MILD AND SELECTIVE PALLADIUM-CATALYZED PYRIDYLIC ALLYLATION OF 4-ALKYLPYRIDINES

FAIZAN RASHEED

A THESIS SUBMITTED TO THE FACULTY OF GRADUATE STUDIES IN PARTIAL FULFILLMENT OF THE REQUIREMENTS FOR THE DEGREE OF MASTER OF SCIENCE

GRADUATE PROGRAM IN CHEMISTRY

YORK UNIVERSITY

TORONTO, ONTARIO

MARCH 2019

Abstract

Pyridines and related heterocycles enjoy widespread occurrence in biologically relevant natural products and drug-like molecules. Therefore, new methods that facilitate their synthesis and incorporation into drug-like structures will likely have a significant impact on the drug development process. This is especially true when these methods accomplish selective functionalization and allow a broad functional group tolerance. Reported herein is a new strategy for the selective allylation of 4-alkylpyridine derivatives. Our methodology exploits well-established alkylidene dihydropyridine intermediates as substrates for a Pd-catalyzed decarboxylative allylation reaction, which installs a synthetically versatile allyl group at the 4-pyridylic position. The use of a weak base and the absence of a Lewis acid in our method enables the allylation of 4-alkylpyridines with exceptional functional group tolerance. Moreover, the compatibility of the proposed pyridylic allylation strategy extends beyond simple 4-alkylpyridines to more sophisticated 3- and 4-disubstituted pyridines. The regioselectivity of the method is also explored with substrates bearing multiple pyridylic sites.

Acknowledgments

I would like to extend my deepest gratitude to Dr. Arturo Orellana for his support and mentorship. His passion for organic chemistry has always been a source of inspiration for me and I feel fortunate that I was given an opportunity to pursue graduate studies under his supervision. I would like to thank him teaching me the importance of integrity and professionalism, and for encouraging me to develop critical-thinking and problem-solving skills. I regard him as an incredible role model.

Dr. Pierre Potvin and Dr. Gino Lavoie, it is an honor to have you on my supervisory committee. I am truly grateful to you for providing your constructive criticism during my research evaluations.

I would like to acknowledge Dr. Howard Hunter for his exceptional expertise in NMR spectroscopy. His support and guidance with various NMR experiments helped a great deal for the completion of this research and for that, I am thankful to him.

To my colleagues, the time I spent in the Orellana lab is truly memorable because of you and I will cherish these fond memories for the rest of my life. I would like to acknowledge and thank Nour Wasfy for her assistance during this research. Minhao Zhang, Anmol Dhesi and Isabelle Hunter, your friendship has been vital for the completion of this work and I wish you the best for your future endeavors. To Jiaqui Shi and Shrey Desai, it has been a privilege to work with you. I thank you for your willingness to engage in chemistry discussions and sharing insightful ideas. To Dr. Andrei Nikolaev, Dr. Aashik Sayyad and Dr. Liam O'Donnell, I really appreciate your advice and suggestions on my research.

To my friends outside York University; Craig Day, Jee Kwak, Murtaza Hassan, Ibrahim Saboor, Mujtaba Jiwani, Minhaj Kabir and Saud Pirzada among others, I am truly grateful to have you all in my life. Your friendship kept me sane during my graduate studies and I thank you for your support and kindness.

Without unconditional love and endless support from my family, especially my parents, I cannot even imagine being successful at anything in life. Thank you for taking care of me and encouraging me to be honest and hardworking. To my wife, Mariam; thank you for your patience and generosity. Your presence in my life is a blessing.

Table of Contents

List of Schemes

List of Tables

List of Figures

List of Abbreviations

1D	1 dimensional
2D	2 dimensional
ACS	American Chemical Society
Alloc-Cl	allyl chloroformate
BINAP	2,2′-bis(diphenylphosphino)-1,1′-binaphthyl
Boc	*tert*-butyloxycarbonyl
COSY	Correlation Spectroscopy
dba	dibenzylidene acetone
DBU	1,8-diazabicyclo[5.4.0]undec-7-ene
DCM	dichloromethane
DEPT	Distortionless Enhancement by Polarization Transfer
DMBQ	2,6-dimethoxybenzoquinone
DME	dimethoxy ethane
DMSO	dimethylsulfoxide
DPEPhos	bis[(2-diphenylphosphino)phenyl] ether
Dppe	1,2-bis(diphenylphosphino)ethane
Dppf	1,1'-bis(diphenylphosphino)ferrocene
$E1_{cb}$	Elimination unimolecular-conjugate base
ee	Enantiomeric excess
Et	ethyl
Et_2O	diethyl ether
EtOAc	ethyl acetate
Eq.	equation
equiv.	equivalents
EWG	electron withdrawing group
FDA	Food and Drug Administration
GPCR	G-protein-coupled receptor
h	hour(s)

HMBC	Heteronuclear Multiple Bond Correlation.
HSQC	Heteronuclear Single Quantum Coherence
Hz	Hertz
IR	Infrared
LDA	lithium diisopropyl amide
LiHMDS	lithium hexamethyldisilazide
L_n	ligand(s) (n = number of ligands)
min	minute(s)
NMR	Nuclear Magnetic Resonance
p	para
ppm	parts per million
R_f	retention factor
r.t.	Room Temperature
S_N2	Substitution Nucleophilic Bimolecular
TBS	*tert*-Butyldimethylsilyl
tert	Tertiary
THF	tetrahydrofuran
TLC	Thin Layer Chromatography
XantPhos	4,5-bis(diphenylphosphino)-9,9-dimethylxanthene

Chapter 1: Introduction

1.1 Transition metal catalysis in organic synthesis.

Synthetic organic chemistry is an evolving science; new synthetic strategies and methods are developed continually to deal with the challenges brought forward by complex natural products and even small molecules. At the heart of most syntheses is the construction and derivatization of a carbon backbone. Therefore, the development of efficient and environmentally benign ways to form new carbon-carbon bonds in a controlled fashion is of utmost significance. In the last few decades, the area of transition metal catalysis has seen tremendous growth. Owing to their ability to access multiple oxidation states, transition metals can participate in oxidation-reduction reactions, a trait that is essential to their use as catalysts in organic synthesis. Transition metals coordinate to various functional groups by engaging their d-orbitals, and hence, facilitate the *in situ* formation of reactive intermediates *via* well understood elementary steps to furnish C-C bonds that are otherwise difficult to make through conventional means (e.g. sp^2-sp^2 coupling for biaryl synthesis).[1] These reactions find widespread practical applications in industry, drug discovery and process development as they often exhibit remarkable functional group tolerance. As catalysts, transition metals allow synthetically useful transformations to occur under mild conditions, increase atom economy and in many cases reduce the formation of environmentally toxic waste products. Transition metal catalysis has revolutionized modern synthetic organic chemistry and therefore, in recognition of its global impact, many recent landmark achievements have been awarded the Nobel Prize in Chemistry: the development of asymmetric osmium-catalyzed oxidations and ruthenium-catalyzed hydrogenations (2001),[2] ruthenium-, tungsten- and molybdenum-catalyzed olefin metathesis (2005)[3] and palladium-catalyzed cross-coupling reactions (2010).[4] The development of highly active transition metal catalysts remains an active area of research in organic and organometallic chemistry mainly to (1) carry out synthetically challenging transformations such as sp^3-sp^3 coupling[5] and C-H activation,[6] (2) understand the

underlying mechanisms and (3) reduce the catalyst loading[7] and progress towards catalyst recycling.

1.2 Palladium in organometallic catalysis.

1.2.1 General introduction.

Palladium is one of the most popular transition metals employed for catalysis in organic chemistry. It mediates several types of reactions such as hydrogenation[8], oxidation[9], nucleophilic substitution[10] and cross-coupling[11] reactions. Palladium can interconvert between two preferred oxidation states, Pd(0) and Pd(II), and therefore, it readily participates in reversible two-electron oxidation-state changes, leading to facile oxidative addition and reductive elimination. Since many Pd(II) complexes are air- and water-stable (such as $Pd(OAc)_2$ and $PdCl_2$), they can be conveniently employed as precursors to Pd(0) in homogenous catalysis. With the development of structurally-complex phosphines, the role of ligands has become crucial in Pd-catalyzed reactions as they impart characteristic properties to the metal for bond-making and bond-breaking processes.[12] Therefore, the electronic and physical properties of the phosphine ligands have been extensively studied and characterized by various parameters including the Tolman electronic parameter (TEP),[13] Tolman cone angle[14] and bite angle[15] etc. The optimization of the activity, selectivity and stability of Pd catalysts can be expediently achieved by varying these ligands around the metal center. Several metal-catalyzed reactions proceed *via* activation of π-bonds in arenes, alkenes and alkynes, which are commonly occurring functional groups in organic molecules. Like other relatively more expensive precious metals such as Au, Pt and Ir etc., Pd can efficiently interact with these π-bonds and initiate bond-making/bond-breaking activity.[16] Moreover, Pd-catalyzed reactions often exhibit exceptional tolerance for the polar functional groups and heterocycles that commonly occur in biologically active compounds.[17]

1.2.2 Carbon-carbon bond forming reactions catalyzed by palladium:

Unlike non-precious transition metals such as Ni and Cu, the reaction mechanisms of Pd-catalyzed reactions are now well established and consist of known elementary steps.[18] In most catalytic cycles, the oxidative addition of Pd(0) across a C-X bond (X = halide or a pseudohalide such as triflate) leads to the formation of aryl-, alkenyl- or alkylpalladium(II) species. An organometallic or main group organic species (C-M) bearing the suitable carbon fragment then undergoes transmetallation with the Pd(II) complex, as shown in Scheme 1. This results in the formation of a new Pd(II) complex bearing both carbon fragments to be coupled. Upon reductive elimination, a new carbon-carbon bond is formed and Pd(0) is regenerated.

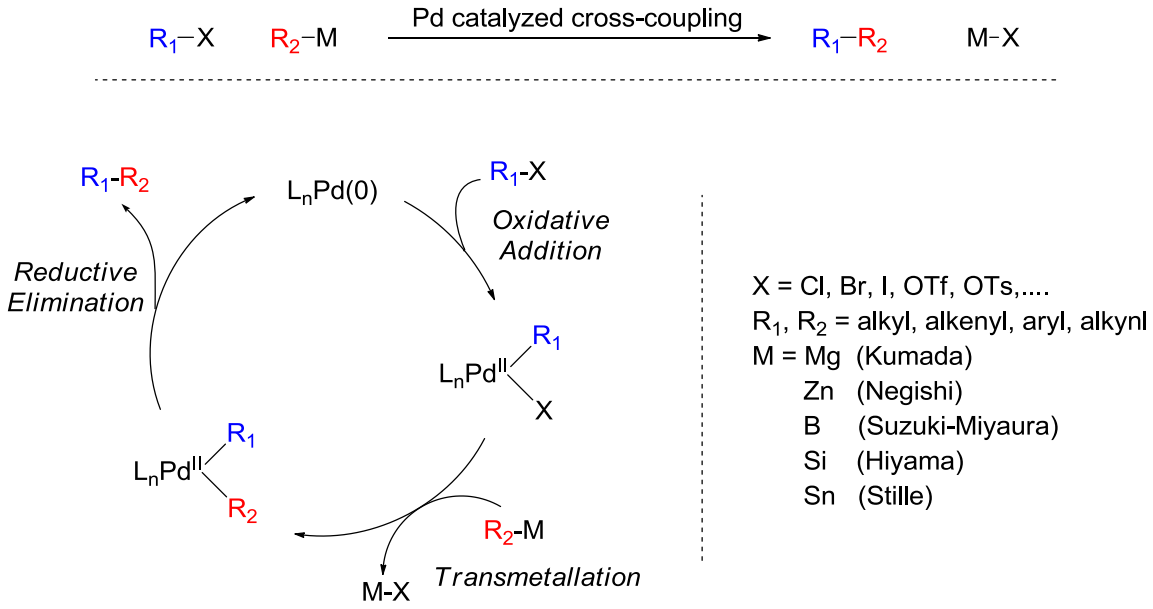

Scheme 1. General equation and mechanism of palladium-catalyzed cross-coupling reactions.

This general mechanism for C-C bond formation represents a fundamental class of Pd-catalyzed transformations called 'cross-coupling' reactions. Several named reactions belonging to this class have evolved in the last few decades such as Suzuki,[19] Stille[20] and Negishi[21] reactions, which essentially differ in the type of organometallic species employed for

transmetallation (Scheme 1). In contrast, the Heck[22] reaction, which does not require a stoichiometric organometallic reagent, proceeds through migratory insertion of an olefin to aryl- or vinylpalladium(II) species (Scheme 2). The new Pd(II) species formed then undergoes β-hydride elimination to release the product bearing a new carbon-carbon double bond and a PdH complex. An added base facilitates the reductive elimination of HX to regenerate Pd(0).

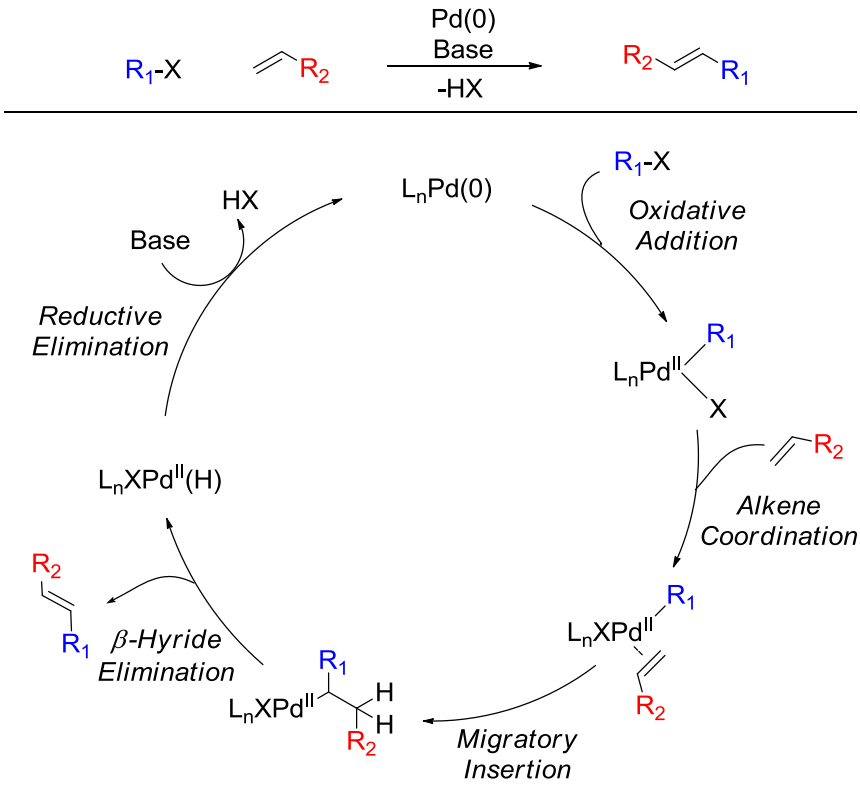

Scheme 2. General equation and mechanism of the Heck reaction.

The Pd-catalyzed reaction of terminal alkynes with aryl or vinyl halides in the presence of Cu(I) as a co-catalyst is known as the Sonogashira[23] coupling (Scheme 3). While the development of cross-coupling reactions to directly install alkyl fragments is still a challenge, this reaction along with the Heck reaction serves as an excellent alternative in most cases, as alkynes and alkenes can be conveniently transformed to the corresponding alkanes by catalytic hydrogenation. One of the few well-established strategies to conduct sp^3-sp^3 coupling is to use

the Tsuji-Trost allylation reaction. This reaction involves Pd-catalyzed substitution of an allylic electrophile with a carbon- or heteroatom-based nucleophile (Scheme 3). The mechanism and synthetic utility of the Tsuji-Trost reaction is discussed in detail in the following sections.

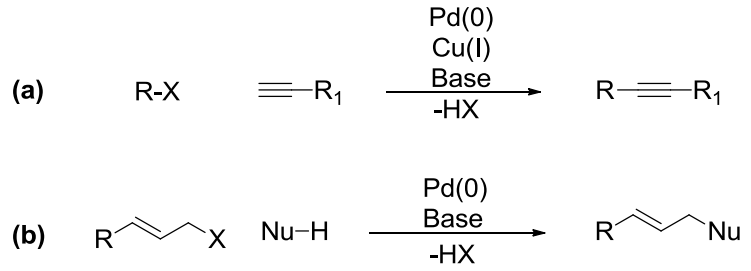

Scheme 3: General equations of **(a)** the Sonagashira coupling reaction **(b)** the Tsuji-Trost allylation reaction

1.3 Palladium-catalyzed allylic substitution.

1.3.1 Early development.

In 1965, Tsuji and co-workers reported the first ever palladium-mediated allylation of stabilized carbon nucleophiles. They treated allylpalladium(II) chloride dimer with the sodium salt of diethyl malonate and recovered a 1:1 mixture of mono- and dialkylated product (Eq. 1).[24]

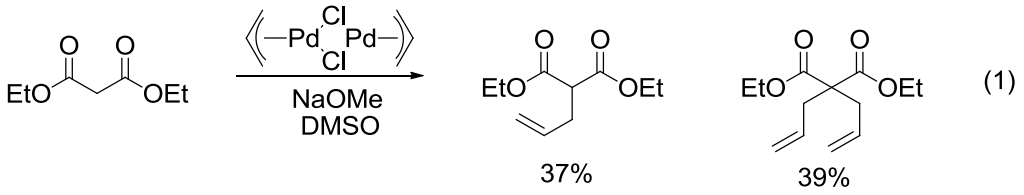

(1)

The electrophilic behavior of the η^3- bound allylpalladium complex was extraordinary as the organometallic compounds of the main group metals such as allylMgBr were known to be nucleophilic. More importantly, this discovery led to the beginning of an exciting and innovative area of research in organometallic catalysis. Preliminary results from Tsuji's work paved the way for the incorporation of the Pd-mediated allylation into a catalytic process. In 1970, the Hata[25] and Atkins[26] groups independently published their work on palladium-catalyzed allylation of phenyl allyl ethers and allylic alcohols respectively, with various carbon and heteroatom nucleophiles (Scheme 4). After these initial reports, the early development of palladium-catalyzed allylation chemistry focused on 'soft' carbanions as nucleophiles, namely anions derived from pronucleophiles bearing electron-withdrawing groups such as β-dicarbonyl compounds, and allylic halides. Over the years, the reaction has been thoroughly investigated and the scope has been expanded to accommodate C, N, P, S and O-based nucleophiles.

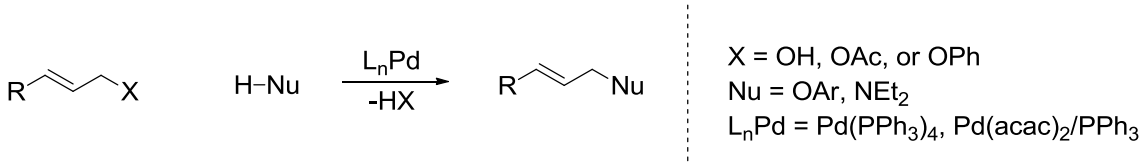

Scheme 4. First examples of Pd-catalyzed allylic substitution by Hata and Atkins.

Trost and co-workers in 1977 published the first ever Pd-catalyzed enantioselective allylic substitution reaction.[27] Using a simple $Pd(PPh_3)_4$ catalyst and a camphor-derived phosphine-based chiral ligand, they managed to isolate the enantioenriched allylation product of diethylmalonate from a racemic allylic ester (Eq. 2). This ground-breaking discovery led to the development of more sophisticated chiral catalysts exhibiting remarkable enantioselectivity in C-C bond formation. In recognition of the pioneering work done by Tsuji and Trost, the Pd-catalyzed allylic substitution reaction is now known as the Tsuji-Trost allylation reaction.[28]

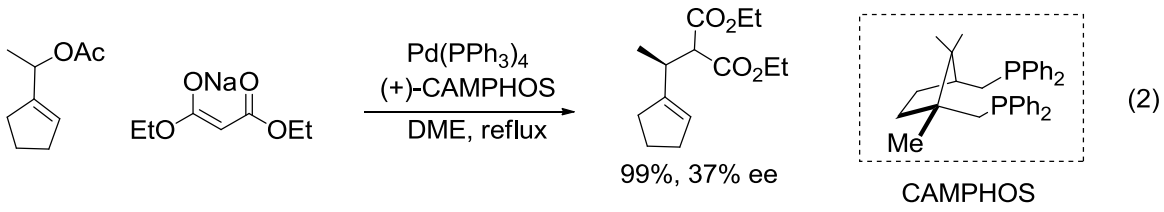

1.3.2 Mechanism of the Tsuji-Trost allylation.

In a typical Tsuji-Trost reaction, an activated allylic substrate, such as an allylic halide or alcohol protected as an acetate or carbonate, undergoes palladium-catalyzed substitution with a carbon or heteroatom nucleophile (Scheme 3b). The mechanism invoked for this transformation involves oxidative addition of Pd(0) to the allylic electrophile to generate the (η^3-allyl)Pd(II) intermediate. In most cases, the leaving group is not bound to the metal center and exists as a counterion of the cationic allyl complex. The nucleophile then intercepts the (η^3-allyl)palladium(II) complex and, upon reductive elimination, the substitution product is released from the catalytic cycle and Pd(0) is regenerated (Scheme 5).

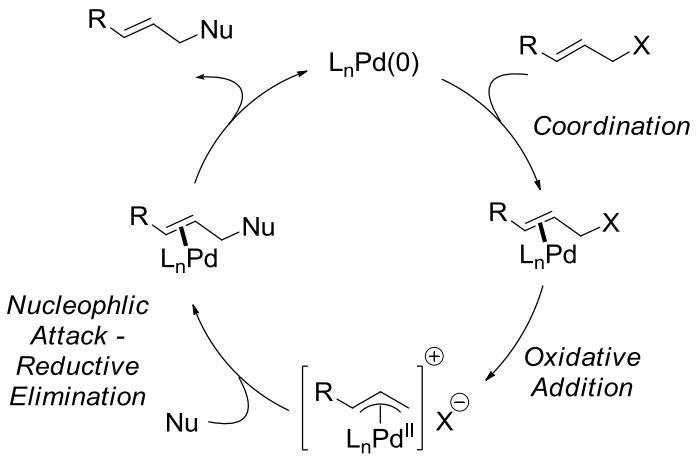

Scheme 5. Catalytic cycle of Pd-catalyzed allylic substitution reaction.

1.3.3 Generating (η^3-allyl)palladium complexes.

Allylpalladium complexes are well understood catalytic intermediates since they are often isolable and can be conveniently characterized by NMR spectroscopy and X-ray crystallography. Access to structural data allows a thorough understanding of the mechanistic features of their synthesis and reactivity patterns. Oxidative addition across the allylic C-X bond is by far the most common way of generating (η^3-allyl)Pd(II) complexes. The mechanistic studies by Amatore provided evidence for the reversibility of the oxidative addition of allyl acetate with the Pd(0) complex generated from $Pd(dba)_2$ and two equivalents of PPh_3.[29] The reaction between the $Pd(dba)_2$-PPh_3 catalyst system and allyl acetate proceeds *via* a neutral intermediate in which the Pd(0) complex is coordinated to the C-C double bond of the allylic electrophile. This complexation step is also reversible and serves to activate the allylic C-X bond for the ionization step (Scheme 6). Moreover, It has been shown that the Pd-mediated ionization of allyl acetates delivers cationic (η^3-allyl)Pd(II) complexes with an inversion of stereochemistry, as established for S_N2 reactions.[30] Beside halides and acetates, several other allylic substrates, such as allylic ammonium salts,[31] sulfones,[32] sulfides,[33] phosphates[34] and nitro groups,[35] have been explored as potential precursors to π-allylPd.

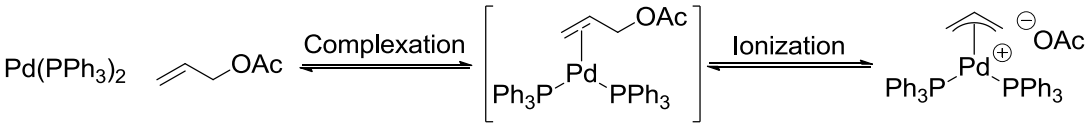

Scheme 6: Formation of cationic η^3-allylPd(II) complex by oxidative addition.

The migratory insertion of 1,3- and 1,2-dienes with (aryl)Pd(II) complexes is an another efficient way of generating (η^3-allyl)Pd(II) complexes. The strategy illustrated in Scheme 7 was first exploited by Stevens and Shier in 1970, as they isolated and characterized a π-allyl intermediate obtained from the carbopalladation of a 1,3-diene substrate (Eq. 3).[36] Similarly, Gore

in 1984 reported the catalytic generation and trapping of a π-allyl complex *via* carbopalladation of an allene using malonate as a nucleophile (Eq. 4).[37]

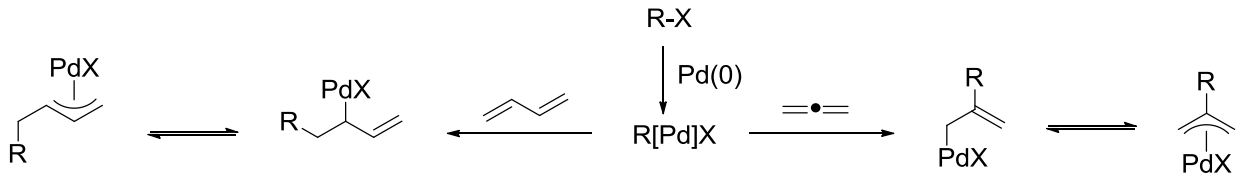

Scheme 7. Generation of η^3-allylpalladium complex by carbopalladation of 1,3 and 1,2-dienes.

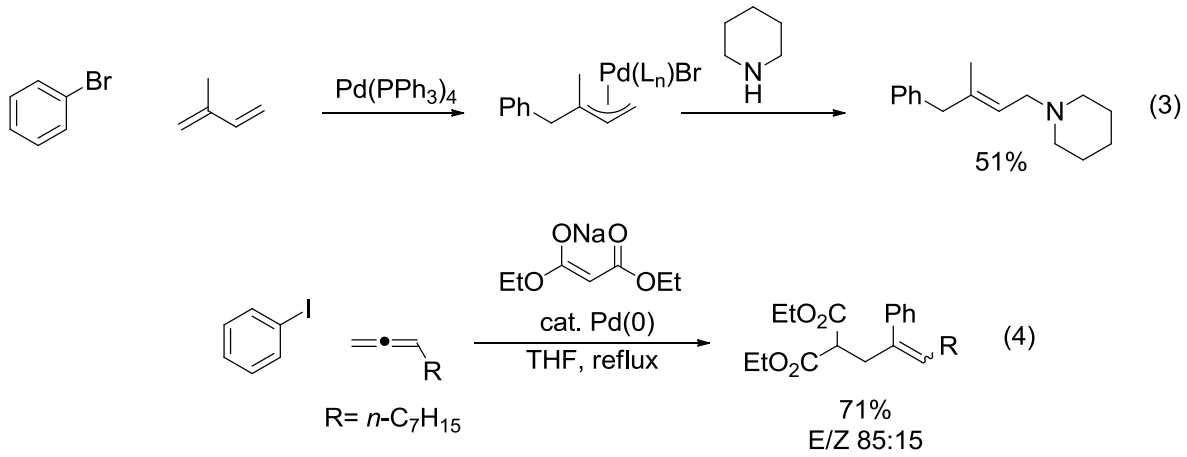

.

More recently, allylic C-H activation has gathered tremendous interest as it allows substitution of unfunctionalized alkenes. The cleavage of an allylic C-H bond has been shown to occur following Pd(II)-olefin coordination in the presence of a suitable ligand and/or additive to afford a (π-allyl)Pd(II) complex. Treatment of the π-allyl with a nucleophile and subsequent reductive elimination delivers the substitution product and Pd(0) complex. However, in order to close the catalytic cycle, stoichiometric oxidants such as DMBQ can be used to re-oxidize Pd(0) to Pd(II) as reported by Chen and White (Eq. 5).[38]

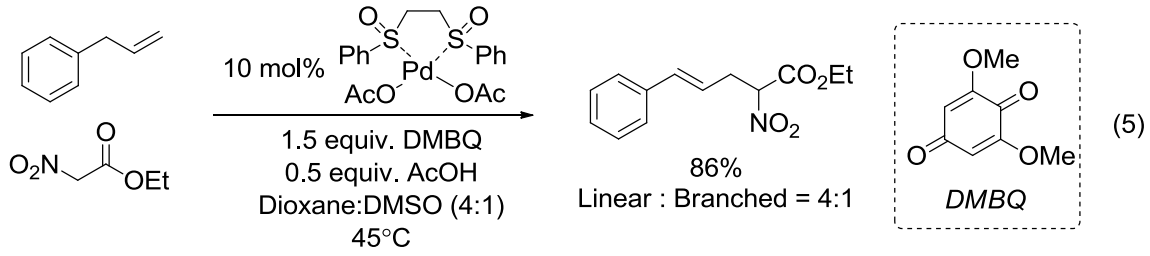

1.3.4 Trapping (π-allyl)palladium complexes with nucleophiles.

(η^3-Allyl)Pd complexes being electrophilic, can be intercepted by various carbon and heteroatom nucleophiles, thereby allowing the formation of C-C and C-heteroatom bonds. The mechanism of nucleophilic attack is governed primarily by the nature of the incoming nucleophile and determines the stereochemical outcome of allylic substitution. Based on the pK_a of pronucleophiles (conjugate acids), Trost and Van Vranken recognized two distinct classes of nucleophiles in the Tsuji-Trost allylation reactions:[39] (1) stabilized or 'soft' carbon nucleophiles bearing one or two electron withdrawing groups such as enolates, malonates and those derived from pronucleophiles with pK_a values lower than 25 and (2) unstabilized or 'hard" nucleophiles such as borate, organozinc, organostannane and those derived from pronucleophiles with pK_a values higher than 25. The former approaches a π-allylpalladium intermediate on the face opposite the metal and directly attacks the metal-bound allyl moiety in an 'outer-sphere' manner. The attack of the nucleophile on the C1 or C3 allylic carbon leads to an η^3 to η^2 shift and affords a Pd(0)-olefin complex. The allylation product is subsequently released from the complex and Pd(0) becomes readily available to carry out further catalysis. Trost and coworkers demonstrated the stereochemical outcome of the outer-sphere reductive elimination with cyclic and acyclic models. The oxidative addition of Pd(0) to *cis* cyclohexenyl acetate generates the π-allyl intermediate with an inversion of stereochemistry. This is followed by an outer-sphere attack of the sodium salt of dimethylmalonate on the face opposite the metal, resulting in the net retention of configuration (Scheme 8).[40]

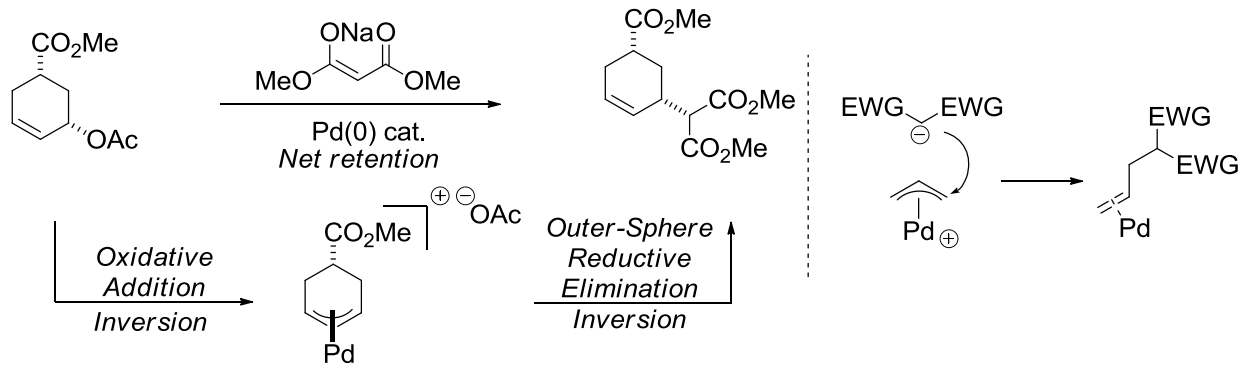

Scheme 8. Mechanism of Pd-catalyzed allylic substitution for 'soft' nucleophiles.

In contrast, 'hard' nucleophiles such as organometallic compounds of main group metals directly attack the metal center and, *via* transmetallation, generate a Pd(II) complex bearing both allyl group and the carbon fragment to be coupled. Therefore, the incoming nucleophile is incorporated into the coordination sphere of Pd (Scheme 9). Upon inner-sphere reductive elimination, the allylation product is released with a net inversion of stereochemistry.[41]

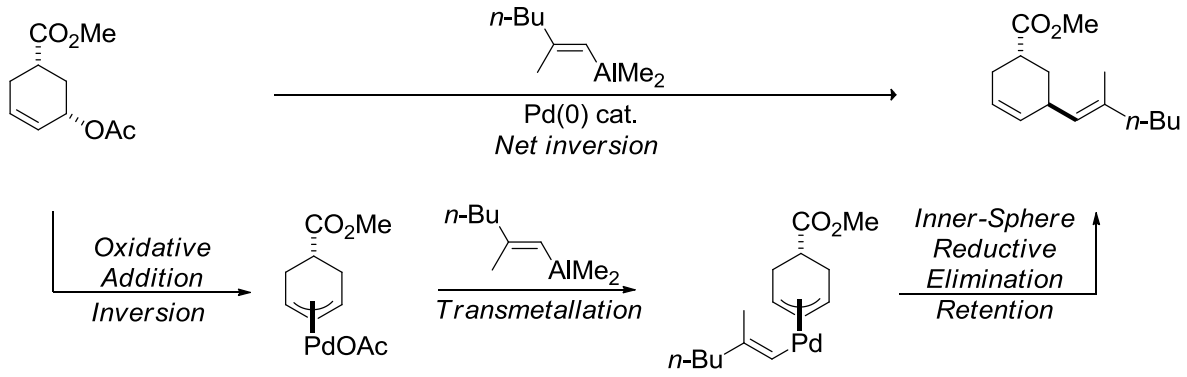

Scheme 9. Mechanism of Pd-catalyzed allylic substitution for 'hard' nucleophiles.

1.4 Palladium-catalyzed decarboxylative allylation.

When a β-keto allyl ester is treated with a base at high temperature, it transforms into an α-allyl,β-keto carboxylic acid by undergoing a [3,3] sigmatropic rearrangement and, upon decarboxylation yields an α-allyl ketone. This transformation, known as Carroll rearrangement, is effectively a decarboxylative allylation (Scheme 10).[42]

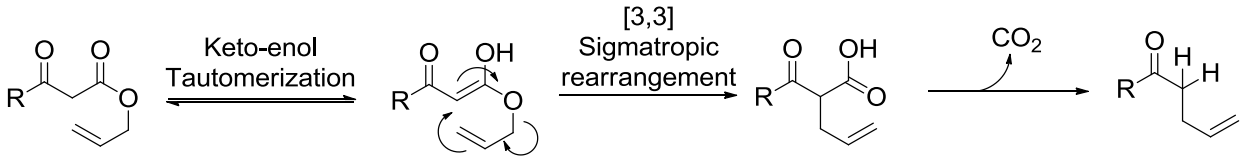

Scheme 10. Mechanism of the Carroll rearrangement.

In 1980, Tsuji[43] and Saegusa[44] (Scheme 11) almost simultaneously showed that the aforementioned transformation can be performed under much milder conditions with a catalytic amount of Pd(0). More importantly, a remarkable feature of the methods reported by Tsuji and Saegusa was the use of Pd-mediated decarboxylation as a tool to generate the nucleophile, thereby replacing the need to introduce preformed enolates.

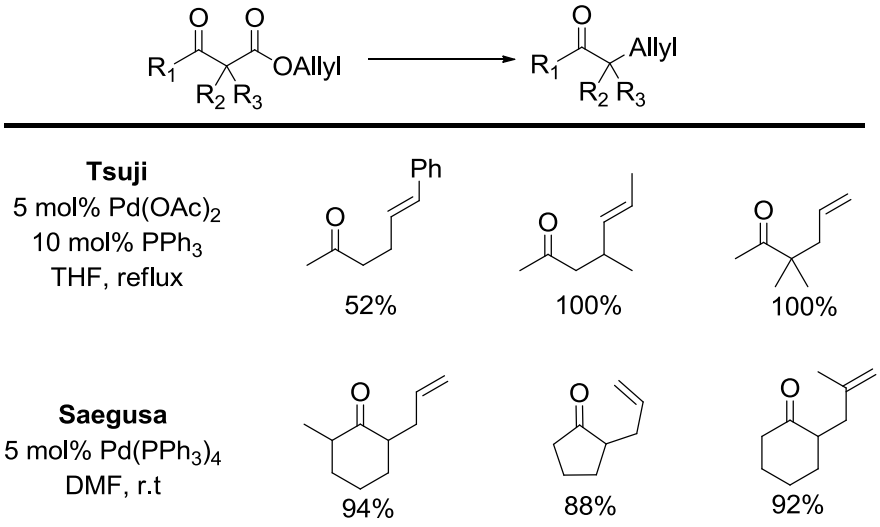

Scheme 11. Pd-catalyzed decarboxylative allylation of β-keto allyl esters by Tsuji and Saegusa.

An interesting development came through in 1982 when Tsuji employed carbonate as a leaving group on the allylic electrophile for the first time.[45] It was hypothesized that an allylic carbonate upon oxidative addition by a Pd(0) catalyst, would spontaneously undergo decarboxylation, leading to the formation of an alkoxide base *in situ*. Deprotonation of acidic pronucleophiles by the *in situ* generated alkoxide and subsequent reductive elimination delivered the allylic substitution product in the absence of any added base (Eq. 6). The attack of the alkoxide on the (π-allyl)palladium complex was found to be much slower than that of the carbon nucleophile. Therefore, the use of allylic carbonates furnished the C-C bond in essentially neutral conditions.

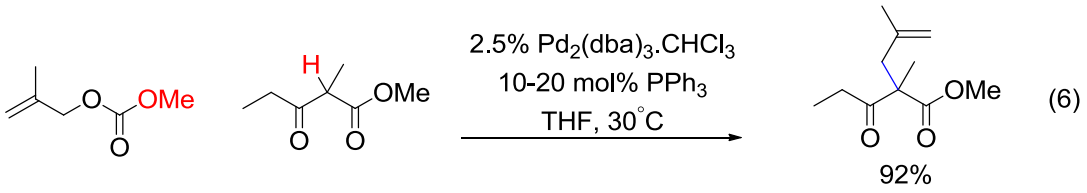

(6)

In a typical cross-coupling reaction, the reagents used for transmetallation are organometallic compounds of B, Sn, Cu or Zn. Such reagents are often relatively expensive, toxic or highly basic and are prepared from other functionalized precursors (e.g. the corresponding halide). Moreover, they generate stoichiometric amounts of sometimes hazardous organometallic by-product that can be difficult to remove and may complicate product purification. Decarboxylative coupling, on the other hand requires widely available and inexpensive carboxylic acid derivatives to generate organometallic reagents by CO_2 extrusion. It gives rise to site-specific organometallic intermediates, unlike coupling by C-H activation where the regioselective formation of such intermediates can be a challenge.[46] Moreover, often the only stoichiometric by-product is CO_2, which is non-toxic and can easily escape the reaction mixture.

1.5 Importance of heterocycles in medicinal chemistry.

Nitrogen-containing heterocycles play a crucial role in medicinal chemistry. A study on structural diversity among small-molecule drugs revealed the presence of N-heterocycles in 59% of all U.S. FDA-approved pharmaceuticals. Moreover, it was found that pyridines are the second-most commonly occurring of all N-heterocycles.[47] These heterocycles commonly serve as tools to manipulate lipophilicity, polarity and the number of hydrogen-bond donor/acceptors in the drug candidates, which can have a profound effect on their pharmacological and physiochemical properties.[48] Therefore, new methods that can facilitate their incorporation into the drug-like compounds are likely to have a significant impact on the drug discovery process. Recently, there has been a call for organic chemists to collaborate with the drug-discovery community to design methodologies for the synthesis of molecules associated with increased clinical success or lead-like compounds.[49] For a successful lead-oriented approach, the methods to be developed must have a high functional-group tolerance to construct a wide range of biologically-relevant products with lead-like properties. As a result, the development of practical methods for the synthesis and derivatization of pyridines and related heterocycles is a new focus of academic research in organic synthesis. In this regard, mild methods that generate new C-C bonds at the pyridylic position are of particular interest. This is especially true when they give rise to tertiary stereogenic centers because the resulting scaffolds are known to be privileged motifs in medicinal chemistry (Figure 1).[50]

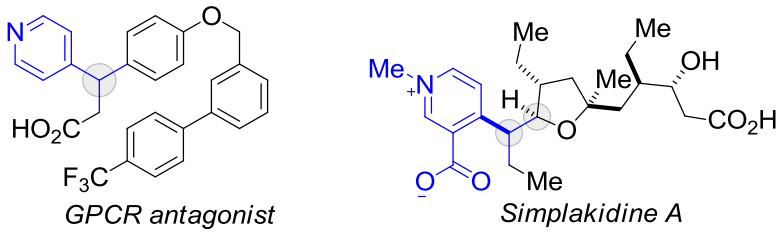

Figure 1. Biologically active heterocycles bearing tertiary pyridylic centers.

1.6 Transition metal-catalyzed pyridylic allylation:

Allyl groups are perhaps the most synthetically versatile among all the hydrocarbon functional groups that can be installed on an organic molecule. The utility of an allyl group as a synthetic handle is evidenced by a variety of transformations that it can undergo including ozonolysis,[51] epoxidation,[52] hydroboration,[53] dihydroxylation[54] and olefin metathesis.[55] An allyl group can be installed by the treatment of a suitable carbon or heteroatom nucleophile with an allylic electrophile (e.g. the deprotonation of 4-methylpyridine by *n*-BuLi, followed by treatment with allyl bromide). However, such reactions often fail to provide the desired regio- and stereo-selectivity for the synthesis of complex drugs and natural products. Therefore, in the last decade, several transition metal-catalyzed methods involving π-allyl intermediates have appeared for the enantio- and/or diastereoselective allylation at the pyridylic site to access tertiary pyridylic motifs.

1.6.1 Tunge's decarboxylative allylation of heteroaromatic alkanes.

Tunge developed the Pd-catalyzed decarboxylative allylation of pyridines from the corresponding allyl esters.[56] This method has been extended to other heterocycles and generates products with adjacent stereogenic centers in a highly diastereoselective manner. However, it requires formation of the allylic ester and is limited to functionalization at the 2-position of the pyridine (Eq. 7).

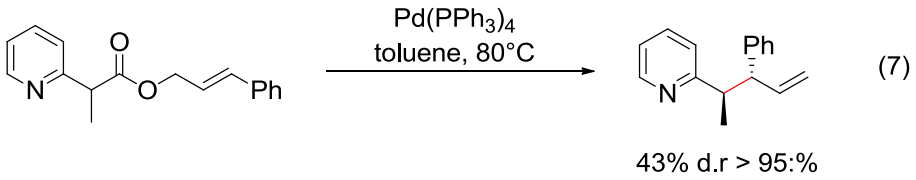

(7)

43% d.r > 95:%

The pyridylic nucleophile generated in Tunge's reaction appears to intercept π-allyl intermediates at the more substituted carbon, which is contrary to the commonly observed preference of a nucleophilic attack at the (π-allyl)Pd system. Moreover, such high diastereoselectivity for C-C bond formation with acyclic nucleophiles is rarely associated with Pd-

catalyzed allylation reactions. Based on preliminary investigations, Tunge and co-workers proposed the following mechanism (Scheme 12) to explain the unusual regio- and diastereoselectivity of their method: (1) Pd(0) ionizes the allylic ester to form (π-allyl)Pd(II) complex **A** and the corresponding heteroaromatic carboxylate, (2) the ring-nitrogen of the heteroaromatic then attacks at the least-substituted terminus of complex **A** to form N-alkylpyridinium intermediate **B**, (3) which facilitates decarboxylation of the carboxylate species to from dearomatized intermediate **C**, and finally (4) the [3,3] sigmatropic (aza-Cope) rearrangement of **C** affords the allylation product with the observed regio- and diastereoselectivity.

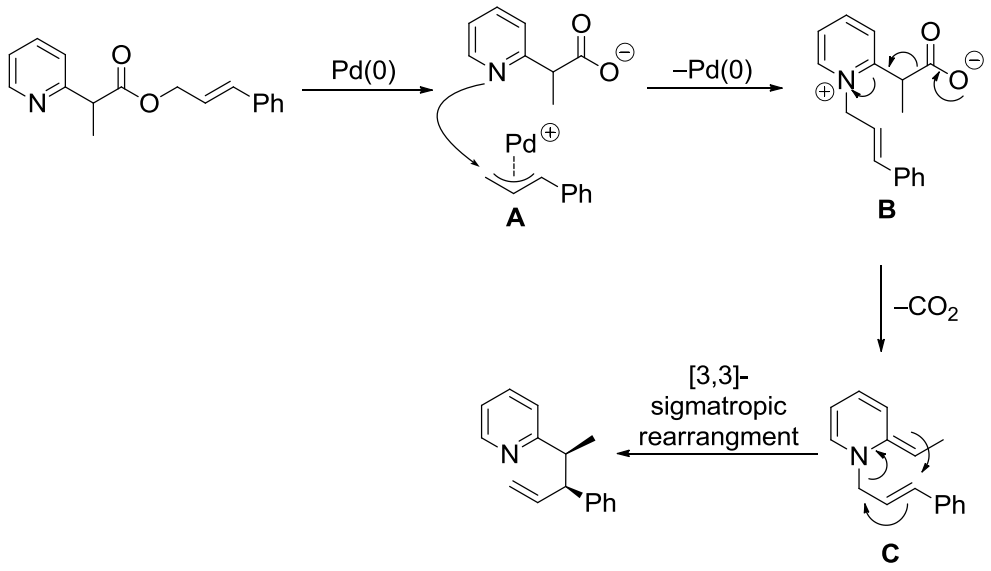

Scheme 12: Mechanism of Tunge's decarboxylative allylation of heteroaromatic alkanes.

1.6.2 Trost's Pd-catalyzed lateral allylation of nitrogen-containing aromatic heterocycles.

Trost has developed the use of pyridine-boron trifluoride complexes to generate soft nucleophiles for highly enantioselective palladium-catalyzed asymmetric pyridylic allylation reactions.[57] Besides using a strong Lewis acid (BF_3), this methodology also requires the use of a strong base to generate the 2-methylpyridine-derived nucleophiles, thereby diminishing the

functional group tolerance of the reaction. Furthermore, the method is limited to allylation at the 2-position of the pyridine as 4-methylpyridine was found to be incompatible with the reported reaction conditions. Consequently, in a competition experiment between the 2- and 4- pyridylic positions with 2,4-lutidine as the substrate, the allylation occurs exclusively at the 2-postion (Eq. 8).

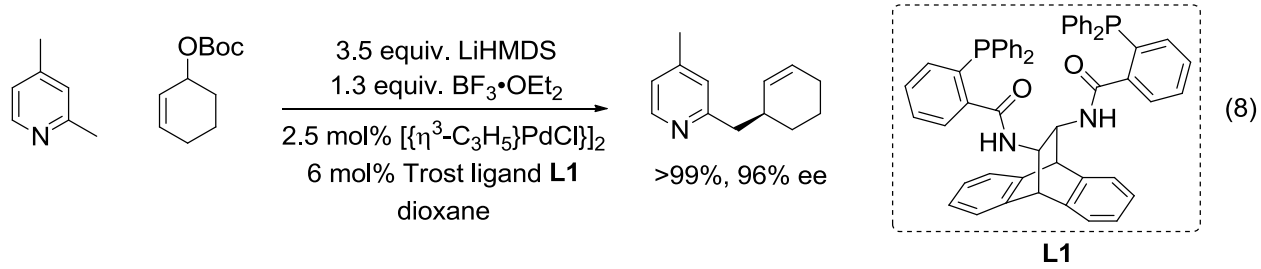

(8)

To investigate the soft nature of pyridine-boron trifluoride nucleophiles in Pd-catalyzed allylation reactions, they conducted the reaction using a *trans*-disubstituted stereochemical probe and the anion generated from 2-picoline. A single diastereomer of the allylation product, with net retention of configuration at the allylic position, was obtained exclusively, suggesting an outer-sphere reductive elimination for the allylic substitution reaction (Eq. 9).

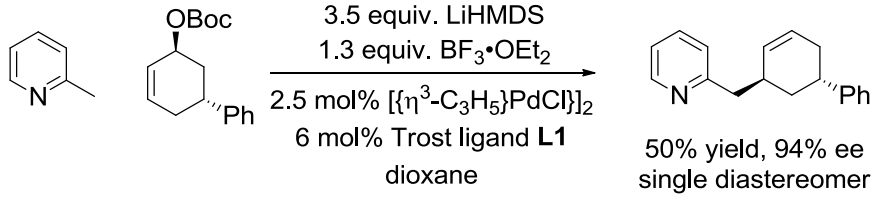

(9)

The same group also reported that 2-ethylpyridine-derived nucleophiles (incompatible with the previously reported conditions in Eq. 8 and 9) can be allylated in a highly diastero and enantioselective manner by introducing 1.0 equivalent of *n*-BuLi to the metalated pyridine-boron trifluoride complex generated with 3.0 equivalents of LiHMDS.[57] It is worth mentioning that *n*-BuLi without the added LiHMDS proved insufficient for the reaction. Presumably, *n*-BuLi serves to

quantitatively deprotonate the HMDS that is formed after the initial deprotonation event with LiHMDS, driving the equilibrium in favor of metalated pyridine complex. The method exhibits excellent diastereoselectivity for C-C bond formation, which originates from the formation of a single geometric isomer of the nucleophile upon deprotonation, because of steric demands imposed by the Lewis acid (Scheme 13).

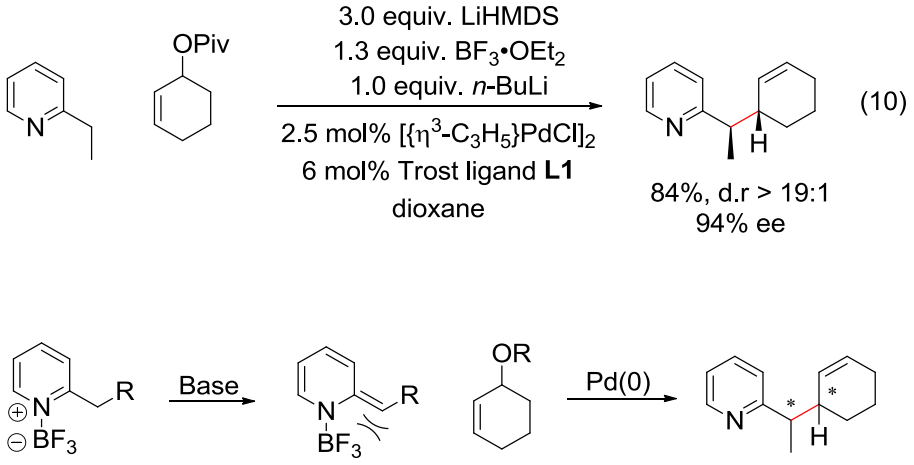

Scheme 13: Trost's hypothesis for the diastereoselective allylation of 2-ethylpyridine-derived nucleophiles

Later, Trost and coworkers managed to expand the scope of allylic substitutions to poly-nitrogenated heterocycles such as pyrimidine, pyrazine, pyridazine, etc. These heterocycles, being more electron-deficient than pyridines, did not require Lewis acid activation (Eq. 11).[58]

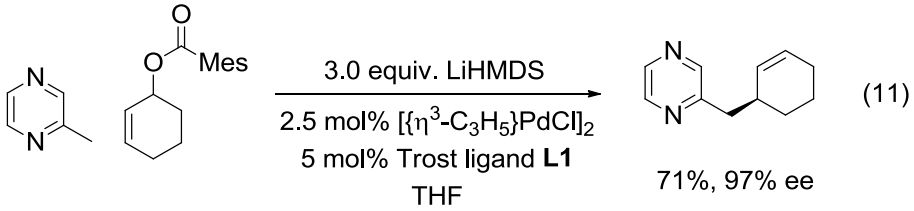

1.6.3. Walsh's method for the allylation of diarylmethanes.

Walsh and co-workers have shown that the anions generated by deprotonation of diarylmethanes can serve as soft nucleophiles in Pd-catalyzed allylation reactions, undergoing the double inversion mechanism.[59] The Trost group has demonstrated similar reactivity for the pyridylic nucleophiles generated in their method by virtue of BF_3 coordination to the ring nitrogen, which could effectively lower the pK_a of the 2-methylpyridine derived pronucleophiles below the threshold of 25 for 'soft' nucleophiles (Eq. 9). However, the retention of stereochemistry at the allylic leaving group in the absence of a Lewis acid suggests that the cut-off between 'hard' and 'soft' nucleophiles should be increased from a pK_a of 25 to at least 32 (Eq. 12). Walsh's method enables benzylic allylation of a variety of diarylmethane derivatives including, 2- , 3-, and 4-benzylpyridines in excellent yields (Scheme 14). However, the use of a strong base limits the functional-group tolerance of the method, and could pose an issue of pyridylic selectivity for allylation when dealing with substrates bearing multiple pyridylic sites.

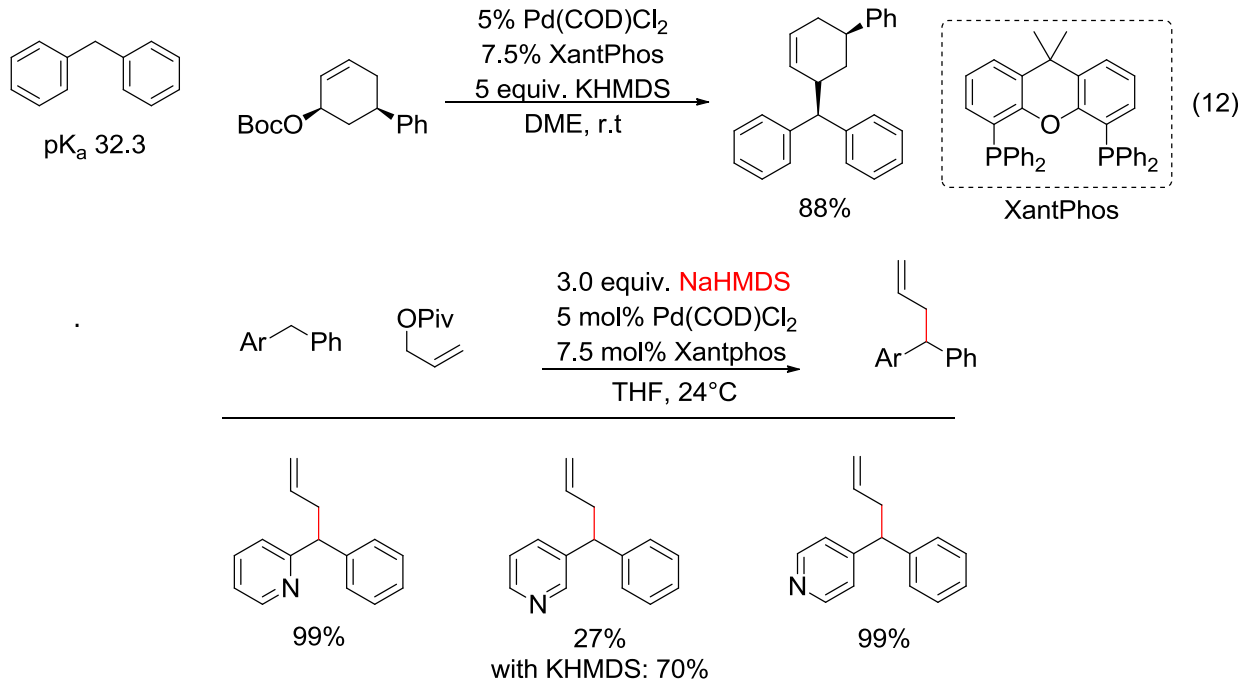

Scheme 14: Allylation of 2-, 3- and 4-benzylpyridine using Walsh's method.

1.6.4 Sawamura's base-free method for pyridylic allylation.

Sawamura and co-workers developed a Pd-catalyzed method for pyridylic allylation by using new, chiral diamidophosphite monodentate ligands.[60] A remarkable feature of their method is the use of allylic carbonates as π-allyl precursors, which allows allylation to occur in the absence of any added base. The mechanism proposed by the Sawamura group (Scheme 15) suggests that the π-allylpalladium(II) complex generated in their reaction serves two purposes: (1) it acts as a Lewis acid that coordinates to the ring-nitrogen and facilitates 'soft enolization' of 2-alkylpyridines by the *in situ* generated alkoxide base, thereby circumventing the need to introduce a stoichiometric Lewis acid and (2) it acts as an electrophile and enables C-C bond formation at the 2-pyridylic site. The authors do not comment on the nature of the reductive elimination step in their method.

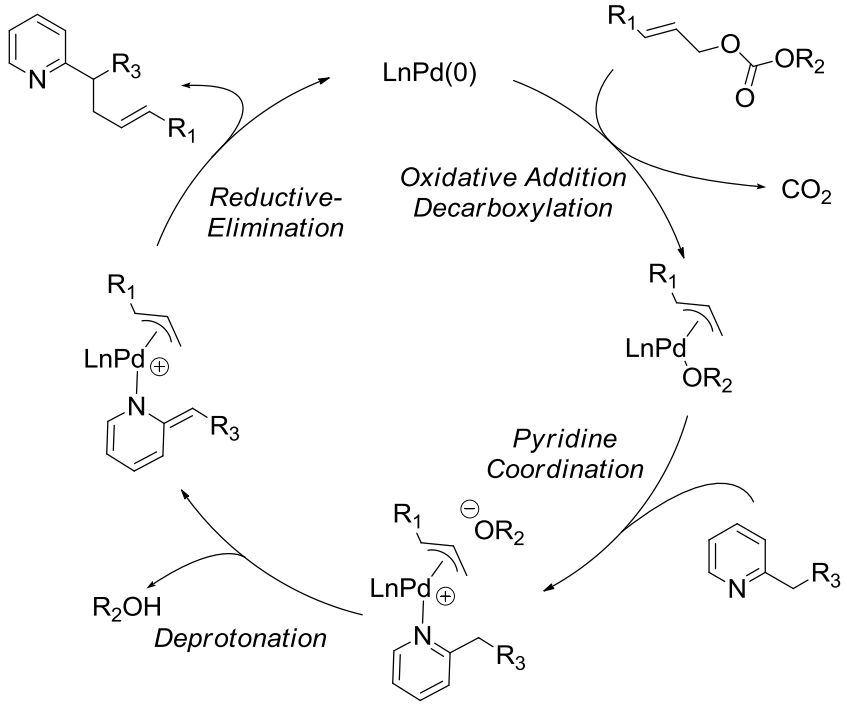

Scheme 15: Proposed mechanism of Sawamura's base-free method for pyridylic allylation

Although the method is limited to functionalization at the 2-pyridylic site, they have shown that it allows selective allylation in the presence of more acidic α-carbonyl C-H bonds (Eq. 13). Furthermore, the method enables lateral allylation at the C2 substituent, in the presence of a C4 alkyl substituent. However, the issue of regioselective allylation at the 4-pyridylic site under mild conditions remains unaddressed.

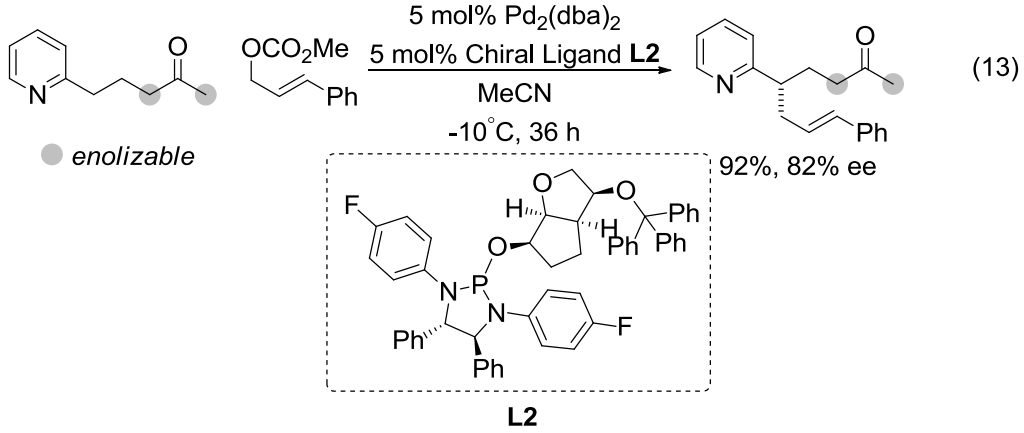

(13)

L2

1.6.5 You's method for the Ir-catalyzed allylation of 2-methylpyridine derivatives

The You group has developed a method for Ir-catalyzed enantioselective lateral allylation with highly unstablized nucleophiles generated *in situ* from 2-methylpyridines (Eq. 14).[61] Like Trost's method, the strategy requires the use of a strong Lewis acid (BF_3•OEt_2) to activate the ring nitrogen and increase the acidity of the pyridylic position. It employs a strong base (LiHMDS) to generate the required nucleophile, which significantly lowers the functional group tolerance of the method. Moreover, the issue of pyridylic selectivity for allylation with substrates containing multiple pyridylic sites has not been addressed.

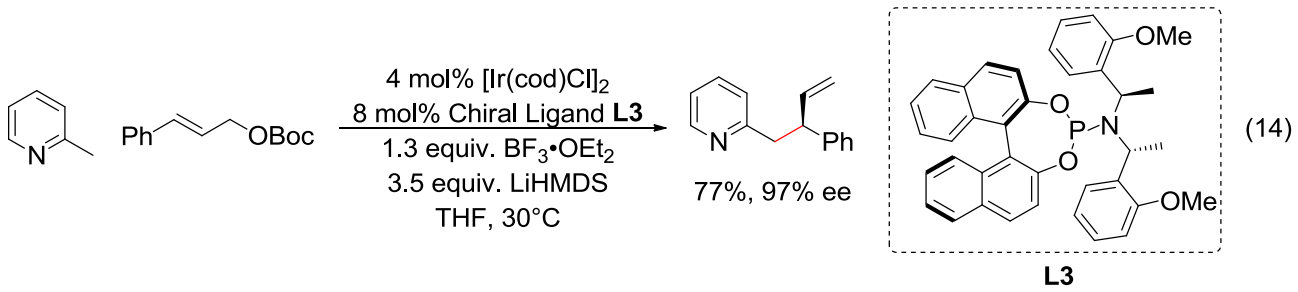

(14)

1.6.6 Lundgren's strategy for the benzylation of allylic electrophiles.

Recently, the Lundgren group reported the use of pre-decarboxylative coupling with aryl acetic acids for both Ir- and Pd-catalyzed asymmetric benzylation of allylic electrophiles.[62] The mechanistic hypothesis proposed by Lundgren suggests that the reaction proceeds *via* a pathway in which C-C bond formation at the benzylic/pyridylic site takes place before the decarboxylation event to afford the functionalized carboxylic acid, which upon decarboxylation leads to the desired allylation product. Unlike methods developed by the Trost, Walsh and You groups, the use of a relatively mild base (i.e. DBU) permits allylation of substrates bearing functional groups that are otherwise sensitive to strong bases. Lundgren's method enables allylation at the 2- and 4-pyridylic sites in good yields and high enantioselectivity. However, it necessitates the formation of pyridyl acetic acids or their corresponding allyl carbonate derivatives.

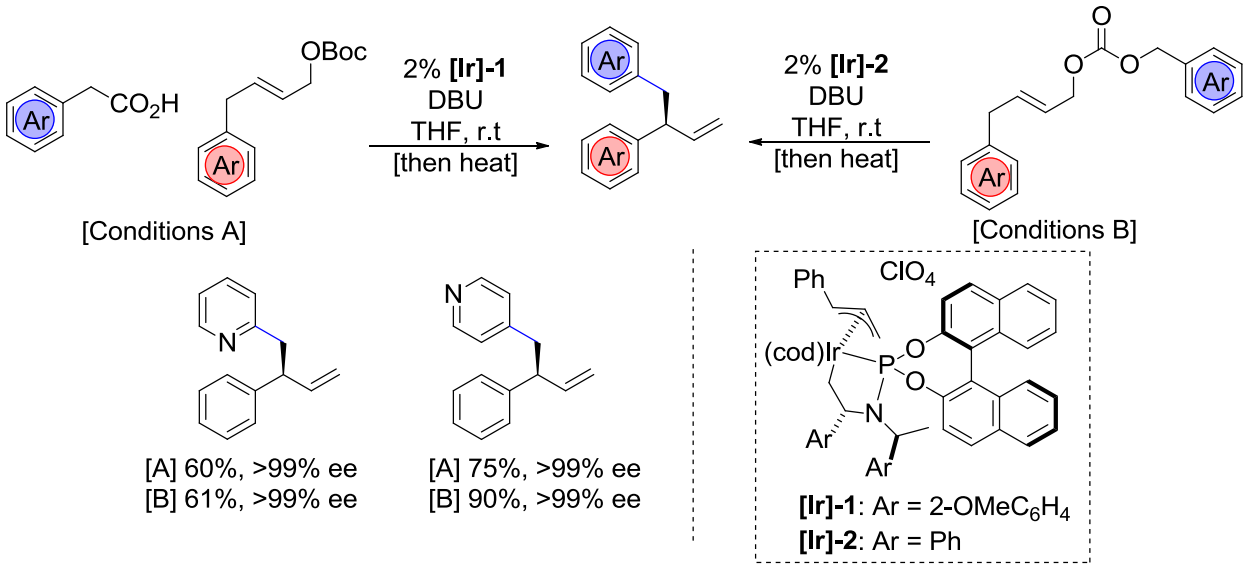

1.7 Proposed strategy for pyridylic allylation.

Given the utility of pyridines in drug discovery, we aimed to develop an alternative method for pyridylic allylation that would avoid the use of strong acids and strong bases, and therefore tolerate a wider range of functional groups. It is now well established that pyridines can be activated towards nucleophilic attack on the aromatic ring by reaction with acyl chlorides and chloroformates to form the corresponding pyridinium ions.[63] The reaction of pyridines with chloroformates has also been employed as a method for 'soft enolization' at the pyridylic position of the ring.[64] Notably, pyridines enolized in this manner have been used in palladium-catalyzed arylation reactions.[65] Curiously, allyl chloroformate has not been used in this manner. It seemed reasonable then to use allyl chloroformate to activate the pyridine ring towards enolization with a mild base. Treatment of the resulting intermediate (I, Scheme 16) with a palladium catalyst would result in a decarboxylative allylation of the pyridine to afford C-C bond formation at the 4-pyridylic site. The proposed mechanism for the palladium-catalyzed step bears similarity to the Tsuji-Trost reaction. Specifically, a Pd(0)L catalyst ionizes the alloc protecting group as previously established for the deprotection of alloc-protected amines,[66] generating a carboxylate that could spontaneously lose CO_2 to rearomatize the pyridine ring, yielding the stabilized pyridylic anion (see reactive intermediate II in scheme 16).

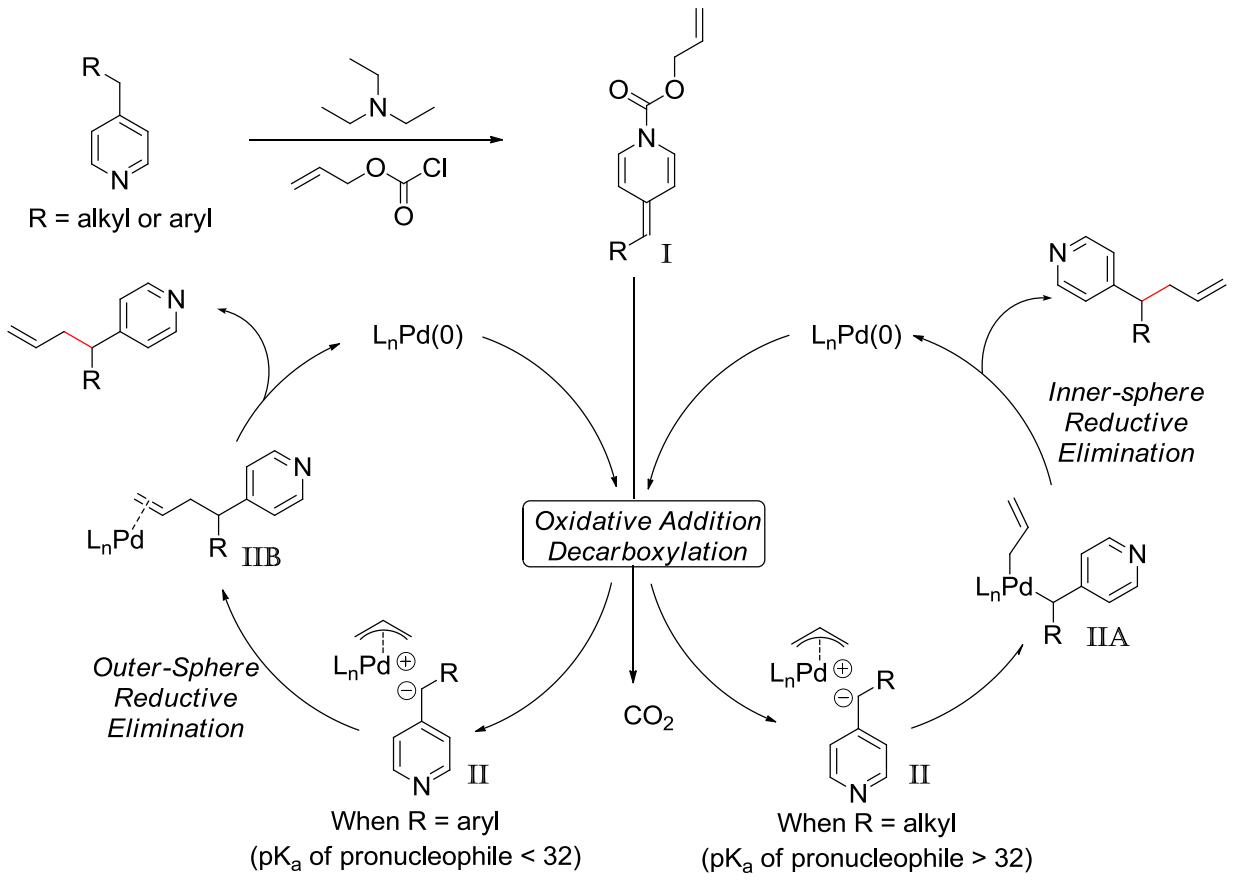

Scheme 16. Proposed strategy for the allylation of 4-alkylpyridines and expected mechanistic dichotomy for reductive elimination based on the pK_a of pronucleophiles.

A recent report by Walsh has revealed that 1,1-diarylmethanes with pK_a values of up to 32 behave as soft nucleophiles in Pd-catalyzed allylation reactions.[59] Therefore, based on the pK_a values of pronucleophiles, we group 4-alkylpyridines into two classes: (1) 4-benzylpyridine and its derivatives with pK_a values lower than the threshold of 32 for 'soft' nucleophiles, and (2) 4-alkylpyridines with pK_a values higher than the threshold of 32 to behave as 'hard' nucleophiles. It is reasonable to expect the latter class of 4-alkylpyridines to undergo inner-sphere reductive elimination where the pyridylic anion is incorporated into the coordination sphere of palladium(II). Moreover, change in the binding mode of the allyl ligand from η^3 to η^1 as the nucleophile binds to metal seems likely to accommodate for four-coordinate alkylpalladium(II) species (Complex **IIA**, scheme 16).

Chapter 2: Results and Discussion.

2.1 Proof of concept.

The utility of alkylidene dihydropyridines as precursors to complex alkaloids is well established.[67] Moreover, they have been shown to participate in Pd-catalyzed Heck reactions,[68] aldol condensation[69] and Au-catalyzed cyclization[70] for the derivatization of heterocycles. Exploiting the pre-established reaction conditions for the synthesis of alkylidene dihydropyridines from 4-alkylpyridines, we treated 4-benzylpyridine with allyl chloroformate and triethylamine in diethyl ether. The reaction mixture was heated to reflux for 30 minutes to afford a dark yellow suspension of the de-aromatized intermediate (**1a'**) with triethylammonium chloride salt (Eq. 15).

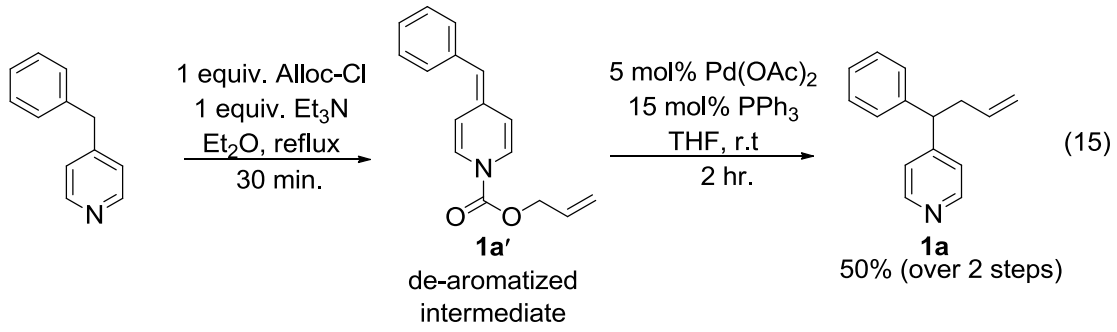

(15)

Evidence for the formation of **1a'** was obtained by ^{1}H-NMR spectroscopic analysis of the reaction mixture. The diagnostic features of the ^{1}H-NMR spectrum include: (1) the disappearance of doublets at 8.48 and 7.09 ppm representing protons belonging to the pyridine ring of 4-benzylpyridine and (2) the appearance of broad peaks in the alkene region (5.5 ppm to 7 ppm) representing protons belonging to the dihydropyridine moiety. Such broadening of peaks is commonly observed for Boc-protected amines and is attributed to the existence of equilibrating rotamers because of slow rotation around the amide bond.[71] The reaction mixture was filtered through a cotton plug to remove the salt and then concentrated under low pressure. Alkylidene dihydropyridine **1a'** was subjected to Pd-catalyzed decarboxylative allylation using a $Pd(OAc)_2$-PPh_3 catalyst system. To our delight, the reaction had reached completion within 2 hours and the

desired allylation product (**1a**) was obtained after water work-up and flash chromatography purification in 50% yield over two steps. The NMR and IR spectroscopic data of **1a** was found to be in agreement with those reported by Walsh and co-workers.[59]

2.2 Reaction development.

A moderate yield of 50% from the first experiment was a source of encouragement for us and we decided to explore the concept by developing the reaction for a broad range of substrates. For this purpose, we thought the best strategy would be to optimize both steps individually by changing the variables involved in each step. Once the optimized conditions are identified, the functional group compatibility of the method was to be established by subjecting various substrates to the reaction conditions. Moreover, we planned to design and synthesize substrates bearing multiple pyridylic sites to explore the regioselectivity of the method.

2.2.1 Optimization of reaction conditions for the synthesis of alkylidene dihydropyridine.

At this point, we did not know which of the two steps was low-yielding so we decided to quantify the alkylidene dihydropyridine intermediate formed in the first part of the synthesis. Quantitative NMR spectroscopy was employed as the intermediate was found to be sensitive to silica during flash chromatography purification. Using 1,4-bis(trichloromethyl)benzene as an internal standard, the yield of the first step was 61% (Entry 1, Table 1). As the isolated yield of allylation product over two steps was 50%, we inferred that the decarboxylative allylation had to be relatively high-yielding.

Table 1. Optimization of reaction conditions for the synthesis of alkylidene dihydropyridine.

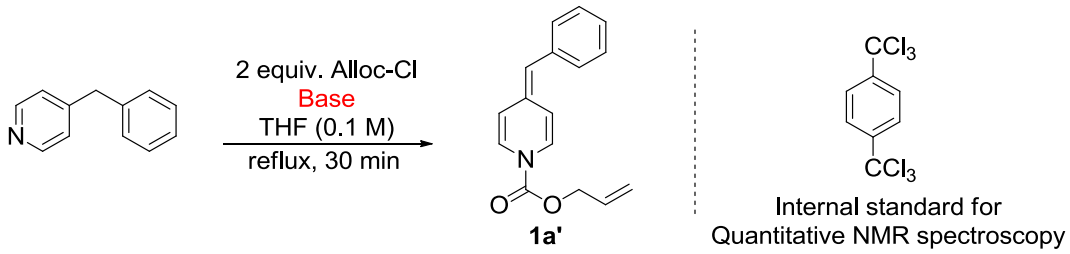

Entry	Base	Equiv.	Isolation Procedure	Q-NMR Yield
1	Triethylamine	1	Salt filtration (trituration)	61 %
2	Triethylamine	1	Water workup	62 %
3	Triethylamine	2	Salt filtration	77 %
4	DBU	2	Phosphate buffer workup (pH = 5.5)	96 %

To maximize the yield of the dearomatized intermediate, we doubled the amount of base and Alloc-Cl in the reaction mixture. By doing so, we could increase the yield of the intermediate to 77% (Table 1, Entry 3). Instead of filtering the ammonium salt, we tried removing it by a water work-up and interestingly, the yield did not change, indicating that the intermediate was stable to treatment with brine (Table 1, Entry 2). To increase the isolated yield further, we treated the substrate with two equivalents of 1,8- diazabicyclo[5.4.0]undec-7-ene (DBU), which is a moderately strong base (pK_a = 16). Excess DBU was removed by treatment with a mildly acidic phosphate buffer (pH = 5.5) and the yield of the de-aromatized intermediate was found to be 96% (Table 1, Entry 4). With the same $Pd(OAc)_2/PPh_3$ catalyst system for decarboxylative allylation, we were pleased to find an increase of 28% (from 50 to 78%) in the yield of the allylation product (**1a**) over two steps. Removal of excess base and the ammonium salt was necessary after the de-aromatization step as their presence appeared to complicate the subsequent decarboxylative

allylation by presenting a complex mixture of pyridines. The ammonium salt could potentially serve a proton source for the pyridylic anion generated during the decarboxylative allylation step, thereby resulting in the formation of starting pyridine **1**. In the presence of excess base, Pd-catalyzed decarboxylative allylation is known to afford a mixture of mono- and bis-allylated products, which can be difficult of separate.[72]

2.2.2 Ligand screen for Pd-catalyzed decarboxylative allylation.

The dearomatized intermediate (**1a'**) of 4-benzylpyridine is expected to undergo outer-sphere reductive elimination in the Pd-catalyzed decarboxylative allylation reaction, according to a recent report by Walsh.[59] Presumably, this may not be true for other 4-alkylpyridines with an sp^3 center at the position *beta* to the pyridine ring (e.g. **2** in Scheme 17), as they are expected to behave as 'hard' nucleophiles exhibiting inner-sphere reductive elimination *via* alkylpalladium(II) intermediates (Complex II, Scheme 17). Metal complexes that contain β-hydrogen-bearing alkyl ligands are prone to decomposition through a competing β-hydride elimination pathway, which affords an olefin and a metal hydride complex (**2b** and complex III, scheme 17). β-Hydride elimination necessitates the formation of a metal-carbon bond. Moreover, M-C_α and C_β-H bonds must be able to align with each other in a syn co-planar fashion for the β-hydride elimination to occur. With 4-benzylpyridine as the substrate, the catalyst was forced to undergo reductive elimination to afford the allylation product **1a** exclusively, as there is no β-hydrogen to abstract. Therefore, we chose to use the dearomatized intermediate (**2a'**) of 4-(2-phenylethyl)pyridine as the substrate for ligand screening, as it potentially allowed for β-hydride elimination (**2b**) along with reductive elimination (**2a**). By providing accessibility for β-hydride elimination, efforts were made towards gaining insights into the nature of the reductive elimination step and, developing a method that allows allylation of 4-alkylpyridines in excellent yields.

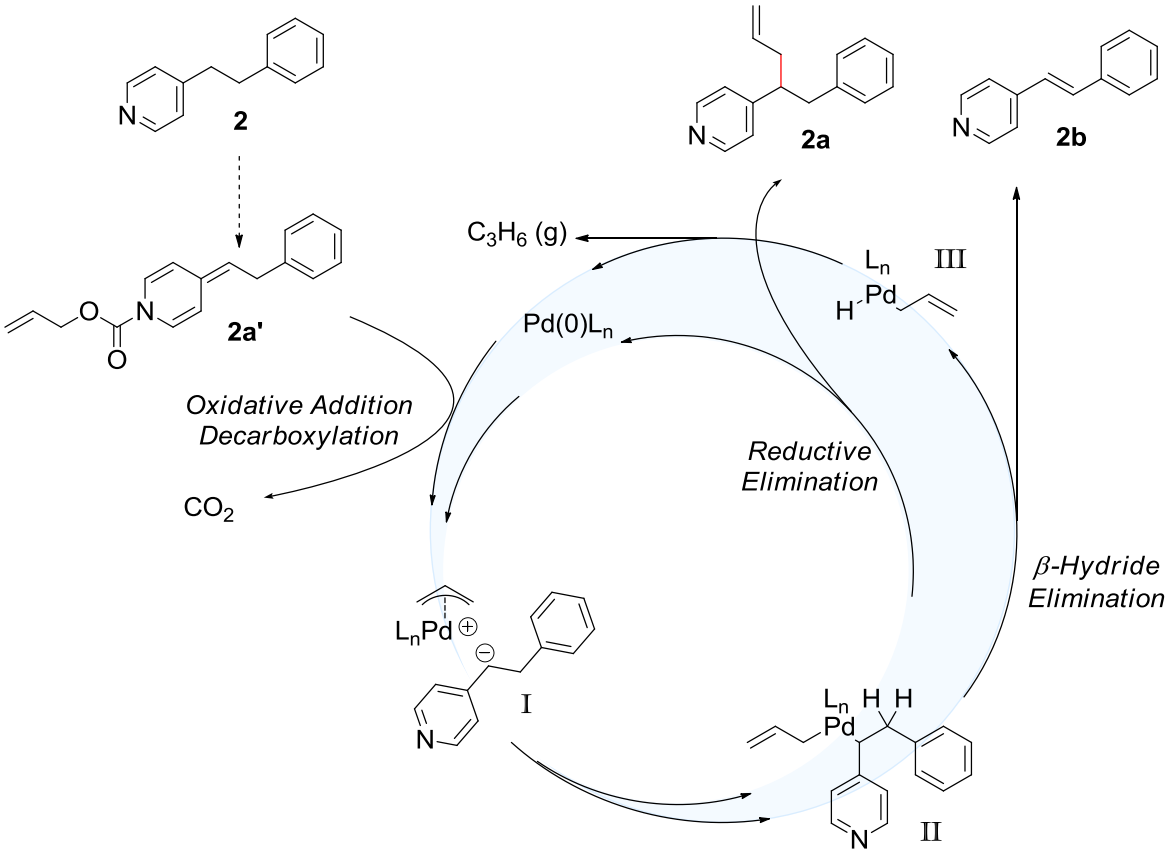

Scheme 17: Expected mechanism of Pd-catalyzed decarboxylative allylation with 'hard' 4-alkylpyridines.

In order to identify a catalyst system that affords high yield for the desired allylation product, we planned to screen a variety of mono and bidentate phosphine ligands. Generally, for phosphine-assisted cycles, the catalytic species responsible for oxidative addition has 2 monodentate or 1 bidentate ligand in the coordination sphere, making it a 14-electron Pd(0) complex.[73] To obtain a consistent 2 :1 ratio of P:Pd in the reaction mixture, we decided to employ $Pd(dba)_2$, which is a source of Pd(0) and does not need to be activated by reduction with phosphine. To expedite the ligand screening process, we synthesized the dihydropyridine intermediate (**2a'**) on a gram scale and upon isolation with a mildly acidic buffer (pH = 5.5), we divided it into fractions of known mass. Each fraction was subjected to a unique ligand to screen a large variety of ligands in an efficient manner. The yields of the allylation (**2a**) and elimination

products (**2b**) were determined by NMR spectroscopic analysis of the crude mixture and are reported over two steps in Table 2.

Table 2. Ligand screen data for the Pd-catalyzed decarboxylative allylation.[a,b]

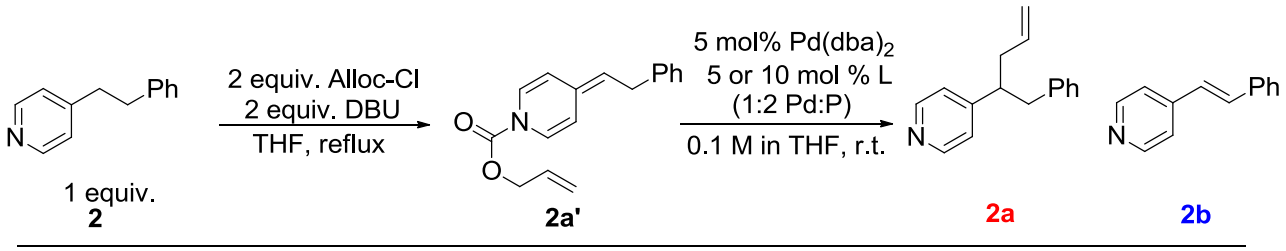

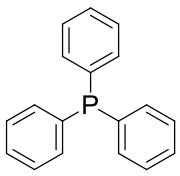

1. 73%, 0%

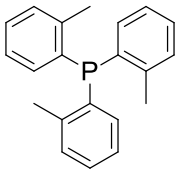

2. 23%, 0%

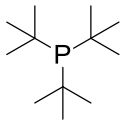

3. 24%, 13%[c]

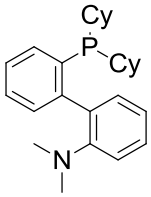

4. 48%, 0%

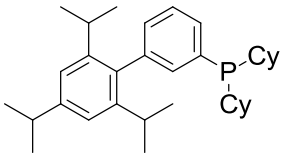

5. 71%, 0%

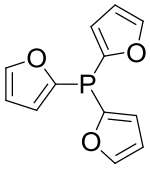

6. 48%, 17%

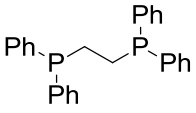

7. 31%, 15%

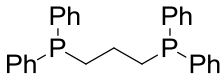

8. 22%, 41%

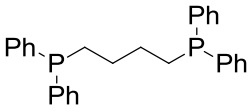

9. 42%, 0%

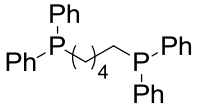

10. 63%, 0%

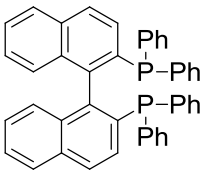

11. 56%, 0%

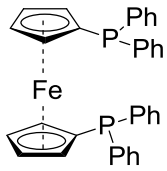

12. 68%, 0%

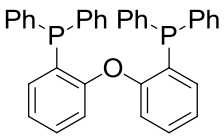

13. 73%, 0%

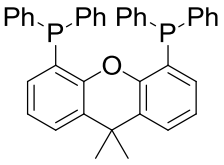

14. 75%, 0%

(a) All reactions were conducted under an inert atmosphere of argon
(b) In the absence of a phosphine ligand, **2b** was observed exclusively in 25% yield.
(c) Used as tetrafluoroborate phosphonium salt with 20% $CsCO_3$

The ligand screen data show an interesting correlation between the nature of the ligand and its influence on the reactivity of the catalyst. For all monodentate ligands tested, the yield appears to be a cumulative effect of both steric and electronic properties of the ligand. Highly electron-rich ligands with wide cone angles such as tri(o-tolyl)phosphine and tri(*tert*-butyl)phosphine afforded the desired allylation products in low yields (ligand **2**, 23% and Ligand **3**, 24%). It is known that electron-rich phosphines stabilize the metal in its lower oxidation state and could potentially disfavor reductive elimination.[13] Triphenylphosphine gave the best yield (ligand **1**, 73%) of all the monodentate ligands tested. Buchwald ligands, DavePhos and XPhos (ligand **4**, 48% and **5**, 71%) also gave substantial yields, possibly due to their high steric bulk.

Bidentate phosphines are known to stabilize the catalyst due to the chelating effect. Over the last few decades, the effect of the P-M-P bite angle on the behavior of the catalyst has been extensively studied in many reactions.[74] van Leeuwan in his review has highlighted the positive effect of large bite angles on the catalytic turnover in allylic alkylations, especially when using soft nucleophiles, as they tend to attack the metal-bound allylic moiety instead of the metal center.[15] Bidentate ligands with small bite angles, namely dpp-ethane (Ligand **7**, 31%) and dpp-propane (Ligand **8**, 22%) gave low yields for the desired allylation product, and generated a significant amounts of the dehydrogenation product (**2b**). An increase in the yield occurred with dpp-pentane (ligand **10,** 63%), BINAP (ligand **11,** 56%) and dppf (ligand **12,** 68%), as they have relatively wider bite angles. The yield of the allylation product increased to 73 and 75% with DPEPhos (ligand **13**) and XantPhos (ligand **14**) respectively, which is consistent with the trend as they have the widest bite angles of all the ligands tested. The appearance of the dehydrogenation product (**2b**) with ligands **3**, **6**, **7** and **8** suggests that a competing β-hydride elimination pathway is indeed taking place. Since a prerequisite for β-hydride elimination is the formation of a metal-carbon bond, the formation of **2b** is indicative of an inner-sphere interaction between the pyridylic anion and the Pd catalyst in our reaction.

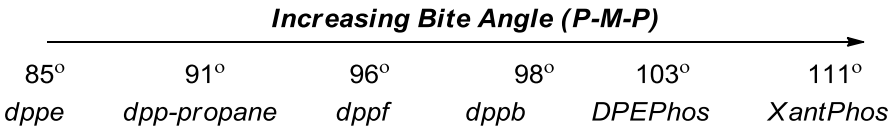

Figure 2. Bite angles (P-M-P) of some bidentate phosphines with $Pd(dba)_2$ as reported by van Leeuwen.[74]

Bidentate ligands with large bite angles consistently provided the allylation product in high yields but none was substantially superior to triphenylphosphine. However, we chose XantPhos for future reaction development as bidentate phosphines should exhibit greater stability than monodentate phosphines. In fact, XantPhos and other closely related phosphines have gained tremendous popularity as highly effective ligands for transition metal-catalyzed allylation reactions.[75] Since the yields obtained in the ligand screen were based on quantitative ^{1}H NMR spectroscopy, the allylation reaction of **2** was repeated in an isolated experiment using the $Pd(dba)_2$-XantPhos catalyst system. The resulting product **2a** was purified using flash chromatography and isolated in 78% yield. We hypothesized that the yield could be further improved by eliminating the work-up steps after both the dihydropyridine formation and allylation reaction. Therefore, we implemented the following adjustments that provided the allylation product **2a** in 92% isolated yield using 1 mol% catalyst loading (Eq. 16):

1) Three equivalents of Et_3N were used in the dihydropyridine formation. This allowed a) the full conversion of the starting pyridine **2** to the dihydropyridine intermediate **2a′**, and b) isolation of **2a′** by trituration with diethyl ether thereby avoiding the buffer workup previously required to remove DBU.
2) No work-up was done after the allylation step; the reaction mixture was concentrated and directly purified using flash chromatography

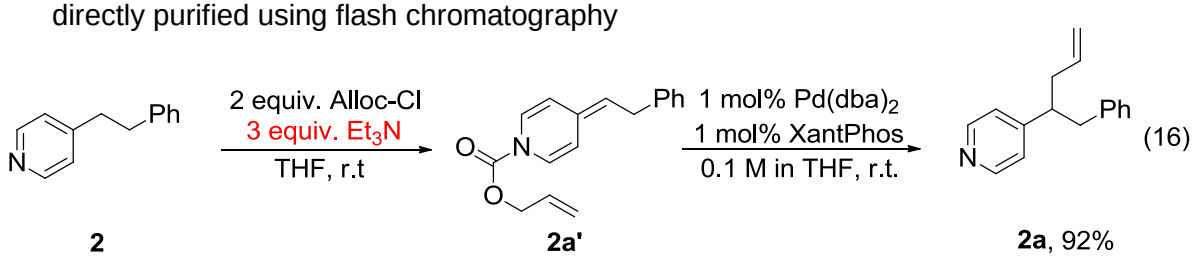

2.3 Substrate Synthesis.

2.3.1 General strategies for the synthesis of 4-alkylpyridines.

Having identified the optimal conditions for pyridylic allylation, we sought to explore the functional group compatibility and its limitations. Substrates for the proposed reaction are either commercially available or can be prepared from readily available reagents in one or two steps. We planned to create a collection of substrates from picoline (4-methylpyridine) as it can be deprotonated by lithium diisopropylamide (LDA) and upon treatment with a suitable bromo electrophile the desired substrate can be obtained (Scheme 18). This strategy proved successful in affording several 4-alkylpydirine derivatives, each bearing a unique functional group. Benzyl (**9**), alkynyl (**5**), nitrile (**7**) and acetal (**8**) derivatives etc., are some of the synthetically-useful substrates that were obtained from the alkylation of 4-picoline.

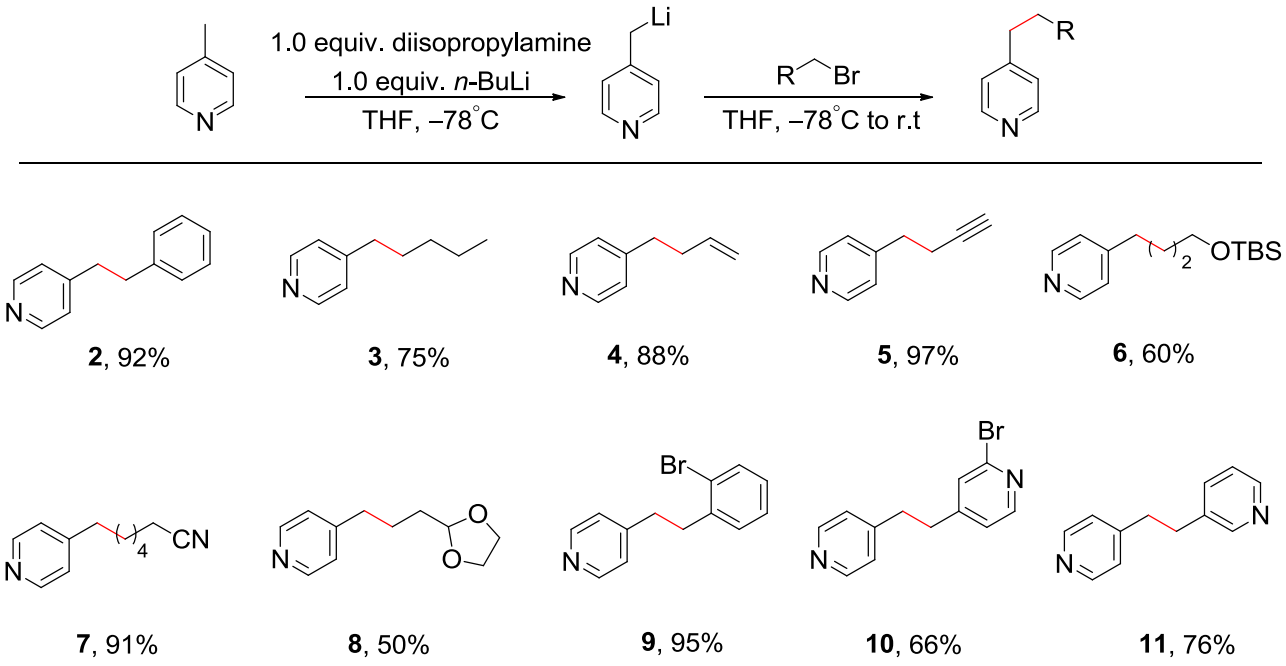

Scheme 18. Synthesis of 4-alkylpyridines from 4-methylpyridine

One major limitation of the methods reported by the Trost,[76,57] Walsh[59] and You[61] groups for pyridylic allylation is the use of a strong base to generate the required pyridylic nucleophile. Consequently, functional groups (e.g. protic groups and electrophiles) that would quench strongly basic organometallic reagents are incompatible with their methods. Although Sawamura's base-free method enables allylation in the presence of more acidic α-carbonyl C-H bonds (Eq. 13), it is limited to functionalization at the 2-pyridylic site. Realizing the value of carbonyl groups as useful synthetic handles, we considered synthesizing 4-alkylpyridine derivatives, bearing aldehyde, ketone and ester functional groups, to explore their compatibility with the optimized reaction conditions. Deprotection of acetal **8** with 1M HCl conveniently afforded the required aldehyde substrate (**12**, Eq. 17)

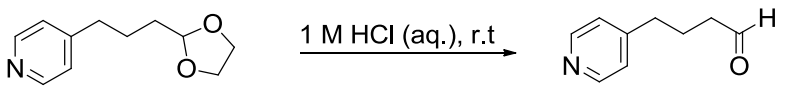

8 **12**, 65% (17)

The alkylation strategy illustrated in Scheme 18 was attempted to synthesize the ester and ketone substrates. However, when the 4-picoline anion was subjected to the appropriate α-bromo carbonyl electrophiles, a complex mixture of products was observed. Presumably, side-products arising from the competing reaction i.e. 1,2-addition of the nucleophile to carbonyl group, was complicating the synthesis. Therefore, ketone **13** (Eq. 18) and ester **14** (Eq. 19) were prepared by the Horner-Wadsworth-Emmons reaction[77] between 4-pyridinecarboxaldeyhde and the appropriate phosphonate, followed by transfer hydrogenation of *trans*-alkenes **13.1** and **14.1** using Pd on charcoal as catalyst. The observed *trans* selectivity for alkene formation in Horner-Wadsworth-Emmons reactions is well established.[78]

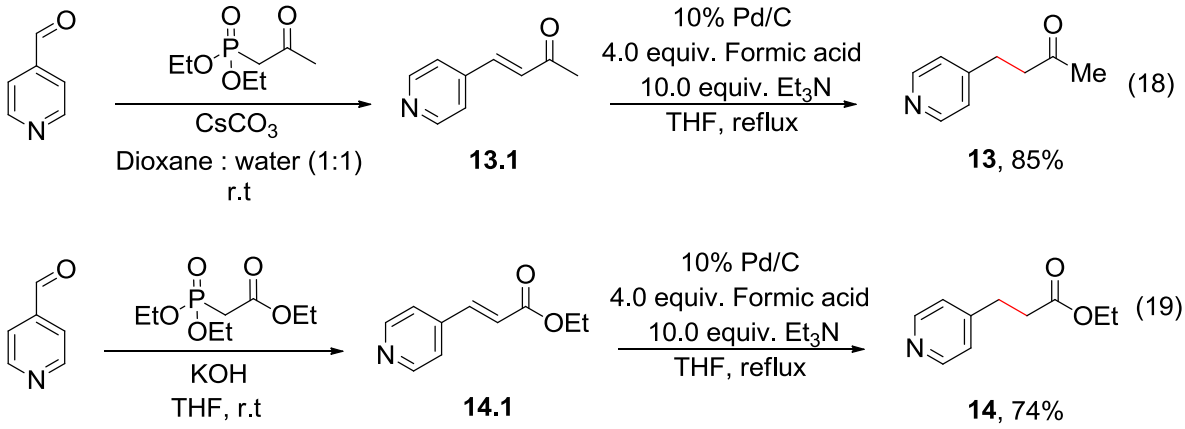

Treatment of 2 and 4-vinylpyridines with Lewis or Bronsted acids has been shown to activate the polarized alkene moiety towards conjugate addition with heteroatom nucleophiles.[79] Therefore, sulfone **15** (Eq. 20) and tertiary amine **16** (Eq. 21) derivatives of 4-alkylpyridine were synthesized by the conjugate addition of appropriate nucleophiles on 4-vinylpyridine under acidic conditions in quantitative yields.

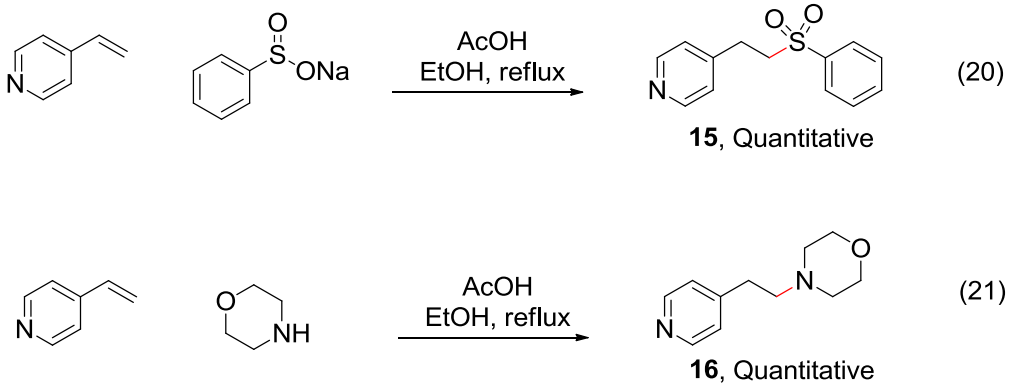

2.3.2 Synthesis of 4-alkylpyridines bearing C3 substituents.

To synthesize 4-alkylpyridines derivatives bearing substituents at the 3-position of the pyridine ring, Knochel's method[80] for direct alkylation of 3-substituted pyridines was considered. The reaction involves activation of a 3-subsitituted pyridine (preferably an electron-withdrawing group) with BF_3, followed by addition of a suitable alkylmagnesium bromide at the 4-position. The immediate product of addition is a 1,4-dihydropyridine derivative, that is then oxidized to the corresponding pyridine by chloranil (Eq. 22). The use of LiCl-activated *n*-butylmagnesium bromide afforded the 4-alkylpyridine derivatives of ethyl nicotinate (**17**) and 3-cyanopyridine (**18**) in good yields. In these reactions, LiCl serves to enhance the nucleophilic character of the Grignard reagent through disaggregation of the organometallic clusters, as reported by Knochel.[81] The cyano group in substrate **18** was conveniently transformed to the *tert*-butyl amide (**19**) by a Ritter reaction with *tert*-butyl acetate in the presence of conc. H_2SO_4 (Eq. 23). Substrates **17**, **18** and **19** contain useful synthetic handles, namely ester, nitrile and secondary amide groups, respectively, that can be exploited for further functionalization of the pyridines into well decorated structures.

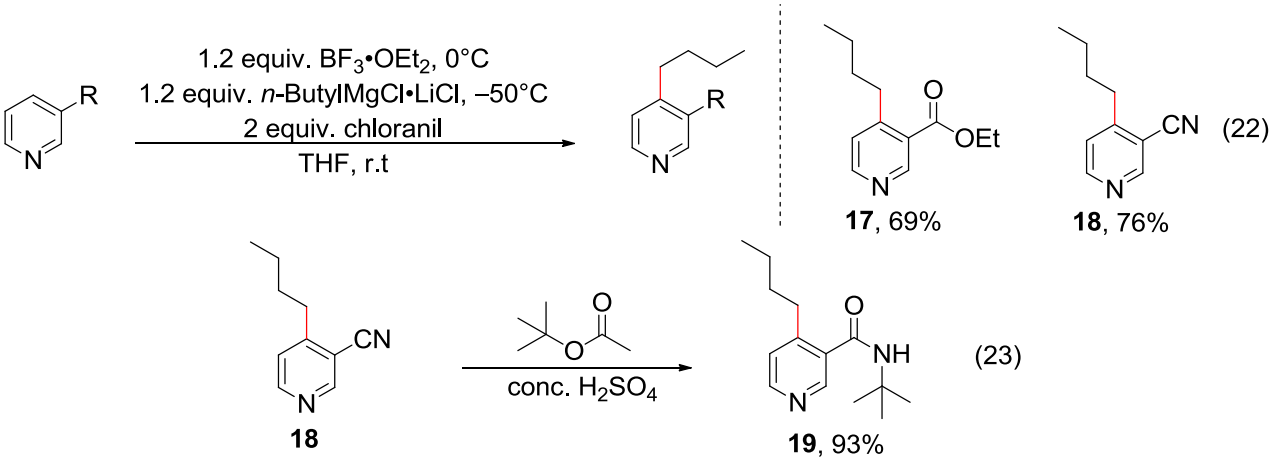

Direct alkylation of 3-phenylpyridine using Knochel's method to synthesize substrate **20** bearing a phenyl at the 3-position failed, presumably because the phenyl group is not sufficiently electron-withdrawing. Alternatively, a three-step procedure was employed (Scheme 19). In the

first step, 3-iodo-4-methylpyridine (**20.1**) was synthesized by diazotization and subsequent iodination of 3-amino-4-methylpyridine (Sandmeyer-type reaction). Crude **20.1** was subjected to the Suzuki cross-coupling reaction with phenylboronic acid to afford 3-phenyl-4-methylpyridine (**20.2**) in 66% yield over two steps. Substrate **20** was obtained by deprotonation of **20.2** with LDA and treatment with 1-bromopropane.

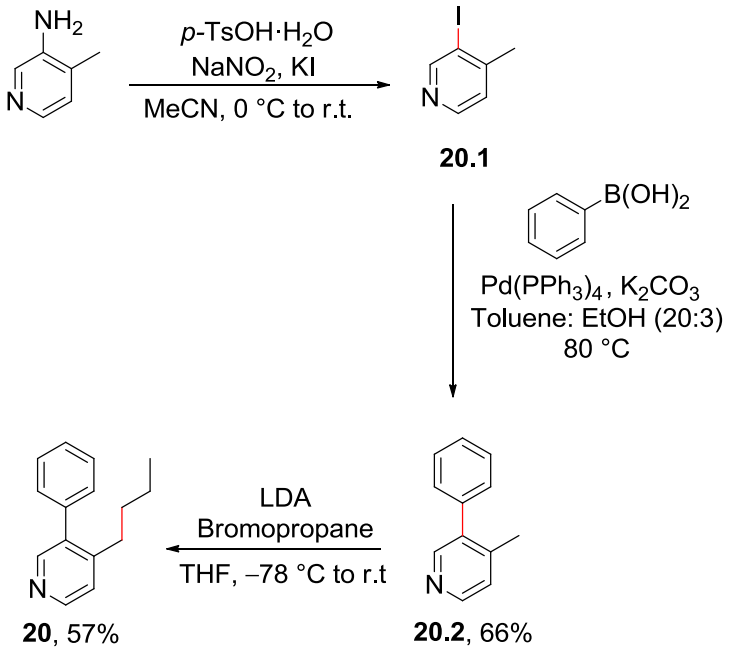

Scheme 19. Multistep synthesis of substrate **20**

Furthermore, substrate **21** containing a carbamate functional group at the 3-postion was synthesized by Boc protection of 3-amino-4-methylpyridine. Subsequent alkylation of the C4 methyl substituent by treatment with *n*-BuLi (2 equivalents) and benzyl bromide delivered **21** in 54% yield (Scheme 20).

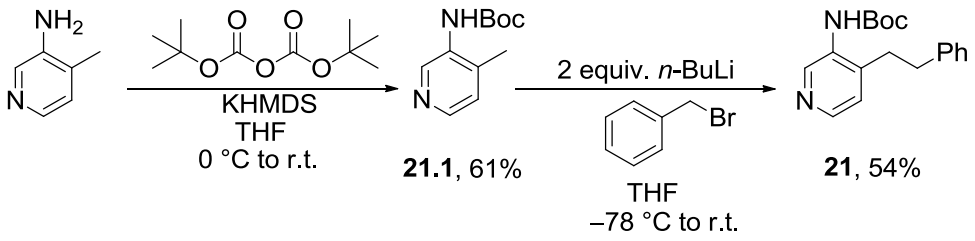

Scheme 20. Synthesis of substrate **21**

2.3.3 Synthesis of substrates bearing 2- and 4-pyridylic positions.

Previously-developed methods for pyridylic allylation exploited the coordination of Lewis acids (e.g. $BF_3{\cdot}OEt_2$) to significantly lower the acidity at the 2-pyridylic site. Upon deprotonation with a suitable base, the pyridylic anion generated by this strategy exhibits exceptional regioselectivity for allylation at the 2-pyridylic site (Eq. 9). Moreover, the proximity of the ring nitrogen in 2-alkylpyridines to the 2-pyridylic site has been exploited by Tunge and coworkers to initiate [3,3]-sigmatropic rearrangements via N-allylpyridinium intermediates, in their regio- and diastereoselective decarboxylative allylation method (Scheme 12). Clearly, these strategies would fail to install an allyl group at the 4-pyridylic position in the presence of an enolizable alkyl substituent at the 2-position. To our knowledge, there are no methods for the site selective transition metal-catalyzed allylation of 4-alkylpyridines. Therefore, efforts were made to design and synthesize substrates bearing 2- and 4-pyridylic positions to investigate the regioselectivity of our method. The two-step synthesis of substrate **22** is illustrated in Scheme 21. In the first step, treatment of 2-cyanopyridine with the 4-picoline anion delivered ketone **22.1** upon acid hydrolysis. The Wolff-Kishner reduction was employed to reduce the ketone down to the alkane level, which afforded substrate **22** in 90% yield over the two steps.

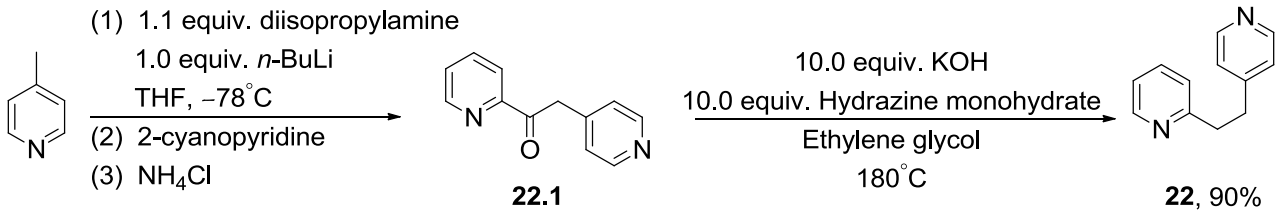

Scheme 21. Synthesis of substrate **22**

A similar substrate (**23**) containing two unique pyridylic sites connected *via* a phenyl linker, was also synthesized. The synthesis of **23** began with the alkylation of 4-picoline to afford (2-phenethyl)pyridine derivative **23.1** in 65% yield (Scheme 22). Reduction of the ester with lithium borohydride ($LiBH_4$) to the alcohol (**23.2**), followed by treatment with triphenylphosphine and bromine (in the absence of a base), afforded 4-alkylpyridine derivative **23.3** as a hydrobromide salt. Alkylation of **23.3** with the 2-picoline anion resulted in the formation of **23** in good yield.

Note: Synthesis of substrate **23** was designed and conducted by Nour Wasfy from the Orellana lab.

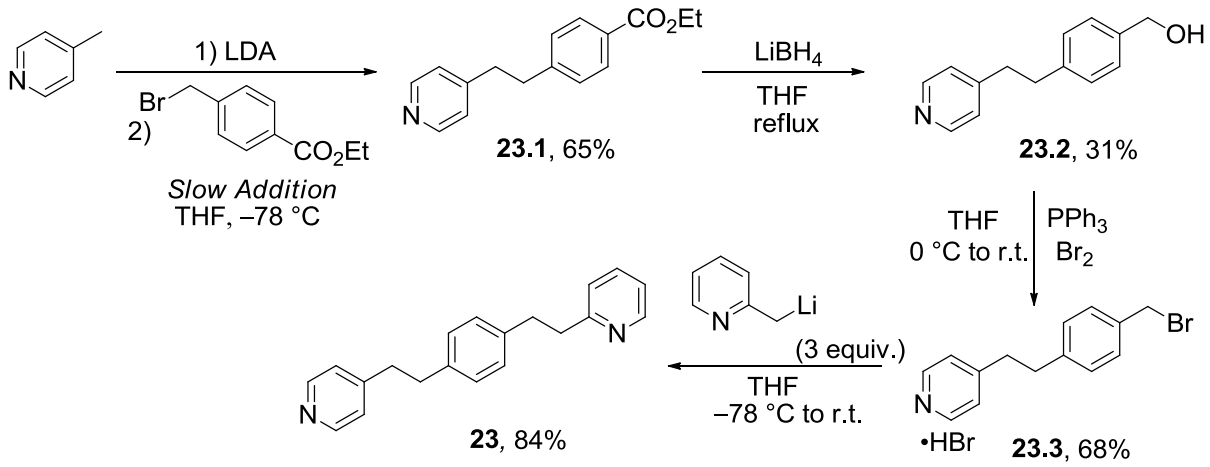

Scheme 22. Synthesis of substrate **23**

Lastly, in order to synthesize 2,4-dialkylpyridine **24,** we alkylated 2-bromo-4-methylpyridine using LDA and bromoethane to afford 2-bromo-4-propylpyridine (**24.1**) in 58%

yield. The Pd-catalyzed Kumada coupling of **24.1** with ethylmagnesium bromide delivered **24** in nearly quantitative yield (Scheme 23).

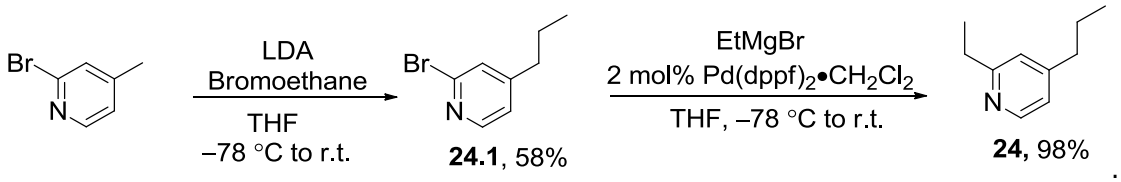

Scheme 23. Synthesis of substrate **24**

2.4 Substrate scope of the method.

2.4.1. Scope of mono-substituted 4-alkylpyridine derivatives.

We were delighted to learn that the method enjoys wide functional group tolerance as suggested by allylation products of compatible substrates shown in Table 3. To explore the possibility of competing side reactions such as β-hydride elimination, the substrates under investigation have a methylene group adjacent to the pyridylic site (except 4-benzylpyridine). Interestingly, the elimination product was not observed with the optimized reaction conditions for any substrate. 4-Benzyl and 4-pentylpyridine provide the allylation products in good yields (Entry 1, 93% and Entry 3, 78%). Substrates bearing benzylic (Entry 10, 84%), allylic (Entry 5, 72%) and propargylic (Entry 6, 63%) sites were found to be compatible and the corresponding allylation products were recovered in good yields. For **9**, no competing side-product from oxidative addition across C-Br bond was observed. A quaternary pyridylic site can be generated in excellent yield (Entry 4, 95%). The reaction tolerates silyl-protected alcohols and acetals (Entry 7, 84% and Entry 9, 73%). These protecting groups will not survive strong Lewis acids like $BF_3.OEt_2$ and therefore, are incompatible with the methods developed by Trost,[76] Walsh[82] and You.[61] This reaction also tolerates tertiary amines (Entry 14, 77%) and a range of substrates bearing electrophilic functional

groups with enolizable α-protons namely, nitriles (Entry 8, 78%), ketones (Entry 12, 71%), esters (Entry 13,90%), and even aldehydes (Entry 11, 61%).

Table 3. Substrate scope of mono-substituted 4-alkylpyridine derivatives

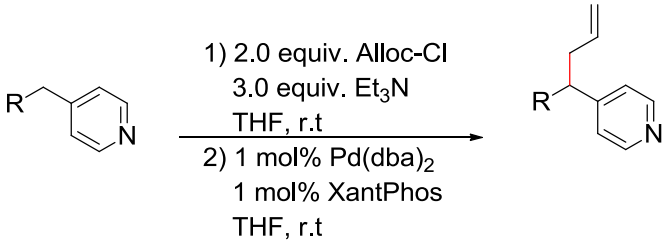

Entry	Substrate	Product	Yield
1	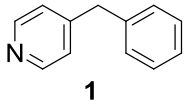 **1**	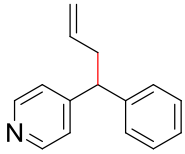 **1a**	93%
2	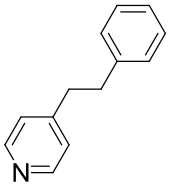 **2**	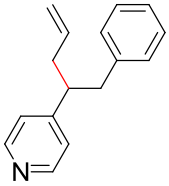 **2a**	92%
3	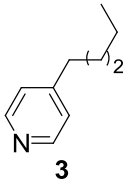 **3**	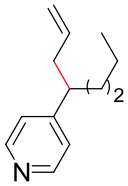 **3a**	78%
4	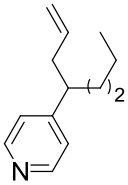 **3a**	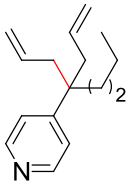 **3aa**	95%

5	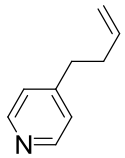 **4**	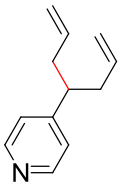 **4a**	72%
6	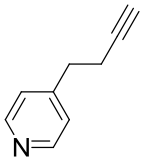 **5**	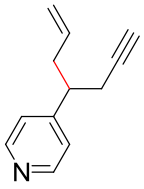 **5a**	63%
7	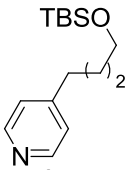 **6**	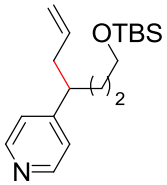 **6a**	84%
8	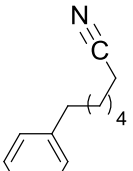 **7**	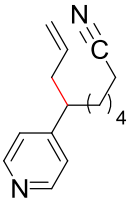 **7a**	78%
9	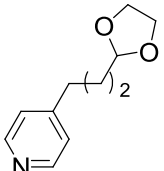 **8**	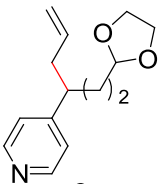 **8a**	73%
10	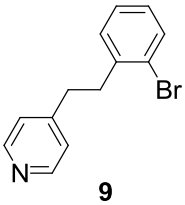 **9**	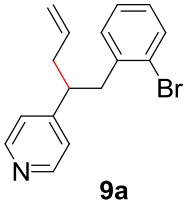 **9a**	84%

11	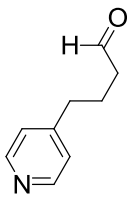 **12**	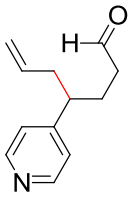 **12a**	61%
12	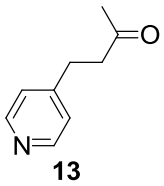 **13**	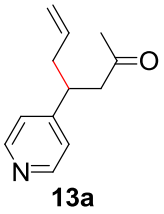 **13a**	71%
13	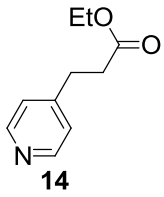 **14**	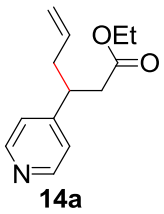 **14a**	90%
14	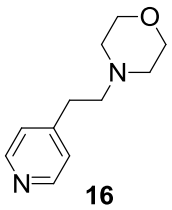 **16**	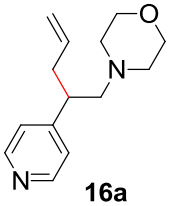 **16a**	77%

Substrates **15** containing a sulfone functional group was successful in transforming to the corresponding enolized intermediate. However, when treated with the Pd catalyst, the alkylidene dihydropyridine intermediate failed to furnish the desired allylation product. Instead, the NMR spectroscopic analysis of the crude mixture revealed the formation of equimolar amounts of 4-vinylpyridine and the product of allylation at the sulfur center (**15a**, Eq.22).

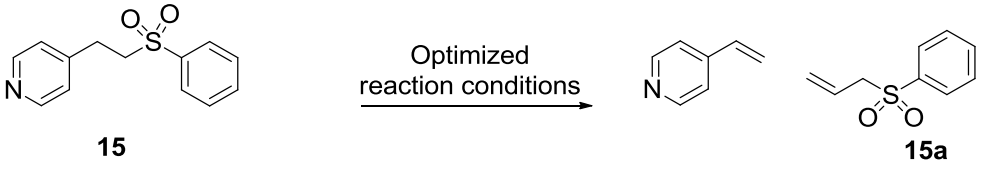

15 **15a** (22)

This reactivity pattern is attributed to the β-position of the electron-withdrawing sulfur substituent with respect to the pyridine ring. According to the proposed mechanism of pyridylic allylation, the treatment of the enolized intermediate of substrate **15** with Pd(0) generates an anion at the pyridylic site. Presumably, the electron-pair from the pyridylic site moves to the β-carbon to form a double bond, eliminating the sulfinate ion in the process, as established for $E1_{cb}$ elimination reactions. The attack of the sulfinate ion on the π-allylpalladium complex can result in the formation of the observed allylation product (Scheme 24).

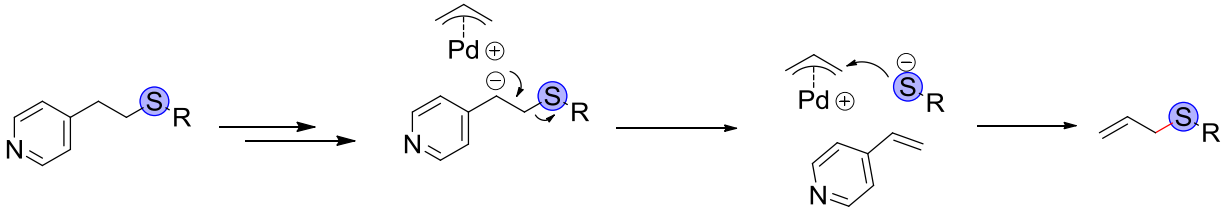

Scheme 24: Proposed mechanism for the observed products with substrate **15**

2.4.2 Scope of 4-alkylpyridine derivatives bearing C3 substituents.

Encouraged by our success with monosubstituted pyridines, we began to investigate the scope of 4-alkylpyridines bearing substituents at the 3-postion on the ring (Table 4). Substrate **20** bearing a phenyl group at the 3-position afforded the expected allylation product in good yield (Entry 4). 4-Alkylpyridines with functional groups at the 3-position, such as nitrile (Entry 2), amide (Entry 3), ester (Entry 1) and carbamate (Entry 5) also provided the desired products. It is worth mentioning that the amide (**19**) and carbamate (**21**) derivatives of 4-alkylpyridine contain acidic C-H bonds and are prone to deprotonation with the methods developed by Trost, Walsh and You, potentially leading to side-products. To our delight, the reaction afforded the desired allylation products (**19a** and **21a**) in good yields.

Table 4: Substrate scope of the 4-alkylpyridine derivatives bearing C3 substituents.

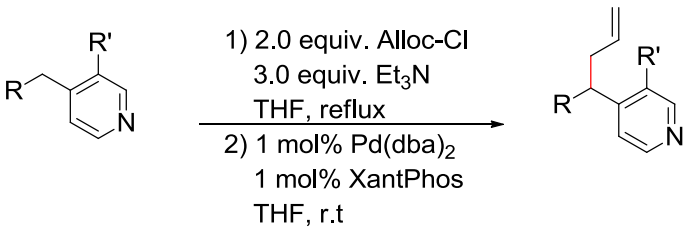

Entry	Substrate	Product	Yield
1	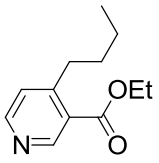 **17**	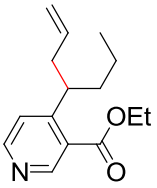 **17a**	90%
2[a]	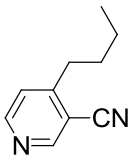 **18**	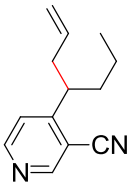 **18a**	30%
3	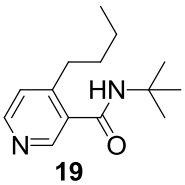 **19**	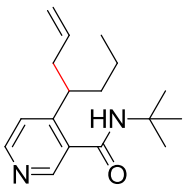 **19a**	73%
4[a,b]	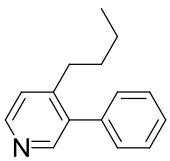 **20**	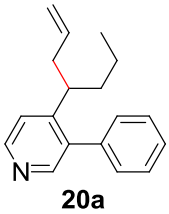 **20a**	88%
5[a,b]	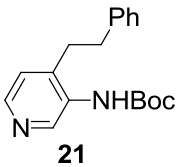 **21**	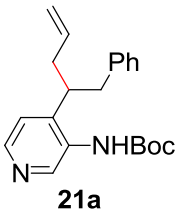 **21a**	65%

[a] 0.5% $Pd_2(dba)_3 \cdot CHCl_3$ was used instead of $Pd(dba)_2$

[b] Formation of the alkylidene dihydropyridine intermediates occurred at room temperature.

Substrates **17**, **18** and **19** bearing electron-withdrawing groups at the 3-postion, were relatively slower to convert to their respective enolized intermediates at room temperature and therefore, needed to be heated to reflux in THF for full conversion. Moreover, when the C3 substituent was a cyano group (**18**), only 50% conversion (by NMR spectroscopy) to the de-aromatized intermediate was observed in refluxing THF overnight and the product **18a** was recovered with an overall isolated yield of 30%. The nucleophilic ability, a property that describes the kinetic aspects of substitution reactions, is generally accepted to be in a good correlation with the basicity.[83] Therefore, the observed decline in nucleophilicity with pyridines bearing electron-withdrawing substituents, can be rationalized based on the pK_a values of the corresponding pyridine derivatives (Table 5). The pK_a of pyridinium species for 3-cyanopyridine (Entry 2) is 2 pK_a units lower than the corresponding amide (Entry 4) and ester (Entry 3) derivatives. Therefore, the ring nitrogen in 3-cyano pyridine is expected to be poorly nucleophilic leading to sluggish reactivity. In order to increase the yield of the dearomatized intermediate of **18**, the use of DMAP as a catalyst was considered. DMAP serves as excellent acyl transfer agent and is commonly employed to accelerate the formation of amides in DCC coupling reactions. Unfortunately, this attempt failed to achieve any fruitful results.

Table 5: Experimental pK_a of various 3-substituted pyridines

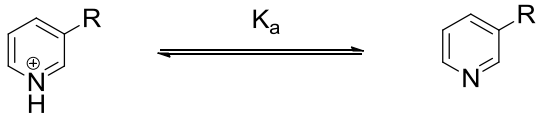

Entry	R	Experimental pK_a of pyridinium in aqueous solution[84,85]
1	-H	5.30
2	-CN	1.30-1.45
3	$-CO_2Et$	3.40
4	$-CO_2NH_2$	3.35
5	-Ph	4.87
6	-Me	5.68

2.4.3 Scope of systems with multiple pyridylic sites.

Interestingly, 2-alkylpyridine derivatives were found to be incompatible with the optimized reaction conditions as they could be not be converted to their respective dihydropyridine intermediates (Scheme 25). Moreover, 2,4-dialkylpyridine **24** failed to undergo enolization at either pyridylic sites. 2-Benzylpyridine (**25**) and ethyl nicotinate derivative **26** bearing relatively more acidic pyridylic sites also could not be transformed to the corresponding alkylidene dihydropyridine derivatives.

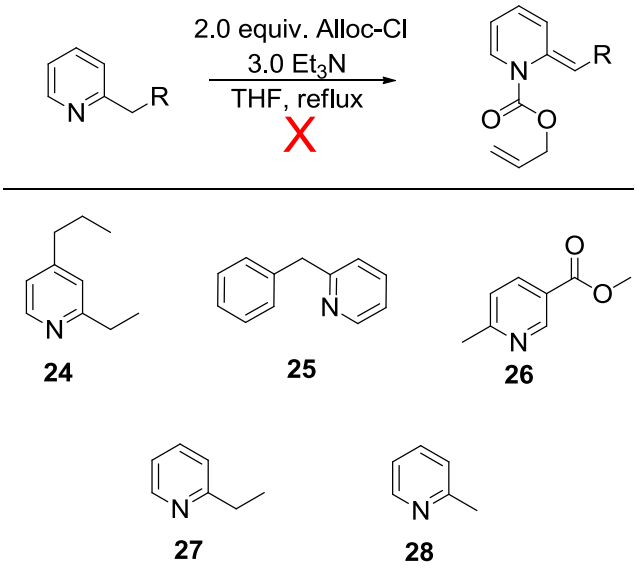

Scheme 25: Substrates found incompatible with the optimized conditions for de-aromatization.

In order to better understand the underlying problem, we conducted control experiments with substrates **24**, **27** and **28**. They were treated with allyl chloroformate in the absence of a base. Unfortunately, the 1-acylpyridinium species was not formed in any case. We reasoned that steric hindrance caused by the substituent at the 2-postion on the ring, inhibited the nucleophilic attack on allyl chloroformate. This rationale for the observed behavior was confirmed when a substrate bearing 2- and 4-alkylpyridines (i.e. **22**) was subjected to the optimized conditions for de-aromatization. We learned that the 4-alkylpyridine fragment is enolized exclusively. However, the treatment of intermediate **22a′** with the $Pd(dba)_2$-XantPhos catalyst system, resulted in its decomposition. The Pd-catalyzed decarboxylative allylation of **22a′** failed to deliver the desired allylation product, perhaps due to interference from the 2-alkylpyridine fragment (see the 5-membered palladacycle intermediate in Eq. 23).

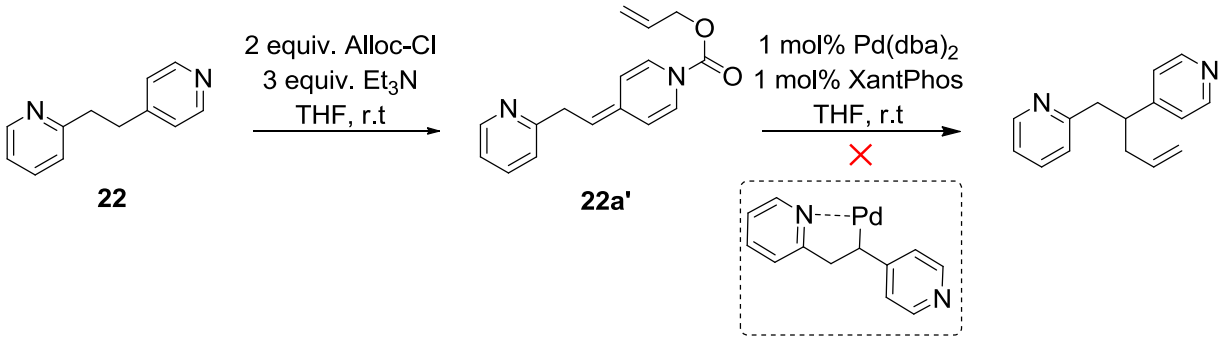

(23)

The inability of 2-alkylpyridine derivatives to form alkylidene dihydropyridine was unfortunate. However, we realized that this structure-based divergence could be exploited to achieve 4-selective allylation in systems with multiple pyridylic sites. To disengage the presumed interaction with the 2-alkylpyridine fragment, we modified substrate **23** to contain a phenyl spacer which isolates the two pyridines. For this purpose, substrate **23** was synthesized *via* a multi-step sequence illustrated in Scheme 21. To our delight, **23** was found to be compatible with our method, as it afforded the desired isomer of allylation product **23a** (functionalized at the 4-alkylpyridine moiety) exclusively in 74% yield over two steps (Figure 3).

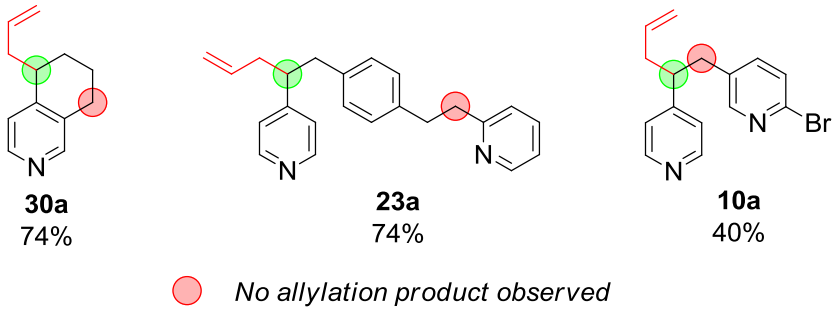

Figure 3. The allylation products of substrates bearing multiple pyridylic sites.

The complete structural characterization of **23a** was accomplished by various NMR experiments. The pyridylic tertiary center bearing the allyl group was indicated by a positive signal at δ = 47.2 ppm in the DEPT-135 spectrum. The correlation of the pyridylic tertiary center to the 4-substituted ring and the allyl moiety was established by thorough inspection of the 2D-COSY,

2D-HSQC and 2D-HMBC spectra of **23a**. Substrate **10** containing 3- and 4-alkylpyridines delivered allylation product **10a** in modest yield, likely due to interference by the bromo-substituent on the 3-alkylpyridine moiety. In this substrate, bromo-substituent serves to prevent the formation of 3-alkylpyridinium species. The formation of 3-alkylpyridinium species is permitted in the absence of a C2 blocking substituent as in 3-benzylpyridine (**29**). However, the 3-pyridylic site is not acidic enough to be deprotonated by a weak base like triethylamine to afford the corresponding dihydropyridine intermediate (Eq. 24). Therefore, tetraisoquinoline **30** bearing 3- and 4-alkyl substituents can be selectively allylated at the 4-postion in good yield (**30a**).

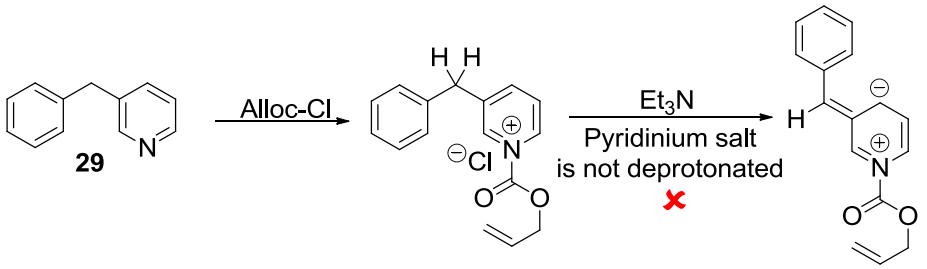

(24)

Similar to substrate **10** but without a C2 blocking substituent on the 3-alkylpyridine moiety, substrate **11** when subjected to allyl chloroformate in the presence of triethylamine undergoes de-aromatization at the 4-alkylpyridine moiety exclusively. However, the treatment of dihydropyridine intermediate **11a′** with Pd(0) catalyst affords a mixture of starting pyridine derivative **11** and the allylation product **11a**, based on the NMR spectroscopic analysis of the crude mixture (Eq. 25). Multiple attempts to separate the constituents of the mixture by flash chromatography failed. Consequently, the yield and identity of the expected product **11a** could not be determined.

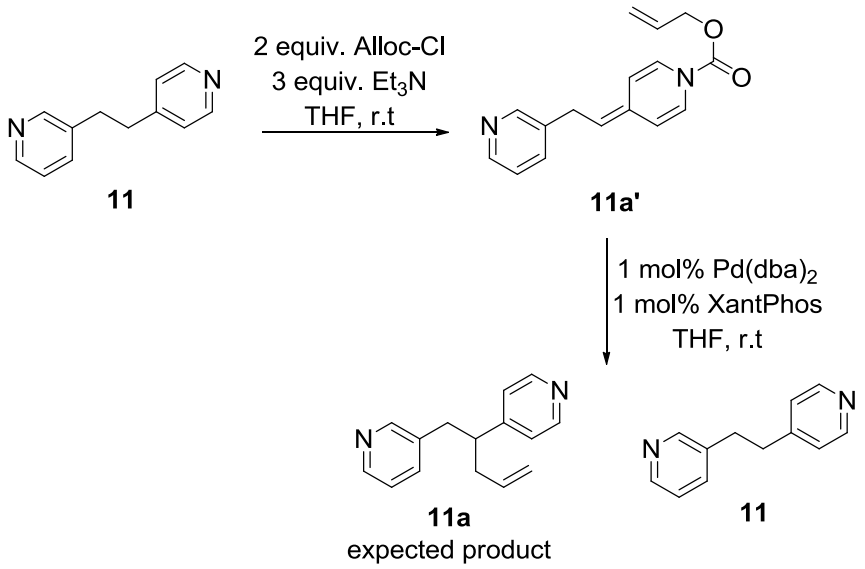

(25)

2.5 Conclusion.

In conclusion, we have developed an effective methodology for the Pd-catalyzed pyridylic allylation of 4-alkylpyridines. We learned that the use of allyl chloroformate in the presence of triethylamine serves as a convenient way to de-aromatize 4-alkylpyridine derivatives. The resulting alkylidene dihydropyridine intermediates can readily participate in a Pd-catalyzed decarboxylative allylation reaction to install an allyl group at the 4-pyridylic site. The mild reaction conditions of our method enable allylation of 4-alkylpyridines bearing functional groups that are sensitive to strong organometallic bases and Lewis acids (e.g. aldehydes, esters, acetals etc.) in good yields. Unfortunately, 2-alkylpyridines and 4-alkylpyridine derivatives that contain C2 substituents on the pyridine ring fail to form the 1-acylpyridinium species required for their enolization and therefore, are incompatible with our method. We have also exploited the reactivity differences of 2, 3- and 4-alkylpyridines towards pyridinium formation or deprotonation to carry out selective allylation of 4-alkylpyridines in systems with multiple pyridylic sites. We expect that this work will become a valuable tool for complex molecule synthesis and medicinal chemistry.

Chapter 3: Experimental

3.1 General Experimental.

All reactions were conducted in flame- or oven-dried glassware under an atmosphere of argon using freshly distilled solvents unless specified otherwise. Dichloromethane (DCM), and toluene were distilled from CaH_2 prior to use. Tetrahydrofuran (THF) was distilled from sodium/benzophenone. Commercial reagents were used as received. Thin-layer chromatography was performed on SiliCycle® silica gel 60 F254 plates. Visualization was carried out using UV light (254 nm) and/or $KMnO_4$, $(NH_4)_2Ce(NO_3)_6$, vanillin, or anisaldehyde solutions. Hexanes (ACS grade) and ethyl acetate (ACS grade) were used as received. Flash column chromatography[86] was carried out using SiliCycle® Silia*Flash*® silica gel (230-400 mesh, 40- 63 µ, 60 Å pore size). ^{1}H-NMR and ^{13}C-NMR spectra were recorded on a Bruker 400 AV, Bruker DRX 600 or Bruker 300 AV spectrometer in chloroform-d (99.8 % deuterated). Spectra recorded using chloroform were calibrated to 7.26 ppm ^{1}H and 77.00 ppm ^{13}C. ^{29}Si-NMR spectra were recorded on Bruker 300 AV spectrometer in chloroform-d (99.8 % deuterated) using TMS in chloroform-d as an external standard. Chemical shifts (δ) are reported in ppm and multiplicities are indicated by s (singlet), d (doublet), t (triplet), q (quartet), p (quintet), sext (sextet), td (triplet of doublets), tt (triplet of triplet) dd (doublet of doublets), dddd (doublet of doublet of doublet of doublets),[87] m (multiplet), br (broad). Coupling constants *J* are reported in Hertz (Hz). Infrared (IR) spectra were recorded as thin films (neat) using AlphaPlatinum ATR, Bruker, diamond crystal FT-IR instrument.

3.2 Preparation of Substrates: Procedures and Structural Data

Procedure 1: *Alkylation of 4-methylpyridine*

A flame-dried round-bottomed flask equipped with a stir bar was charged with freshly distilled diisopropylamine (1.1 equiv.) in THF and cooled to -78 °C. To this solution, *n*-BuLi (1.0 equiv., 1.6 M in hexanes) was added dropwise and the mixture was left to stir for 15 min to form LDA. A solution of 4-methylpyridine (1.0 equiv.) in THF was introduced at the same temperature. This deprotonated picoline was cannulated to a round-bottomed flask containing the suitable electrophile (1.0 equiv.) in THF. The reaction was kept at -78 °C for 1 h and then allowed to warm slowly to room temperature overnight. The reaction was quenched with water, and the aqueous layer was extracted three times with EtOAc. The combined organics were then washed with brine, dried using $MgSO_4$ and concentrated *in vacuo*. Unless otherwise stated, the product was purified by the following method. The crude mixture was dissolved in minimal DCM and was treated with pentane. The resulting suspension was filtered through a cotton plug and the filtrate was concentrated *in vacuo* to obtain the desired product.

Procedure 2: *Direct alkylation of pyridines by Knochel's method*[88]

A flame-dried round-bottomed flask equipped with a stir bar was charged with the appropriate pyridine (1.0 equiv.) as a solution in THF and cooled to 0 °C. BF_3•OEt_2 (1.1 equiv.) was added dropwise and the mixture was stirred for 15 min. The reaction mixture was then cooled to -50 °C and to it was added a THF solution of the required alkyl Grignard reagent (1.3 equiv.). After 30 min, chloranil (2.0 equiv.) was added and the mixture was warmed up to room temperature and stirred for 2 additional hours. The reaction was then quenched with $NH_4OH_{(aq.)}$ (1.0 mL/mmol of pyridine), filtered through a pad of Celite® and extracted three times with diethyl ether. The combined organics were then washed with brine and dried with $MgSO_4$. The product was concentrated *in vacuo* and purified using flash chromatography.

4-(2-Phenylethyl)pyridine **2** (CAS: 2116-64-5)

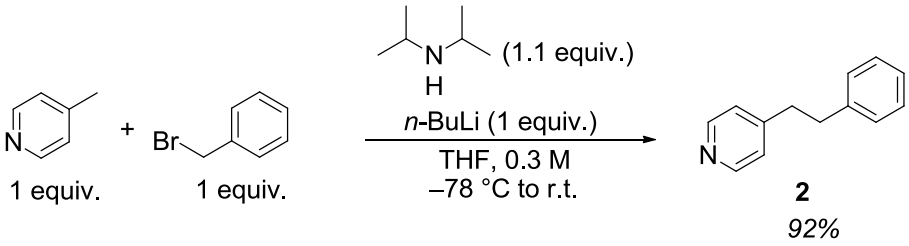

Substrate **2** was synthesized according to **procedure 1** using 4-picoline (0.52 g, 5.6 mmol, 1.0 equiv.) and benzyl bromide as the electrophile (0.96 g, 5.6 mmol, 1.0 equiv.). Purification was done according to **procedure 1** to obtain the product as a yellow solid (0.94 g, 5.1 mmol, 92% yield). Spectral data of this compound is consistent with that reported in the literature.[89]

^{1}H-NMR (400 MHz, $CDCl_3$)
δ 8.48 (d, *J* = 5.6 Hz, 2 H), 7.30-7.19 (m, 3 H), 7.15 (d, *J* = 7.6 Hz, 2 H), 7.08 (d, *J* = 5.6 Hz, 2 H), 2.93 (br, 4 H).

^{13}C-NMR (100 MHz, $CDCl_3$)
δ 150.4, 149.7, 140.6, 128.4, 128.3, 126.2, 123.9, 37.0, 36.5.

4-Pentylpyridine **3** (CAS: 2961-50-4)

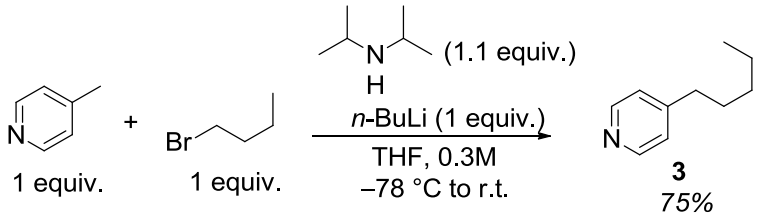

Substrate **3** was synthesized according to **procedure 1** using 4-picoline (0.75 g, 8.0 mmol, 1.0 equiv.) and 1-bromobutane as the electrophile (1.11 g, 8.00 mmol, 1.0 equiv.). The product was purified by flash chromatography and obtained as a yellow oil (0.90 g, 6.0 mmol, 75% yield). Spectral data is consistent with that reported in the literature.[90]

Chromatography: 20% EtOAc in hexane (R_f = 0.27).

^{1}H-NMR (400 MHz, $CDCl_3$)
δ 8.47 (d, *J* = 5.6 Hz, 2 H), 7.09 (d, *J* = 5.6 Hz, 2 H), 2.59 (t, *J* = 7.6 Hz, 2 H), 1.62 (tt, *J* = 7.6, 7.2 Hz, 2 H), 1.36-1.27 (m, 4 H), 0.89 (t, *J* = 7.2 Hz, 3 H).

^{13}C-NMR (100 MHz, $CDCl_3$)
δ 152.0, 149.8, 124.1, 35.4, 31.5, 30.2, 22.6, 14.1.

4-(But-3-en-1-yl)pyridine **4** (CAS: 45814-04-8)

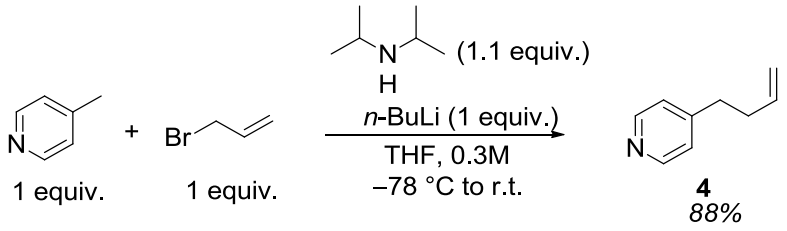

Substrate **4** was synthesized according to **procedure 1** using 4-picoline (0.98 g, 10.5 mmol, 1.0 equiv.) and allyl bromide as the electrophile (1.30 g, 10.5 mmol, 1.0 equiv.). The product was purified according to **procedure 1** and obtained as a yellow oil (1.2 g, 9.3 mmol, 88% yield). Spectral data is consistent with that reported in the literature.[91]

^{1}H-NMR (400 MHz, $CDCl_3$)
δ 8.51 (d, *J* = 5.6 Hz, 2 H), 7.13 (d, *J* = 5.6 Hz, 2 H),
5.84 (dddd, *J* = 17.2, 10.0, 6.8, 6.8 Hz, 1 H), 5.06-4.99 (m, 2 H),
2.75-2.71 (m, 2 H), 2.44-2.38 (m, 2 H).

^{13}C-NMR (100 MHz, $CDCl_3$)
δ 150.1, 149.2, 136.5, 123.5, 115.2, 34.0, 33.7.

4-(3-Butyn-1-yl)pyridine **5** (CAS: 103440-64-8)

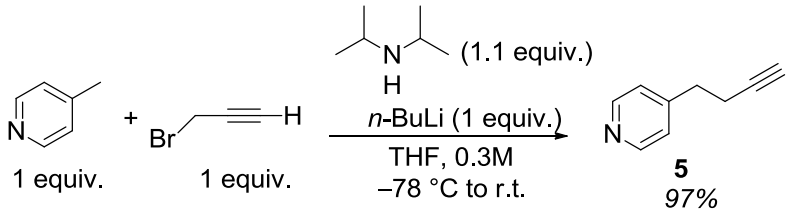

Substrate **5** was synthesized according to **procedure 1** using 4-picoline (0.71 g, 7.6 mmol, 1.0 equiv.) and propargyl bromide as the electrophile (1.08 g, 7.6 mmol, 1.0 equiv.). The product was purified according to **procedure 1** and obtained as a white solid (0.98 g, 7.4 mmol, 97% yield).

^{1}H-NMR (400 MHz, $CDCl_3$)
δ 8.52 (dd, *J* = 4.4, 1.6 Hz, 2 H), 7.16 (d, *J* = 6.0 Hz, 2 H),
2.84 (t, *J* = 7.2 Hz, 2 H), 2.52 (dt, *J* = 7.2, 2.8 Hz, 2 H), 1.99 (t, *J* = 2.8 Hz, 1 H).

^{13}C-NMR (100 MHz, $CDCl_3$)
δ 150.0, 149.2, 124.0, 82.9, 69.8, 34.1, 19.5.

IR Alpha-Platinum ATR, Bruker, diamond crystal
υ = 3180, 2955, 1602, 1558 cm^{-1}

HRMS ESI
Calculated mass for $(M+H)^+$ of C_9H_9N is 132.0808 found 132.0806.

4-(4-((tert-Butyldimethylsilyl)oxy)butyl)pyridine **6**

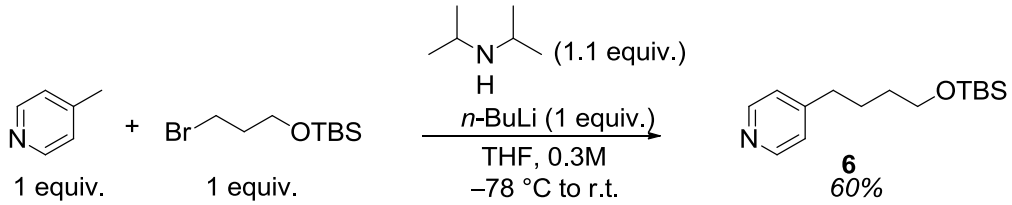

Substrate **6** was synthesized according to **procedure 1** using 4-picoline (0.85 g, 9.1 mmol, 1.0 equiv.) and (3-bromopropoxy)-*tert*-butyldimethylsilane as the electrophile (2.30 g, 9.1 mmol, 1.0 equiv.). The product was purified by flash chromatography and obtained as a yellow oil (1.60 g, 5.48 mmol, 60% yield).

Chromatography: 40% EtOAc in hexane (R_f. = 0.56).

^{1}H-NMR (400 MHz, $CDCl_3$)
δ 8.48 (d, *J* = 5.6 Hz, 2 H), 7.10 (d, *J* = 5.6 Hz, 2 H), 3.62 (t, *J* = 6.4 Hz, 2 H), 2.62 (t, *J* = 7.6 Hz, 2 H), 1.78-1.66 (m, 2 H), 1.57-1.52 (m, 2 H), 0.91 (s, 9 H), 0.06 (s, 6 H).

^{13}C-NMR (100 MHz, $CDCl_3$)
δ 151.2, 149.4, 123.6, 62.4, 34.7, 31.9, 26.3, 25.7, 18.1, -5.5.

^{29}Si-NMR (80 MHz, $CDCl_3$)
δ 18.74

IR Alpha-Platinum ATR, Bruker, diamond crystal
υ = 2894, 2857, 1602 cm^{-1}

HRMS ESI
Calculated mass for $(M+H)^+$ of $C_{15}H_{27}NOSi$ is 266.1935 found 266.1928.

4-Pyridineheptanenitrile **7** (CAS: 154939-07-8)

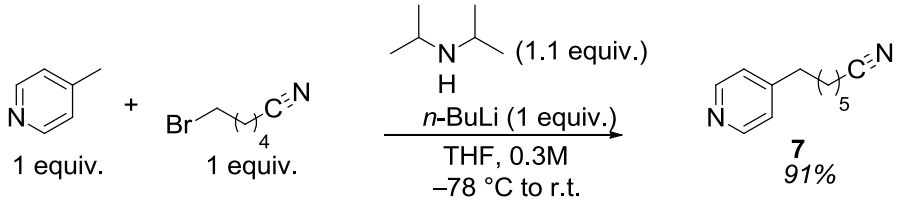

Substrate **7** was synthesized according to **procedure 1** using 4-picoline (0.50 g, 5.4 mmol, 1.0 equiv.) and 6-bromo-hexanenitrile as the electrophile (0.95 g, 5.4 mmol, 1.0 equiv.). The product was purified according to **procedure 1** and obtained as a yellow oil (0.92 g, 4.9 mmol, 91% yield). Spectral data is consistent with that reported in the literature.[92]

^{1}H-NMR (400 MHz, $CDCl_3$)
δ 8.49 (dd, *J* = 5.0, 1.6 Hz, 2 H), 7.09 (d, *J* = 5.6 Hz, 2 H),
2.61 (t, *J* = 7.6 Hz, 2 H), 2.34 (t, *J* = 7.2 Hz, 2 H), 1.69-1.62 (m, 4 H),
1.53-1.45 (m, 2 H), 1.40-1.37 (m, 2 H).

^{13}C-NMR (100 MHz, $CDCl_3$)
δ 151.1, 149.5, 123.7, 119.6, 34.9, 29.8, 28.2, 28.1, 25.1, 17.0.

4-(3-(1,3-Dioxolan-2-yl)propyl)pyridine **8** (CAS: 639089-29-5)

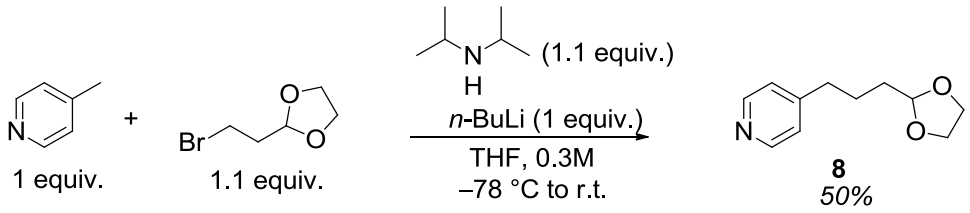

Substrate **8** was synthesized according to **procedure 1** using 4-picoline (1.06 g, 11.4 mmol, 1.0 equiv.) and 2-(2-bromoethyl)-1,3-dioxolane as the electrophile (2.06 g, 12.5 mmol, 1.1 equiv.). The product was purified by flash chromatography and obtained as a yellow oil (1.10 g, 5.69 mmol, 50% yield). Spectral data is consistent with that reported in the literature.[93]

Chromatography: 100% EtOAc (R_f. = 0.50).

^{1}H-NMR (400 MHz, $CDCl_3$)
δ 8.48 (d, *J* = 5.6 Hz, 2 H), 7.11 (d, *J* = 5.6 Hz, 2 H), 4.87 (t, *J* = 4.4 Hz, 1 H), 3.99-3.93 (m, 2 H), 3.92-3.81 (m, 2 H), 2.65 (t, *J* = 7.2 Hz, 2 H), 1.79-1.68 (m, 4 H).

^{13}C-NMR (100 MHz, $CDCl_3$)
δ 151.1, 149.8, 123.9, 104.2, 65.0, 35.0, 33.3, 24.6.

4-(2-Bromophenethyl)pyridine **9**

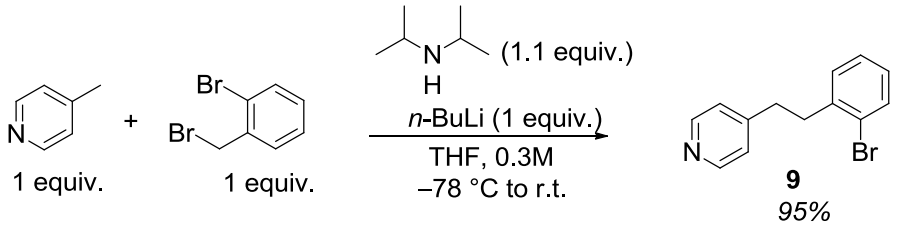

Substrate **9** was synthesized according to **procedure 1** using 4-picoline (0.36 g, 3.9 mmol, 1.0 equiv.) and 2-bromobenzyl bromide as the electrophile (0.98 g, 3.9 mmol, 1.0 equiv.). The product was purified according to **procedure 1** and obtained as a yellow oil (0.97 g, 3.7 mmol, 95% yield).

^{1}H-NMR (400 MHz, $CDCl_3$)
δ 8.49 (d, *J* = 6.0 Hz, 2 H), 7.55 (d, *J* = 8.0 Hz, 1 H), 7.22-7.19 (m, 1 H), 7.13-7.06 (m, 4 H), 3.06-3.02 (m, 2 H), 2.93-2.89 (m, 2 H).

^{13}C-NMR (100 MHz, $CDCl_3$)
δ 149.8, 149.5, 139.6, 132.6, 130.2, 127.8, 127.3, 124.1, 123.6, 36.8, 35.0.

IR Alpha-Platinum ATR, Bruker, diamond crystal
υ = 3066, 3023, 2930, 1599, 1559 cm^{-1}

HRMS ESI
Calculated mass for $(M+H)^+$ of $C_{13}H_{12}BrN$ is 262.0226 found 262.0223.

2-Bromo-5-(2-(pyridin-4-yl)ethyl)pyridine **10**

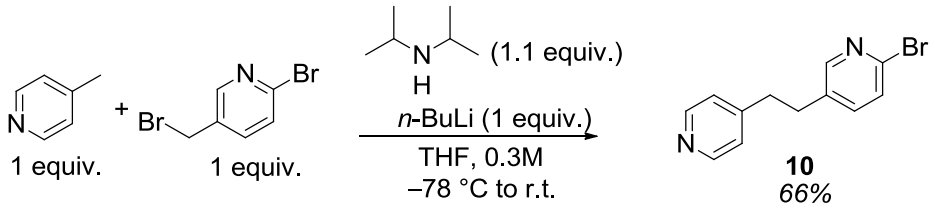

Substrate **10** was synthesized according to **procedure 1** using 4-picoline (0.090 g, 1.0 mmol, 1.0 equiv.) and 2-bromo-5-(bromomethyl)pyridine as the electrophile (0.25 g, 1.0 mmol, 1.0 equiv.). The product was purified by flash chromatography and obtained as a white solid (0.17 g, 0.66 mmol, 66% yield).

Chromatography: 3% MeOH in EtOAc (R_f. = 0.41).

^{1}H-NMR (400 MHz, $CDCl_3$)
δ 8.48 (d, *J* = 5.6 Hz, 2 H), 8.14 (d, *J* = 2.4 Hz, 1 H), 7.35 (d, *J* = 8.0 Hz, 1 H), 7.26 (dd, *J* = 8.0, 2.4 Hz, 1 H), 7.03 (d, *J* = 5.6 Hz, 2 H), 2.89 (br, 4 H).

^{13}C-NMR (100 MHz, $CDCl_3$)
δ 150.0, 149.9, 149.0, 139.9, 138.5, 135.1, 127.7, 123.7, 36.2, 32.8.

IR Alpha-Platinum ATR, Bruker, diamond crystal
υ = 3032, 2923, 1597, 1579, 1557 cm^{-1}

HRMS ESI
Calculated mass for $(M+H)^+$ of $C_{12}H_{11}BrN_2$ is 263.0178 found 263.0170.

3-(2-(pyridin-4-yl)ethyl)pyridine **11**

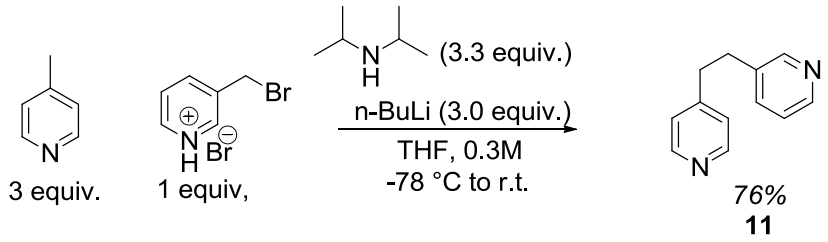

Substrate **11** was synthesized according to **Procedure 1** using 4-picoline (0.78 g, 8.4 mmol, 3.0 equiv.) and 3-(bromomethyl)pyridine•HBr salt as the electrophile (0.70 g, 2.8 mmol, 1.0 equiv.). The product was purified by flash chromatography and was obtained as an orange oil (0.39 g, 2.1 mmol, 76% yield).

Chromatography: 5% Et_3N : 25% Hexane : 70% EtOAc (R_f = 0.25)

^{1}H-NMR (400 MHz, $CDCl_3$)
δ 8.48 (d, *J* = 5.6 Hz, 2 H), 8.45 (d, *J* = 4.8 Hz, 1 H), 8.42 (s, 1 H), 7.42 (d, *J* = 7.6 Hz, 2 H), 7.19 (dd, *J* = 7.6, 4.8 Hz, 1 H), 7.06 (d, *J* = 5.6 Hz, 2 H), 2.93 (br, 4 H).

^{13}C-NMR (100 MHz, $CDCl_3$)
δ 149.8, 149.8, 149.5, 147.7, 135.8, 135.7, 123.8, 123.2, 36.5, 33.5.

IR Alpha-Platinum ATR, Bruker, diamond crystal
υ = 3026, 2928, 1599, 1575, 1558 cm^{-1}

HRMS ESI
Calculated mass for $(M+H)^+$ of $C_{12}H_{12}N_2$ is 185.1073 found 185.1072.

4-(Pyridin-4-yl)butanal **12** (CAS: 192643-84-8)

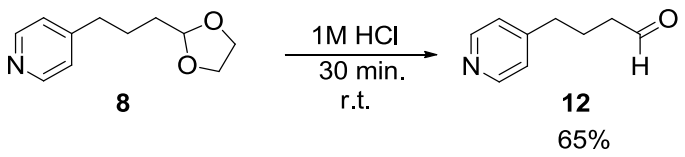

8 **12**

65%

Acetal **8** (0.35 g, 1.8 mmol, 1.0 equiv.) was dissolved in 1 M $HCl_{(aq)}$ (10 mL) in a round-bottomed flask equipped with a stir bar. The solution was stirred for 30 min at room temperature and subsequently washed twice with DCM. The aqueous solution was then neutralized using saturated aqueous $NaHCO_3$ solution and extracted three times with DCM. The combined organics were washed with brine, dried over $MgSO_4$, filtered and concentrated *in vacuo* to afford **12** as a colorless oil (0.17 g, 1.2 mmol, 65% yield) which was used without further purification. Spectral data is consistent with that reported in the literature.[94]

^{1}H-NMR (400 MHz, $CDCl_3$)
δ 9.77 (s, 1 H), 8.49 (d, *J* = 5.2 Hz, 2 H), 7.10 (d, *J* = 5.2 Hz, 2 H),
2.64 (t, *J* = 7.6 Hz, 2 H), 2.47 (t, *J* = 7.2 Hz, 2 H), 1.96 (tt, *J* = 7.6, 7.2 Hz, 2 H).

^{13}C-NMR (100 MHz, $CDCl_3$)
δ 201.3, 150.0, 149.4, 123.6, 42.6, 33.9, 22.1.

4-(Pyridin-4-yl)butan-2-one **13** (CAS: 35250-71-6)

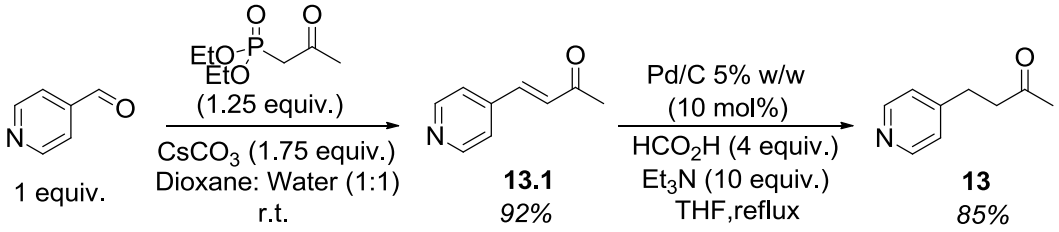

Horner-Wadsworth-Emmons Reaction – A solution of $CsCO_3$ (2.85 g, 8.75 mmol, 1.75 equiv.) in a 1:1 mixture of 1,4-dioxane and distilled water (10 mL) was made in a round-bottomed flask equipped with a stir bar. To this solution diethyl (2-oxopropyl)phosphonate (1.04 g, 6.25 mmol, 1.25 equiv.) was added and the mixture was left to stir for 30 min. before 4-pyridinecarboxaldehyde (0.54 g, 5.0 mmol, 1.0 equiv.) was introduced. Upon completion of the reaction, as indicated by TLC, the mixture was diluted with EtOAc and washed with brine three times. The organic layer was dried over $MgSO_4$ and concentrated *in vacuo*. The crude mixture was flushed through a plug of silica with EtOAc to afford **13.1** (CAS: 10416-53-2) as brown solid (0.68 g, 4.60 mmol, 92% yield). Spectral data is consistent with that reported in the literature.[95]

Data for **13.1**

^{1}H-NMR (400 MHz, $CDCl_3$)
δ 8.66 (d, *J* = 5.6 Hz, 2 H), 7.41 (d, *J* = 16.4 Hz, 1 H), 7.38 (d, *J* = 5.6 Hz, 2 H), 6.84 (d, *J* = 16.4 Hz, 1 H), 2.41 (s, 3 H).

^{13}C-NMR (100 MHz, $CDCl_3$)
δ 197.9, 150.9, 141.9, 140.3, 130.9, 122.1, 28.1.

4-(Pyridin-4-yl)butan-2-one **13** (CAS: 35250-71-6)

Hydrogenation – A flame-dried round-bottomed flask equipped with a stir bar was charged with α,β-unsaturated ketone **13.1** (0.44 g, 3.0 mmol, 1.0 equiv.) in THF (17 mL), triethylamine (4.0 mL, 30 mmol, 10.0 equiv.), 5% w/w Pd/C (0.64 g, 0.29 mmol, 10 mol%) and formic acid (0.55 mL, 12 mmol, 4.0 equiv.). The flask was then equipped with a condenser and heated under reflux for 4 h. The reaction mixture was then diluted with EtOAc and filtered through a pad of Celite®. The filtrate was concentrated *in vacuo* and subsequently flushed through a plug of silica to afford **13** a yellow oil (0.38 g, 2.6 mmol, 85% yield). Spectral data is consistent with that reported in the literature.[90]

Data for **13**

^{1}H-NMR (400 MHz, $CDCl_3$)
δ 8.49 (d, *J* = 5.2 Hz, 2 H), 7.11 (d, *J* = 5.2 Hz, 2 H), 2.89 (t, *J* = 7.2 Hz, 2 H), 2.77 (t, *J* = 7.2 Hz, 2 H), 2.16 (s, 3 H).

^{13}C-NMR (100 MHz, $CDCl_3$)
δ 206.9, 150.1, 149.9, 124.2, 43.7, 30.1, 28.9.

Ethyl 3-(pyridin-4-yl)propanoate **14** (CAS: 52809-19-5)

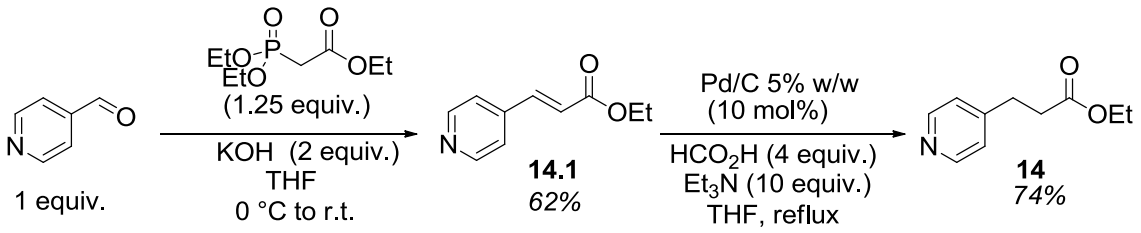

Horner-Wadsworth-Emmons Reaction - A flame-dried round-bottomed flask equipped with a stir bar was charged with finely-ground KOH (0.56 g, 10 mmol, 2.0 equiv.) and THF (10 mL) and cooled to 0 °C. Triethyl phosphonoacetate (1.40 g, 6.25 mmol, 1.25 equiv.) in THF (7 mL) was added and the mixture was left to stir for 30 min. 4-Pyridinecarboxaldehyde (0.54 g, 5.0 mmol, 1.0 equiv.) in THF (7 mL) was then introduced and the flask was warmed to room temperature and left to stir overnight. The reaction mixture was diluted with diethyl ether and dried with $MgSO_4$. Upon filtration through a pad of Celite® and concentration, product **14.1** (CAS: 24489-96-1) was obtained as a white solid. The product was further purified by a short plug of silica using EtOAc as eluent (0.55 g, 3.1 mmol, 62% yield). Spectral data is consistent with that reported in the literature.[96]

Data for **14.1**

^{1}H-NMR (400 MHz, $CDCl_3$)
δ 8.64 (d, *J* = 5.6 Hz, 2 H), 7.59 (d, *J* = 16.0 Hz, 1 H), 7.36 (d, *J* = 5.6 Hz, 2 H), 6.58 (d, *J* = 16.0 Hz, 1 H), 4.28 (q, *J* = 7.2 Hz, 2 H), 1.34 (t, *J* = 7.2 Hz, 3 H).

^{13}C-NMR (100 MHz, $CDCl_3$)
δ 166.2, 150.8, 141.8, 123.1, 122.0, 61.2, 14.4.

Ethyl 3-(pyridin-4-yl)propanoate **14** (CAS: 52809-19-5)

Hydrogenation - A flame-dried round-bottomed flask equipped with a stir bar was charged with α,β-unsaturated ester **14.1** (0.90 g, 5.1 mmol, 1.0 equiv.) in THF (17 mL), triethylamine (7.1 mL, 51 mmol, 10.0 equiv.), 5% w/w Pd/C (1.1 g, 0.51 mmol, 10 mol%) and formic acid (0.77 mL, 20 mmol, 4.0 equiv.). The flask was then equipped with a condenser and heated under reflux for 4 h The reaction mixture was then diluted with EtOAc and filtered through a pad of Celite® to remove the palladium catalyst. The filtrate was concentrated *in vacuo* and subsequently flushed through a plug of silica to afford product **14** as a yellow oil (0.68 g, 3.8 mmol, 74% yield). Spectral data is consistent with that reported in the literature.[97]

Data for **14**

^{1}H-NMR (400 MHz, $CDCl_3$)
δ 8.51 (d, *J* = 5.6 Hz, 2 H), 7.14 (d, *J* = 5.6 Hz, 2 H), 4.13 (q, *J* = 7.2 Hz, 2 H), 2.95 (t, *J* = 7.6 Hz, 2 H), 2.64 (t, *J* = 7.6 Hz, 2 H), 1.23 (t, *J* = 7.2 Hz, 3 H).

^{13}C-NMR (100 MHz, $CDCl_3$)
δ 172.1, 149.8, 149.4, 123.6, 60.6, 34.4, 30.0, 14.1.

4-(2-(phenylsulfonyl)ethyl)pyridine **15** (CAS: 65003-03-4)

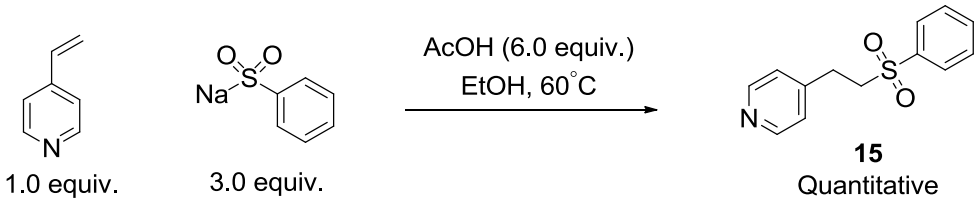

To a 50 mL round-bottomed flask equipped with a stir bar was added 4-vinylpyridine (0.53 g, 5.0 mmol, 1.0 equiv.), benzenesulfinic acid sodium salt (2.46 g, 15.0 mmol, 3.0 equiv.) and EtOH (20 mL). AcOH (1.80 mL, 30.0 mmol, 6.0 equiv.) was then added and the mixture was heated to 60°C overnight. The reaction mixture was then diluted with EtOAc and neutralized using a saturated solution of $NaHCO_3$ (30 mL). The aqueous phase was extracted three times with EtOAc and the combined organics were washed with brine, dried using $MgSO_4$, and concentrated *in vacuo*. The product was purified a short plug of silica using EtOAc as eluent and obtained as a yellow solid (1.25 g, 5.00 mmol, 100% yield). Spectral data of **15** is consistent with that reported in the literature.[98]

^{1}H-NMR (300 MHz, $CDCl_3$)
δ 8.45 (d, *J* = 6.0 Hz, 2 H), 7.90 (dt, *J* = 7.2, 1.5 Hz, 2 H),
7.65 (tt, *J* = 7.2 Hz, 1.5 Hz, 1 H), 7.55 (tt, *J* = 7.2, 1.5 Hz, 2 H),
7.03 (d, *J* = 6.0 Hz, 2 H), 3.35 (m, 2 H), 3.03 (m, 2 H).

^{13}C-NMR (75 MHz, $CDCl_3$)
δ 150.0, 146.3, 138.6, 133.9, 129.4, 128.0, 123.4, 56.0, 27.9.

4-[2-(4-Morpholinyl)ethyl]pyridine **16** (CAS: 28487-18-5)

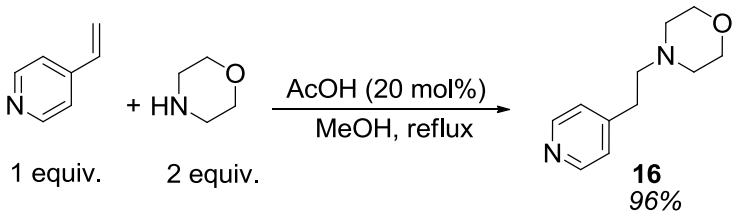

To a 25 mL round-bottomed flask equipped with a stir bar was added 4-vinylpyridine (0.60 mL, 5.5 mmol, 1.0 equiv.), morpholine (0.96 mL, 11.0 mmol, 2.0 equiv.) and MeOH (7 mL). AcOH (0.06 mL, 1.1 mmol, 20 mol%) was then added and the mixture was heated to reflux overnight. The reaction mixture was then diluted with EtOAc and neutralized using a saturated solution of $NaHCO_3$. The aqueous phase was extracted three times with EtOAc and the combined organics were washed with brine, dried using $MgSO_4$, and concentrated *in vacuo*. The product was purified using flash chromatography and obtained as a yellow solid (1.2 g, 5.3 mmol, 96% yield). Spectral data of **16** is consistent with that reported in the literature.[94]

Chromatography: 5% Et_3N :3.3% MeOH :91.7% EtOAc (R_f. = 0.33).

^{1}H-NMR (400 MHz, $CDCl_3$)
δ 8.49 (dd, *J* = 4.4, 1.6 Hz, 2 H), 7.14 (d, *J* = 6.0 Hz, 2 H), 3.73 (t, *J* = 4.4 Hz, 4 H), 2.80 (dd, *J* = 8.4, 5.6 Hz, 2 H), 2.61 (dd, *J* = 8.4, 5.6 Hz, 2 H), 2.51 (t, *J* = 4.4 Hz, 4 H).

^{13}C-NMR (100 MHz, $CDCl_3$)
δ 149.6, 149.1, 124.0, 66.8, 59.2, 53.5, 32.5.

Ethyl 4-butylnicotinate **17**

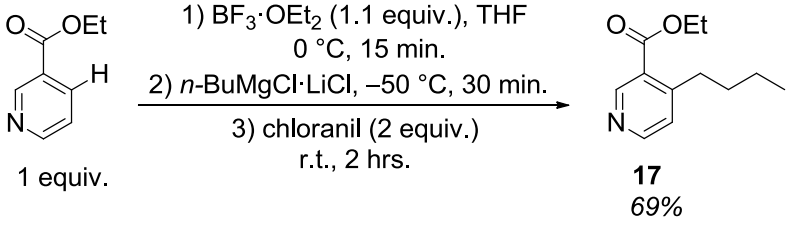

1 equiv.

17
69%

Substrate **17** was synthesized according to **procedure 2** using 3-ethyl nicotinate (0.76 g, 5.0 mmol, 1.0 equiv.) and *n*-BuMgCl•LiCl (11 mL, 7.9 mmol, 1.6 equiv., 0.7 M in THF). The product was purified by flash chromatography and obtained as a colorless oil (0.71 g, 3.5 mmol, 69% yield).

Chromatography: 3.33% Et_3N in hexanes (R_f. = 0.20).

^{1}H-NMR (300 MHz, $CDCl_3$)
δ 9.03 (s, 1 H), 8.56 (d, *J* = 5.1 Hz, 1 H), 7.17 (d, *J* = 5.1 Hz, 1 H), 4.39 (q, *J* = 7.2 Hz, 2 H), 2.97 (t, *J* = 7.8 Hz, 2 H), 1.63-1.55 (m, 2 H), 1.45-1.36 (m, 5 H), 0.94 (t, *J* = 7.2 Hz, 3 H)

^{13}C-NMR (100 MHz, $CDCl_3$)
δ 166.3, 153.7, 152.1, 151.7, 126.1, 125.4, 61.3, 33.6, 33.0, 22.8, 14.3, 14.0

IR Alpha-Platinum ATR, Bruker, diamond crystal
υ = 2959, 2932, 2872, 1719, 1590, 1556 cm^{-1}

HRMS ESI

Calculated mass for $(M+H)^+$ of $C_{12}H_{17}NO_2$ is 208.1332 found 208.1326.

4-Butyl-3-pyridinecarbonitrile **18** (CAS: 1713287-19-4)

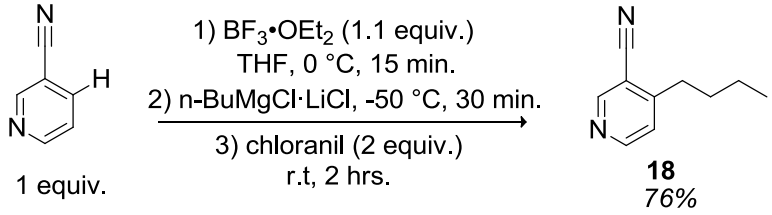

Substrate **19** was synthesized according to **procedure 2** using 3-cyanopyridine (0.78 g, 7.5 mmol, 1.0 equiv.) and *n*-BuMgCl•LiCl (4.87 mL, 9.74 mmol, 2.0 M, 1.3 equiv.). The product was purified by flash chromatography and obtained as a colorless oil (0.91 g, 5.7 mmol, 76% yield).

Chromatography: 20% EtOAc in hexanes (R_f. = 0.40).

^{1}H-NMR (400 MHz, $CDCl_3$)
δ 8.77 (s, 1 H), 8.64 (d, *J* = 5.2 Hz, 1 H), 7.26 (d, *J* = 5.2 Hz, 1 H), 2.82 (t, *J* = 7.6 Hz, 2 H), 1.70-1.62 (m, 2 H), 1.44-1.35 (m, 2 H), 0.97 (t, *J* = 7.2 Hz, 3 H).

^{13}C-NMR (100 MHz, $CDCl_3$)
δ 155.6, 153.1, 152.7, 124.1, 116.1, 110.6, 34.0, 32.1, 22.4, 13.9.

IR Alpha-Platinum ATR, Bruker, diamond crystal
υ = 2958, 2932, 2872, 2228, 1589, 1553 cm^{-1}

HRMS ESI
Calculated mass for $(M+H)^+$ of $C_{10}H_{12}N_2$ is 161.1073 found 161.1077.

N-(*tert*-Butyl)-4-butylnicotinamide **19** (CAS: 331969-16-5**)**

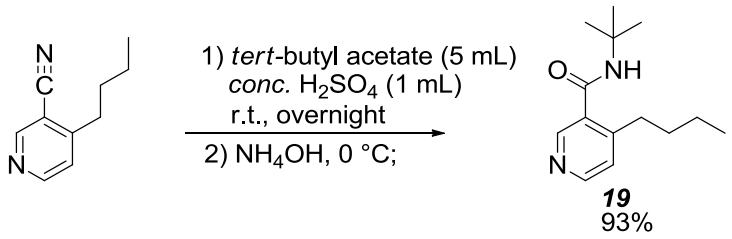

To a round-bottomed flask containing a solution of 3-cyano-4-butylpyridine (0.40 g, 2.5 mmol, 1.0 equiv.) in *tert*-butyl acetate (5 mL) was added concentrated H_2SO_4 (1 mL), and the mixture was stirred at room temperature overnight. The solution was then diluted with water and carefully neutralized by adding NH_4OH (3 mL) at 0 °C. The aqueous phase was extracted three times with a 1:1 mixture of hexane-EtOAc and the combined organics were washed with brine, dried ($MgSO_4$), filtered, and concentrated *in vacuo*. The residue was chromatographed on silica gel to afford the product as a white solid (0.54 g, 2.3 mmol, 93% yield). Spectral data of **19** is consistent with that reported in the literature.[99]

Chromatography: 70%-90% EtOAc in hexanes (R_f. = 0.34).

^{1}H-NMR (400 MHz, $CDCl_3$)
δ 8.50 (s, 1 H), 8.48 (d, *J* = 5.2 Hz, 1 H), 7.14 (d, *J* = 5.2 Hz, 1 H), 5.64 (br, 1 H), 2.76 (t, *J* = 7.6 Hz, 2 H), 1.59 (p, *J* = 7.6 Hz, 2 H), 1.47 (s, 9 H), 1.37 (qt, *J* = 7.6, 7.2 Hz, 2 H), 0.93 (t, *J* = 7.2 Hz, 3 H).

^{13}C-NMR (100 MHz, $CDCl_3$)
δ 167.4, 150.7, 150.3, 147.5, 133.8, 124.9, 52.4, 32.9, 32.5, 29.0, 22.9, 14.1.

4-Butyl-3-phenylpyridine **20**

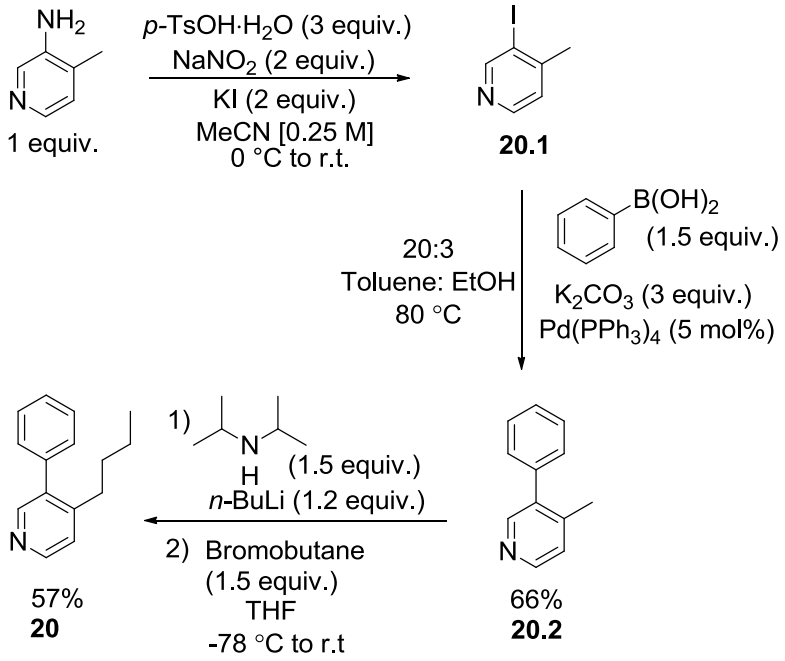

*Synthesis of 3-iodo-4-methylpyridine (**20.1**)* - To a solution of 3-amino-4-methylpyridine (0.40 g, 3.7 mmol, 1.0 equiv.) and *p*-TsOH•H_2O (2.11 g, 11.1 mmol, 3.0 equiv.) in MeCN (15 mL) was added dropwise a solution of $NaNO_2$ (0.51 g, 7.4 mmol, 2.0 equiv.) and KI (1.23 g, 7.40 mmol, 2.0 equiv.) in distilled water (5 mL) at 0°C over 15 min. After 1 h the reaction mixture was warmed to room temperature then treated with saturated aqueous $NaHCO_3$ (30 mL) and saturated aqueous $NaHSO_3$ (30 mL). The aqueous phase was extracted with EtOAc three times and the combined organics were washed with brine, dried with $MgSO_4$ and concentrated *in vacuo* to afford **20.1** (CAS: 38749-96-1) as a yellow oil, which was used in the next step without further purification. Spectral data was found to be consistent with that reported in the literature.[100]

Data for **20.1**

^{1}H-NMR (400 MHz, $CDCl_3$)
δ 8.85 (s, 1 H), 8.37 (d, *J* = 5.0 Hz, 1 H), 7.18 (d, *J* = 5.0 Hz, 1 H), 2.41 (s, 3 H).

^{13}C-NMR (100 MHz, $CDCl_3$)
δ 154.9, 150.4, 148.8, 125.4, 100.6, 27.3.

4-Butyl-3-phenylpyridine **20**

Suzuki coupling – A flame-dried flask equipped with a stir bar was charged with **20.1**, phenylboronic acid (0.60 g, 4.9 mmol, 1.5 equiv.), K_2CO_3 (1.37 g, 9.90 mmol, 3.0 equiv.) and $Pd(PPh_3)_4$ (0.19 g, 0.16 mmol, 5 mol%) and kept under an atmosphere of argon. To this mixture was added freshly distilled toluene (20 mL) and anhydrous EtOH (3 mL) and the resulting solution was heated to 80 °C. After 3 h, the flask was cooled to room temperature and then diluted with EtOAc and washed with brine three times. The organic phase was dried with $MgSO_4$ and concentrated *in vacuo*. The crude mixture was purified by flash chromatography to afford **20.2** (CAS: 19352-29-5) as a colorless oil (0.37 g, 2.2 mmol, 66% yield). Spectral data is consistent with that reported in the literature.[101]

Chromatography: 30% EtOAc in Toluene (R_f. = 0.33).

Data for **20.2**

^{1}H-NMR (400 MHz, $CDCl_3$)
δ 8.44 (br, 2 H), 7.47-7.34 (m, 3 H), 8.37 (d, *J* = 7.6 Hz, 2 H), 7.19 (d, *J* = 4.8 Hz, 1 H), 2.29 (s, 3 H).

^{13}C-NMR (100 MHz, $CDCl_3$)
δ 149.8, 148.2, 144.4, 137.8, 137.6, 129.2, 128.3, 127.5, 125.1, 19.7.

4-Butyl-3-phenylpyridine **20**

*Alkylation of **20.2*** – Substrate **20** was synthesized according to **procedure 1** using **20.2** (0.30 g, 1.8 mmol, 1.0 equiv.) and 1-bromopropane as the electrophile (0.33 g, 2.7 mmol, 1.5 equiv.). The product was purified by flash chromatography and obtained as a colorless oil (0.32 g, 1.0 mmol, 57% yield).

Chromatography: 40% EtOAc in hexanes (R_f. = 0.40).

Data for **20**

^{1}H-NMR (400 MHz, $CDCl_3$)
δ 8.47 (d, *J* = 4.8 Hz, 1 H), 8.41 (s, 1 H), 7.45-7.36 (m, 3 H), 7.30-7.28 (m, 2 H), 7.19 (d, *J* = 4.8 Hz, 1 H), 2.58 (t, *J* = 7.6 Hz, 2 H), 1.46 (p, *J* = 7.6 Hz, 2 H), 1.22 (qt, *J* = 7.2, 7.6 Hz, 2 H), 0.79 (t, *J* = 7.2 Hz, 3 H).

^{13}C-NMR (100 MHz, $CDCl_3$)
δ 150.1, 149.1, 148.4, 137.9, 137.5, 129.3, 128.3, 127.5, 123.8, 32.2, 31.9, 22.3, 13.7.

IR Alpha-Platinum ATR, Bruker, diamond crystal
υ = 2957, 2929, 2861, 1597 cm^{-1}

HRMS ESI
Calculated mass for $(M+H)^+$ of $C_{15}H_{17}N$ is 212.1434 found 212.1430.

tert-Butyl (4-phenethylpyridin-3-yl)carbamate **21**

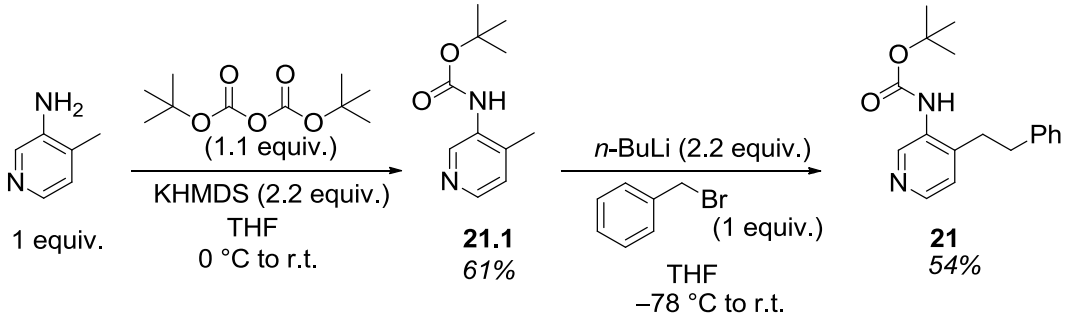

<u>*Boc- protection of 3-amino-4-methylpyrdine*</u> – A flame-dried round-bottomed flask equipped with a stir bar was charged with 3-amino-4-methylpyridine (0.50 g, 4.6 mmol, 1.0 equiv.) and freshly distilled THF (10 mL) and kept under an atmosphere of argon. While stirring at 0 °C, KHMDS solution (20.2 mL, 10.2 mmol, 2.2 equiv., 0.5 M in toluene) was introduced dropwise. After stirring for 30 min, the mixture was allowed to warm to room temperature then a solution of di-*tert*-butyl dicarbonate (1.10 g, 5.09 mmol, 1.1 equiv.) in dry THF (10 mL) was added. The reaction was monitored by TLC and upon completion, the reaction mixture was concentrated *in vacuo* then quenched with of 0.1 M $HCl_{(aq)}$ (20 mL). The aqueous phase was extracted with DCM three times and the combined organics were washed with brine, dried with $MgSO_4$ and concentrated *in vacuo*. The crude mixture was purified by silica gel chromatography to afford **21.1** (CAS: 180253-66-1) as yellow solid (0.58 g, 2.8 mmol, 61% yield). The spectral data was found to be consistent with that reported in the literature.[102]

Chromatography: 60% EtOAc in hexanes (R_f. = 0.40).

Data for **22.1**

^{1}H-NMR (400 MHz, $CDCl_3$)
δ 8.82 (br, 1 H), 8.21 (d, *J* = 4.8 Hz, 1 H), 7.06 (d, *J* = 4.8 Hz, 1 H), 6.52 (br, 1 H), 2.24 (s, 3 H), 1.49 (s, 9 H).

^{13}C-NMR (100 MHz, $CDCl_3$)
δ 152.9, 145.1, 143.9, 138.0, 133.4, 125.0, 80.9, 28.2, 17.3.

tert-Butyl (4-phenethylpyridin-3-yl)carbamate **21**

*Alkylation of **21.1*** – A flame-dried round-bottomed flask equipped with a stir bar was cooled to −78 °C and charged with *n*-BuLi (1.90 mL, 4.75 mmol, 2.2 equiv., 2.5 M in hexanes) and freshly distilled THF (20 mL) under an atmosphere of argon. A solution of **21.1** (0.45 g, 2.2 mmol, 1.0 equiv.) in dry THF (5 mL) was then added dropwise and the resulting mixture was allowed to stir for 1 h. Benzyl bromide (0.37 g, 2.2 mmol, 1.0 equiv.) was introduced and the solution was maintained at −78 °C for 1 h, then slowly warmed to room temperature. Upon completion as indicated by TLC, the reaction was quenched with water and the aqueous phase was extracted with EtOAc three times. The combined organics were washed with brine, dried with $MgSO_4$ and concentrated *in vacuo*. The crude mixture was purified by flash chromatography to afford **21** as a white solid (0.35 g, 1.2 mmol, 54% yield).

Chromatography: 50-65% EtOAc in Hexane (R_f. = 0.30).

Data for **21**

^{1}H-NMR (400 MHz, $CDCl_3$)
δ 8.78 (br, 1 H), 8.29 (d, *J* = 4.8 Hz, 1 H), 7.31-7.21 (m, 3 H), 7.12 (d, *J* = 7.6 Hz, 1 H), 7.07 (d, *J* = 4.8 Hz, 1 H), 5.94 (br, 1 H), 2.95-2.85 (m, 4 H), 1.49 (s, 9 H).

^{13}C-NMR (100 MHz, $CDCl_3$)
δ 153.1, 145.8, 145.3, 141.7, 140.4, 132.7, 128.7, 128.5, 128.4, 126.5, 123.8, 80.9, 35.3, 32.7, 28.2.

IR Alpha-Platinum ATR, Bruker, diamond crystal
υ = 3179, 2971, 2931, 1705, 1600, 1566, 1530 cm^{-1}

HRMS ESI
Calculated mass for $(M+H)^+$ of $C_{18}H_{22}N_2O_2$ is 299.1754 found 299.1753.

2-(2-(Pyridin-4-yl)ethyl)pyridine **22**

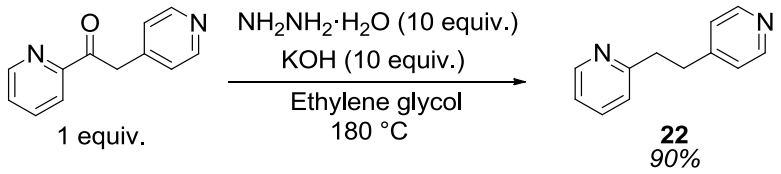

A round-bottomed flask equipped with a stir bar and a condenser was charged with a solution of 1-(pyridin-2-yl)-2-(pyridin-4-yl)ethenone (0.43 g, 2.2 mmol, 1.0 equiv.) in ethylene glycol (10 mL). Hydrazine monohydrate (1.1 mL, 2.17 mmol, 1.0 equiv.) was introduced at room temperature and the solution was then heated to 180 °C for 1 h and then cooled to ~80 °C. Potassium hydroxide pellets (1.21 g, 21.7 mmol, 10.0 equiv.) were then carefully added in small portions and the reaction mixture was again heated to 180 °C for 1 h. The reaction mixture was allowed to cool to room temperature and then diluted with Et_2O. The organic phase was washed with brine three times, dried over $MgSO_4$ and concentrated *in vacuo*. The crude mixture was flushed through a short plug of silica gel with EtOAc as eluent to afford **22** as an orange oil (0.36 g, 1.9 mmol, 90% yield).

^{1}H-NMR (400 MHz, $CDCl_3$)
δ 8.51 (d, *J* = 4.4 Hz, 1 H), 8.47 (d, *J* = 5.6 Hz, 2 H), 7.52 (t, *J* = 7.6 Hz, 1 H), 7.09-7.00 (m, 4 H), 3.08-2.99 (m, 4 H).

^{13}C-NMR (100 MHz, $CDCl_3$)
δ 160.0, 150.3, 149.5, 149.3, 136.3, 123.8, 122.9, 121.3, 38.6, 34.8.

IR Alpha-Platinum ATR, Bruker, diamond crystal
υ = 3024, 2928, 1590, 1568 cm^{-1}

HRMS ESI
Calculated mass for $(M+H)^+$ of $C_{12}H_{12}N_2$ is 185.1073 found 185.1071.

2-(4-(2-(Pyridin-4-yl)ethyl)phenethyl)pyridine **23**

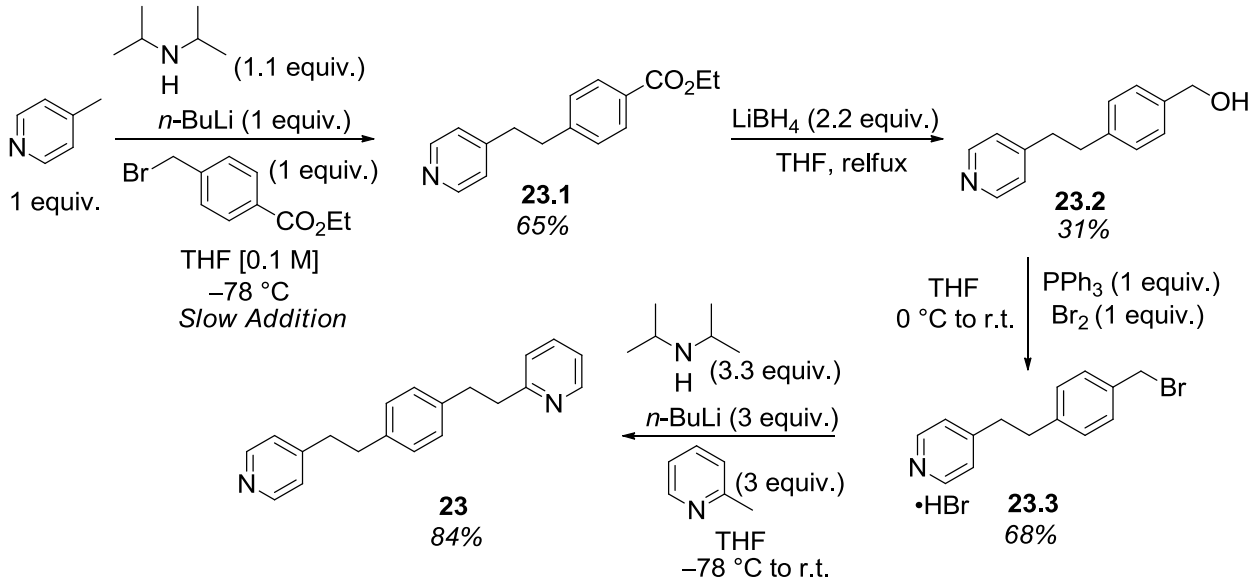

Alkylation of 4-methylpyridine – **23.1** was synthesized according to **Procedure 1** using 4-picoline (0.80 g, 8.6 mmol, 1.0 equiv.) and ethyl-4-bromomethylbenzoate as the electrophile (2.08 g, 8.60 mmol, 1.0 equiv.). The crude mass was purified by flash chromatography to afford **23.1** (CAS: 1802629-62-4) as a white solid (1.43 g, 5.58 mmol, 65% yield). Spectral data is consistent with that reported in the literature.[103]

Chromatography: 80% EtOAc in hexanes (R_f. = 0.46).

Data for **23.1**

^{1}H-NMR (400 MHz, $CDCl_3$)
δ 8.48 (dd, *J* = 4.8, 1.6 Hz, 2 H), 7.95 (d, *J* = 8.4 Hz, 2 H),
7.20 (d, *J* = 8.4 Hz, 2 H), 7.05 (d, *J* = 6.4 Hz, 2 H), 4.36 (q, *J* = 7.2 Hz, 2 H),
3.01-2.91 (m, 4 H), 1.39 (t, *J* =7.2 Hz, 3 H).

^{13}C-NMR (100 MHz, $CDCl_3$)
δ 166.6, 150.0, 149.9, 146.0, 129.9, 128.8, 128.6, 124.0, 61.0, 36.7, 36.6, 14.5.

2-(4-(2-(Pyridin-4-yl)ethyl)phenethyl)pyridine **23**

*Reduction of **23.1*** – A flame-dried round-bottomed flask equipped with a stir bar was charged with a solution of ester **23.1** (1.43 g, 5.58 mmol, 1.0 equiv.) in dry THF (50 mL). $LiBH_4$ (0.15 g, 6.70 mmol, 1.20 equiv.) was then added and the reaction was heated to reflux and left to stir overnight. A second portion of $LiBH_4$ (0.15 g, 6.70 mmol, 1.2 equiv.) was added and after 2 h, the reaction was quenched with a saturated solution of $NaHCO_3$ and extracted with EtOAc three times. The combined organics were washed with brine, dried using $MgSO_4$ and concentrated *in vacuo*. The crude mixture was purified by flash chromatography to afford **23.2** as a white solid (0.36 g, 1.7 mmol, 31% yield).

Chromatography: 100% EtOAc (R_f. = 0.34).

Data for **23.2**

^{1}H-NMR (400 MHz, $CDCl_3$)
δ 8.46 (dd, *J* = 4.8, 1.6 Hz, 2 H), 7.29 (d, *J* = 8.0 Hz, 2 H),
7.14 (d, *J* = 8.0 Hz, 2 H), 7.05 (dd, *J* = 4.8, 1.6 Hz, 2 H), 4.67 (s, 2 H),
2.94-2.91 (m, 4 H), 1.97 (br, 1 H).

^{13}C-NMR (100 MHz, $CDCl_3$)
δ 150.6, 149.8, 140.2, 139.1, 128.7, 127.4, 124.1, 65.2, 36.7, 37.1, 36.3.

IR Alpha-Platinum ATR, Bruker, diamond crystal
υ = 3158, 2879, 1603, 1558 cm^{-1}

HRMS ESI
Calculated mass for $(M+H)^+$ of $C_{14}H_{15}NO$ is 214.1226 found 214.1216.

2-(4-(2-(Pyridin-4-yl)ethyl)phenethyl)pyridine **23**

*Bromination of **23.2*** – A flame-dried round-bottomed flask equipped with a stir bar was charged with triphenylphosphine (0.32 g, 1.2 mmol, 1.0 equiv.) and dry THF (5 mL), and cooled to 0 °C. Bromine (0.06 mL, 1.2 mmol, 1.0 equiv.) was then added dropwise and the mixture was left to stir for 20 min. A solution of alcohol **23.2** (0.26 g, 1.2 mmol, 1.0 equiv.) in THF (7 mL) was introduced at the same temperature and then the flask was allowed to warm to room temperature. After an overnight reaction, the pyridinium salt (**23.3**) precipitated out of the mixture and was isolated using vacuum filtration as a white solid (0.29 g, 0.83 mmol, 68% yield) which was used in the next step without further purification.

Data for **23.3**

^{1}H-NMR (400 MHz, $CDCl_3$)
δ 8.64 (d, *J* = 6.8 Hz, 2 H), 7.62 (d, *J* = 6.8 Hz, 2 H), 7.33 (d, *J* = 8.0 Hz, 2 H), 7.06 (d, *J* = 8.0 Hz, 2 H), 4.67 (s, 2 H), 3.23 (t, *J* = 7.4 Hz, 2 H), 3.06 (t, *J* = 7.4 Hz, 2 H).

^{13}C-NMR (100 MHz, $CDCl_3$)
δ 162.8, 140.2, 138.6, 137.0, 129.8, 128.9, 127.1, 37.9, 35.6, 33.0.

IR Alpha-Platinum ATR, Bruker, diamond crystal
δ = 3370, 3091, 3052, 1634, 1594 cm^{-1}

HRMS ESI
Calculated mass for $(M+H)^+$ of $C_{14}H_{15}Br_2N$ is 355.9644 found $(C_{14}H_{15}BrN+H-HBr)^+$ 276.0400

2-(4-(2-(Pyridin-4-yl)ethyl)phenethyl)pyridine **23**

*Alkylation of **23.3** using 2-methylpyridine* – **23** was synthesized according to **Procedure 1** using 2-picoline (0.23 g, 2.5 mmol, 3.0 equiv.) and **23.3** (0.30 g, 0.82 mmol, 1.0 equiv.) as the electrophile. The product was purified using flash chromatography and obtained as a white solid (0.20 g, 0.69 mmol, 84% yield).

Chromatography: 3% MeOH in EtOAc (R_f. = 0.44).

Data for **23**

^{1}H-NMR (400 MHz, $CDCl_3$)
δ 8.56 (d, *J* = 4.4 Hz, 1 H), 8.48 (dd, *J* = 4.4, 1.6 Hz, 2 H), 7.56 (td, *J* = 7.6, 1.6 Hz, 1 H), 7.13-7.04 (m, 8 H), 3.10-3.01 (m, 4 H), 2.89 (br, 4 H).

13C-NMR (100 MHz, $CDCl_3$)
δ 161.4, 150.7, 149.8, 149.5, 139.6, 138.4, 136.4, 128.7, 128.5, 124.1, 123.1, 121.3, 40.4, 37.2, 36.2, 35.7.

IR Alpha-Platinum ATR, Bruker, diamond crystal
υ = 2922, 2856, 1587, 1566 cm^{-1}

HRMS ESI
Calculated mass for $(M+H)^+$ of $C_{20}H_{20}N_2$ is 289.1699 found 289.1688.

2-Ethyl-4-propylpyridine **24**

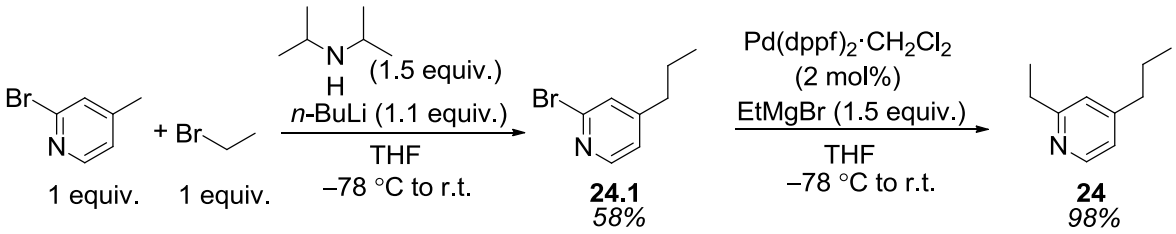

Alkylation of 2-bromo-4-methylpyridine – **24.1** was synthesized according to **procedure 1** using 2-bromo-4-methylpyridine (0.75 g, 4.4 mmol, 1.0 equiv.) and bromoethane as the electrophile (0.71 g, 6.5 mmol, 1.5 equiv.). The product was purified by flash chromatography and obtained as a yellow oil (0.51 g, 2.5 mmol, 58% yield).

Chromatography: 10% EtOAc in hexanes (R_f. = 0.44).

Data for **24.1**

^{1}H-NMR (400 MHz, $CDCl_3$)
δ 8.23 (d, *J* = 4.8 Hz, 1 H), 7.30 (s, 1 H), 7.05 (d, *J* = 4.8 Hz, 1 H),
2.55 (t, *J* = 7.2 Hz, 2 H), 1.65 (sext, *J* = 7.2 Hz, 2 H), 0.94 (t, *J* = 7.2 Hz, 3 H).

^{13}C-NMR (100 MHz, $CDCl_3$)
δ 154.7, 149.8, 142.3, 128.0, 123.1, 36.8, 23.3, 13.6.

IR Alpha-Platinum ATR, Bruker, diamond crystal
υ = 2961, 2932, 2872, 1587, 1540 cm^{-1}

HRMS ESI
Calculated mass for $(M+H)^+$ of $C_8H_{10}BrN$ is 200.0069 found 200.0070.

2-Ethyl-4-propylpyridine **24**

*Kumada coupling of **24.1***– A flame-dried round-bottomed flask equipped with a stir bar was charged with a solution of **24.1** (0.20 g, 1.0 mmol, 1.0 equiv.) in freshly distilled THF (10 mL) under an atmosphere of argon then cooled to −78 °C. $Pd(dppf)_2Cl_2 \bullet CH_2Cl_2$ (0.016 g, 0.020 mmol, 2 mol%) was introduced and the reaction mixture was allowed to stir for 5 min. at −78 °C. Ethylmagnesium bromide (0.78 mL, 1.5 mmol, 1.5 equiv., 2.0 M) was then added dropwise over 10 min. The resulting solution was stirred for 2 h at −78 °C then slowly warmed to room temperature. The reaction was monitored by TLC and upon completion was quenched with water. The aqueous phase was extracted with EtOAc three times and the combined organics were washed with brine, dried over $MgSO_4$ and concentrated *in vacuo*. The crude mixture was purified by silica gel chromatography to afford **24** as a yellow oil (0.14 g, 0.98 mmol, 98% yield).

Chromatography: 20% EtOAc in hexanes (R_f. = 0.50).

Data for **24**

^{1}H-NMR	(400 MHz, $CDCl_3$) δ 8.36 (d, *J* = 5.0 Hz, 1 H), 6.94 (s, 1 H), 6.88 (d, *J* = 5.0 Hz, 1 H), 2.76 (q, *J* = 7.2 Hz, 2 H), 2.51 (t, *J* = 7.6 Hz, 2 H), 1.62 (sext, *J* = 7.6 Hz, 2 H), 1.27 (t, *J* = 7.2 Hz, 3 H), 0.91 (d, *J* = 7.6 Hz, 3 H).
^{13}C-NMR	(100 MHz, $CDCl_3$) δ 163.2, 151.7, 148.8, 122.1, 121.1, 37.2, 31.2, 23.4, 13.9, 13.6.
IR	Alpha-Platinum ATR, Bruker, diamond crystal υ = 2963, 2933, 2873, 1603, 1559 cm^{-1}
HRMS	ESI Calculated mass for $(M+H)^+$ of $C_{10}H_{15}N$ is 150.1277 found 150.1271.

3.3 Optimization study.

We aimed at developing a two-step protocol for pyridylic allylation that avoids the isolation of the alkylidene dihydropyridine intermediate by aqueous work-up. We envisioned that this would not only expedite the ligand screening process but also be an efficient way to conduct substrate scope studies. For this purpose, the two steps of the method were optimized individually.

Part A: Summary of optimization of the synthesis of alkylidene dihydropyridine

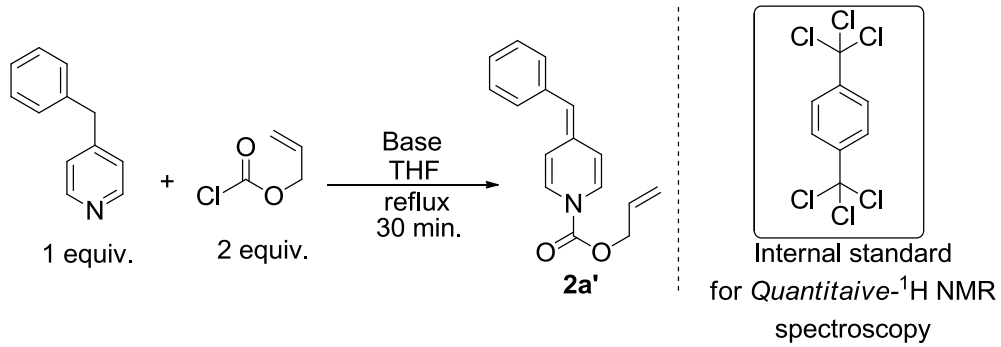

Entry	Base	Equiv.	Isolation Procedure	Q-NMR Yield
1	Et_3N	1	Salt filtration (trituration)	61 %
2	Et_3N	1	Water workup	62 %
3	Et_3N	2	Salt filtration (trituration)	77 %
4	***DBU***	***2***	***Phosphate buffer workup (pH = 5.5)***	***96 %***

Procedure 3: Optimal procedure for the preparation of alkylidene dihydropyridine

4-Benzylpyridine (0.10 g, 0.59 mmol, 1.0 equiv.) and diazabicyclo[5.4.0]undec-7-ene (0.17 g, 1.09 mmol, 2.0 equiv.) were dissolved in dry THF (6 mL) in a two-neck round-bottomed flask equipped with a stir bar and a condenser. The solution was heated to reflux and allyl chloroformate (0.13 g, 1.09 mmol, 1.0 equiv.) was added dropwise. Upon completion (30 min.), the reaction mixture was

diluted with EtOAc and washed with pH 5.5 phosphate buffer three times. The organic phase was then washed with brine, dried over $MgSO_4$ and concentrated *in vacuo* to afford crude **2a'**. The yield was found to be 96% by quantitative ^{1}H-NMR using 1,4-bis(trichloromethyl)benzene as an internal standard.

Part B: Ligand Screen

To expedite the ligand-screening process, pyridine **1** was subjected to optimal reaction conditions for alkylidene dihydropyridine formation as described in **procedure 3**. The resulting crude **1a'** was weighed and split into equal portions by mass; each portion was subjected to $Pd(dba)_2$ (5 mol%) and a phosphine ligand (1 :2 Pd :P) in THF at room temperature under an atmosphere of argon. Each reaction mixture was left to stir overnight then concentrated *in vacuo*. The yields (reported over two steps) of allylation **1a** and elimination **1b** products were determined by quantitative ^{1}H-NMR using 1,4-bis(trichloromethyl)benzene as an internal standard.

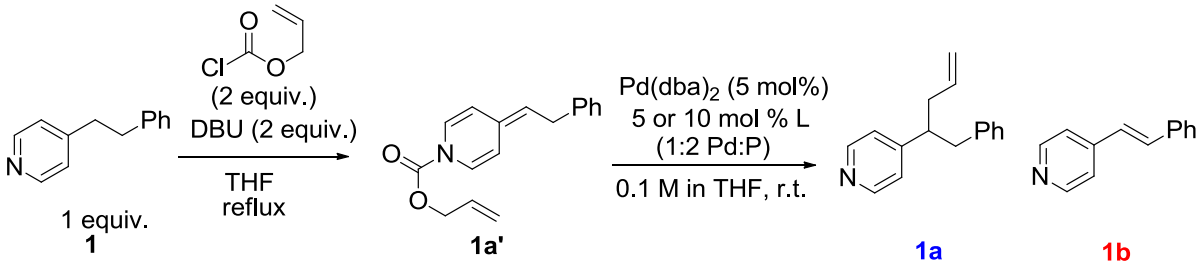

1) no ligand 0%, 25%

2) PPh_3 73%, 0%

3) P(*o*-tol)$_3$ 23%, 0%

4) P(2-furyl)$_3$ 48%, 17%

5) P(t-Bu)$_3$ 24%, 13%

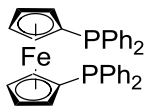

14) dppf: 68%, 0%

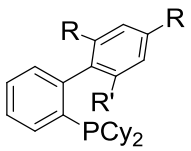

6) R & R' = *i-Pr*: 71%, 0%

7) R = H, R' = NMe_2: 48%, 0%

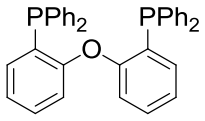

13) DPEPhos: 73%, 0%

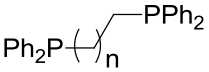

8) n = 1: 31%, 15%

9) n = 2: 22%, 41%

10) n = 3: 42%, 0%

11) n = 4: 63%, 0%

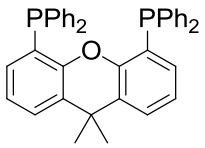

12) XantPhos: 75%, 0%

Triphenylphosphine (entry 2) and bidentate ligands with large bite angles (entries 12-14) provided the allylation product **1a** in good yields. Since complexes with bidentate ligands should display greater stability than those with monodentate ligands, Xantphos was our ligand of choice in future reaction development.

Since the yields obtained in the ligand screen were based off quantitative ^{1}H NMR spectroscopy, the allylation reaction of **1** was repeated following the two-step protocol listed above and using Xantphos as ligand. The resulting product **1a** was purified using flash chromatography and isolated in *78%* yield. We hypothesized that the yield could be further improved by eliminating the work-up steps after both the dihydropyridine formation and allylation reaction. Therefore, we implemented the following adjustments that provided the allylation product **1a** in *92%* isolated yield using 1 mol% catalyst loading:

1) 3 equivalents of triethylamine were used as base in the dihydropyridine formation which allowed a) the full conversion of the starting pyridine **1** to the dihydropyridine intermediate **1a′**, and b) isolation of **1a′** by trituration with diethyl ether thereby avoiding the buffer workup required to remove DBU
2) No work-up was done after the allylation step; the reaction mixture was concentrated and directly purified using flash chromatography

This improved protocol (detailed in **procedure 4**) was used to conduct substrate scope studies.

3.4 Pd-catalyzed pyridylic allylation of 4-alkylpyridines

Procedure 4: General procedure of Pd-catalyzed pyridylic allylation of 4-alkylpyridines

Synthesis of the alkylidene dihydropyridine intermediate: Triethylamine (3.0 equiv.) was added to a solution of the appropriate pyridine (1.0 equiv.) in dry THF (0.1 M) in a two-neck round-bottomed flask equipped with a stir bar. The resulting solution was stirred at room temperature and allyl chloroformate (2.0 equiv.) was added dropwise. Upon disappearance of the starting pyridine, the mixture was concentrated *in vacuo*. The resulting crude mass was suspended in diethyl ether and filtered through a plug of cotton to remove triethylammonium chloride salt. The filtrate was concentrated *in vacuo* to afford a yellow oil which was used in the next step without further purification.

Palladium-catalyzed decarboxylative allylation: To an oven-dried round-bottomed flask equipped with a stir bar, Xantphos (1 mol%) and $Pd(dba)_2$ (1 mol%) were taken. To this flask, freshly distilled THF was added and the resulting solution was allowed to stir for 10 minutes at room temperature under an inert atmosphere of argon. A solution of the alkylidene dihydropyridine intermediate in dry THF was then added to the flask containing the catalyst and the mixture was stirred at room temperature. The reaction was monitored by TLC and upon completion the reaction mixture was concentrated *in vacuo* and purified using flash chromatography, eluting with the indicated solvent mixture to afford the desired product.

4-(1-Phenylbut-3-en-1-yl)pyridine **1a** (CAS: 856856-59-2)

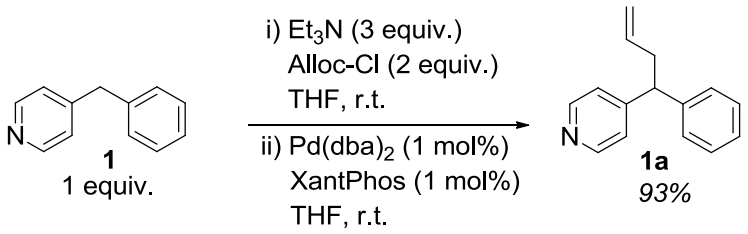

Using **Procedure 4,** 4-benzylpyridine (0.20 g, 1.2 mmol, 1.0 equiv.) provided product **1a** (0.23 g, 1.1 mmol, 93% yield) as a yellow oil. Spectral data of this compound is consistent with that reported in the literature.[82]

Chromatography: 15% acetone in hexane (R_f. = 0.25).

^{1}H-NMR (400 MHz, $CDCl_3$)
δ 8.49 (d, *J* = 5.8 Hz, 2 H), 7.32-7.29 (m, 2 H), 7.23-7.20 (m, 2 H), 7.15 (d, *J* = 5.8 Hz, 2 H), 5.68 (ddt, *J* = 17.0, 10.4, 7.2 Hz, 1 H), 5.04 (d, *J* = 17.0 Hz, 1 H), 4.98 (d, *J* = 10.4 Hz, 1 H), 3.99 (t, *J* = 7.6 Hz, 1 H), 2.81 (t, *J* = 7.2 Hz, 2 H).

^{13}C-NMR (100 MHz, $CDCl_3$)
δ 153.2, 149.8, 142.6, 135.8, 135.7, 128.6, 127.9, 126.8, 123.3, 117.0, 50.5, 39.1.

4-(1-Phenylpent-4-en-2-yl)pyridine **2a**

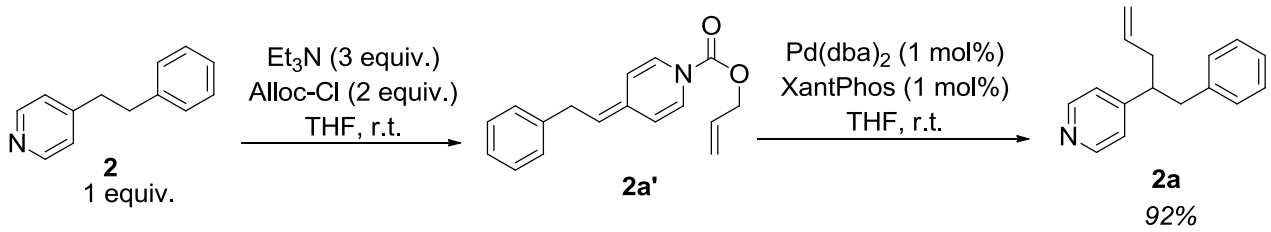

Using **Procedure 4**, pyridine **2** (0.20 g, 1.09 mmol, 1.0 equiv.) provided product **2a** (0.23 g, 1.01 mmol, 93% yield) as a yellow oil.

Chromatography: 20% EtOAc in hexane (R_f. = 0.30).

Data for **2a′**

^{1}H-NMR (300 MHz, $CDCl_3$, at 45°C)
δ 7.28-7.16 (m, 5 H), 6.96 (d, *J* = 5.7 Hz, 1 H), 6.81 (d, *J* = 6.3 Hz, 1 H), 6.01-5.88 (m, 2 H), 5.68 (d, *J* = 7.2 Hz, 1 H), 6.35 (d, *J* = 17.4 Hz, 1 H), 5.28 (d, *J* = 10.2 Hz, 1 H), 4.97 (t, *J* = 7.8 Hz, 1 H), 4.71 (d, *J* = 5.7 Hz, 1 H), 3.38 (d, *J* = 7.8 Hz, 1 H)

^{13}C-NMR (75 MHz, $CDCl_3$, at 52°C)
δ 150.4, 141.2, 131.6, 128.5, 128.3, 128.2, 125.8, 124.6, 122.4, 118.7, 115.6, 114.4, 109.0, 67.3, 33.1

IR Alpha-Platinum ATR, Bruker, diamond crystal
υ = 3026, 1719, 1673, 1300, 1285, 1192, 1127, 1102, 966, 937 cm^{-1}

HRMS ESI
Calculated mass for $(M+H)^+$ of $C_{17}H_{17}NO_2$ is 268.1332, found 268.1328.

Data for **2a**

^{1}H-NMR (400 MHz, $CDCl_3$)

δ 8.45 (d, *J* = 5.6 Hz, 2 H), 7.24-7.13 (m, 3 H), 7.01-7.00 (m, 4 H),
5.63 (dddd, *J* =17.2, 10.4, 6.8, 6.8 Hz, 1 H), 4.97 (d, *J* = 17.2 Hz, 1 H),
4.96 (d, *J* = 10.4 Hz, 1 H), 2.99 (dd, *J* = 12.4, 6.8 Hz, 1 H),
2.97-2.89 (m, 1 H), 2.83 (dd, *J* = 12.4, 7.4 Hz, 1 H), 2.50-2.36 (m, 2 H)

^{13}C-NMR (100 MHz, $CDCl_3$)

δ 153.3, 149.6, 139.3, 136.7, 136.6, 129.1, 128.2, 126.2, 123.3, 117.1, 47.2, 41.9, 39.2.

IR Alpha-Platinum ATR, Bruker, diamond crystal

υ = 3064, 3026, 2923, 1640, 1597, 1557, 1495, 1453, 1413, 910 cm^{-1}

HRMS ESI

Calculated mass for $(M+H)^+$ of $C_{13}H_{17}N$ is 224.1434, found 224.1424.

4-(Oct-1-en-4-yl)pyridine **3a**

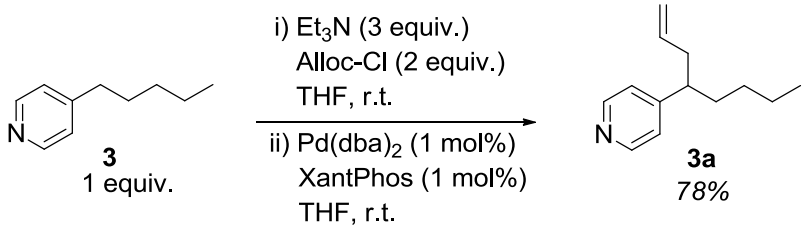

Using **Procedure 4,** pyridine **3** (0.30 g, 2.0 mmol, 1.0 equiv.) provided product **3a** (0.29 g, 1.6 mmol, 78% yield) as a yellow oil.

Chromatography: 20% EtOAc in Hexane (R_f. = 0.40).

^{1}H-NMR (400 MHz, $CDCl_3$)
δ 8.48 (d, *J* = 5.6 Hz, 2 H), 7.05 (d, *J* = 5.6 Hz, 2 H),
5.59 (dddd, *J* = 17.2, 10.0, 7.2, 7.2 Hz, 1 H), 4.92 (d, *J* = 17.2 Hz, 1 H),
4.91 (d, *J* = 10.0 Hz, 1 H), 2.61-2.54 (m, 1 H), 2.40-2.26 (m, 2 H), 1.73-1.64 (m, 1 H),
1.56-1.44 (m, 1 H), 1.31-1.08 (m, 2 H), 0.81 (t, *J* = 7.2 Hz, 3 H).

^{13}C-NMR (100 MHz, $CDCl_3$)
δ 154.4, 149.6, 136.0, 123.2, 116.5, 45.3, 40.5, 34.9, 29.4, 22.6, 13.9.

IR Alpha-Platinum ATR, Bruker, diamond crystal
υ = 3069, 2957, 2927, 2858, 1640, 1597, 1557, 1492, 1465, 1378, 912 cm^{-1}

HRMS ESI
Calculated mass for $(M+H)^+$ of $C_{13}H_{19}N$ is 190.1590, found 190.1582.

4-(4-Allyloct-1-en-4-yl)pyridine **3aa**

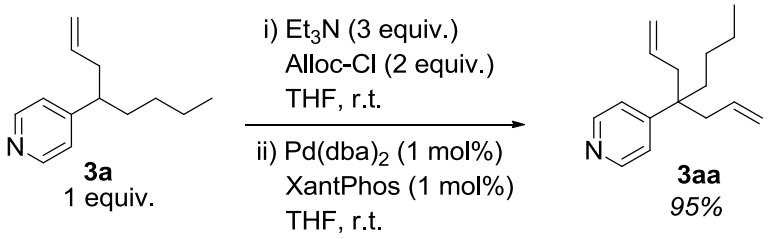

Using **Procedure 4,** pyridine **3a** (0.250 g, 1.32 mmol, 1.0 equiv.) provided product **3aa** (0.290 g, 1.25 mmol, 95% yield) as a colorless oil.

Chromatography: 14% EtOAc in hexanes (R_f. = 0.30).

^{1}H-NMR (600 MHz, $CDCl_3$)
δ 8.52 (d, *J* = 6.0 Hz, 2 H), 7.20 (d, *J* = 6.0 Hz, 2 H),
5.51 (ddt, *J* = 16.2, 10.8, 7.2 Hz, 2 H), 5.00 (d, *J* = 10.8 Hz, 2 H),
5.01 (d, *J* = 16.2 Hz, 2 H), 2.42 (d, *J* = 7.2 Hz, 4 H), 1.64-1.61 (m, 2 H),
1.21 (sext, *J* = 7.2 Hz, 2 H), 1.03-0.96 (m, 2 H), 0.82 (t, *J* = 7.2 Hz, 3 H).

^{13}C-NMR (100 MHz, $CDCl_3$)
δ 155.9, 149.6, 133.6, 122.1, 118.1, 43.5, 41.0, 37.1, 25.4, 23.1, 13.9.

IR Alpha-Platinum ATR, Bruker, diamond crystal
υ = 3076, 2956, 2931, 2862, 1639, 1595, 1455, 1410, 995, 912, 730 cm^{-1}

HRMS ESI
Calculated mass for $(M+H)^+$ of $C_{16}H_{23}N$ is 230.1903, found 230.1898.

4-(Hepta-1,6-dien-4-yl)pyridine **4a**

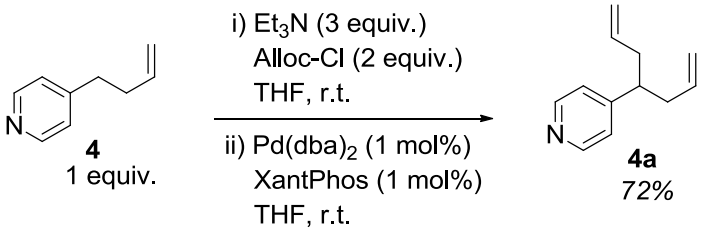

Using **Procedure 4,** pyridine **4** (0.20 g, 1.5 mmol, 1.0 equiv.) provided product **4a** (0.19 g, 1.1 mmol, 72% yield) as a yellow oil.

Chromatography: 25% EtOAc in hexanes (R_f. = 0.30).

^{1}H-NMR (400 MHz, $CDCl_3$)
δ 8.50 (d, *J* = 5.4 Hz, 2 H), 7.07 (d, *J* = 5.4 Hz, 2 H),
5.62 (dddd, *J* = 16.4, 10.8, 7.2, 7.2 Hz, 2 H), 4.97 (dd, *J* = 16.4, 1.2 Hz, 1 H),
4.96 (d, *J* = 10.8 Hz, 1 H), 2.75-2.68 (m, 1 H), 2.47-2.30 (m, 4 H).

^{13}C-NMR (100 MHz, $CDCl_3$)
δ 153.4, 149.6, 135.5, 123.2, 116.9, 44.9, 39.4.

IR Alpha-Platinum ATR, Bruker, diamond crystal
υ = 3075, 2923, 1640, 1597, 1413, 993, 911, 784 cm^{-1}

HRMS ESI
Calculated mass for $(M+H)^+$ of $C_{12}H_{15}N$ is 174.1277, found 174.1275.

4-(Hept-1-en-6-yn-4-yl)pyridine **5a**

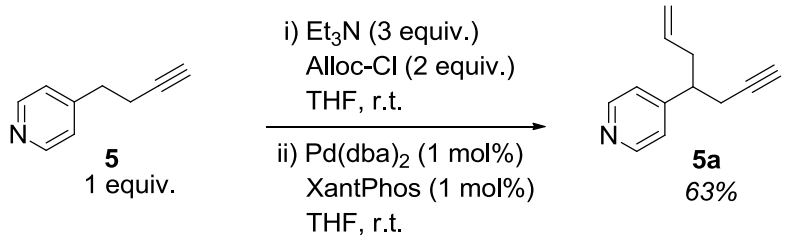

Using **Procedure 4,** pyridine **5** (0.20 g, 1.5 mmol, 1.0 equiv.) provided product **5a** (0.16 g, 0.96 mmol, 63% yield) as a yellow oil.

Chromatography: 33% EtOAc in toluene (R_f. = 0.35).

^{1}H-NMR (400 MHz, $CDCl_3$)
δ 8.53 (d, *J* = 6.0 Hz, 2 H), 7.14 (d, *J* = 6.0 Hz, 2 H),
5.63 (dddd, *J* = 17.2, 10.0, 6.8, 6.8 Hz, 1 H), 5.03 (d, *J* = 17.2, 1 H),
5.03 (d, *J* = 10.0, 1 H), 2.90-2.83 (m, 1 H), 2.62-2.39 (m, 4 H),
1.96 (t, *J* = 2.8 Hz, 1 H).

^{13}C-NMR (100 MHz, $CDCl_3$)
δ 152.2, 149.8, 149.7, 135.0, 134.9, 123.0, 117.6, 81.5, 70.4, 43.6, 38.5, 24.3.

IR Alpha-Platinum ATR, Bruker, diamond crystal
υ = 3298, 2912, 1640, 1599, 1557, 1414, 994, 917, 816 cm^{-1}

HRMS ESI
Calculated mass for $(M+H)^+$ of $C_{12}H_{13}N$ is 172.1121, found 172.1121.

4-(7-((*tert*-Butyldimethylsilyl)oxy)hept-1-en-4-yl)pyridine **6**

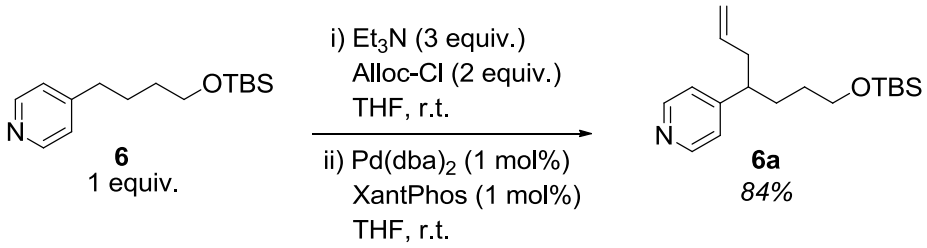

Using **Procedure 4,** pyridine **6** (0.40 g, 1.5 mmol, 1.0 equiv.) provided product **6a** (0.38 g, 1.3 mmol, 84% yield) as a colorless oil.

Chromatography: 40% EtOAc in hexanes (R_f. = 0.40).

^{1}H-NMR (400 MHz, $CDCl_3$)
δ 8.50 (d, *J* = 5.6 Hz, 2 H), 7.07 (d, *J* = 5.6 Hz, 2 H),
5.61 (dddd, *J* = 17.2, 10.4, 7.2, 7.2 Hz, 1 H), 4.95 (d, *J* = 17.2 Hz, 1 H),
4.94 (d, *J* = 10.4 Hz, 1 H), 3.54 (t, *J* = 6.4 Hz, 2 H), 2.65-2.58 (m, 1 H),
2.40-2.31 (m, 2 H), 2.81-2.74 (m, 1 H), 1.65-1.57 (m, 1 H), 1.41-1.31 (m, 2 H),
0.87 (s, 9 H), 0.01 (d, *J* = 2.0 Hz, 6 H).

^{13}C-NMR (100 MHz, $CDCl_3$)
δ 154.2, 149.7, 135.9, 123.3, 116.7, 62.8, 45.1, 40.6, 31.4, 30.5, 25.9, 18.3,
5.34.

^{29}Si-NMR 18.78

IR Alpha-Platinum ATR, Bruker, diamond crystal
υ = 3070, 2951, 2928, 2856, 1641, 1597, 1471, 1413, 1253, 1096, 912, 773 cm^{-1}

HRMS ESI
Calculated mass for $(M+H)^+$ of $C_{18}H_{31}NOSi$ is 306.2248, found 306.2240.

7-(Pyridin-4-yl)dec-9-enenitrile **7a**

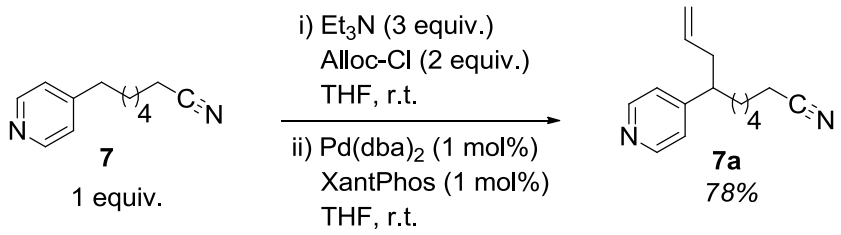

Using **Procedure 4,** pyridine **7** (0.19 g, 1.0 mmol, 1.0 equiv.) provided product **7a** (0.18 g, 0.78 mmol, 78% yield) as a yellow oil.

Chromatography: 67% EtOAc in hexanes (R_f. = 0.30).

^{1}H-NMR (400 MHz, $CDCl_3$)
δ 8.50 (d, *J* = 5.2 Hz, 2 H), 7.06 (d, *J* = 5.2 Hz, 2 H),
5.60 (dddd, *J* = 17.2, 10.4, 7.2, 7.2 Hz, 1 H), 4.95 (d, *J* = 17.2 Hz, 1 H),
4.94 (d, *J* = 10.4 Hz, 1 H), 2.63-2.55 (m, 1 H), 2.40-2.31 (m, 2 H),
2.28 (t, *J* = 7.2 Hz, 2 H), 1.72-1.67 (m, 1 H), 1.62-1.54 (m, 3 H),1.44-1.24 (m, 2 H), 1.20-1.11 (m, 2 H).

^{13}C-NMR (100 MHz, $CDCl_3$)
δ 154.0, 149.8, 135.7, 123.1, 119.6, 116.8, 45.2, 40.5, 34.8, 28.5, 26.5, 25.1, 17.1.

IR Alpha-Platinum ATR, Bruker, diamond crystal
υ = 3071, 2854, 1640, 1558 cm^{-1}

HRMS ESI
Calculated mass for $(M+H)^+$ of $C_{15}H_{20}N_2$ is 229.1699, found 229.1686.

4-(1-(1,3-Dioxolan-2-yl)hex-5-en-3-yl)pyridine **8a**

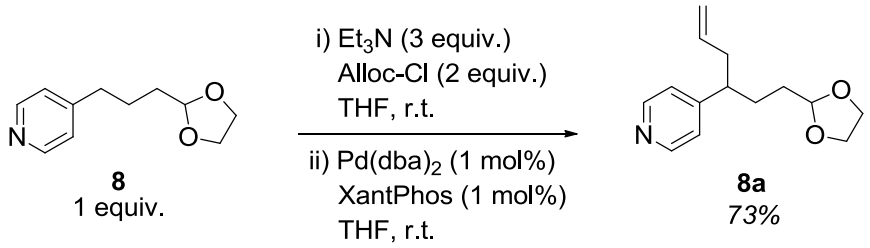

Using **Procedure 4,** pyridine **8** (0.25 g, 1.29 mmol, 1.0 equiv.) provided product **8a** (0.22 g, 0.94 mmol, 73% yield) as a colorless oil.

Chromatography: 80% EtOAc in toluene (R_f. = 0.40).

^{1}H-NMR (400 MHz, $CDCl_3$)
δ 8.51 (br, 2 H), 7.08 (d, *J* = 5.2 Hz, 2 H),
5.60 (dddd, *J* = 16.8, 9.6, 6.8, 6.8 Hz, 1 H), 4.97 (d, *J* = 16.8 Hz, 1 H),
4.95 (d, *J* = 9.6 Hz, 1 H), 4.79 (t, *J* = 4.8 Hz, 1 H), 3.94-3.80 (m, 4 H),
2.43-2.28 (m, 2 H), 1.87-1.82 (m, 1 H),1.72-1.61 (m, 1 H), 1.58-1.40 (m, 2 H).

^{13}C-NMR (100 MHz, $CDCl_3$)
δ 153.7, 149.8, 135.6, 123.2, 116.8, 104.2, 64.9, 64.8, 45.1, 40.5, 31.6, 29.2.

IR Alpha-Platinum ATR, Bruker, diamond crystal
υ = 3071, 2882, 1640, 1598 cm^{-1}

HRMS ESI
Calculated mass for $(M+H)^+$ of $C_{14}H_{19}NO_2$ is 234.1489, found 234.1487.

4-(1-(2-Bromophenyl)pent-4-en-2-yl)pyridine **9a**

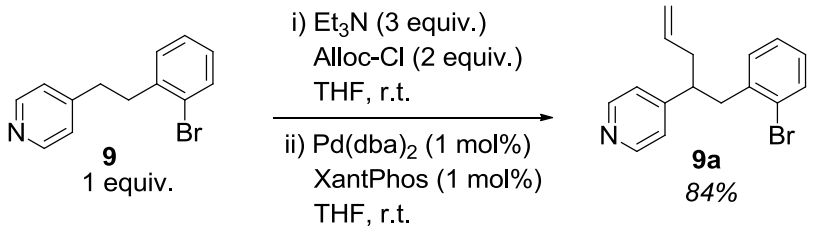

Using **Procedure 4,** pyridine **9** (0.20 g, 0.76 mmol, 1.0 equiv.) provided product **9a** (0.19 g, 0.64 mmol, 84% yield) as a colorless oil.

Chromatography: 50% EtOAc in toluene (R_f. = 0.30).

^{1}H-NMR (400 MHz, $CDCl_3$)
δ 8.45 (d, *J* = 5.2 Hz, 2 H), 7.51 (d, *J* = 7.6 Hz, 1 H), 7.09-7.01 (m, 4 H), 6.85 (d, *J* = 7.6 Hz, 1 H), 5.68 (dddd, *J* = 16.8, 10.0, 6.8, 6.8 Hz, 1 H), 5.00 (d, *J* = 16.8 Hz, 1 H), 4.96 (d, *J* = 10.0 Hz, 1 H), 3.16 (dd, *J* = 13.2, 6.8 Hz, 1 H), 3.12-3.05 (m, 1 H), 2.88 (dd, *J* = 13.2, 8.0 Hz, 1 H), 2.51-2.46 (m, 2 H).

^{13}C-NMR (100 MHz, $CDCl_3$)
δ 152.9, 149.7, 138.7, 135.5, 135.5, 132.9, 131.4, 128.0, 127.1, 124.6, 123.5, 123.3, 117.1, 45.1, 42.3, 39.1.

IR Alpha-Platinum ATR, Bruker, diamond crystal
υ = 3068, 2924, 1639, 1597, 1493, 1470, 1438, 1023, 913, 746 cm^{-1}

HRMS ESI
Calculated mass for $(M+H)^+$ of $C_{16}H_{16}BrN$ is 302.0539, found 302.0540.

2-Bromo-5-(2-(pyridin-4-yl)pent-4-en-1-yl)pyridine **10a**

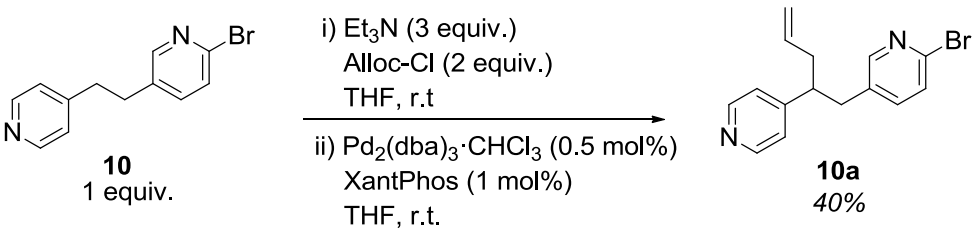

Using **procedure 4,** pyridine **10** (0.075 g, 0.28 mmol, 1.0 equiv.) provided product **10a** (0.035 g, 0.11 mmol, 40% yield) as a colorless oil.

Chromatography: 60-70% EtOAc in hexanes (R_f. = 0.30).

^{1}H-NMR (400 MHz, $CDCl_3$)

δ 8.48 (d, *J* = 4.8 Hz, 2 H), 8.03 (d, *J* = 2.0 Hz, 1 H), 7.28 (d, *J* = 8.4 Hz, 1 H), 7.07 (dd, *J* = 8.4, 2.0 Hz, 1 H), 6.97 (d, *J* = 4.8 Hz, 2 H), 5.67 (dddd, *J* = 17.2, 9.6, 7.2, 7.2 Hz, 1 H), 5.02 (d, *J* = 17.2 Hz, 1 H), 5.01 (d, *J* = 9.6 Hz, 1 H), 2.98 (dd, *J* = 13.2, 5.6 Hz, 1 H), 2.91-2.84 (m, 1 H), 2.77 (dd, *J* = 13.2, 8.8 Hz, 1 H), 2.47-2.37 (m , 2 H).

^{13}C-NMR (100 MHz, $CDCl_3$)

δ 151.9, 150.5, 149.9, 139.9, 139.0, 134.8, 134.0, 127.5, 123.1, 117.7, 46.7, 39.3, 37.9.

IR Alpha-Platinum ATR, Bruker, diamond crystal

υ = 3071.8, 2924.7, 1733.4, 1640.1, 1454.8, 1045.5, 915.6, 815.9 cm^{-1}

HRMS ESI

Calculated mass for $(M+H)^+$ of $C_{15}H_{15}BrN_2$ is 303.0491 found 303.0497.

3-(Pyridin-4-yl)hex-5-enal **12a**

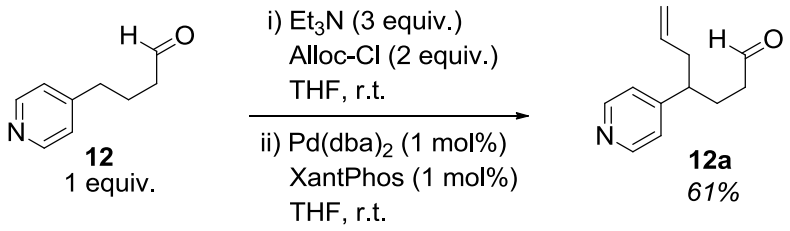

Using **Procedure 4,** pyridine **12** (0.10 g, 0.67 mmol, 1.0 equiv.) provided product **12a** (0.08 g, 0.4 mmol, 61% yield) as a yellow oil.

Chromatography: 70% EtOAc in hexanes (R_f. = 0.30).

^{1}H-NMR (400 MHz, $CDCl_3$)

δ 9.67 (s, 1 H), 8.51 (d, *J* = 5.2 Hz, 2 H), 7.05 (d, *J* = 5.2 Hz, 2 H), 5.60 (dddd, *J* =17.2, 10.0, 6.8, 6.8 Hz, 1 H), 4.96 (d, *J* = 17.2 Hz, 1 H), 4.95 (d, *J* = 10.0 Hz, 1 H), 2.67-2.60 (m, 1 H), 2.39-2.34 (m, 2 H), 2.31-2.27 (m, 2 H), 2.12-2.04 (m, 1 H), 1.87-1.80 (m, 1 H).

^{13}C-NMR (100 MHz, $CDCl_3$)

δ 201.4, 152.9, 149.9, 135.2, 123.1, 117.2, 44.4, 41.6, 40.4, 27.1.

IR Alpha-Platinum ATR, Bruker, diamond crystal

υ = 3074, 2924, 1713, 1640, 1598 cm^{-1}

HRMS ESI

Calculated mass for $(M+H)^+$ of $C_{12}H_{15}NO$ is 190.1226, found 190.1220.

4-(Pyridin-4-yl)hept-6-en-2-one **13a**

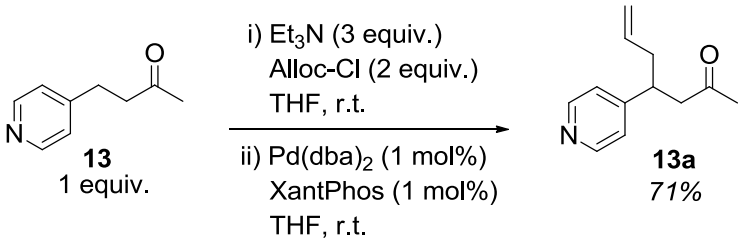

Using **Procedure 4,** pyridine **13** (0.15 g, 1.0 mmol, 1.0 equiv.) provided product **13a** (0.13 g, 0.71 mmol, 71% yield) yield as a yellow oil.

Chromatography: 100% EtOAc (R_f. = 0.40).

^{1}H-NMR (400 MHz, $CDCl_3$)
δ 8.50 (d, *J* = 5.2 Hz, 2 H), 7.11 (d, *J* = 5.2 Hz, 2 H),
5.60 (ddt, *J* =16.2, 9.2, 7.2 Hz, 1 H), 4.98 (d, *J* =16.8 Hz, 1 H),
4.97 (d, *J* = 9.2 Hz, 1 H), 3.27 (m, 1 H), 2.83-2.69 (m, 2 H),
2.35 (t, *J* = 7.2 Hz, 2 H), 2.07 (s, 3 H).

^{13}C-NMR (100 MHz, $CDCl_3$)
δ 206.4, 153.1, 150.0, 149.9, 135.0, 122.9, 117.5, 48.3, 39.9, 39.6, 30.5.

IR Alpha-Platinum ATR, Bruker, diamond crystal
υ = 3070, 2980, 1729, 1641, 1599 cm^{-1}

HRMS ESI
Calculated mass for $(M+H)^+$ of $C_{12}H_{15}NO$ is 190.1226, found 190.1226.

Ethyl 3-(pyridin-4-yl)hex-5-enoate **14a**

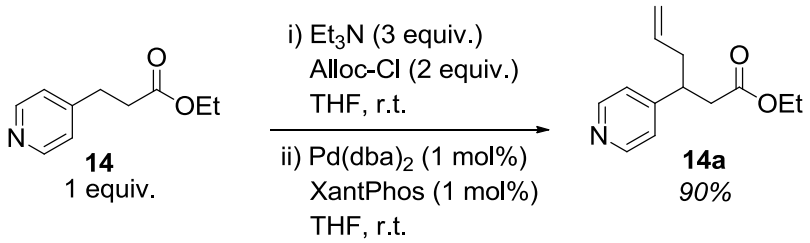

Using **Procedure 4,** pyridine **14** (0.18 g, 1.0 mmol, 1.0 equiv.) provided product **14a** (0.20 g, 0.90 mmol, 90% yield) as a yellow oil.

Chromatography: 60% EtOAc in hexanes (R_f. = 0.25).

^{1}H-NMR (400 MHz, $CDCl_3$)
δ 8.51 (d, *J* = 5.2 Hz, 2 H), 7.12 (d, *J* = 5.2 Hz, 2 H),
5.62 (ddt, *J* = 16.8, 9.2, 7.2 Hz, 1 H),
5.01 (d, *J* = 16.8 Hz, 1 H), 5.00 (d, *J* = 9.2 Hz, 1 H), 4.03 (q, *J* = 7.2 Hz, 2 H),
3.24-3.17 (m, 1 H), 2.72-2.67 (m, 1 H), 2.59-2.53 (m, 1 H), 2.38 (t, *J* = 7.2 Hz, 2 H),
1.14 (t, *J* = 7.2 Hz, 3 H)

^{13}C-NMR (100 MHz, $CDCl_3$)
δ 171.6, 152.5, 149.9, 134.8, 122.9, 117.7, 60.5, 41.1, 39.9, 39.5, 14.1.

IR Alpha-Platinum ATR, Bruker, diamond crystal
υ = 3071, 2931, 2245, 1640, 1598 cm^{-1}

HRMS ESI
Calculated mass for $(M+H)^+$ of $C_{13}H_{17}NO_2$ is 220.1332, found 220.1326.

4-(2-(Pyridin-4-yl)pent-4-en-1-yl)morpholine **16a**

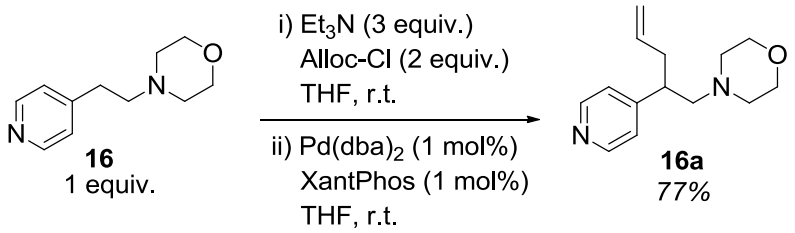

Using **Procedure 4,** pyridine **16** (0.19 g, 1.0 mmol, 1.0 equiv.) provided product **16a** (0.18 g, 0.77 mmol, 77% yield) as a yellow oil.

Chromatography: 5% Et_3N : 60% EtOAc : 35% hexane (R_f. = 0.40).

^{1}H-NMR (400 MHz, $CDCl_3$)
δ 8.50 (d, *J* = 5.6 Hz, 2 H), 7.09 (d, *J* = 5.6 Hz, 2 H),
5.62 (dddd, *J* = 17.2, 10.8, 7.2, 7.2 Hz, 1 H), 4.95 (d, *J* = 17.2 Hz, 1 H),
4.94 (d, *J* = 10.8 Hz, 1 H), 3.62 (t, *J* = 4.4 Hz, 4 H), 2.91-2.84 (m, 1 H),
2.58-2.48 (m, 3 H), 2.40 (t, *J* = 4.4 Hz, 4 H), 2.35-2.27 (m, 1 H).

^{13}C-NMR (100 MHz, $CDCl_3$)
δ 152.9, 149.7, 135.6, 135.6, 123.4, 116.9, 66.9, 63.5, 53.9, 42.6, 37.9.

IR Alpha-Platinum ATR, Bruker, diamond crystal
υ= 3071, 2854, 1640, 1558 cm^{-1}

HRMS ESI
Calculated mass for $(M+H)^+$ of $C_{14}H_{20}N_2O$ is 233.1648, found 133.1646.

Ethyl 4-(hept-1-en-4-yl)nicotinate **17a**

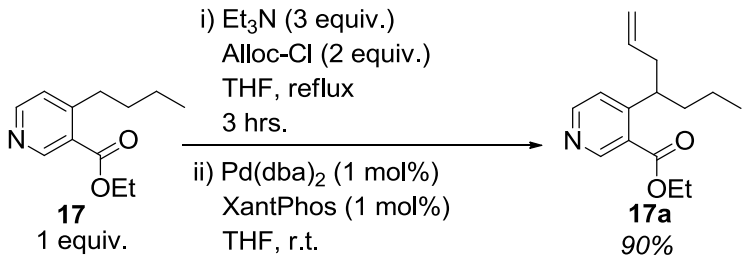

Using **procedure 4** with some modification, pyridine **17** (0.15 g, 0.72 mmol, 1.0 equiv.) in THF (7 mL) was reacted with Et_3N (0.22 g, 2.16 mmol, 3.0 equiv.) and Alloc-Cl (0.17 g, 1.4 mmol, 2.0 equiv.) under reflux for 3 h. The reaction mixture was cooled to room temperature and concentrated under reduced pressure. The resulting crude mass was suspended in diethyl ether and filtered through a plug of cotton to remove triethylammonium chloride salt. The filtrate was concentrated *in vacuo* to afford the corresponding alkylidene dihydropyridine as a yellow oil. The alkylidene dihydropyridine was reacted with a $Pd(dba)_2$ (4 mg, 0.007 mmol, 1 mol%) - XantPhos (4 mg, 0.007 mmol, 1 mol%) catalytic system in THF at room temperature to furnish product **17a** (0.16 g, 0.65 mmol, 90% yield) as a yellow oil.

Chromatography: 20% EtOAc in hexanes (R_f. = 0.30).

^{1}H-NMR (400 MHz, $CDCl_3$)
δ 8.93 (s, 1 H), 8.60 (d, *J* = 5.2 Hz, 1 H), 7.24 (d, *J* = 5.2 Hz, 1 H), 5.65 (dddd, *J* = 16.8, 9.6, 6.8, 6.8 Hz, 1 H), 4.92 (d, *J* = 16.8 Hz, 1 H), 4.92 (d, *J* = 9.6 Hz, 1 H), 4.39 (q, *J* = 7.2 Hz, 2 H), 3.78-3.71 (m, 1 H), 2.41-2.29 (m, 2 H), 1.68-1.53 (m, 2 H), 1.40 (t, *J* = 7.2 Hz, 3 H), 1.39-1.13 (m, 2 H), 0.85 (t, *J* = 7.6 Hz, 3 H).

^{13}C-NMR (100 MHz, $CDCl_3$)
δ 166.7, 155.8, 151.8, 151.7, 151.0, 135.8, 127.5, 121.9, 116.6, 61.3, 40.5, 39.2, 37.3, 20.4, 14.2, 14.1.

IR Alpha-Platinum ATR, Bruker, diamond crystal
υ = 3251, 3070, 2961, 1727, 1654, 1590 cm^{-1}

HRMS ESI
Calculated mass for $(M+H)^+$ of $C_{15}H_{21}NO_2$ is 248.1645, found 248.1641.

4-(Hept-1-en-4-yl)nicotinonitrile **18a**

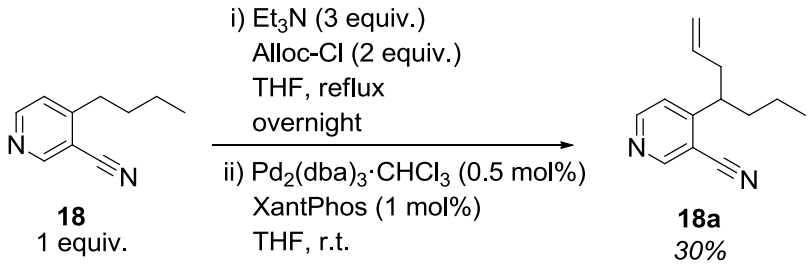

Using **procedure 4**, pyridine **18** (0.30 g, 1.87 mmol, 1.0 equiv.) in THF (18 mL) reacted with Et_3N (0.45 g, 3.7 mmol, 3.0 equiv.) and Alloc-Cl (0.57 g, 5.6 mmol, 2.0 equiv.) under reflux overnight. The reaction mixture was cooled to room temperature and concentrated under reduced pressure. The resulting crude mass was suspended in diethyl ether and filtered through a plug of cotton to remove triethylammonium chloride salt. The filtrate was concentrated *in vacuo* to afford the corresponding alkylidene dihydropyridine (~50% conversion) as a yellow oil. The crude alkylidene dihydropyridine was then reacted with $Pd_2(dba)_3$•$CHCl_3$ (10 mg, 0.009 mmol, 0.5 mol%) - XantPhos (11 mg, 0.018 mmol, 1 mol%) catalytic system in THF at room temperature to furnish product **18a** (0.11 g, 0.56 mmol, 30% yield) as a yellow oil.

Chromatography: 20% EtOAc in hexanes (R_f. = 0.25).

^{1}H-NMR (400 MHz, $CDCl_3$)
δ 8.80 (s, 1 H), 8.69 (d, *J* = 5.4 Hz, 1 H), 7.25 (d, *J* = 5.4 Hz, 1 H), 5.64 (dddd, *J* = 17.2, 10.0, 7.2, 7.2 Hz, 1 H), 4.97 (d, *J* = 10.0 Hz, 1 H), 4.94 (d, *J* = 17.2 Hz, 1 H), 3.21-3.13 (m, 1 H), 2.53-2.47 (m, 1 H), 2.40-2.33 (m, 1 H), 1.80-1.72 (m, 1 H), 1.67-1.62 (m, 1 H), 1.29-1.15 (m, 2 H), 0.88 (t, *J* = 7.2 Hz, 3 H).

^{13}C-NMR (100 MHz, $CDCl_3$)
δ 158.2, 153.1, 152.6, 134.6, 121.9, 117.7, 116.2, 111.2, 43.4, 39.9, 37.1, 20.4, 13.9.

IR Alpha-Platinum ATR, Bruker, diamond crystal
υ = 3061, 2956, 2930, 1640, 1587 cm^{-1}

HRMS ESI
Calculated mass for $(M+H)^+$ of $C_{13}H_{16}N_2$ is 201.1386, found 201.1385.

N-(*tert*-Butyl)-4-(hept-1-en-4-yl)nicotinamide **19a**

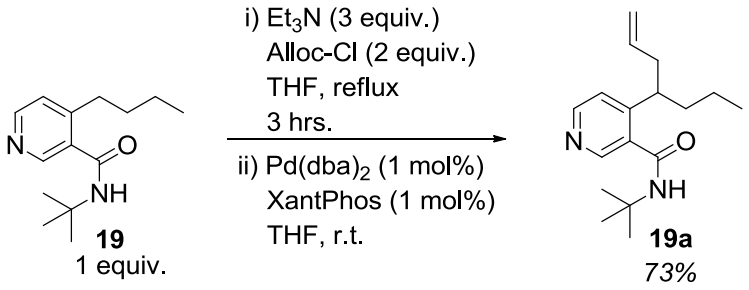

Using **procedure 4**, pyridine **19** (0.15 g, 0.64 mmol, 1.0 equiv.) in THF (6 mL) reacted with Et_3N (0.19 g, 1.92 mmol, 3.0 equiv.) and Alloc-Cl (0.15 g, 1.28 mmol, 2.0 equiv.) under reflux for 3 h. The reaction mixture was then cooled to room temperature and concentrated under reduced pressure. The resulting crude mass was suspended in diethyl ether and filtered through a plug of cotton to remove triethylammonium chloride salt. The filtrate was concentrated *in vacuo* to afford the corresponding alkylidene dihydropyridine as a yellow solid. The crude alkylidene dihydropyridine was then reacted with $Pd(dba)_2$ (4 mg, 0.006 mmol, 1 mol%) - XantPhos (4 mg, 0.006 mmol, 1 mol%) catalytic system in THF at room temperature to furnish product **19a** (0.13 g, 0.47 mmol, 73% yield) as a colorless oil.

Chromatography: 80% EtOAc in hexanes (R_f. = 0.30).

^{1}H-NMR (400 MHz, $CDCl_3$)
δ 8.52 (d, *J* = 5.2 Hz, 1 H), 8.48 (s, 1 H), 7.18 (d, *J* = 5.2 Hz, 1 H), 5.67-5.58 (m, 1 H), 4.93 (d, *J* = 16.0 Hz, 1 H), 4.92 (d, *J* = 11.2 Hz, 1 H), 3.22-3.16 (m, 1 H), 2.42-2.29 (m, 2 H), 1.69-1.57 (m, 2 H), 1.46 (s, 9 H), 1.26-1.11 (m, 2 H), 0.85 (t, *J* = 7.2 Hz, 3 H).

^{13}C-NMR (100 MHz, $CDCl_3$)
δ 167.1, 152.6, 150.3, 147.2, 136.2, 136.1, 121.8, 116.8, 52.3, 40.7, 40.3, 37.7, 28.8, 20.6, 14.0.

IR Alpha-Platinum ATR, Bruker, diamond crystal
υ = 3079, 2959, 2228, 1641, 1687 cm^{-1}

HRMS ESI
Calculated mass for $(M+H)^+$ of $C_{17}H_{26}N_2O$ is 275.2118, found 275.2109.

4-(Hept-1-en-4-yl)-3-phenylpyridine **20a**

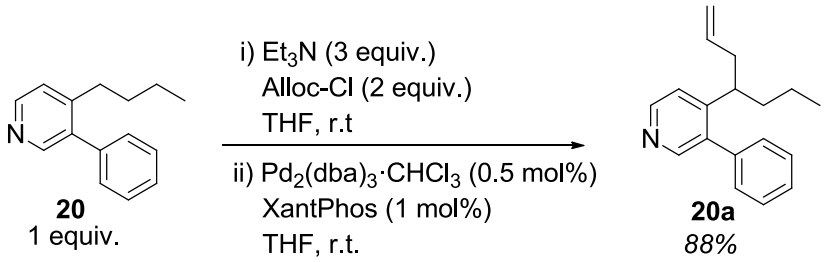

20
1 equiv.

20a
88%

Using **Procedure 4,** pyridine **20** (75 mg, 0.35 mmol, 1.0 equiv.) provided product **20a** (78 mg, 0.31 mmol, 88% yield) as a colorless oil.

Chromatography: 30% EtOAc in hexanes (R_f. = 0.25).

^{1}H-NMR (400 MHz, $CDCl_3$)
δ 8.53 (d, *J* = 5.2 Hz, 1 H), 8.41 (s, 1 H), 7.44-7.36 (m, 3 H), 7.26 (d, *J* = 8.4 Hz, 1 H), 7.22 (d, *J* = 5.2 Hz, 1 H), 5.54 (ddt, *J* = 17.2, 10.4, 7.2 Hz, 1 H), 4.90 (d, *J* = 10.4 Hz, 1 H), 4.89 (d, *J* = 17.2 Hz, 1 H), 2.93-2.85 (m, 1 H), 2.28 (t, *J* = 7.2 Hz, 2 H), 1.60-1.48 (m, 2 H), 1.01-1.01 (m, 2 H), 0.73 (t, *J* = 7.6 Hz, 3 H).

^{13}C-NMR (100 MHz, $CDCl_3$)
δ 152.1, 150.2, 148.6, 138.3, 138.0, 136.0, 129.8, 128.2, 127.4, 121.0, 116.5, 40.8, 39.6, 38.0, 20.4, 14.0.

IR Alpha-Platinum ATR, Bruker, diamond crystal
υ = 3072, 2925, 2724, 1721, 1640, 1598 cm^{-1}

HRMS ESI
Calculated mass for $(M+H)^+$ of $C_{17}H_{19}N$ is 238.1590, found 238.1589.

tert-Butyl (4-(1-phenylpent-4-en-2-yl)pyridin-3-yl)carbamate **21a**

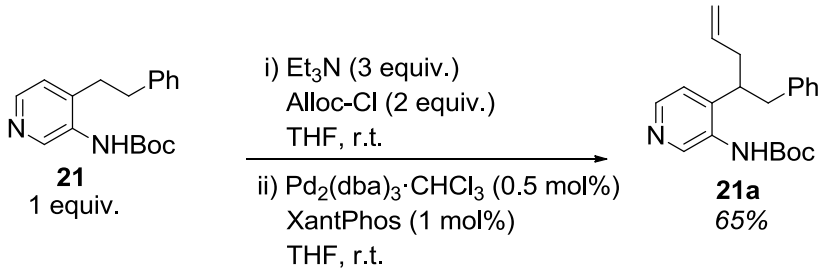

Using **procedure 4,** pyridine **21** (100 mg, 0.33 mmol, 1.0 equiv.) provided product **21a** (73 mg, 0.21 mmol, 65% yield) as a yellow oil.

Chromatography: 60% Et_2O in toluene (R_f. = 0.40).

^{1}H-NMR (400 MHz, $CDCl_3$)
δ 8.59 (br, 1 H), 8.37 (d, *J* = 5.2 Hz, 1 H), 7.23-7.16 (m, 4 H),
6.96 (d, *J* = 6.8 Hz, 2 H), 5.65 (dddd, *J* = 17.2, 10.0, 7.2, 7.2 Hz, 1 H), 5.51 (br, 1 H)
5.02 (d, *J* = 17.2 Hz, 1 H), 5.00 (d, *J* = 10.0 Hz, 1 H), 3.14 (br, 1 H),
3.04 (dd, *J* = 13.2, 6.0 Hz, 1 H), 2.70 (dd, *J* = 13.2, 8.0 Hz, 1 H), 2.53-2.39 (m, 2 H),
1.46 (s, 9 H).

^{13}C-NMR (100 MHz, $CDCl_3$)
δ 153.4, 146.8, 146.4, 139.2, 135.4, 132.6, 128.9, 128.5, 126.6, 121.2, 117.5, 80.7,
41.9, 41.0, 38.7, 28.2.

IR Alpha-Platinum ATR, Bruker, diamond crystal
υ = 3070, 2959, 1719, 1641, 1589 cm^{-1}

HRMS ESI
Calculated mass for $(M+H)^+$ of $C_{21}H_{26}N_2O_2$ is 339.2067, found 339.2071.

2-(2-(pyridin-4-yl)pent-4-en-1-yl)pyridine **22a**

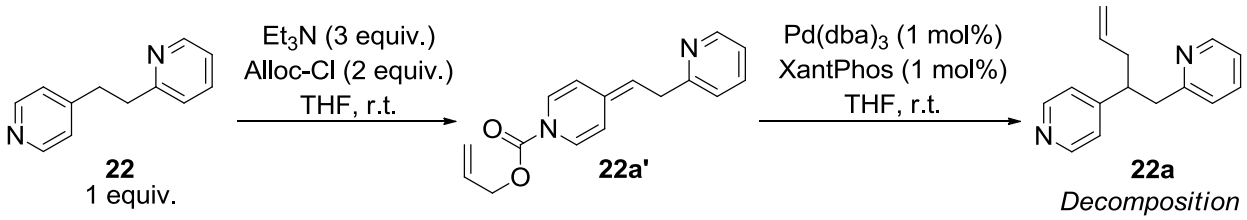

Using **procedure 4,** pyridine **22** (0.10 g, 0.54 mmol, 1.0 equiv.) in THF (5.5 mL) was reacted with Et_3N (0.16 g, 1.6 mmol, 3.0 equiv.) and Alloc-Cl (0.16 g, 1.1 mmol, 2.0 equiv.) at room temperature. Upon disappearance of the starting pyridine, the mixture was concentrated *in vacuo*. The resulting crude mass was suspended in diethyl ether and filtered through a plug of cotton to remove triethylammonium chloride salt. The filtrate was concentrated *in vacuo* to afford the corresponding alkylidene dihydropyridine (**22a'**) as a yellow oil. The crude alkylidene dihydropyridine was subjected to $Pd(dba)_2$ (3 mg, 0.005 mmol, 1 mol%) - XantPhos (3 mg, 0.005 mmol, 1 mol%) catalytic system in THF at room temperature. However, the desired product (**22a**) was not observed after an overnight reaction as **22a'** decomposed.

Data for **22a'**

^{1}H-NMR (300 MHz, $CDCl_3$, at 40°C)
8.51 (d, *J* = 4.5 Hz, 1 H), 7.57 (t, *J* = 7.5 Hz, 1 H), 7.15 (d, *J* = 7.5 Hz, 1 H), 7.10-7.06 (m, 1 H), 6.97 (d, *J* = 7.5 Hz, 1 H), 6.82 (d, *J* = 7.5 Hz, 1 H), 6.01-5.90 (m, 2 H), 5.73 (d, *J* = 7.5 Hz, 1 H), 5.35 (d, *J* = 17.1 Hz, 1 H), 5.28 (d, *J* = 10.5 Hz, 1 H), 5.07 (t, *J* = 7.8 Hz, 1 H), 4.72 (d, *J* = 5.7 Hz, 1 H), 3.58 (d, *J* = 7.8 Hz, 1 H).

^{13}C-NMR (75 MHz, $CDCl_3$, at 55°C)
δ 161.0, 150.4, 149.2, 136.3, 131.6, 129.3, 124.7, 122.5, 122.3, 120.9, 118.8, 115.5, 112.1, 109.0, 67.4, 34.0.

IR Alpha-Platinum ATR, Bruker, diamond crystal
υ = 2921, 1721, 1673, 1589, 1301, 1196, 980, 967.

HRMS ESI
Calculated mass for $(M+H)^+$ of $C_{16}H_{16}N_2O_2$ is 269.1285, found 269.1277.

2-(4-(2-(Pyridin-4-yl)pent-4-en-1-yl)phenethyl)pyridine **23a**

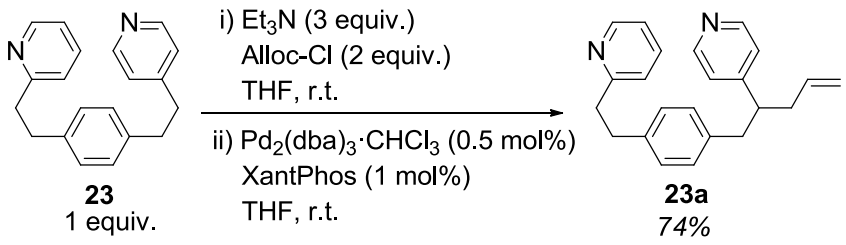

Using **procedure 4**, pyridine **23** (50 mg, 0.17 mmol, 1.0 equiv.) provided product **23a** (42 mg, 0.12 mmol, 74% yield) as a yellow oil.

Chromatography: 3% MeOH in DCM (R_f. = 0.30).

^{1}H-NMR (600 MHz, $CDCl_3$)
8.54 (d, *J* = 4.2 Hz, 1 H), 8.44 (d, *J* = 4.8 Hz, 2 H), 7.54 (td, *J* = 7.8, 1.8 Hz, 1 H), 7.10 (dd, *J* = 4.2, 1.8 Hz, 1 H), 7.01 (d, *J* = 7.8 Hz, 1 H)*, 7.01 (d, *J* = 7.8 Hz, 2 H)*, 6.99 (d, *J* = 4.8 Hz, 2 H), 6.88 (d, *J* = 7.8 Hz, 2 H),
8.54 (dddd, *J* = 16.8, 10.2, 7.2, 7.2 Hz, 1 H), 4.96 (d, *J* = 16.8 Hz, 1 H),
4.95 (d, *J* = 10.2 Hz, 1 H), 3.05-2.87 (m, 6.0 H), 2.78 (dd, *J* = 12.6, 7.2 Hz, 1 H), 2.46-2.35 (m, 2 H).

^{13}C-NMR (150 MHz, $CDCl_3$)
δ 161.2, 153.4, 149.5, 149.3, 139.3, 136.8, 136.2, 135.7, 129.0, 128.3, 123.4, 122.9, 121.1, 117.0, 47.2, 41.5, 40.1, 39.2, 35.5.

IR Alpha-Platinum ATR, Bruker, diamond crystal
υ = 3069.5, 3007.1, 2922.1, 1596.0, 1473.4, 992.8, 817.6, 748.5 cm^{-1}

HRMS ESI
Calculated mass for $(M+H)^+$ of $C_{23}H_{24}N_2$ is 329.2012, found 329.2003.

* Overlapping doublets with identical chemical shifts and coupling constants

2-(4-(2-(Pyridin-4-yl)pent-4-en-1-yl)phenethyl)pyridine **23a**

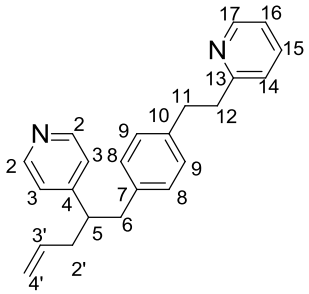

Carbon No.	^{13}C δ (ppm)[a]	^{1}H δ (ppm) (mult; *J* (Hz))[b,c,d]	HMBC Correlations
2	149.5	H-2 : 8.44 (d, *J* = 4.8 Hz)	H-3
3	123.4	H-3 : 6.99 (d, *J* = 4.8 Hz)	H-2, H-5
4	153.4		H-2, H-2'a, H-2'b, H-6a, H-6b, H-5
5	47.2	H-5 : part of the m at 2.99-2.87	H-2'a, H-2'b, H-6a, H-6b, H-3
6	41.5	H-6a : part of the m at 2.99-2.87 H-6b : 2.78 (dd, *J* = 12.6, 7.2 Hz)	H-5, H-8
7	136.8		H-8, H-6a, H-6b
8	129.0	H-8 : 6.88 (d, *J* = 7.8 Hz)	H-6a, H-6b
9	128.3	H-9 : 7.01 (d, *J* = 7.8 Hz)	H-11a, H-11b
10	139.8		
11	35.5	H-11a : part of the m at 2.99-2.87 H-11b : part of the m at 2.99-2.87	H-9, H-12a, H-12b
12	40.1	H-12a : part of the m at 3.05-2.96. H-12b : part of the m at 3.05-2.96	H-11a, H-11b, H-9
13	161.2		H-14, H-15
14	122.9	H-14 : Overlapping with the d at 7.01 (d, *J* = 7.8 Hz)	H-16
15	136.2	H-15 : 7.55 (td, *J* = 7.8, 1.8 Hz)	H-17
16	121.1	H-16 : 7.10 (dd, *J* = 4.2, 1.8 Hz)	H-17, H-14
17	149.3	H-17 : 8.54 (d, *J* = 4.2 Hz)	H-15, H16
2'	39.2	H-2'a : part of the m at 2.46-2.35 H-2'b : part of the m at 2.46-2.35	H-4'a-H-4'b, H-3
3'	135.7	H-3' : 5.61 (dddd, *J* = 16.8, 10.2, 7.2, 7.2 Hz)	H-2'a, H-2'b
4'	117.0	H-4'a : 4.96 (d, *J* = 16.8 Hz) H-4'b : 4.95 (d, *J* = 10.2 Hz)	H-2'a, H-2'b

[a] Recorded at 150 MHz. [b] Recorded at 600 MHz.

[c] Assignments based on HSQC-DEPT and HMBC data

[d] Methylene protons are designated H-Xa and H-Xb arbitrarily

[e] Only those correlations which could be unambiguously assigned are reported.

2-(4-(2-(Pyridin-4-yl)pent-4-en-1-yl)phenethyl)pyridine **23a**

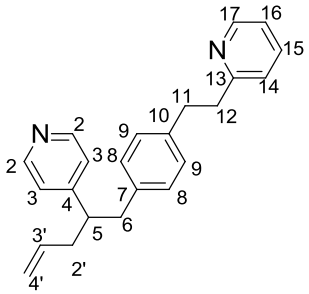

Proton No.	**^{1}H δ (ppm) (mult; *J* (Hz))[a,b,c]**	**COSY Correlations**
H-2	8.44 (d, *J* = 4.8 Hz)	H-3
H-3	6.99 (d, *J* = 4.8 Hz)	H-2
H-5	part of the m at 2.99-2.87	
H-6a	part of the m at 2.99-2.87	H-6b
H-6b	2.78 (dd, *J* = 12.6, 7.2 Hz)	H-6a
H-8	6.88 (d, *J* = 7.8 Hz)	H-9
H-9	7.01 (d, *J* = 7.8 Hz)	H-8
H-11a	part of the m at 2.99-2.87	
H-11b	part of the m at 2.99-2.87	
H-12a	part of the m at 3.05-2.96.	
H-12b	part of the m at 3.05-2.96	
H-14	Overlapping with the d at 7.01 (d, *J* = 7.8 Hz)	H-15, H-16
H-15	7.54 (td, *J* = 7.8, 1.8 Hz)	H-16, H-14
H-16	7.10 (dd, *J* = 4.2, 1.8 Hz)	H-15, H-14
H-17	8.54 (d, *J* = 4.2 Hz)	H-15
H-2'a	part of the m at 2.46-2.35	
H-2'b	part of the m at 2.46-2.35	
H-3'	5.61 (dddd, *J* = 16.8, 10.2, 7.2, 7.2 Hz)	H-2'a, H-2'b, H-4'a, H-4'b
H-4'a	4.96 (d, *J* = 16.8 Hz)	H-3'
H-4'b	4.95 (d, *J* = 10.2 Hz)	H-3'

[a] Recorded at 600 MHz. [b] Assignments based on HSQC-DEPT and HMBC data

[c] Methylene protons are designated H-Xa and H-Xb arbitrarily

[d] Only those correlations which could be unambiguously assigned are reported.

5-Allyl-5,6,7,8-tetrahydroisoquinoline **30a**

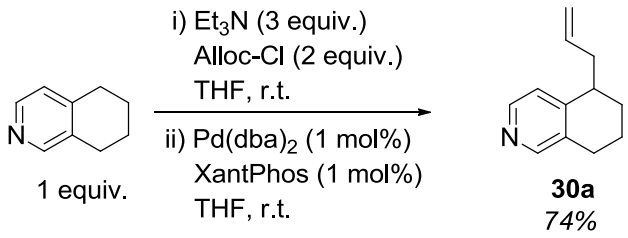

1 equiv. **30a** *74%*

Using **procedure 4**, 5,6,7,8-tetrahydroisoquinoline (0.300 g, 2.25 mmol, 1.0 equiv.) provided product **30a** (0.290 g, 1.67 mmol, 74% yield) as a yellow oil.

Chromatography: 25% EtOAc in toluene (R_f. = 0.25).

^{1}H-NMR (400 MHz, $CDCl_3$)
δ 8.32 (br, 2 H), 7.11 (d, *J* = 5.2 Hz, 1 H),
5.65 (dddd, *J* = 17.2, 10.8, 7.2, 7.2 Hz, 1 H), 5.09 (d, *J* = 15.6 Hz, 1 H),
5.08 (d, *J* = 11.2 Hz, 1 H), 2.89-2.83 (m, 1 H), 2.75 (br, 2 H),
2.54-2.48 (m, 1 H), 2.38-2.30 (m, 1 H), 1.94-1.83 (m, 2 H), 1.80-1.67 (m, 2H).

^{13}C-NMR (100 MHz, $CDCl_3$)
δ 150.5, 149.1, 146.6, 136.4, 136.3, 133.0, 122.9, 116.9, 40.3, 36.7, 26.9, 26.6, 19.6.

IR Alpha-Platinum ATR, Bruker, diamond crystal
υ = 3074, 2933, 2861, 1639, 1592 cm^{-1}

HRMS ESI
Calculated mass for $(M+H)^+$ of $C_{12}H_{15}N$ is 174.1277 found 174.1273.

3.5 ^{1}H,^{13}C and ^{29}Si – NMR spectra

^{1}H (400 MHz, $CDCl_3$) and ^{13}C (100 MHz, $CDCl_3$) – NMR spectra of **2**

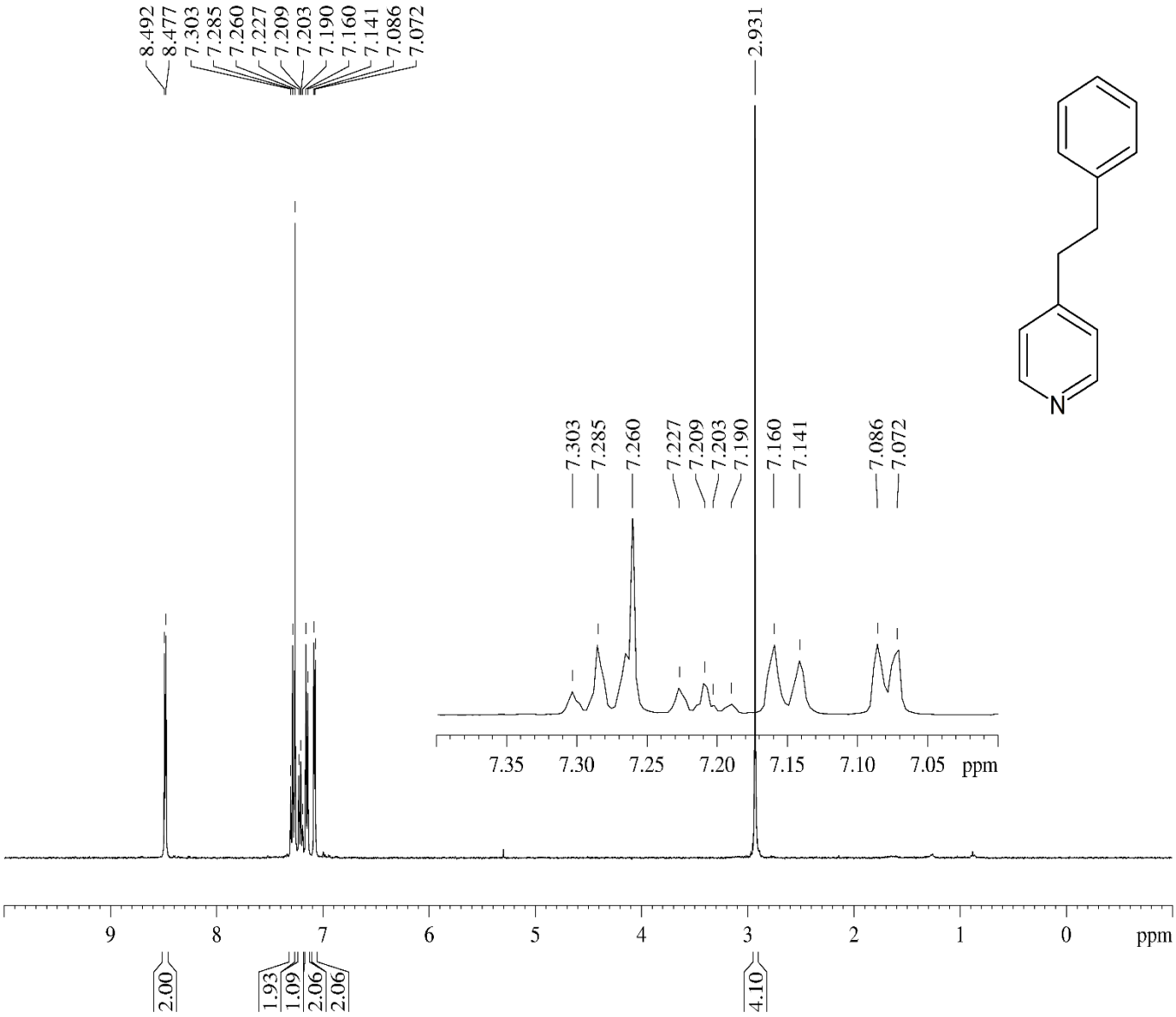

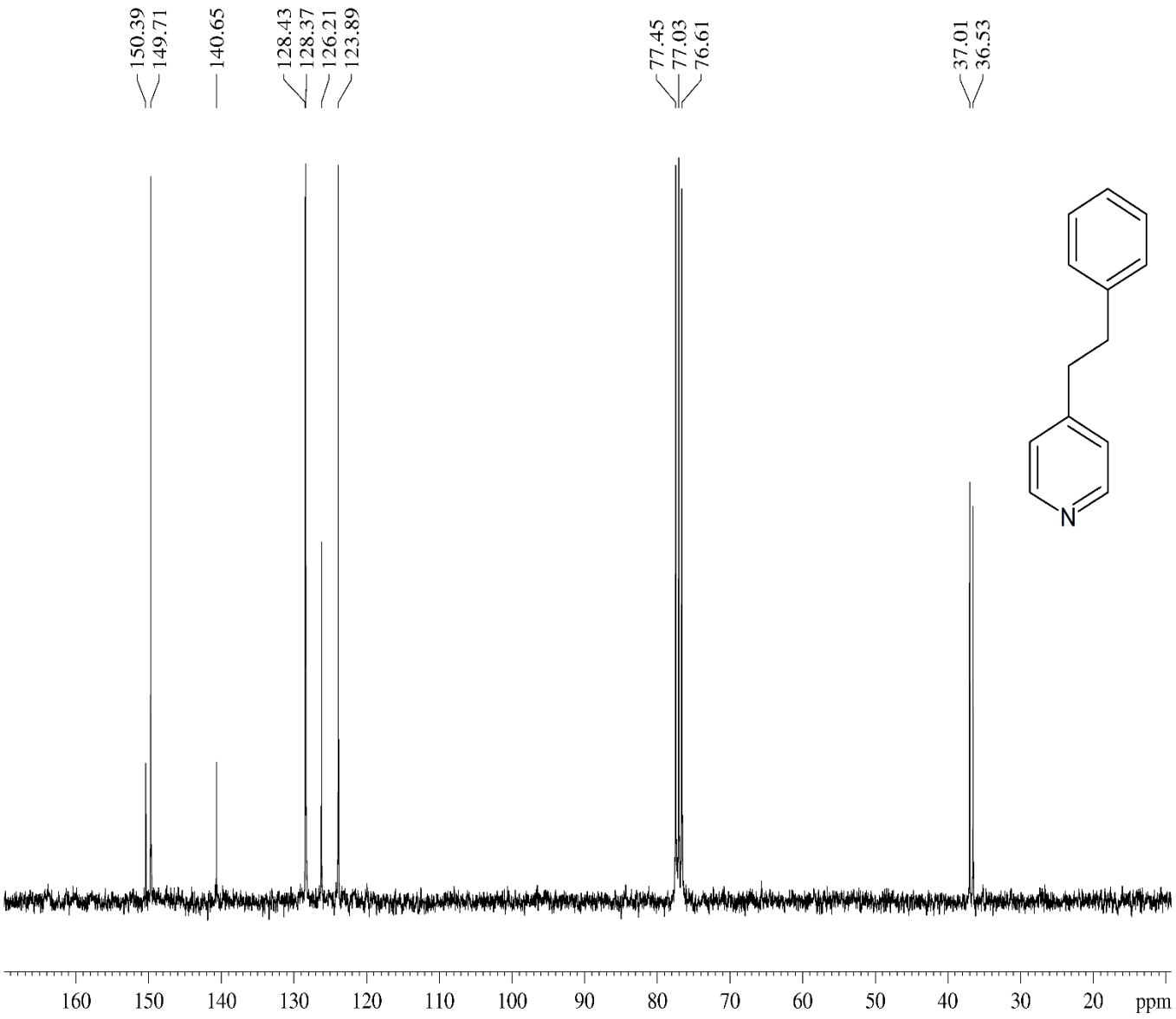
150.39
149.71
140.65
128.43
128.37
126.21
123.89
77.45
77.03
76.61
37.01
36.53
N
160
150
140
130
120
110
100
90
80
70
60
50
40
30
20
ppm

^{1}H (400 MHz, $CDCl_3$) and ^{13}C (100 MHz, $CDCl_3$) – NMR Spectra for **3**

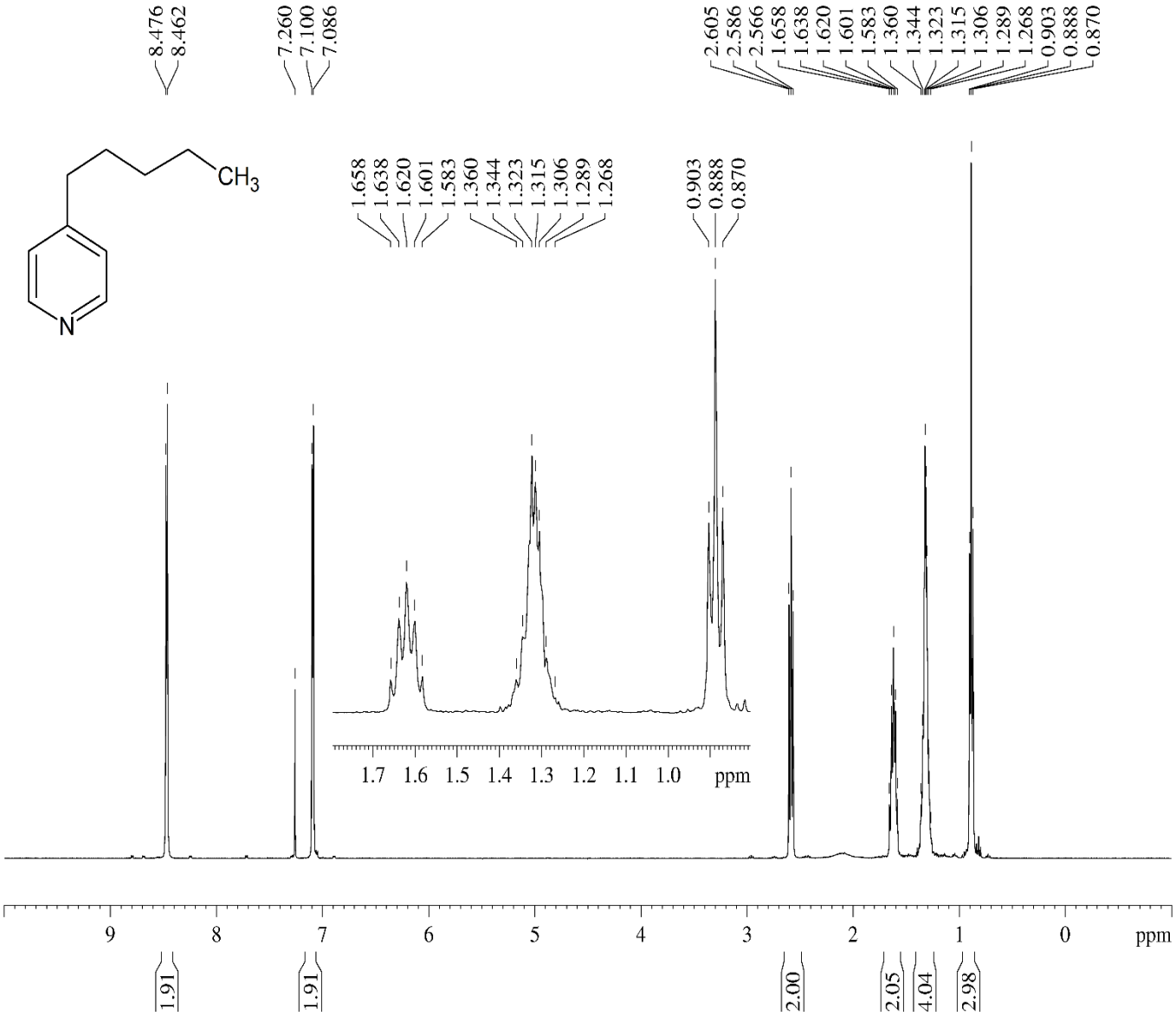

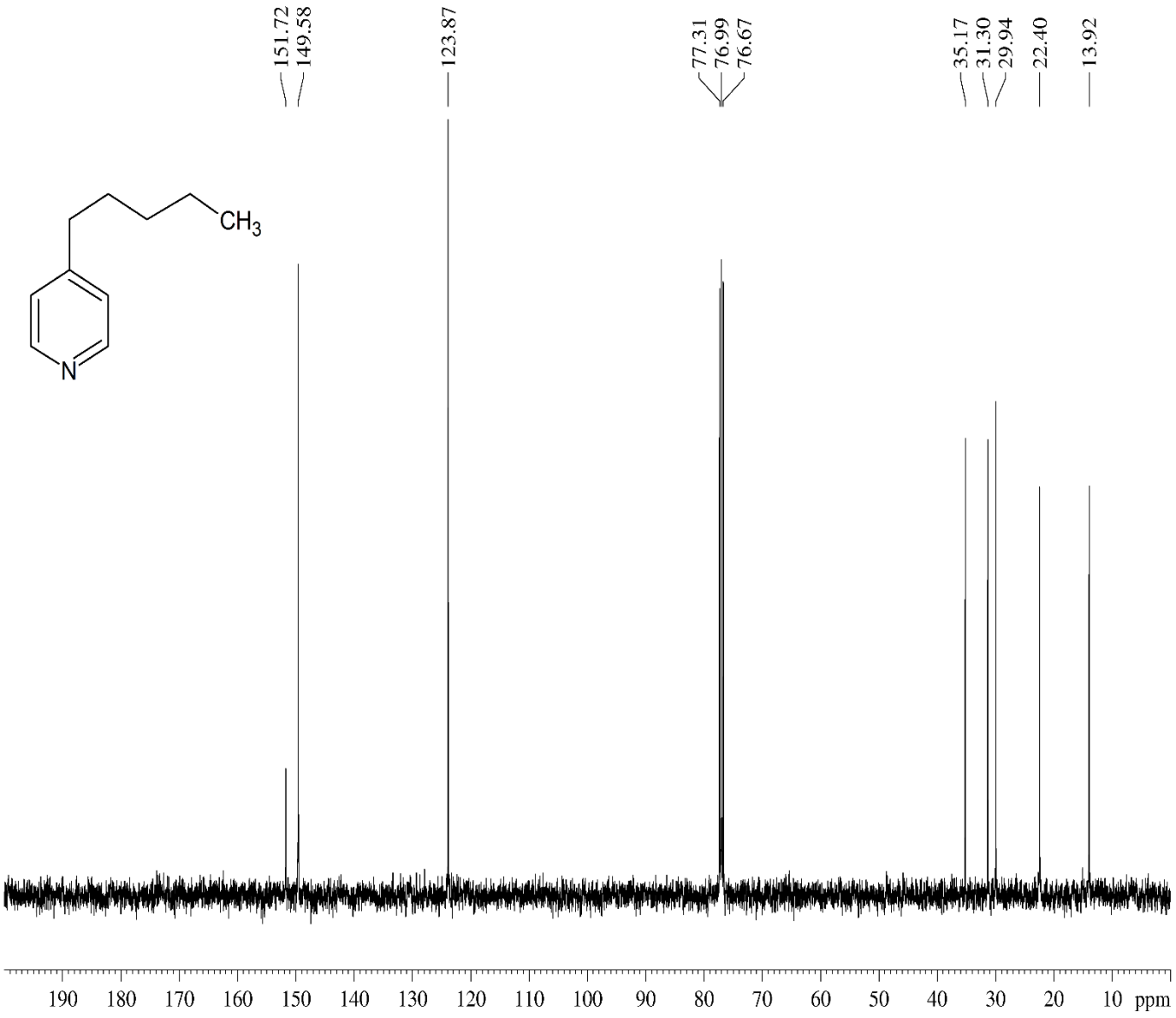
151.72
149.58
123.87
77.31
76.99
76.67
35.17
31.30
29.94
22.40
13.92
CH3
N
190 180 170 160 150 140 130 120 110 100 90 80 70 60 50 40 30 20 10 ppm

^{1}H (400 MHz, $CDCl_3$) and ^{13}C (100 MHz, $CDCl_3$) – NMR Spectra for **4**

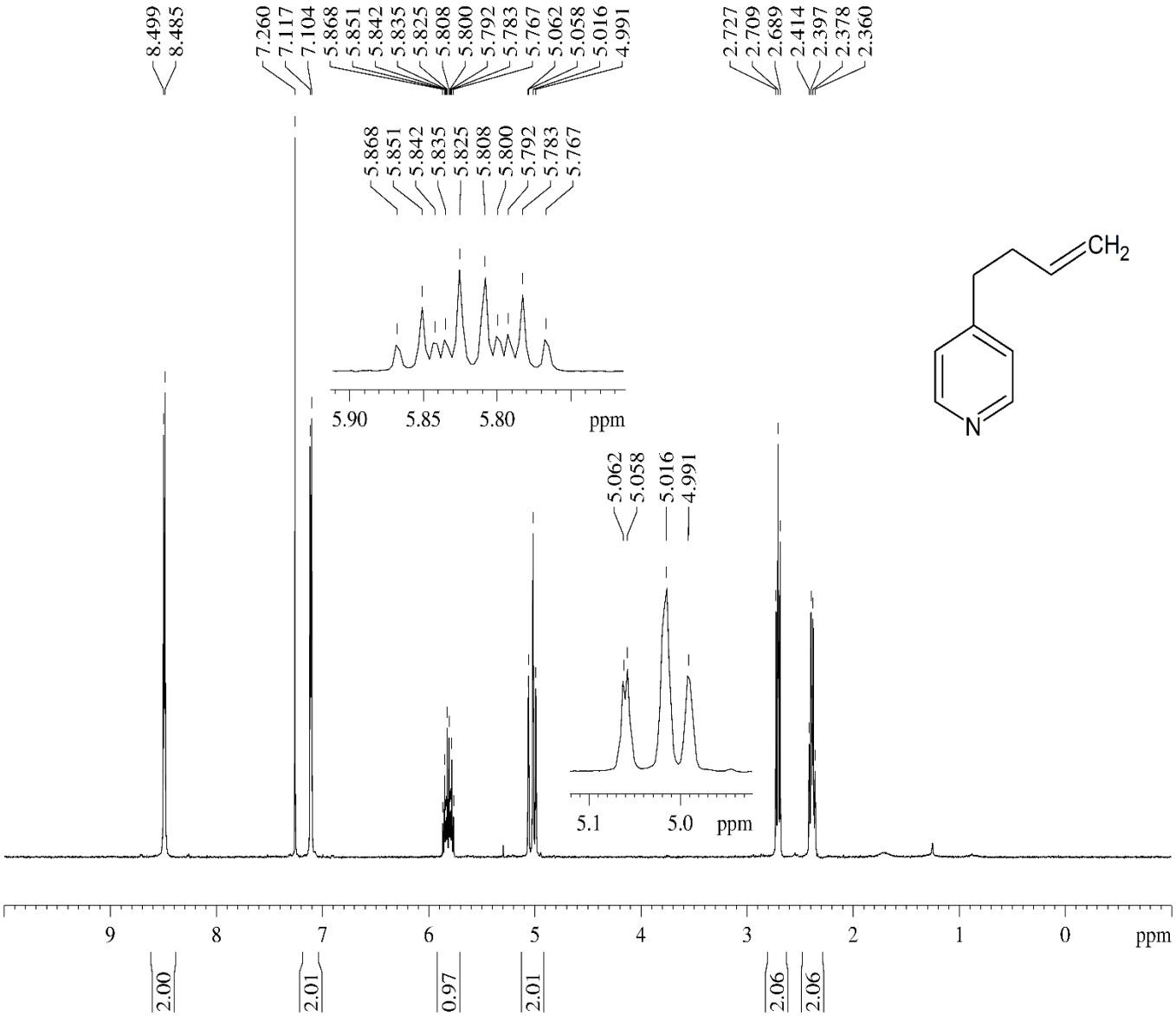

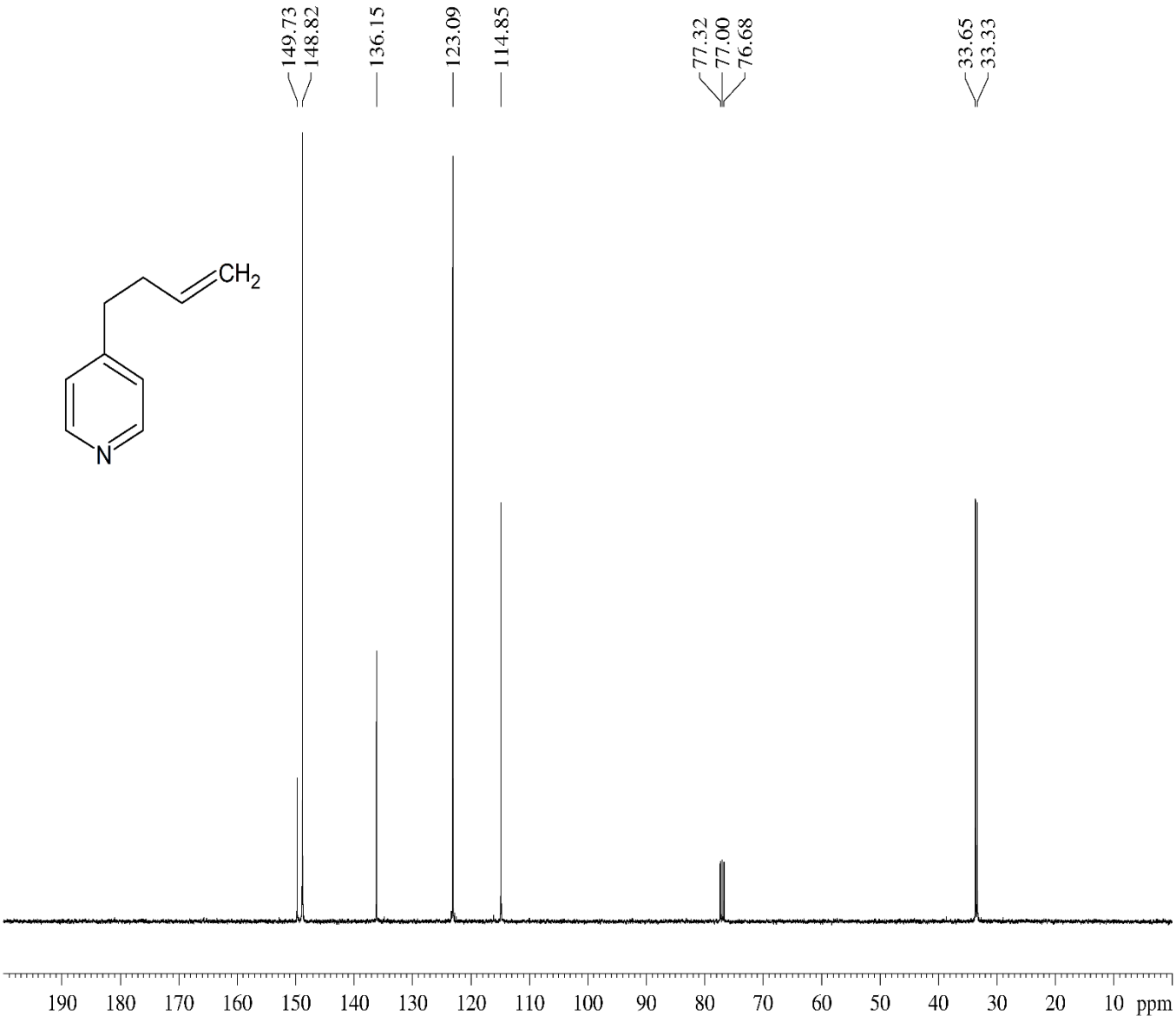
149.73
148.82
136.15
123.09
114.85
77.32
77.00
76.68
33.65
33.33
CH2
N
190 180 170 160 150 140 130 120 110 100 90 80 70 60 50 40 30 20 10 ppm

^{1}H (400 MHz, $CDCl_3$) and ^{13}C (100 MHz, $CDCl_3$) – NMR Spectra for **5**

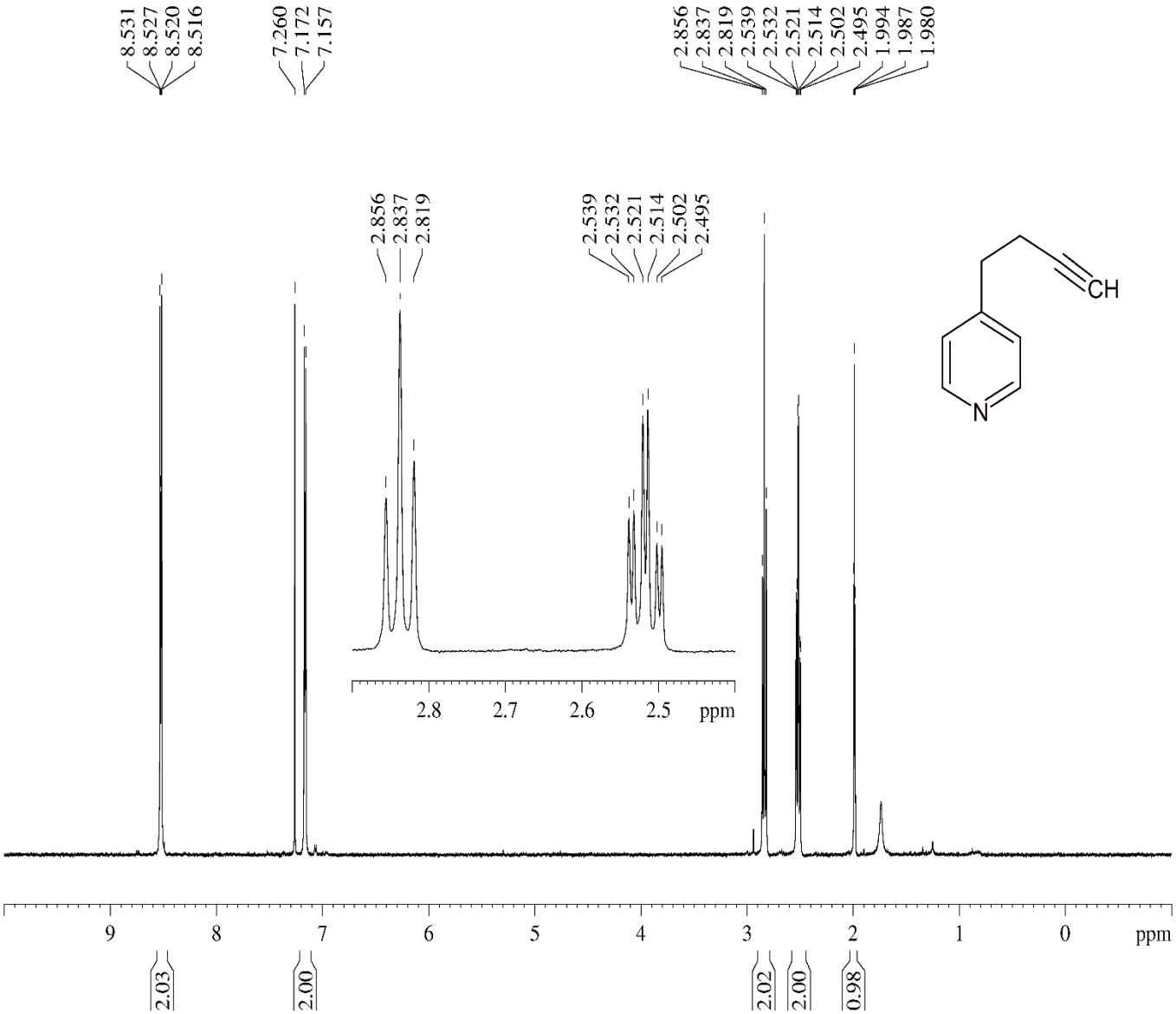

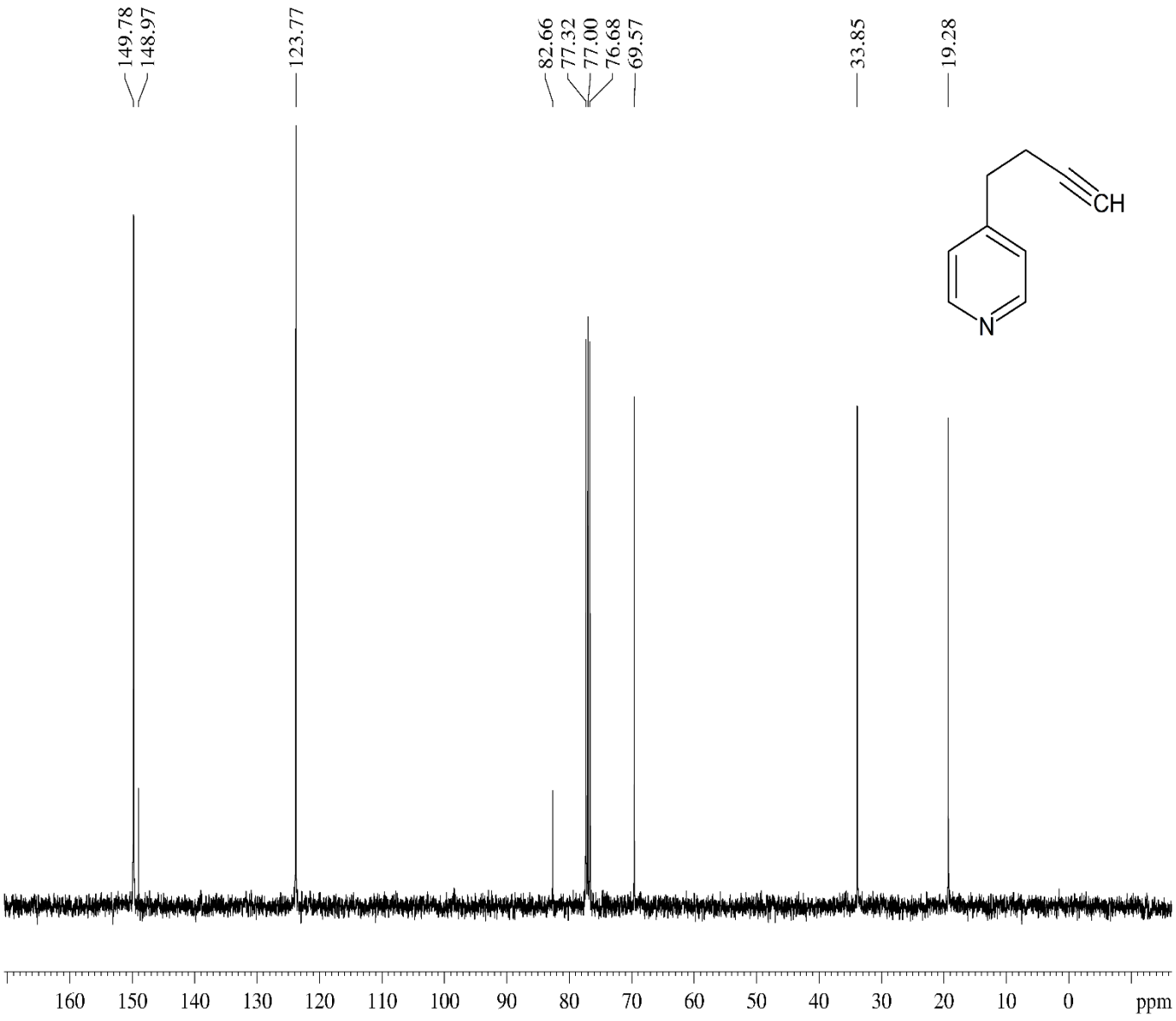
149.78
148.97
123.77
82.66
77.32
77.00
76.68
69.57
33.85
19.28
CH
N
160
150
140
130
120
110
100
90
80
70
60
50
40
30
20
10
0
ppm

^{1}H (400 MHz, $CDCl_3$) and ^{13}C (100 MHz, $CDCl_3$) – NMR Spectra for **6**

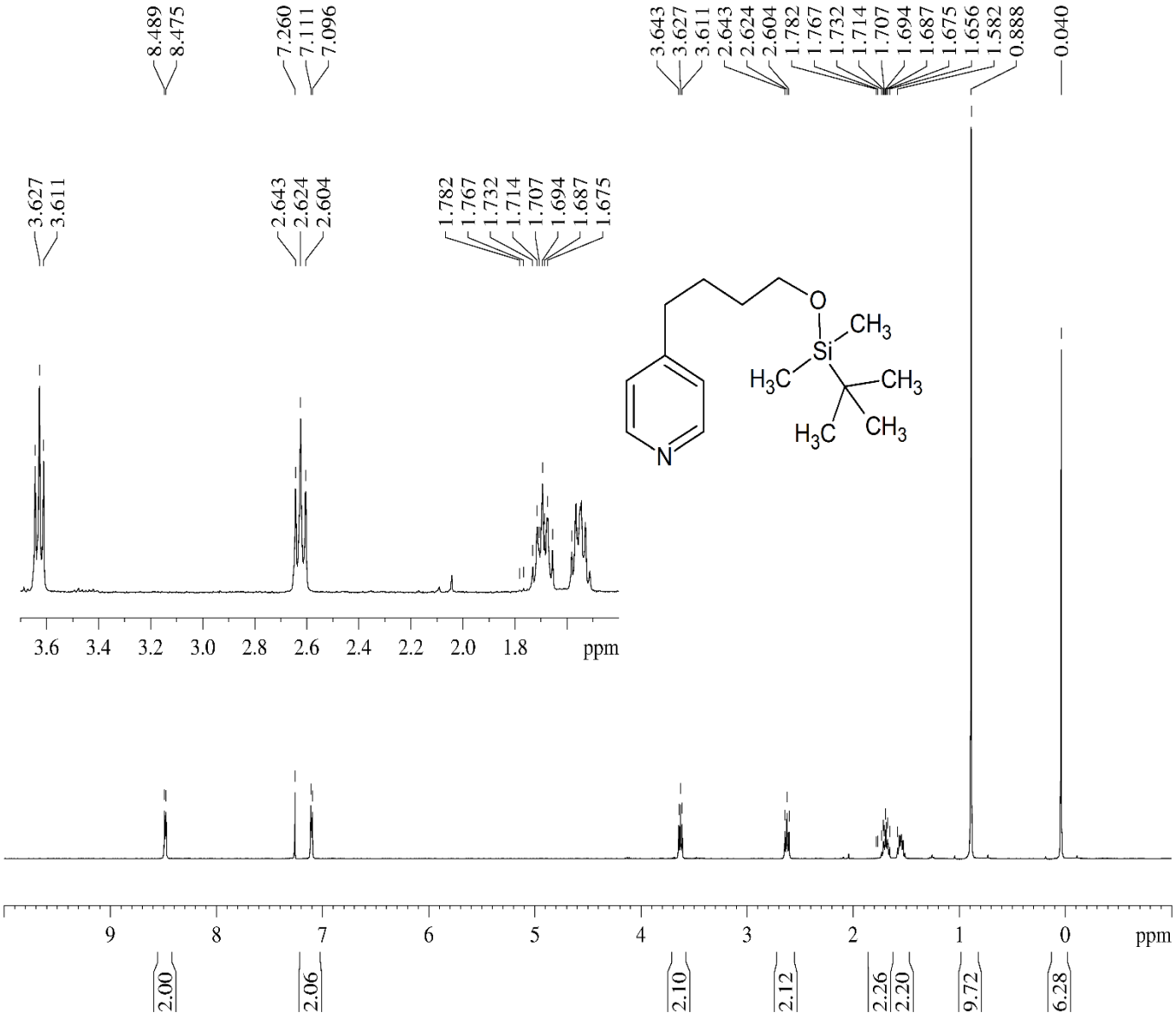

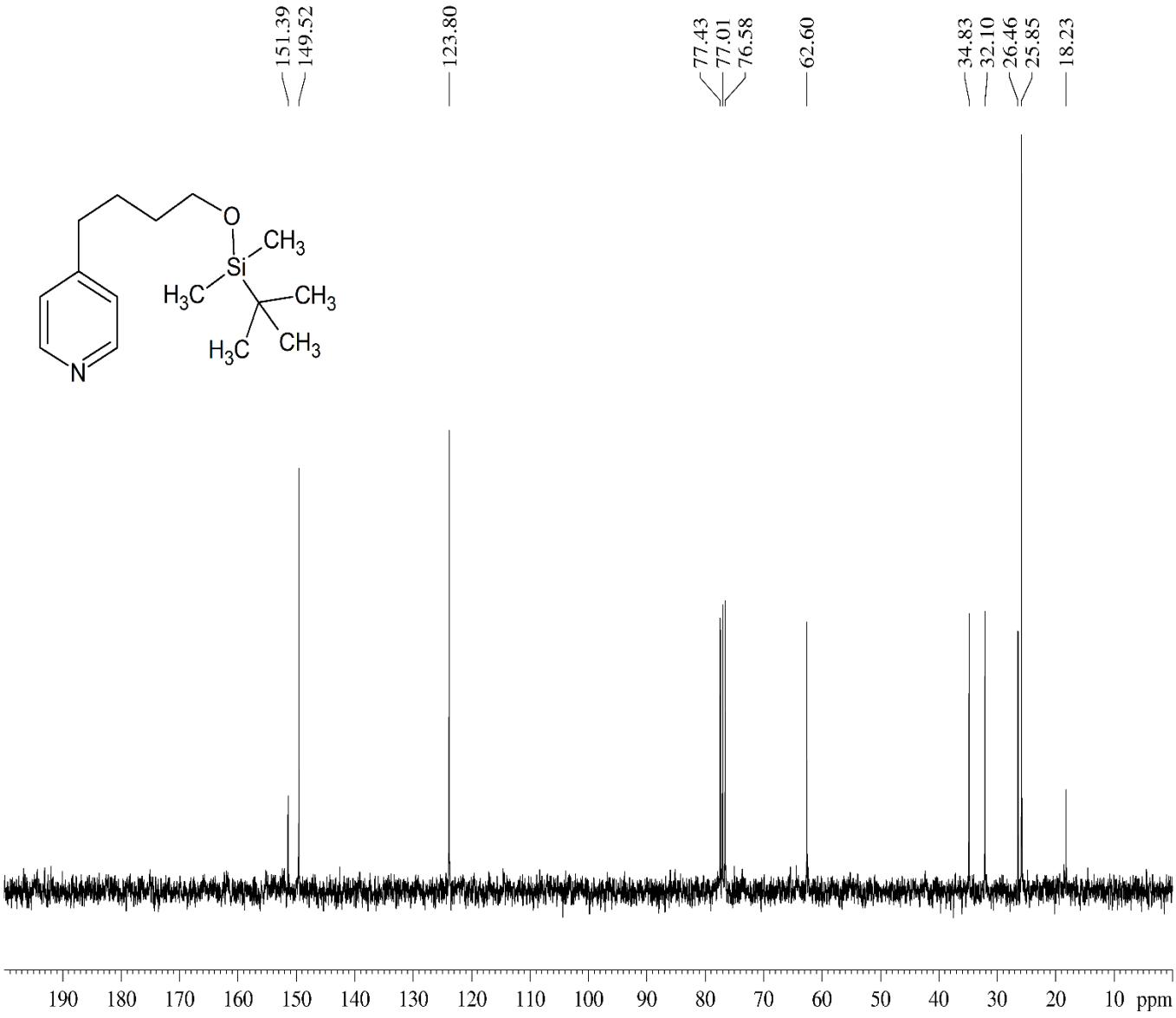
151.39
149.52
123.80
77.43
77.01
76.58
62.60
34.83
32.10
26.46
25.85
18.23
O
Si
CH3
H3C
CH3
H3C
CH3
N
190 180 170 160 150 140 130 120 110 100 90 80 70 60 50 40 30 20 10 ppm

^{29}Si NMR Spectrum for **6** (80 MHz, $CDCl_3$)

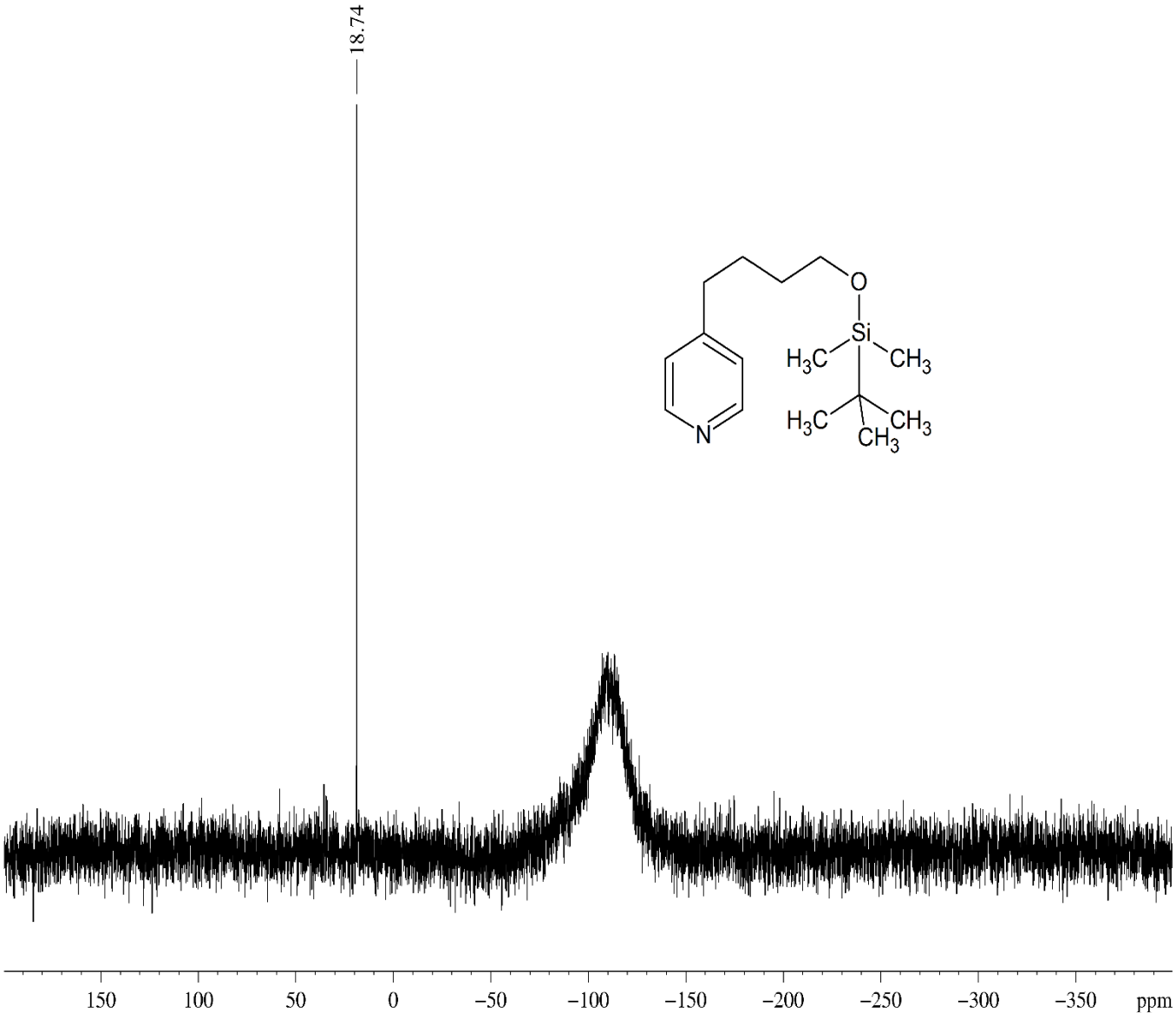

^{1}H (400 MHz, $CDCl_3$) and ^{13}C (100 MHz, $CDCl_3$) – NMR Spectra for **7**

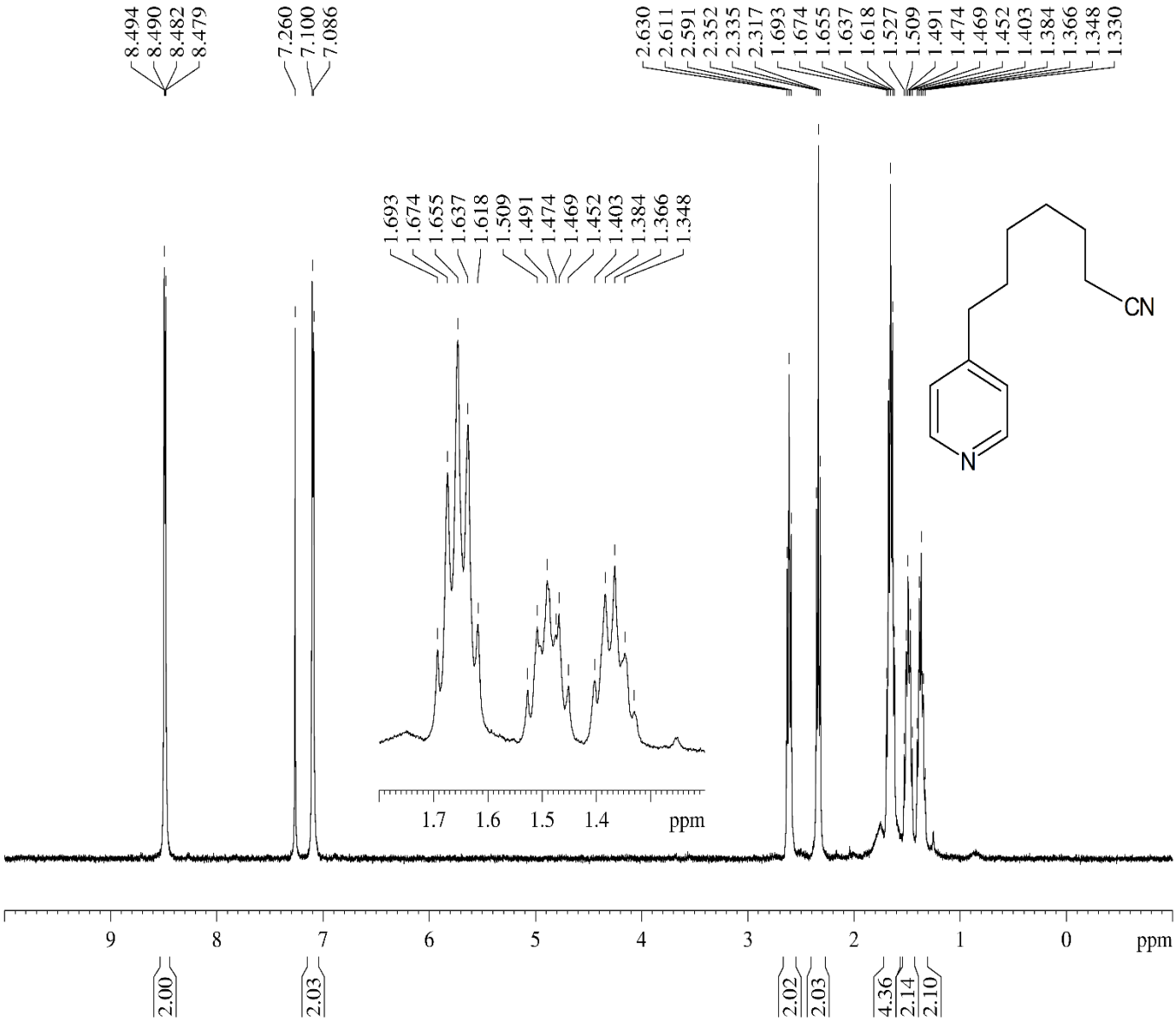

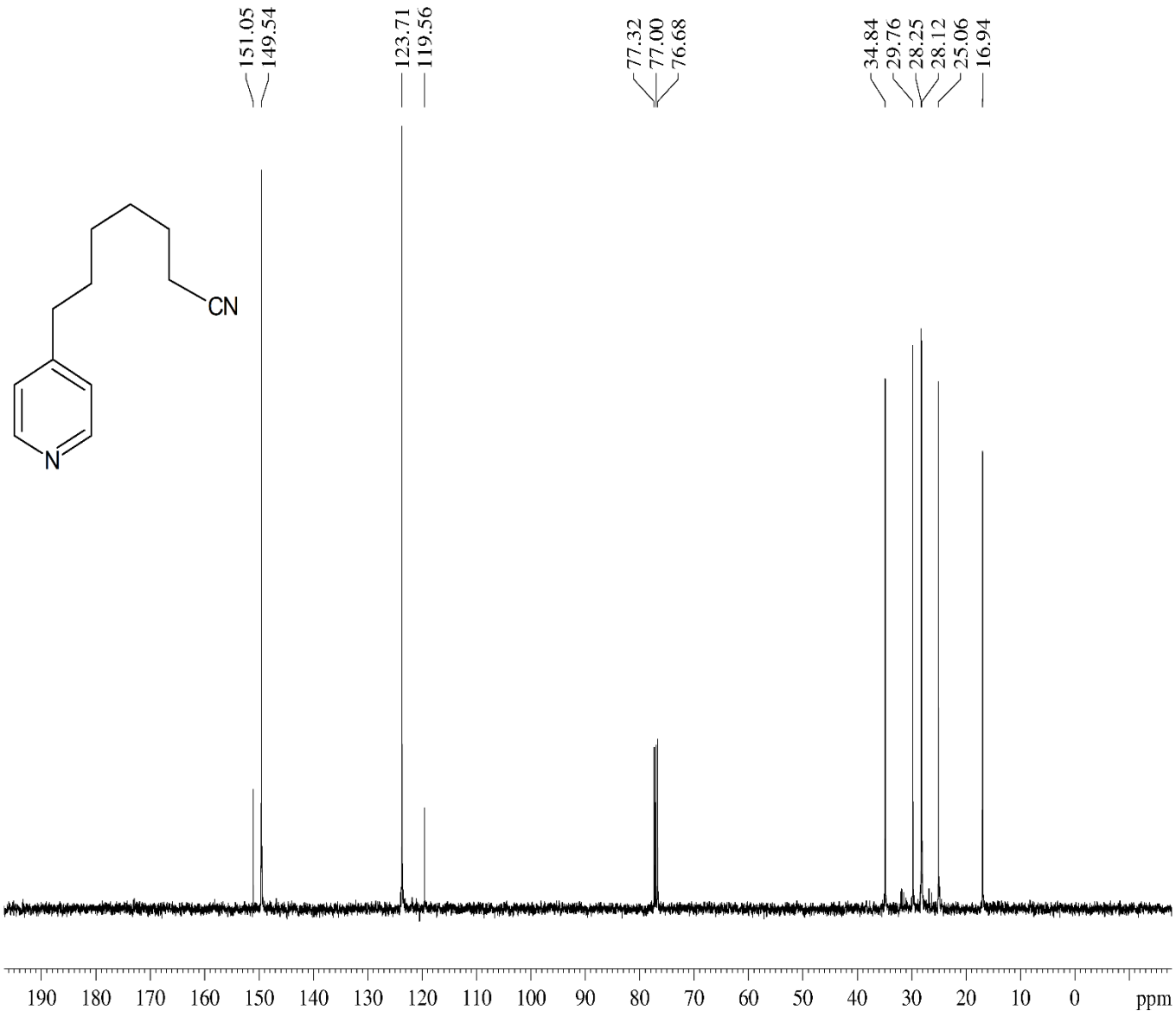
151.05
149.54
123.71
119.56
77.32
77.00
76.68
34.84
29.76
28.25
28.12
25.06
16.94
CN
N
190 180 170 160 150 140 130 120 110 100 90 80 70 60 50 40 30 20 10 0 ppm

^{1}H (400 MHz, $CDCl_3$) and ^{13}C (100 MHz, $CDCl_3$) – NMR Spectra for **8**

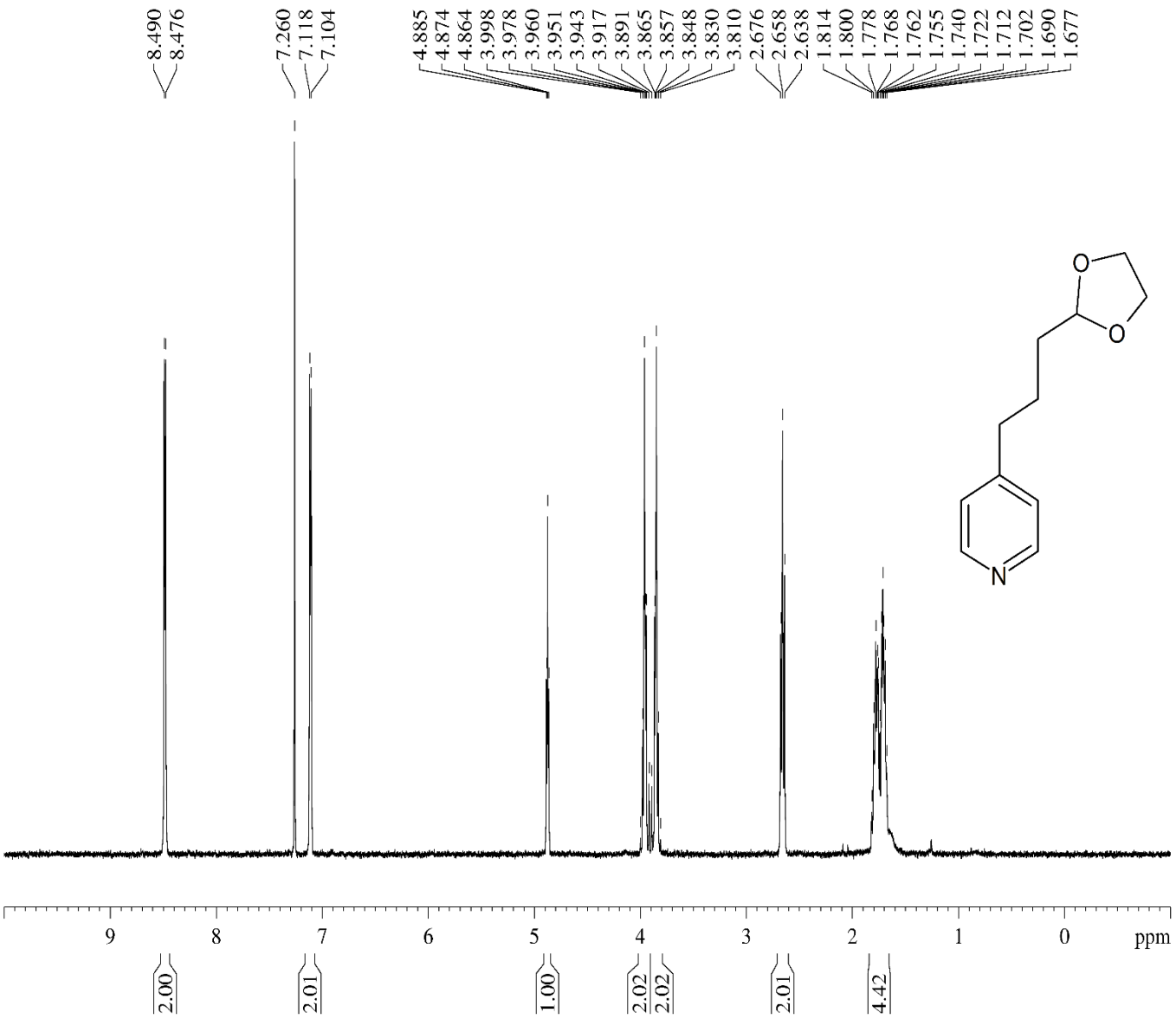

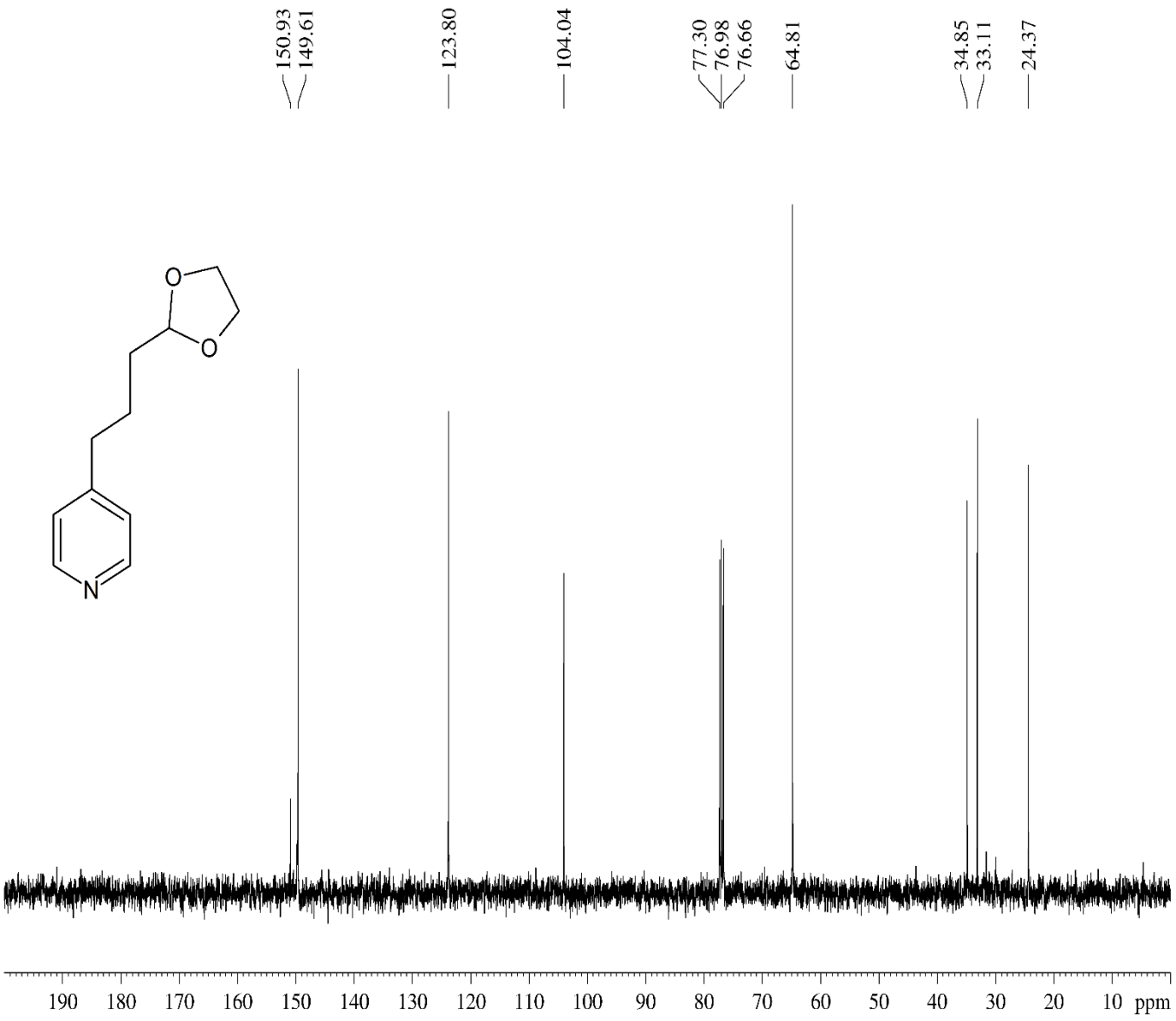
150.93
149.61
123.80
104.04
77.30
76.98
76.66
64.81
34.85
33.11
24.37
O
O
N
190 180 170 160 150 140 130 120 110 100 90 80 70 60 50 40 30 20 10 ppm

^{1}H (400 MHz, $CDCl_3$) and ^{13}C (100 MHz, $CDCl_3$) – NMR Spectra for **9**

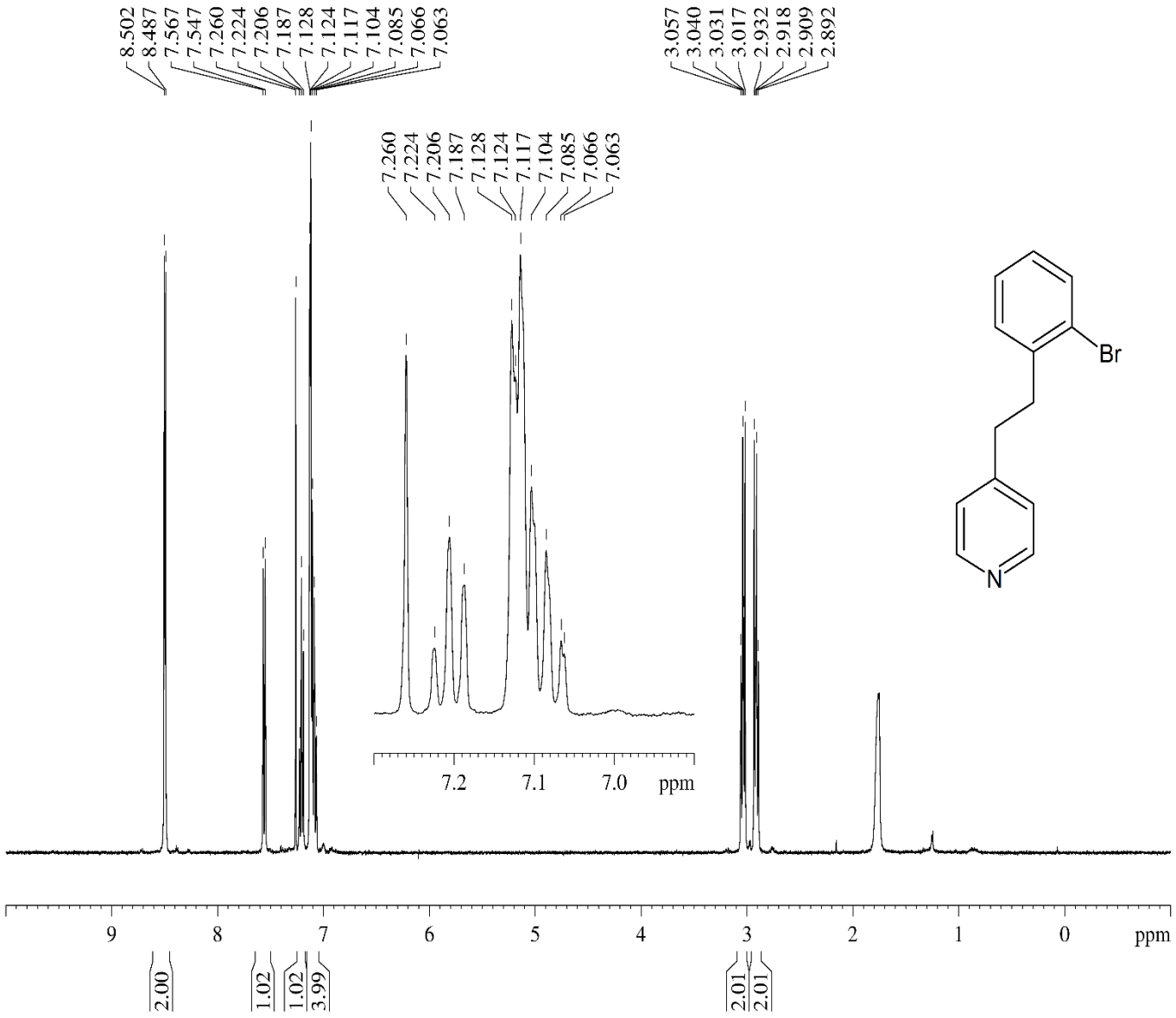

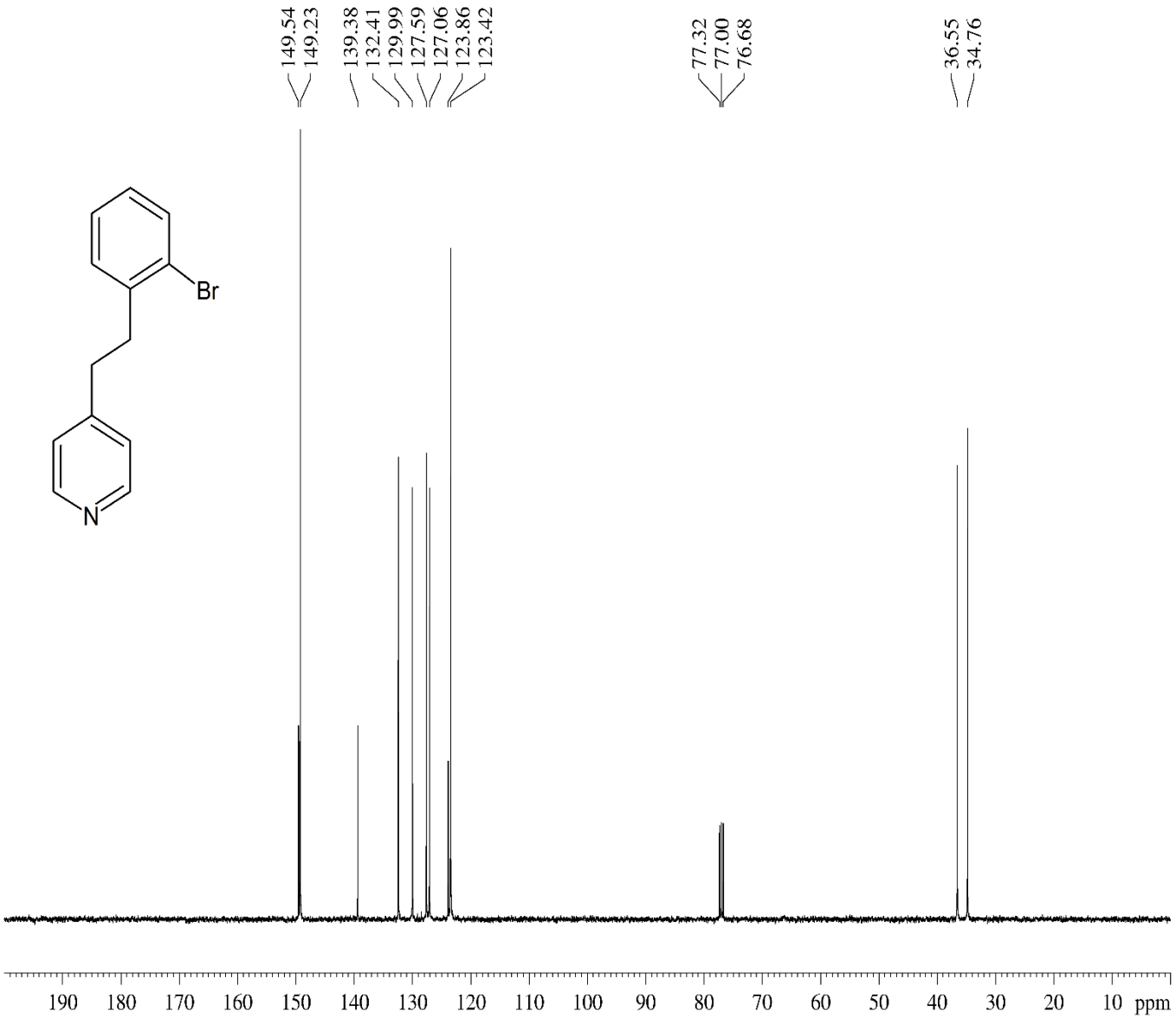
149.54
149.23
139.38
132.41
129.99
127.59
127.06
123.86
123.42
77.32
77.00
76.68
36.55
34.76
Br
N
190
180
170
160
150
140
130
120
110
100
90
80
70
60
50
40
30
20
10
ppm

^{1}H (400 MHz, $CDCl_3$) and ^{13}C (100 MHz, $CDCl_3$) – NMR Spectra for **10**

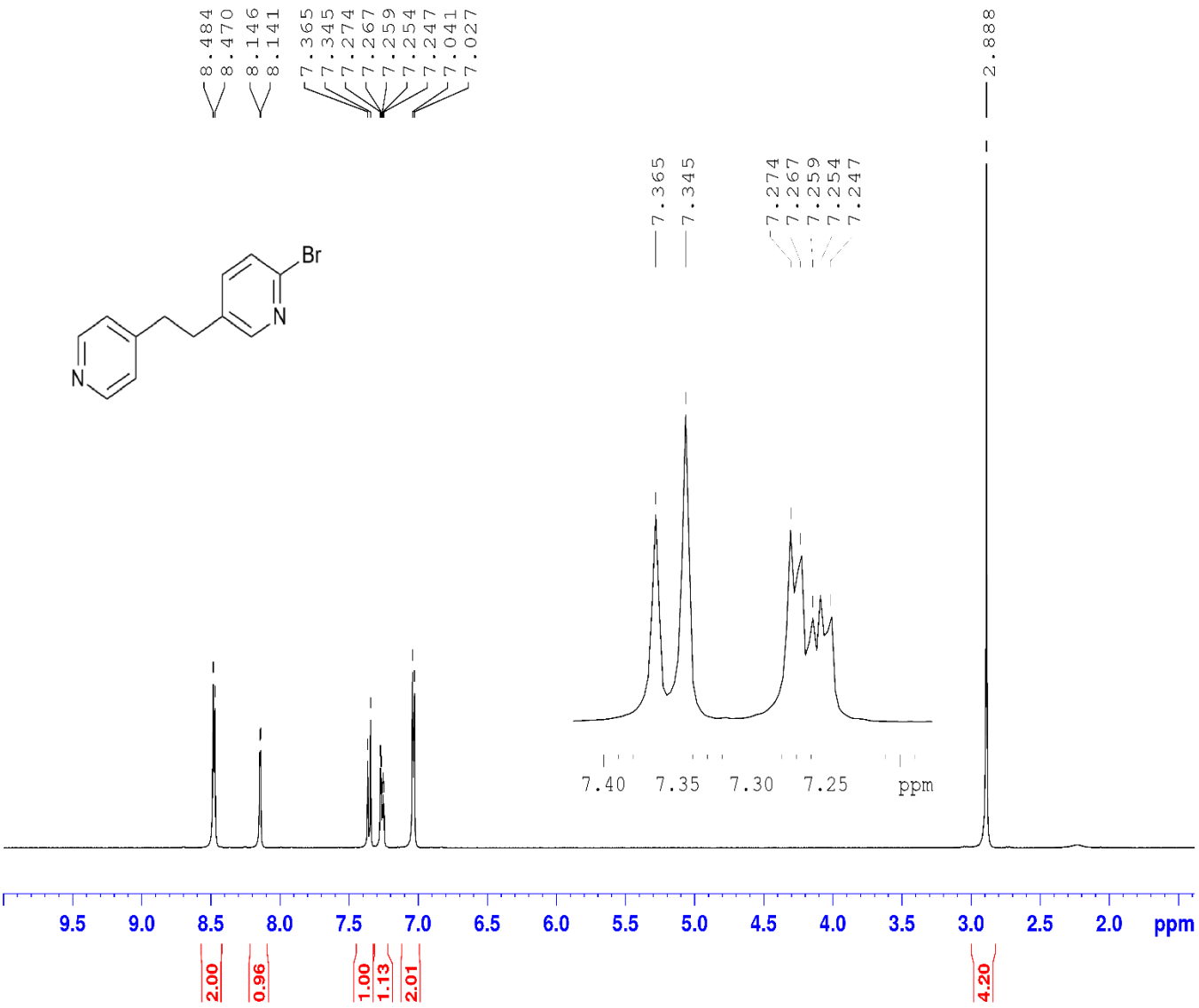

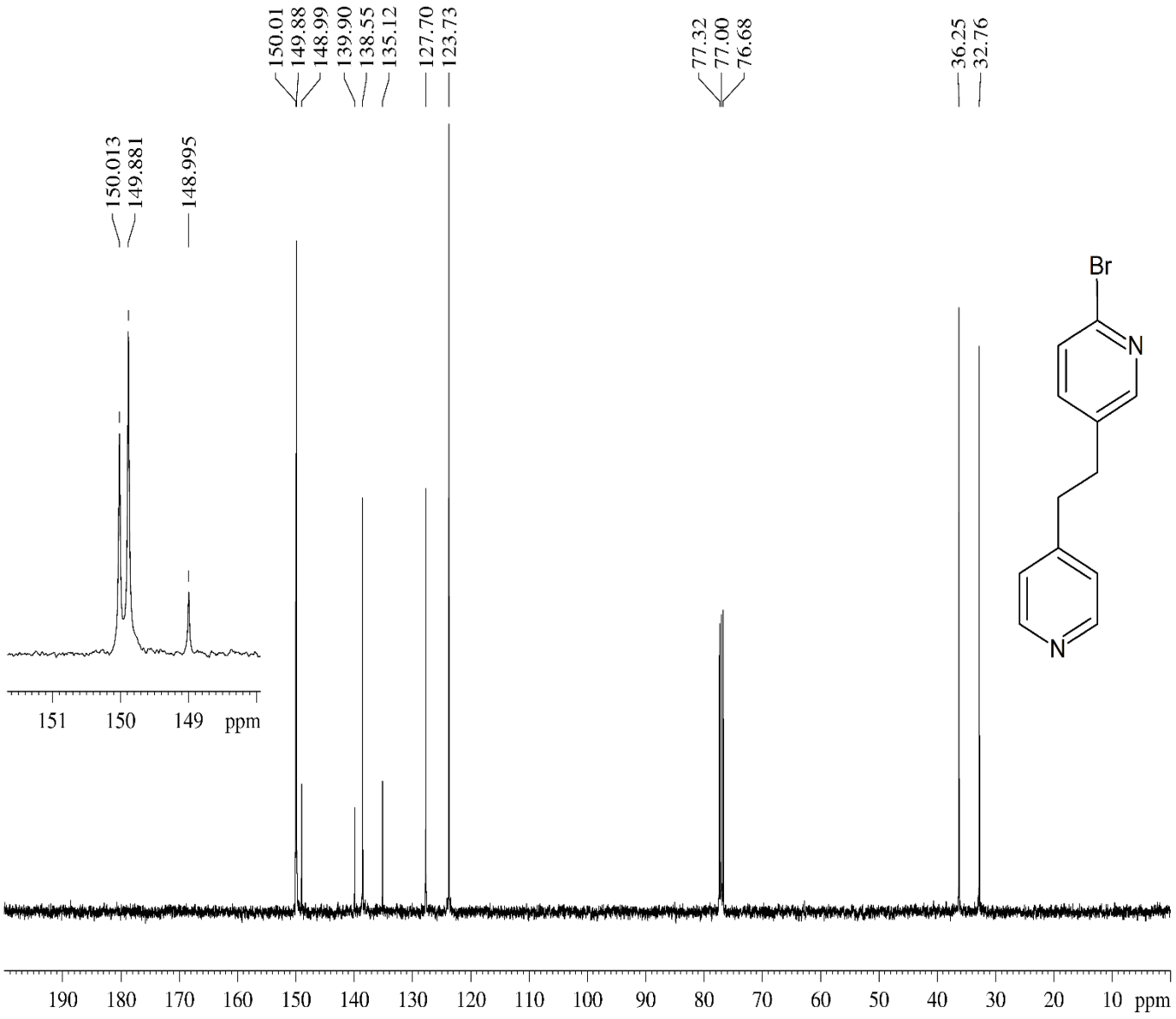
150.01
149.88
148.99
139.90
138.55
135.12
127.70
123.73
77.32
77.00
76.68
36.25
32.76
150.013
149.881
148.995
151
150
149
ppm
Br
N
N
190
180
170
160
150
140
130
120
110
100
90
80
70
60
50
40
30
20
10
ppm

^{1}H (400 MHz, $CDCl_3$) and ^{13}C (100 MHz, $CDCl_3$) – NMR Spectra for **11**

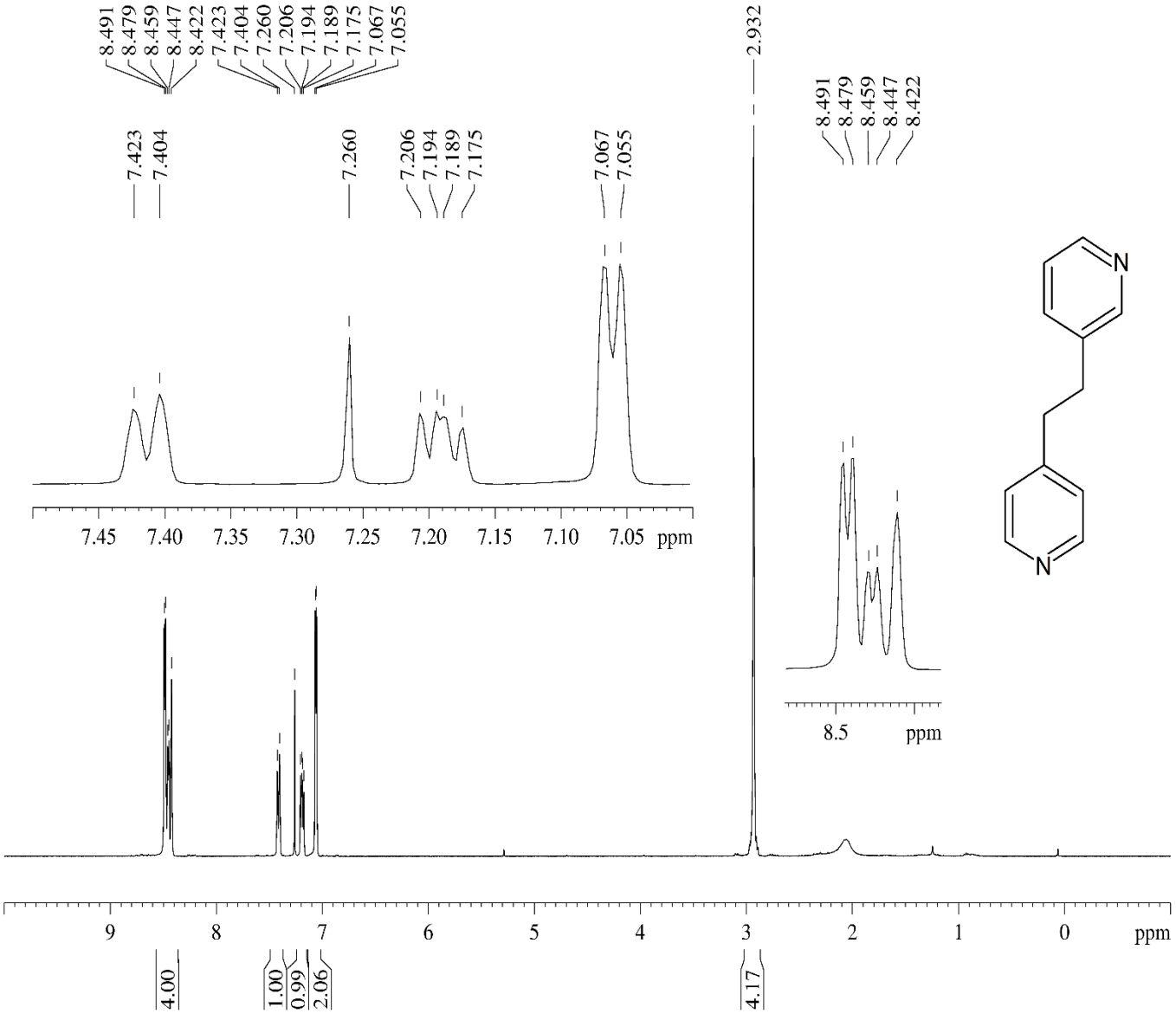

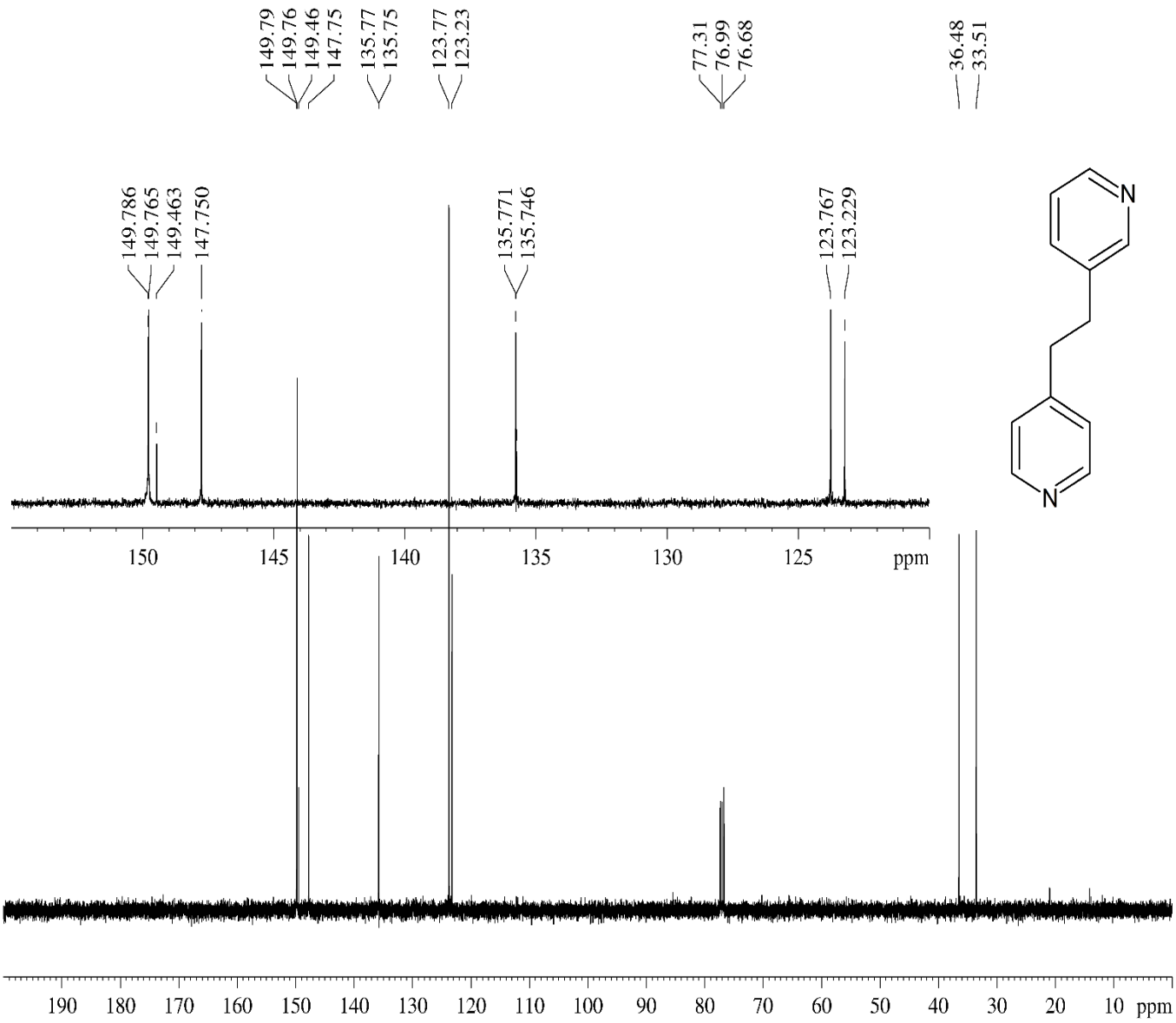
149.79
149.76
149.46
147.75
135.77
135.75
123.77
123.23
77.31
76.99
76.68
36.48
33.51
149.786
149.765
149.463
147.750
135.771
135.746
123.767
123.229
N
N
150
145
140
135
130
125
ppm
190
180
170
160
150
140
130
120
110
100
90
80
70
60
50
40
30
20
10
ppm

^{1}H (400 MHz, $CDCl_3$) and ^{13}C (100 MHz, $CDCl_3$) – NMR Spectra for **12**

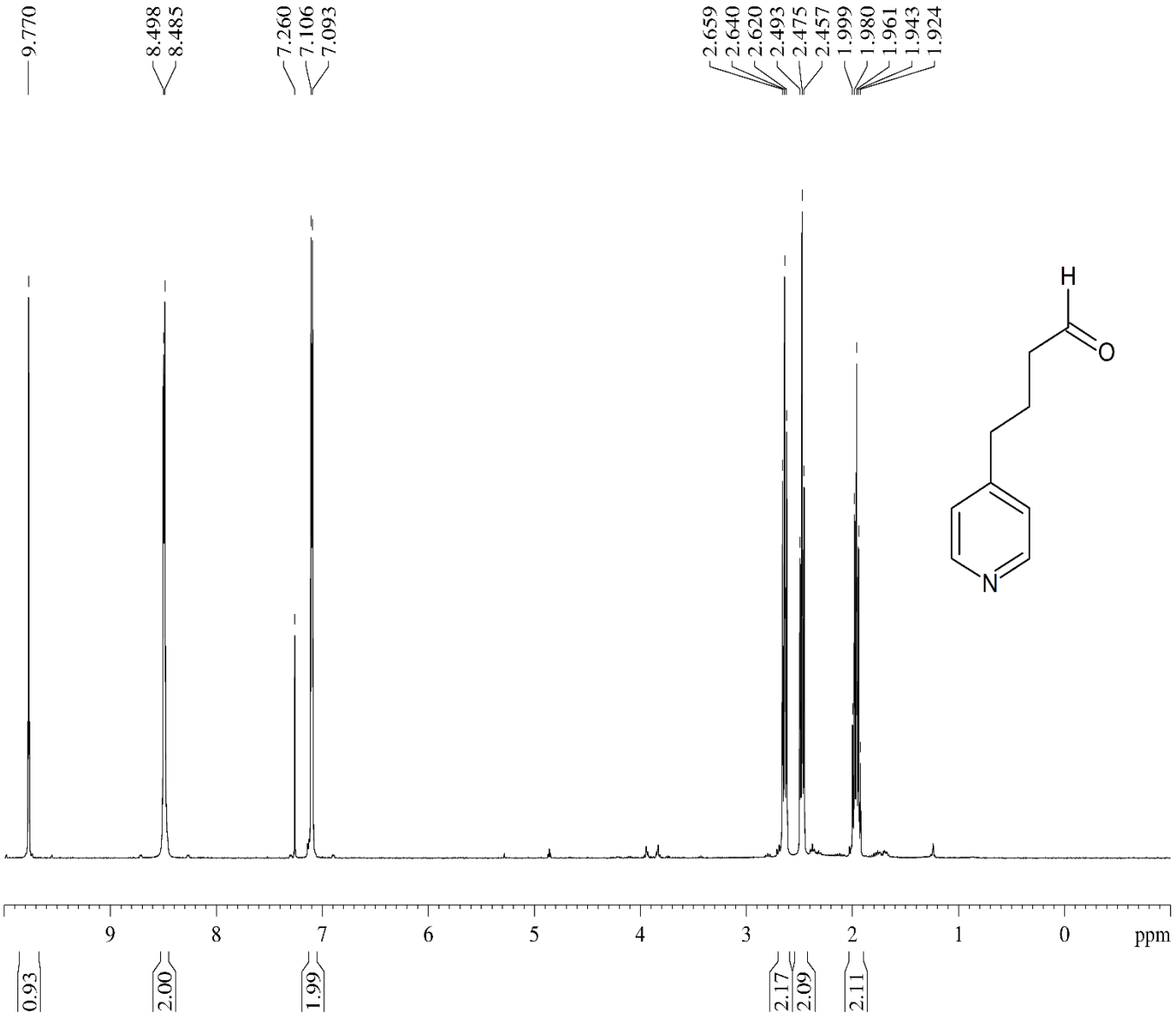

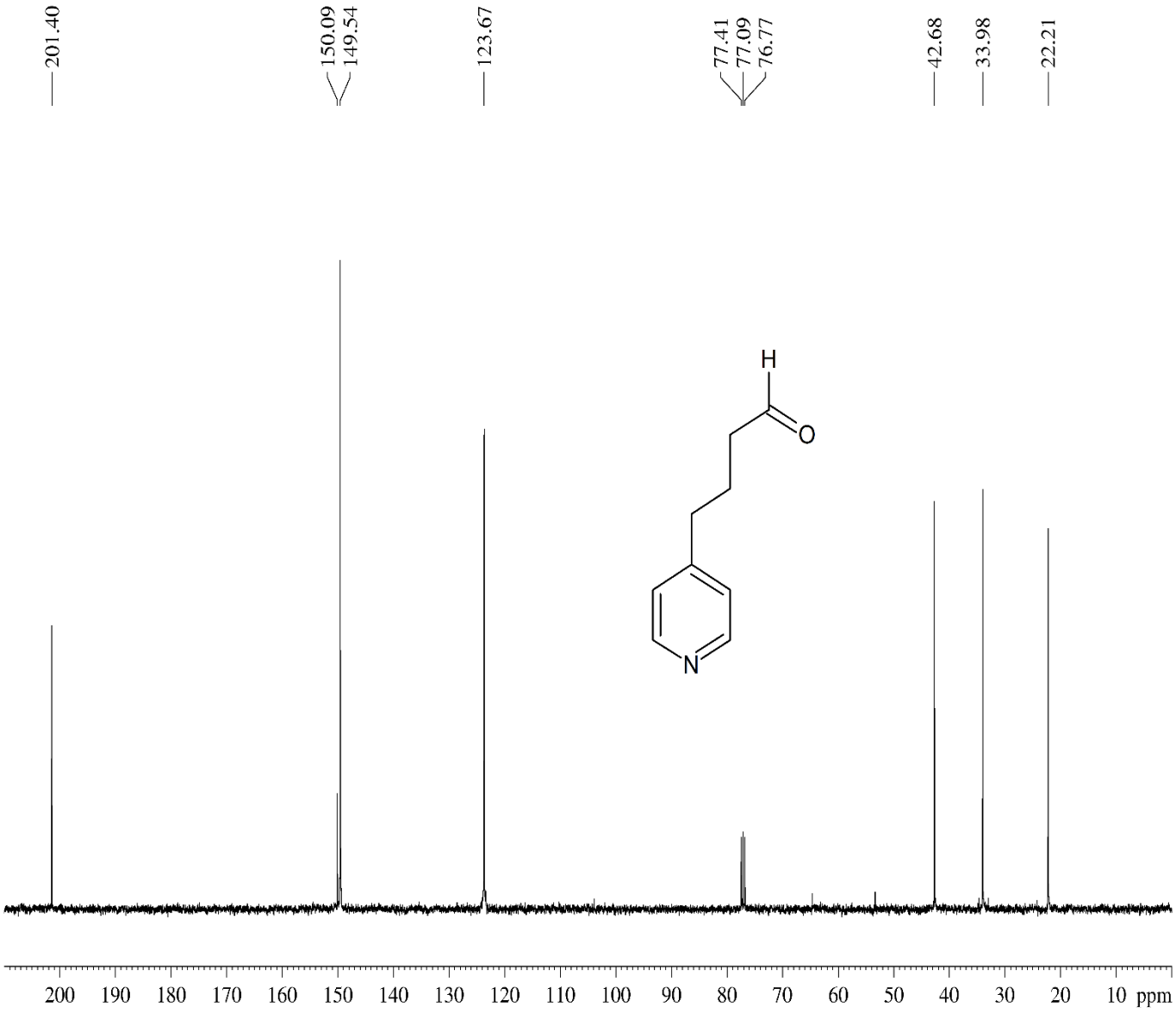
201.40
150.09
149.54
123.67
77.41
77.09
76.77
42.68
33.98
22.21
H
O
N
200 190 180 170 160 150 140 130 120 110 100 90 80 70 60 50 40 30 20 10 ppm

^{1}H (400 MHz, $CDCl_3$) and ^{13}C (100 MHz, $CDCl_3$) – NMR Spectra for **13.1**

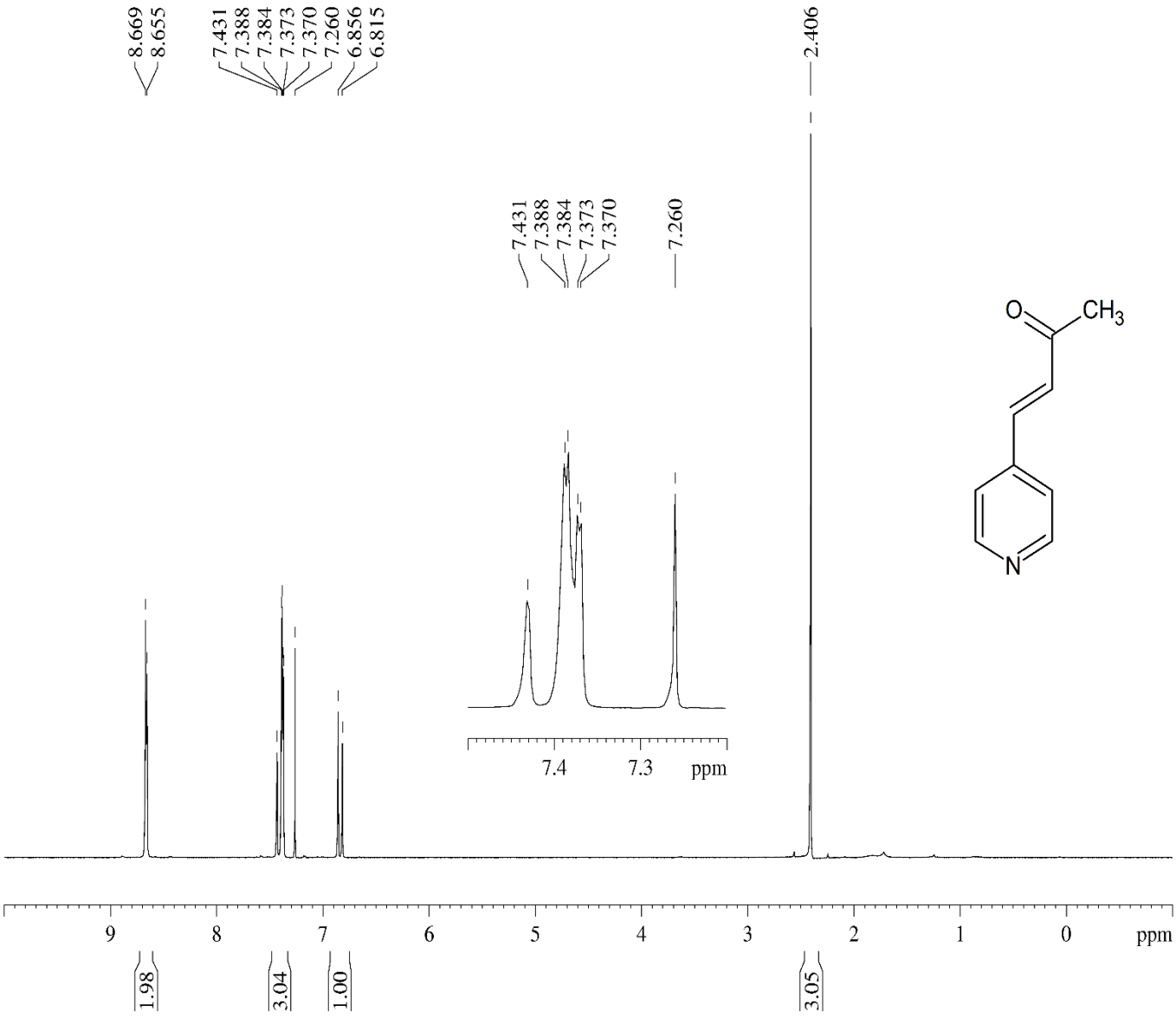

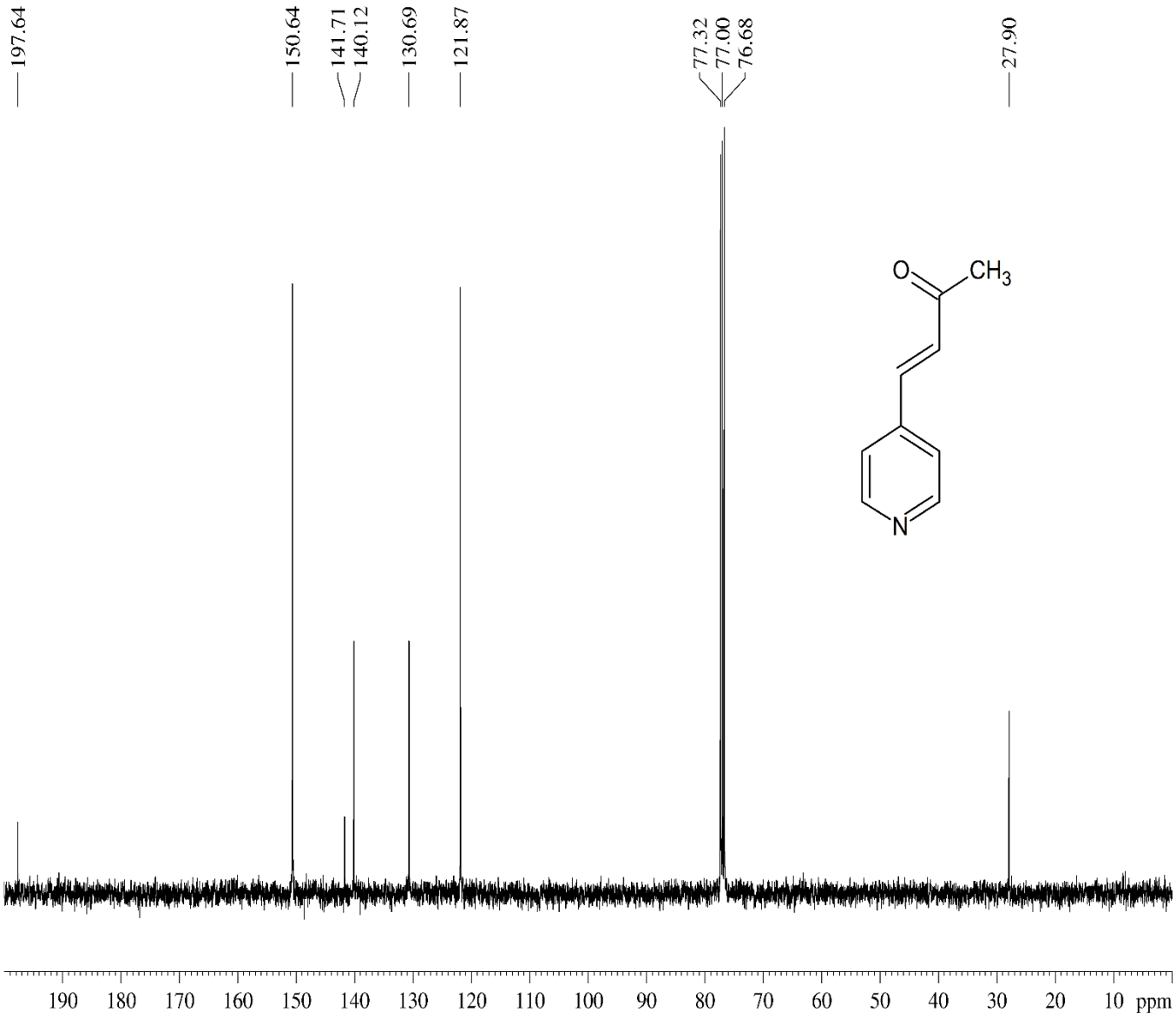
197.64
150.64
141.71
140.12
130.69
121.87
77.32
77.00
76.68
27.90
O
CH3
N
190 180 170 160 150 140 130 120 110 100 90 80 70 60 50 40 30 20 10 ppm

^{1}H (400 MHz, $CDCl_3$) and ^{13}C (100 MHz, $CDCl_3$) – NMR Spectra for **13**

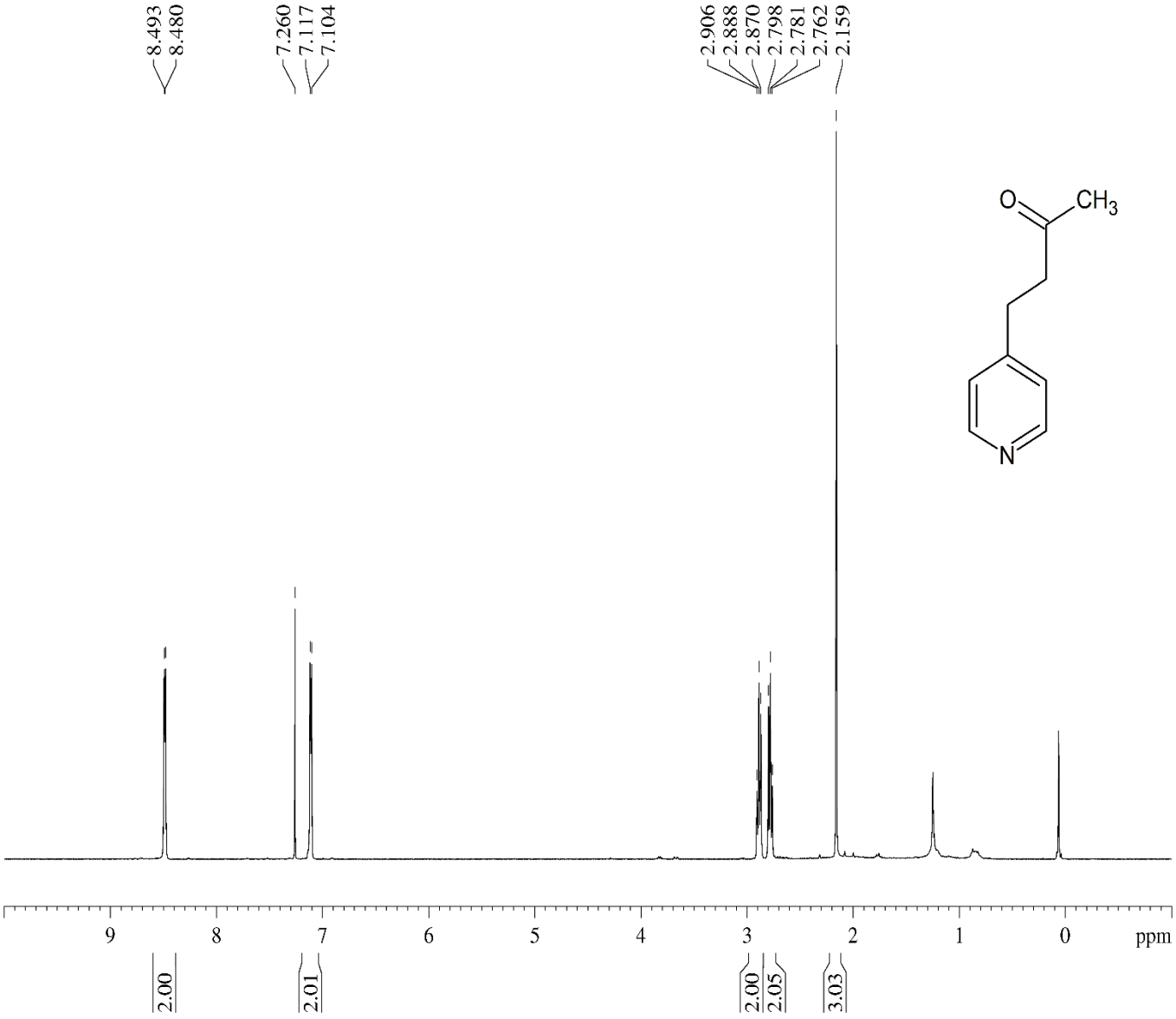

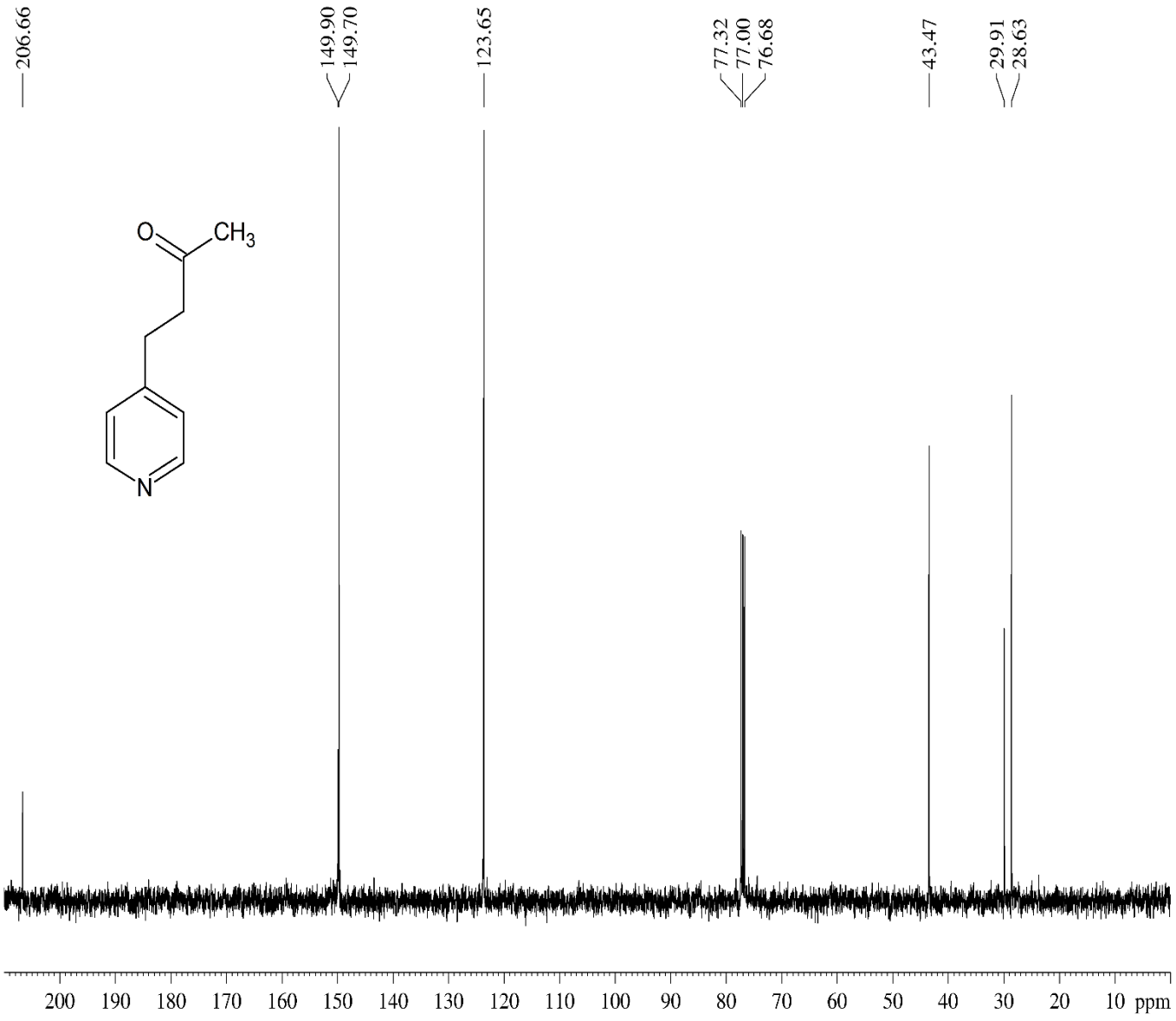
206.66
149.90
149.70
123.65
77.32
77.00
76.68
43.47
29.91
28.63
O
CH3
N
200 190 180 170 160 150 140 130 120 110 100 90 80 70 60 50 40 30 20 10 ppm

^{1}H (400 MHz, $CDCl_3$) and ^{13}C (100 MHz, $CDCl_3$) – NMR Spectra for **14.1**

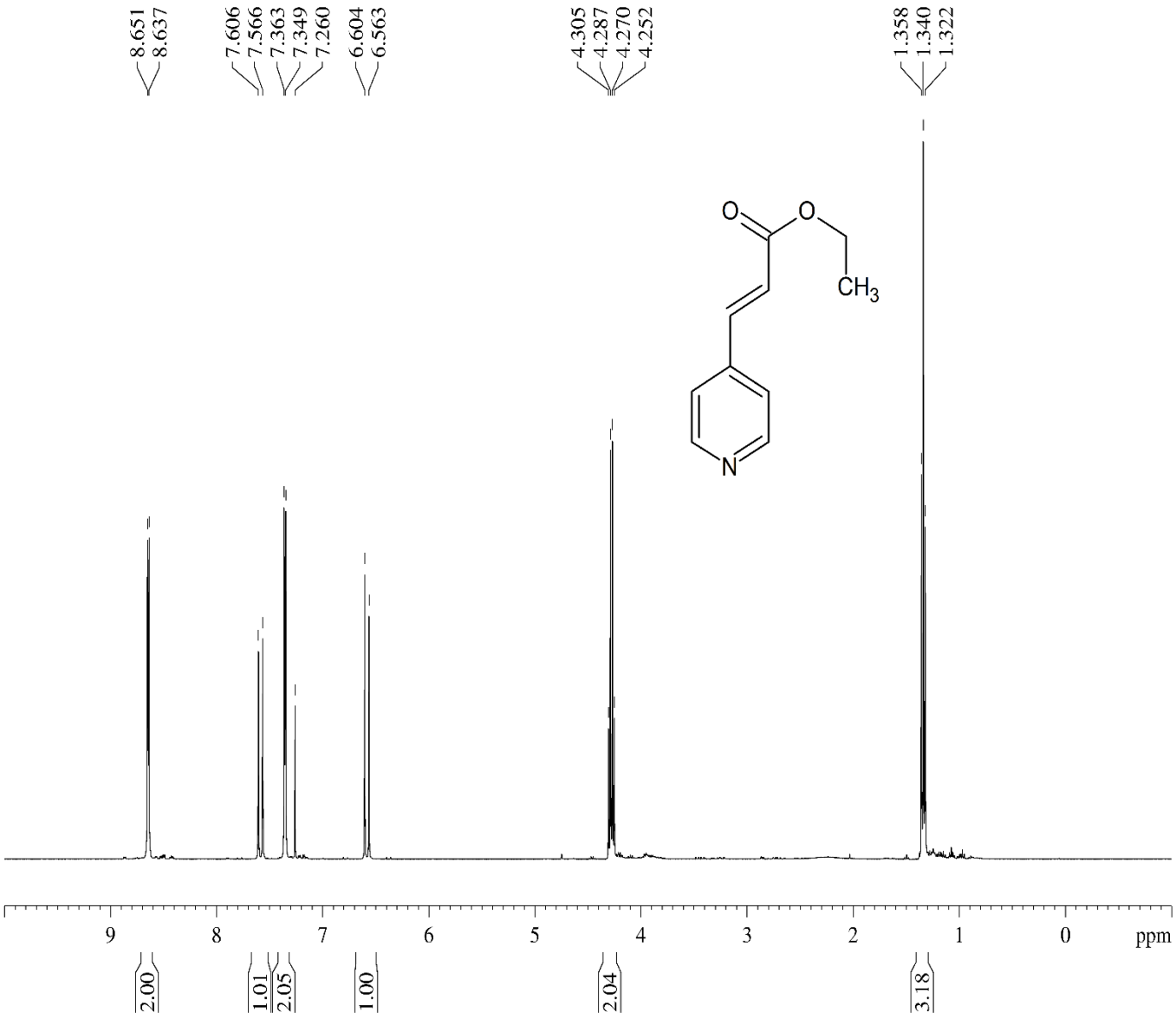

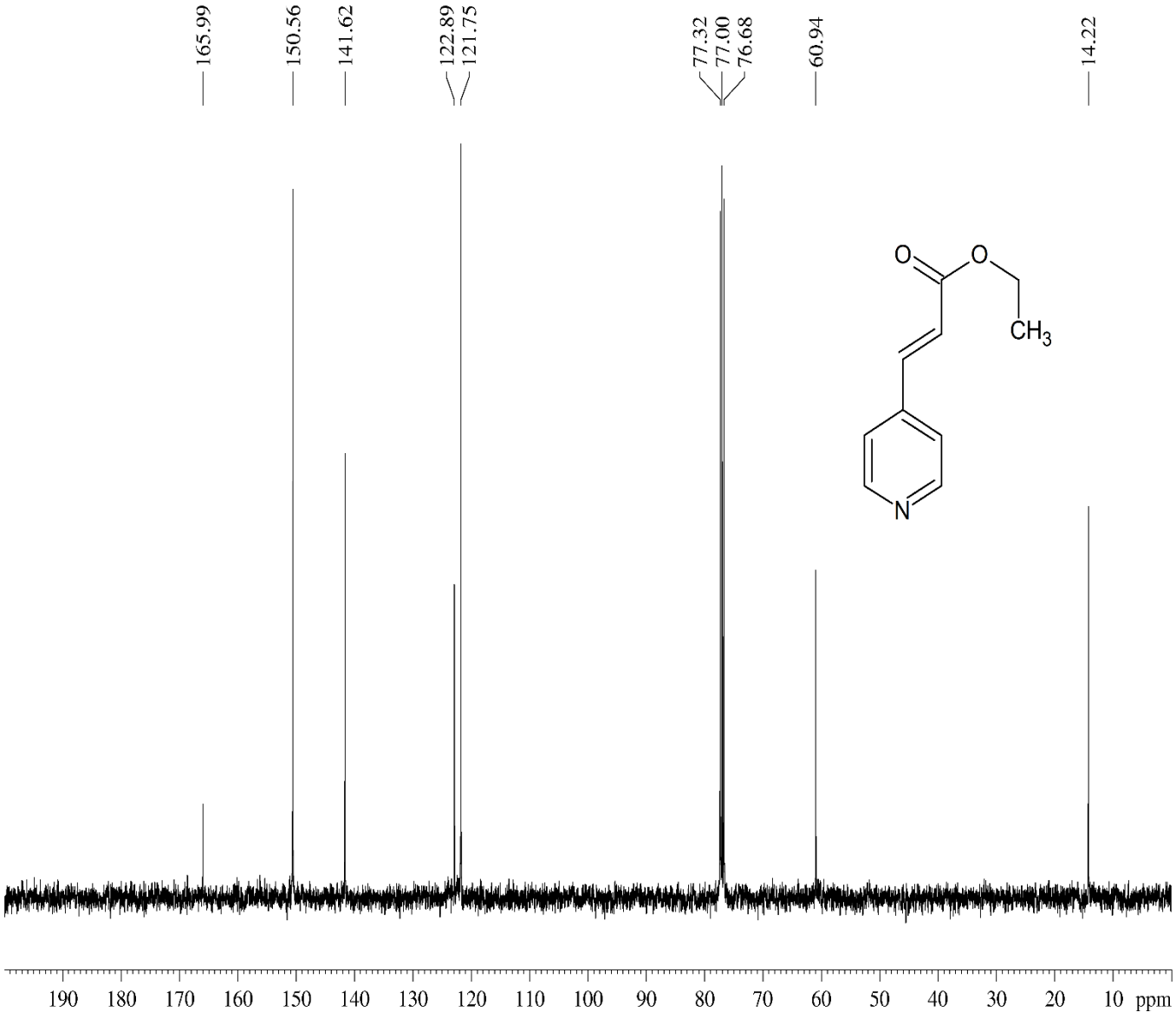
165.99
150.56
141.62
122.89
121.75
77.32
77.00
76.68
60.94
14.22
O
O
CH3
N
190 180 170 160 150 140 130 120 110 100 90 80 70 60 50 40 30 20 10 ppm

^{1}H (400 MHz, $CDCl_3$) and ^{13}C (100 MHz, $CDCl_3$) – NMR Spectra for **14**

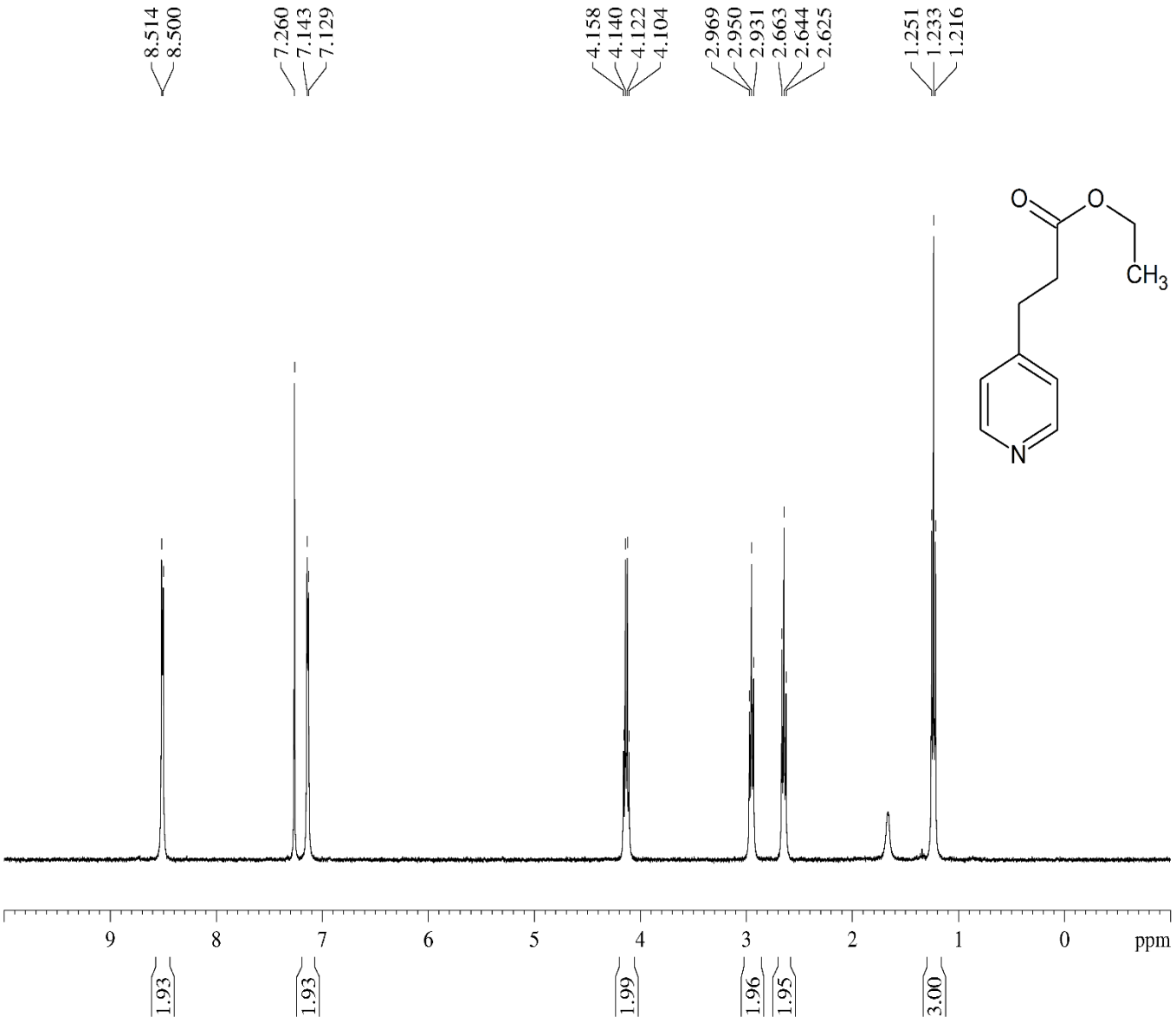

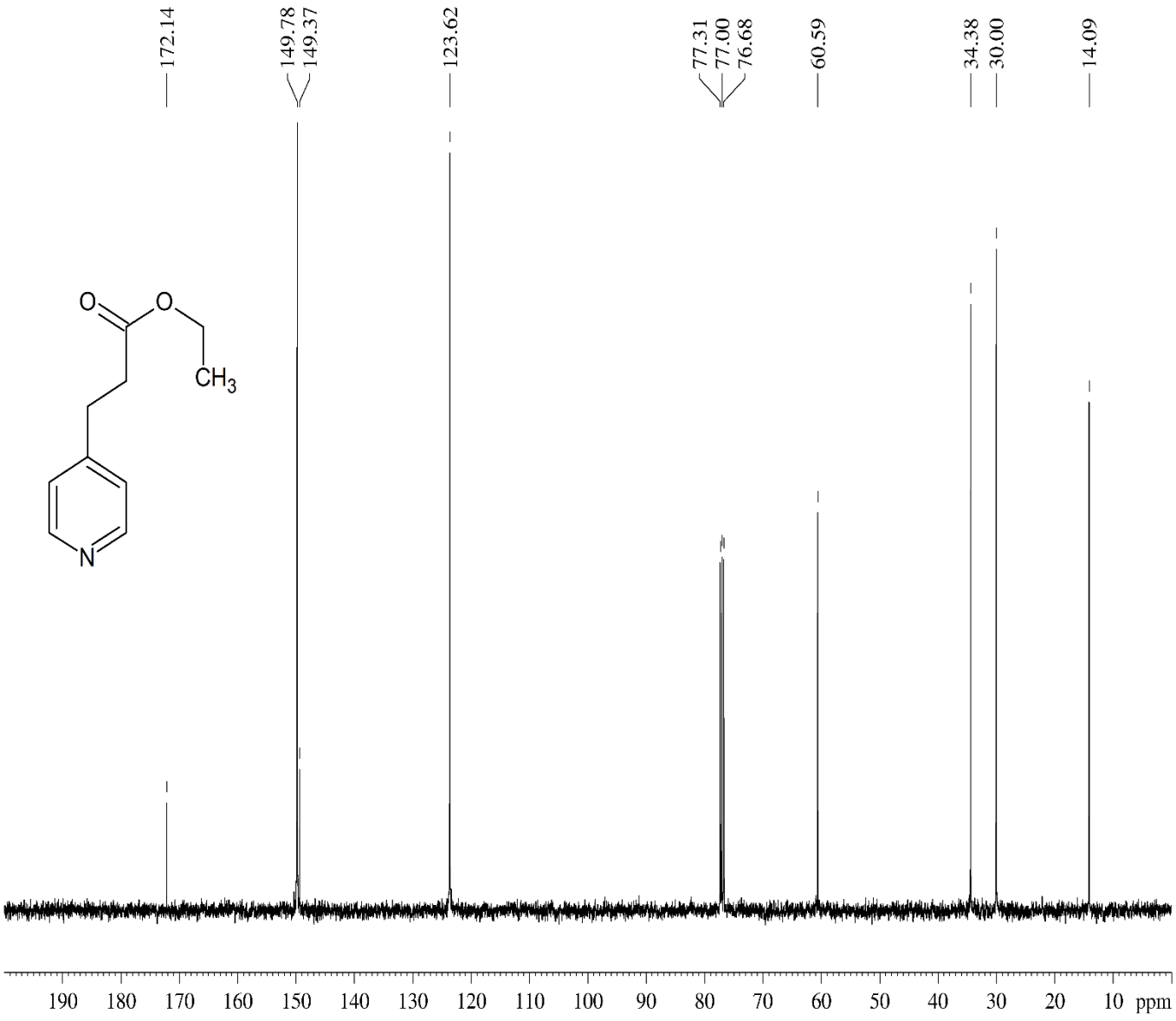
172.14
149.78
149.37
123.62
77.31
77.00
76.68
60.59
34.38
30.00
14.09
O
O
CH3
N
190 180 170 160 150 140 130 120 110 100 90 80 70 60 50 40 30 20 10 ppm

^{1}H (300 MHz, $CDCl_3$) and ^{13}C (75 MHz, $CDCl_3$) – NMR Spectra for **15**

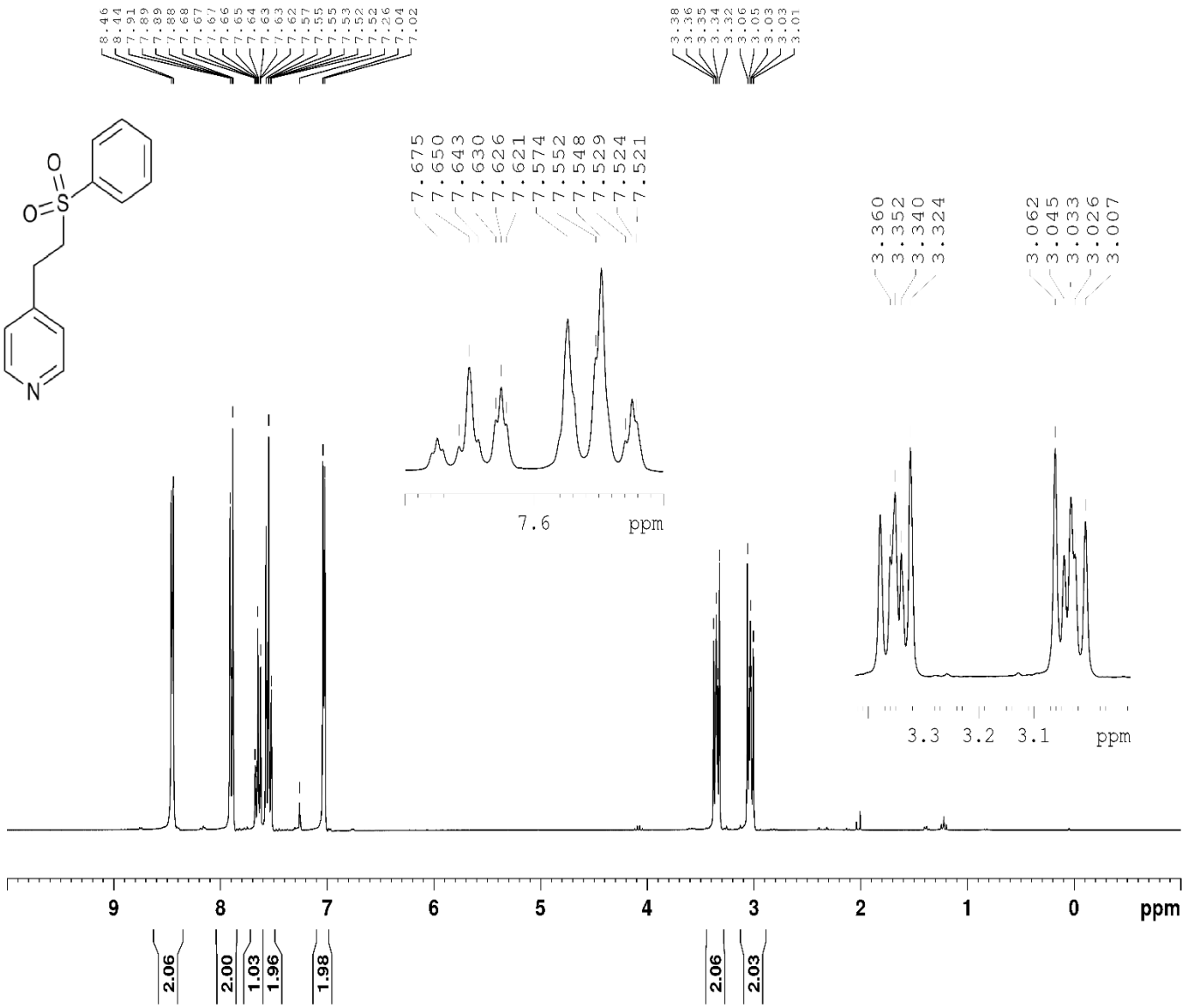

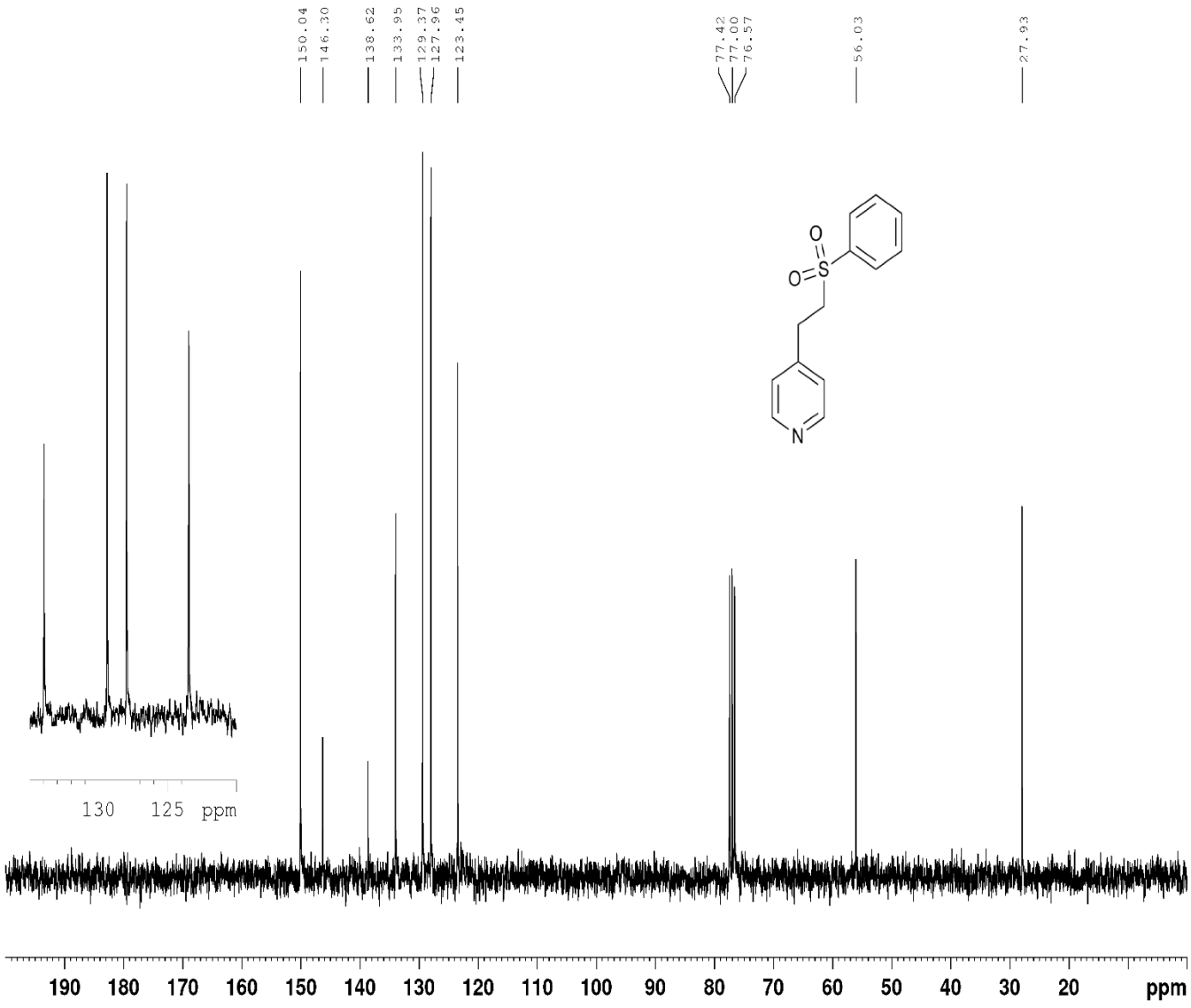
150.04
146.30
138.62
133.95
129.37
127.96
123.45
77.42
77.00
76.57
56.03
27.93
O
O
S
N
130
125
ppm
190
180
170
160
150
140
130
120
110
100
90
80
70
60
50
40
30
20
ppm

^{1}H (400 MHz, $CDCl_3$) and ^{13}C (100 MHz, $CDCl_3$) – NMR Spectra for **16**

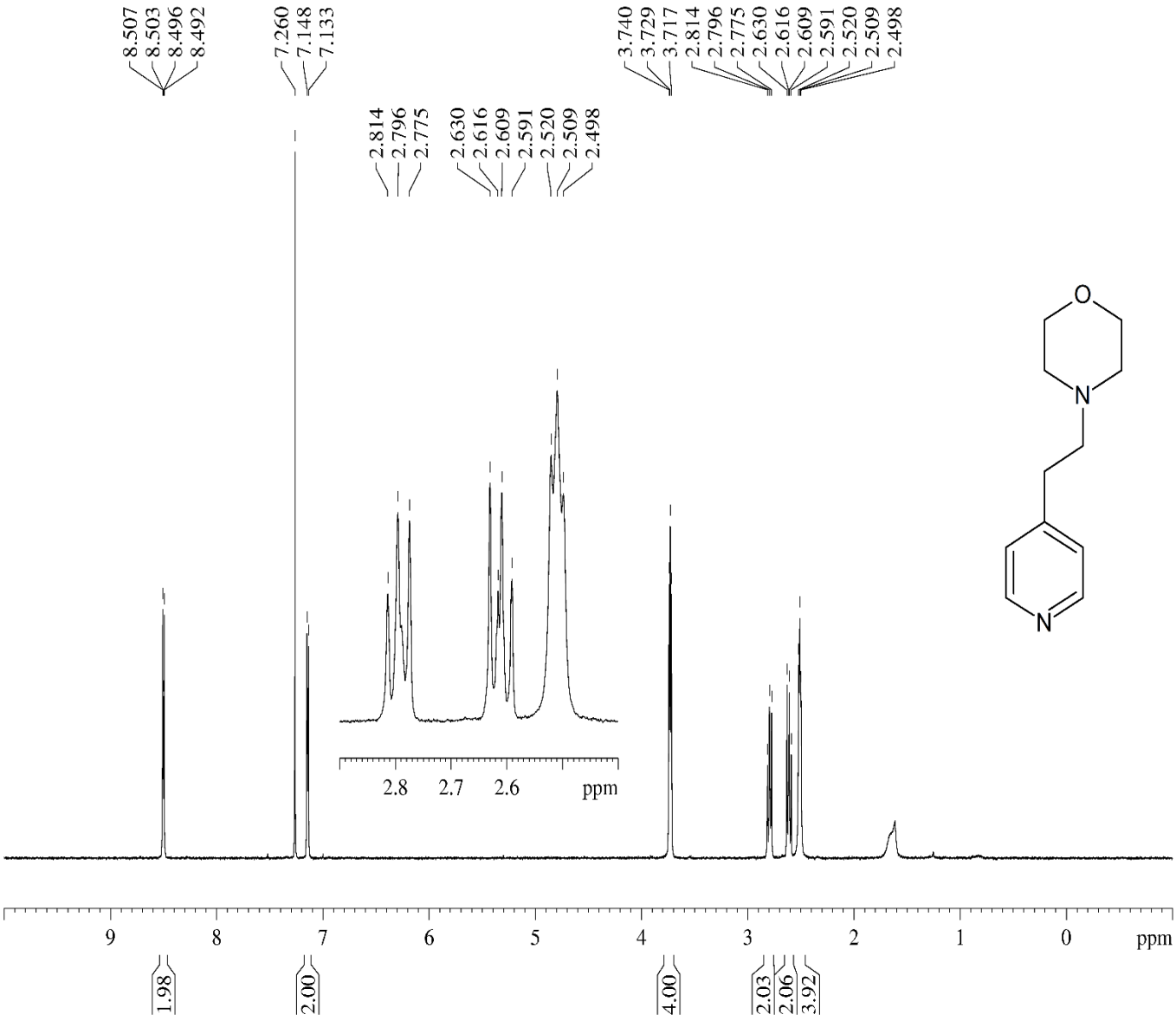

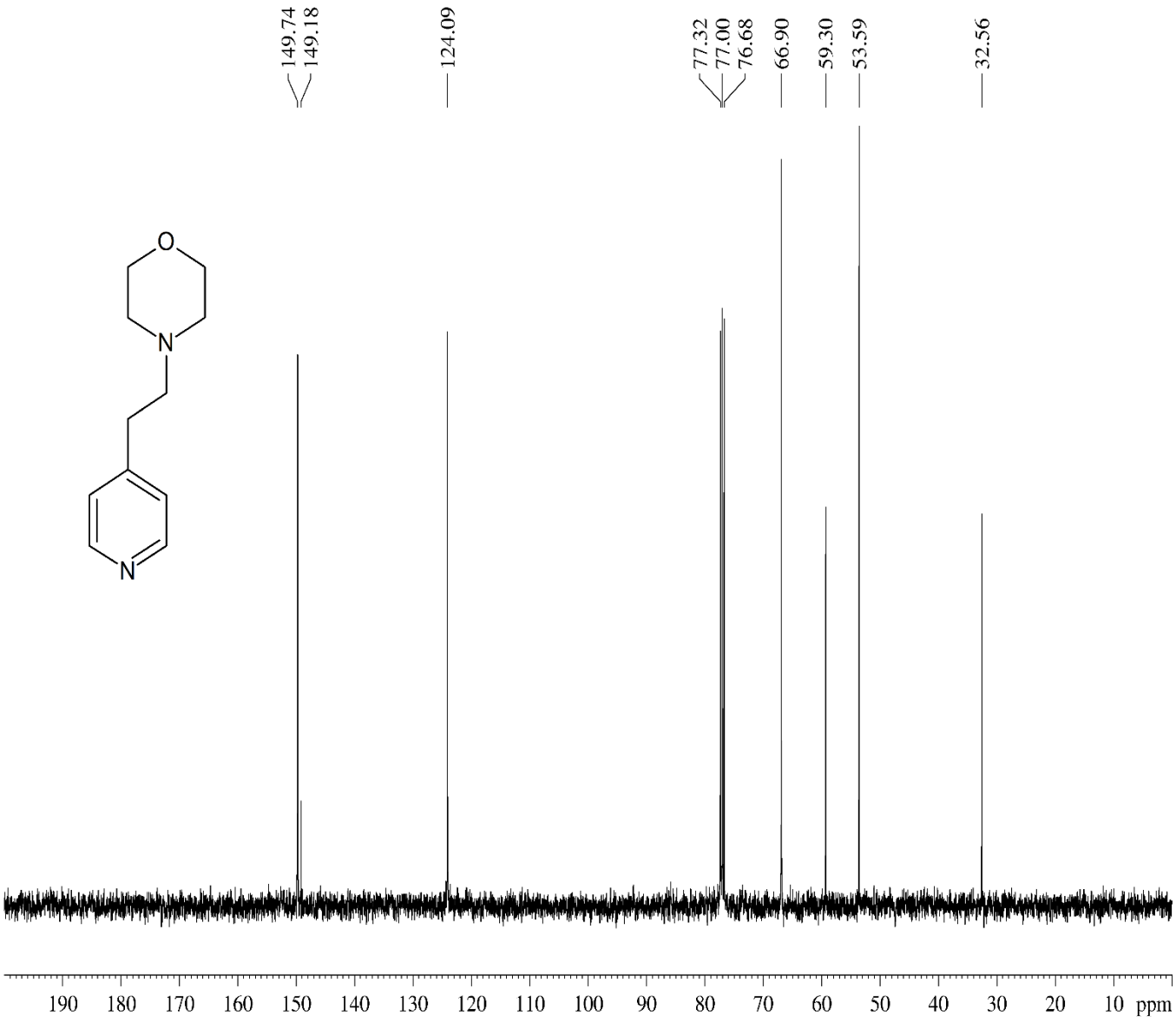
149.74
149.18
124.09
77.32
77.00
76.68
66.90
59.30
53.59
32.56
O
N
N
190 180 170 160 150 140 130 120 110 100 90 80 70 60 50 40 30 20 10 ppm

^{1}H (400 MHz, $CDCl_3$) and ^{13}C (100 MHz, $CDCl_3$) – NMR Spectra for **17**

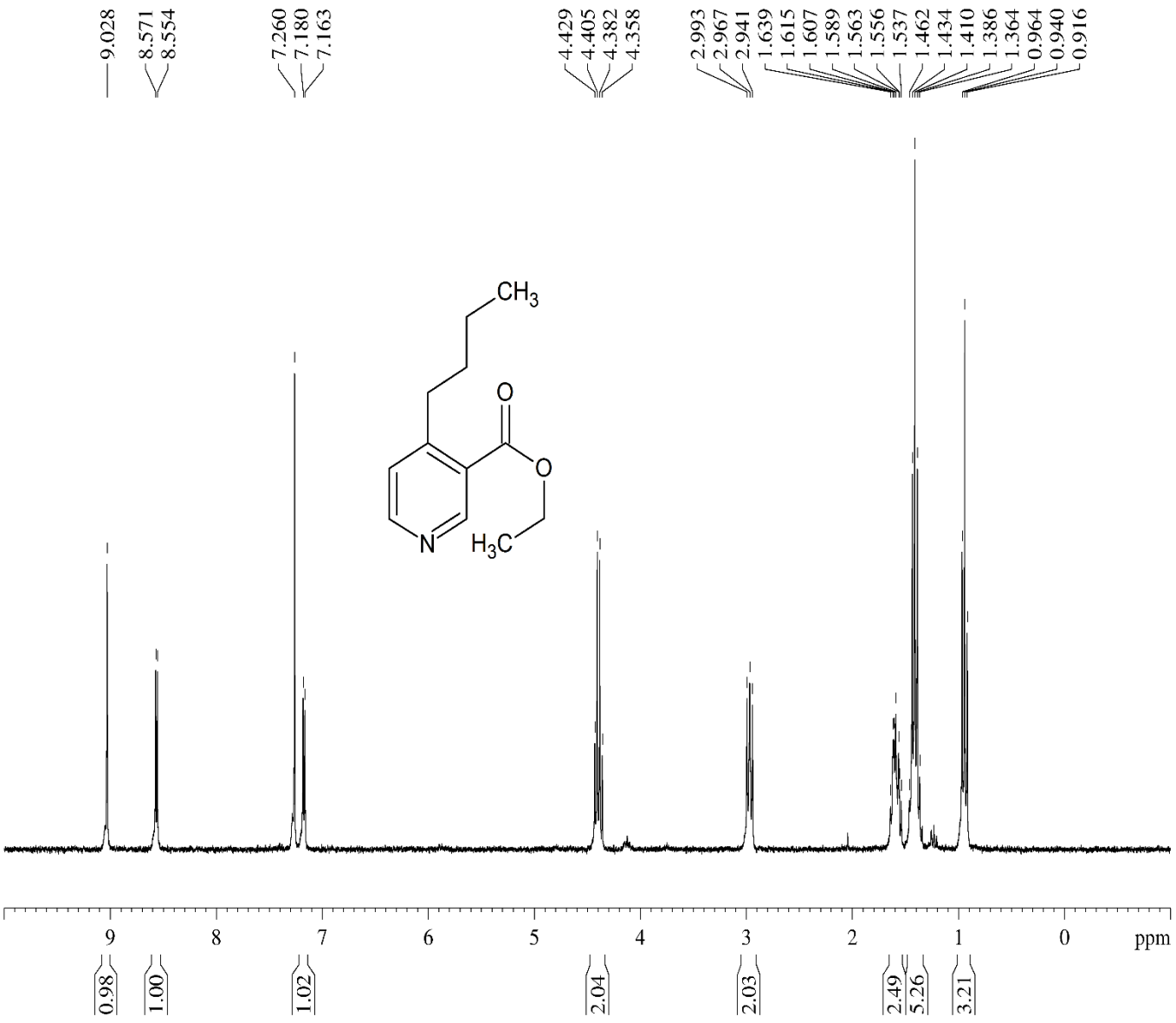

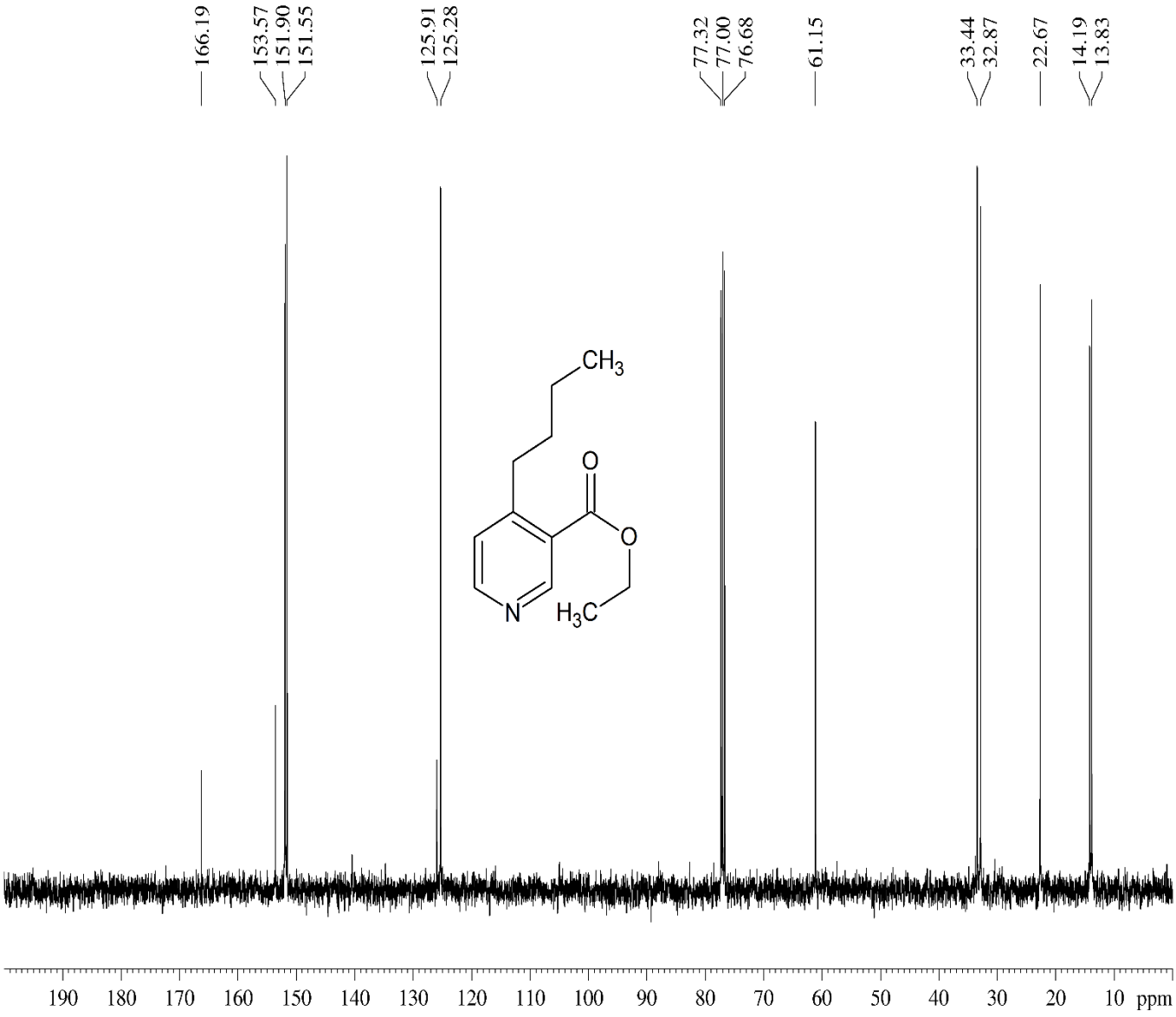
166.19
153.57
151.90
151.55
125.91
125.28
77.32
77.00
76.68
61.15
33.44
32.87
22.67
14.19
13.83
CH3
O
O
N
H3C
190 180 170 160 150 140 130 120 110 100 90 80 70 60 50 40 30 20 10 ppm

^{1}H (400 MHz, $CDCl_3$) and ^{13}C (100 MHz, $CDCl_3$) – NMR Spectra for **18**

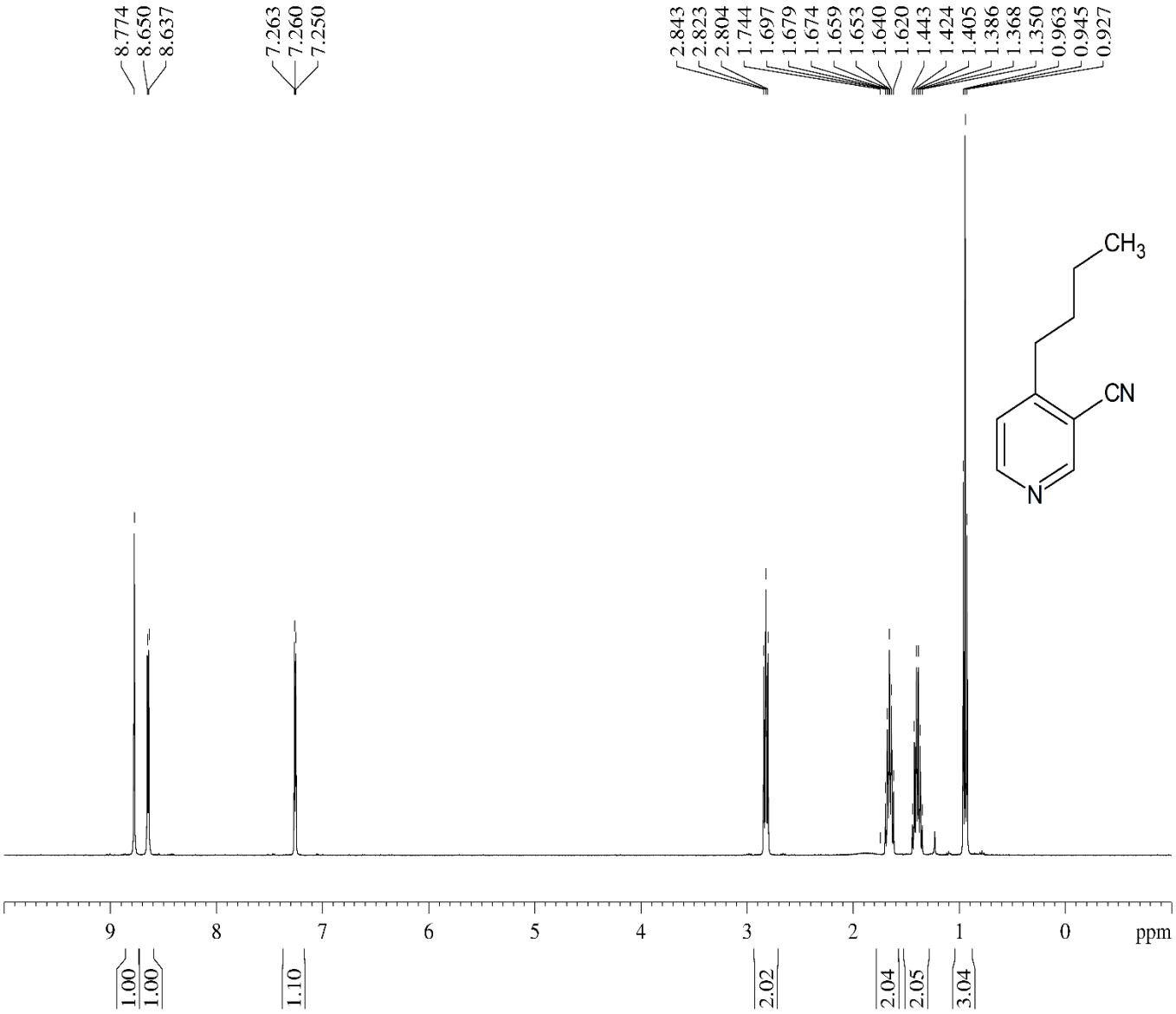

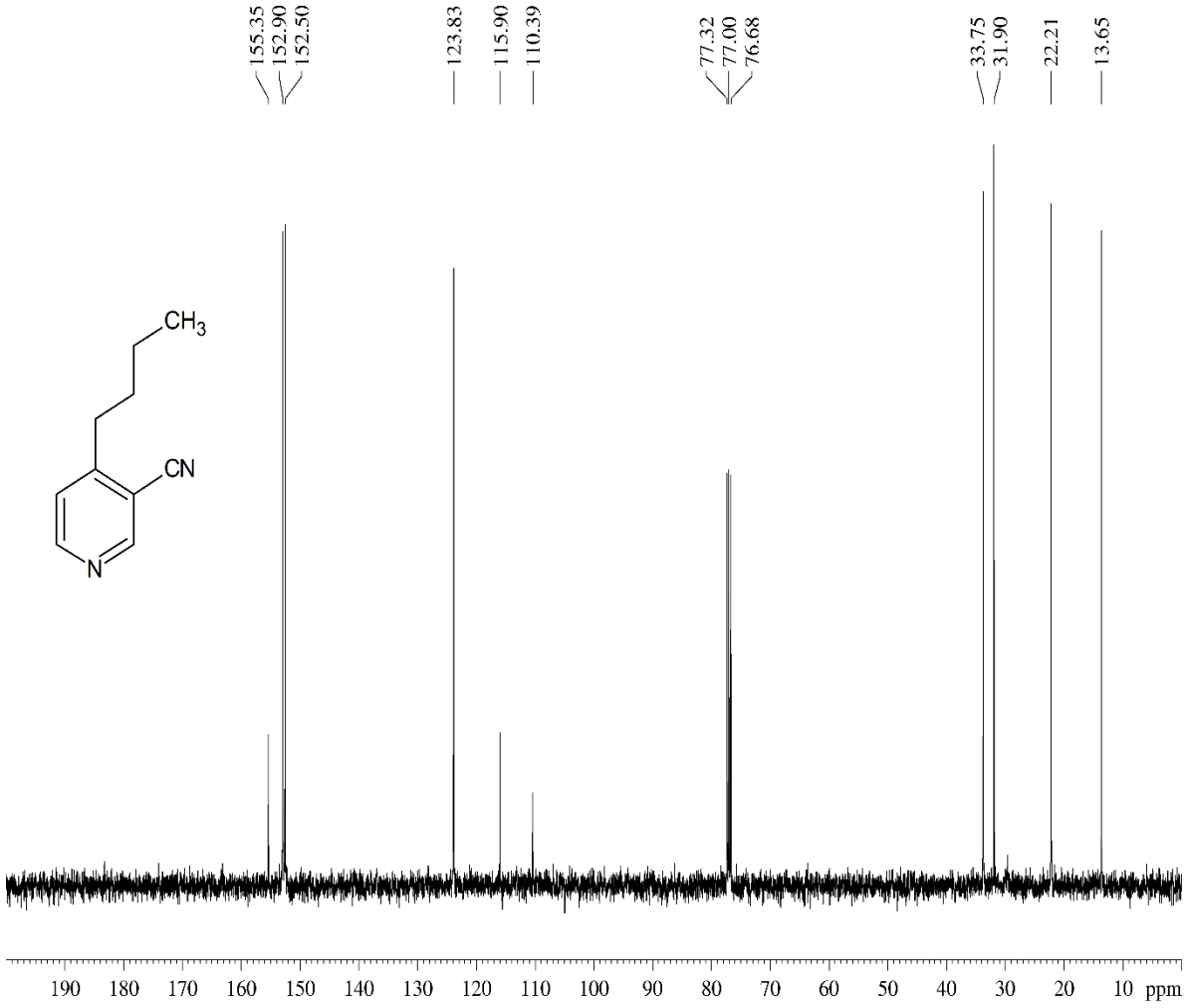
155.35
152.90
152.50
123.83
115.90
110.39
77.32
77.00
76.68
33.75
31.90
22.21
13.65
CH3
CN
N
190 180 170 160 150 140 130 120 110 100 90 80 70 60 50 40 30 20 10 ppm

^{1}H (400 MHz, $CDCl_3$) and ^{13}C (100 MHz, $CDCl_3$) – NMR Spectra for **19**

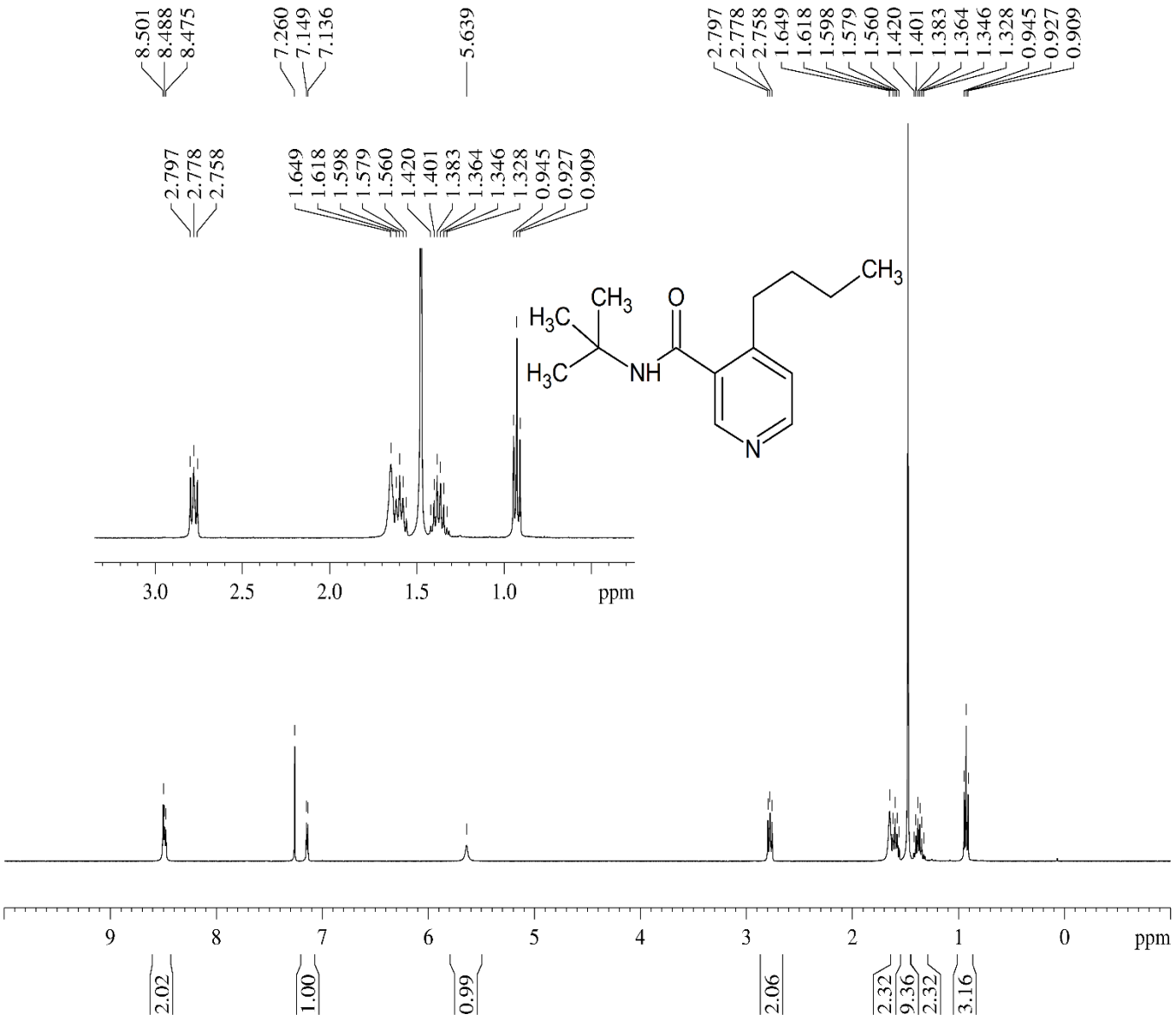

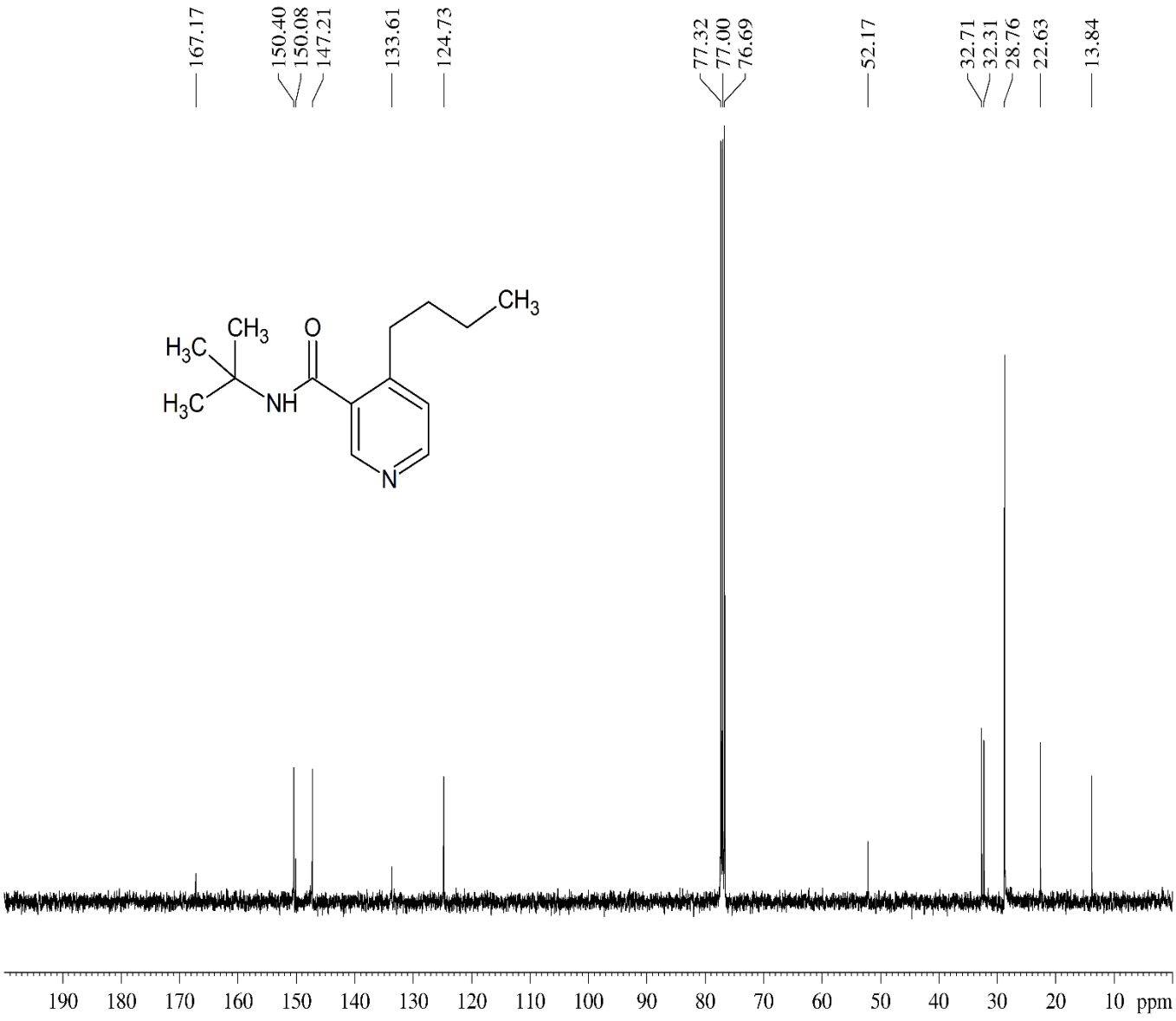
167.17
150.40
150.08
147.21
133.61
124.73
77.32
77.00
76.69
52.17
32.71
32.31
28.76
22.63
13.84
CH3
O
H3C
CH3
H3C
NH
N
190 180 170 160 150 140 130 120 110 100 90 80 70 60 50 40 30 20 10 ppm

^{1}H (400 MHz, $CDCl_3$) and ^{13}C (100 MHz, $CDCl_3$) – NMR Spectra for **20.1**

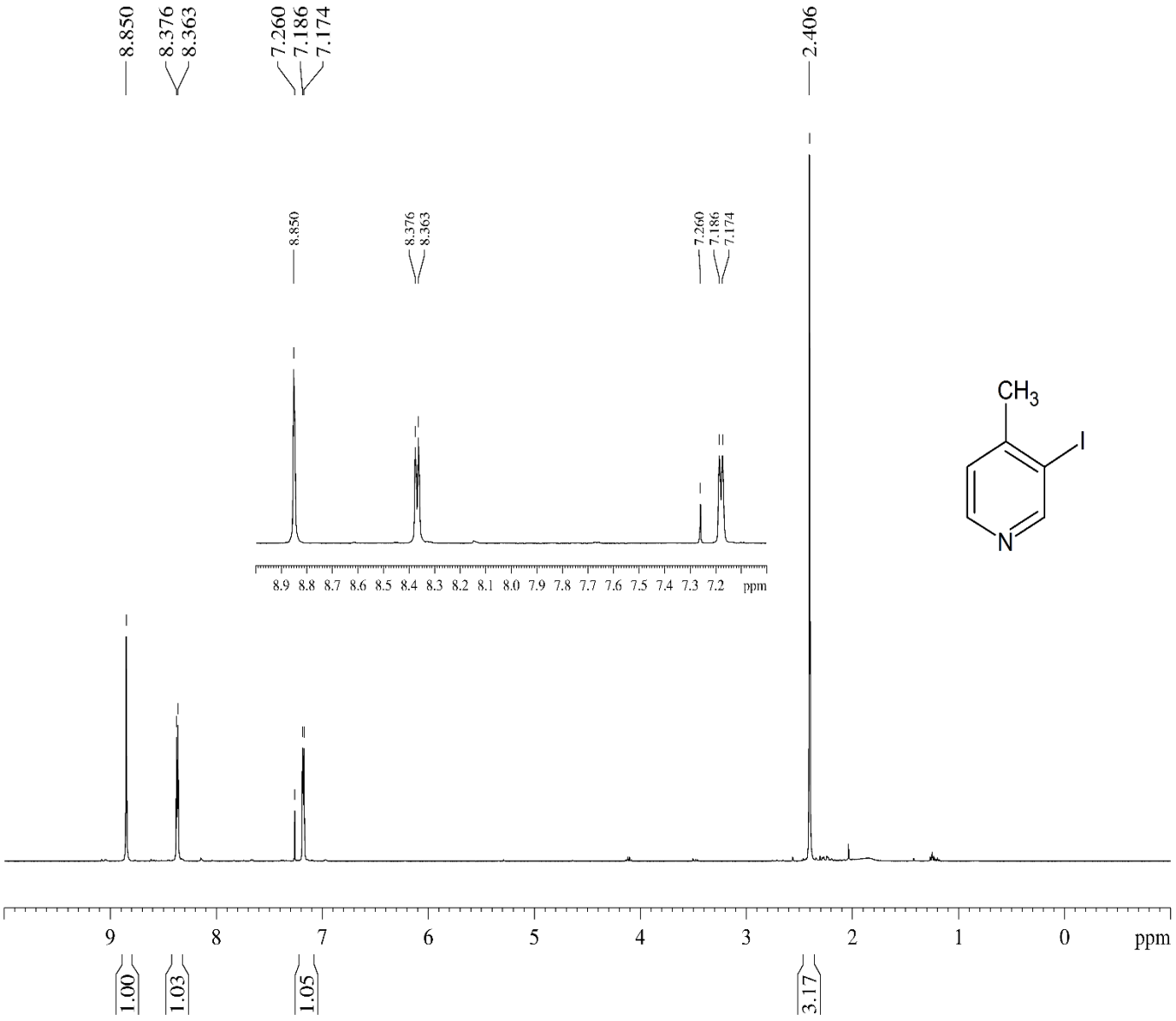

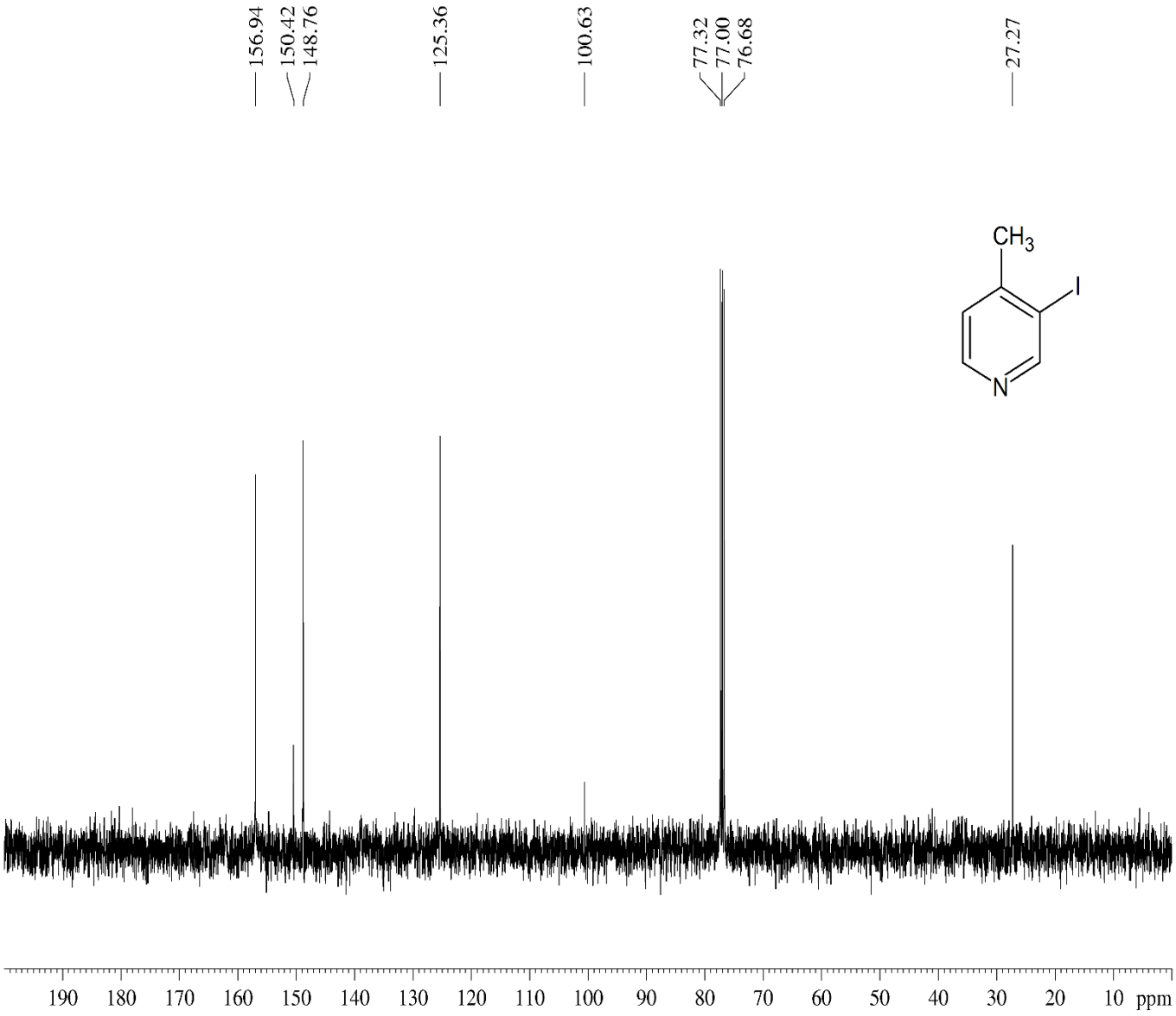
156.94
150.42
148.76
125.36
100.63
77.32
77.00
76.68
27.27
CH3
I
N
190 180 170 160 150 140 130 120 110 100 90 80 70 60 50 40 30 20 10 ppm

^{1}H (400 MHz, $CDCl_3$) and ^{13}C (100 MHz, $CDCl_3$) – NMR Spectra for **20.2**

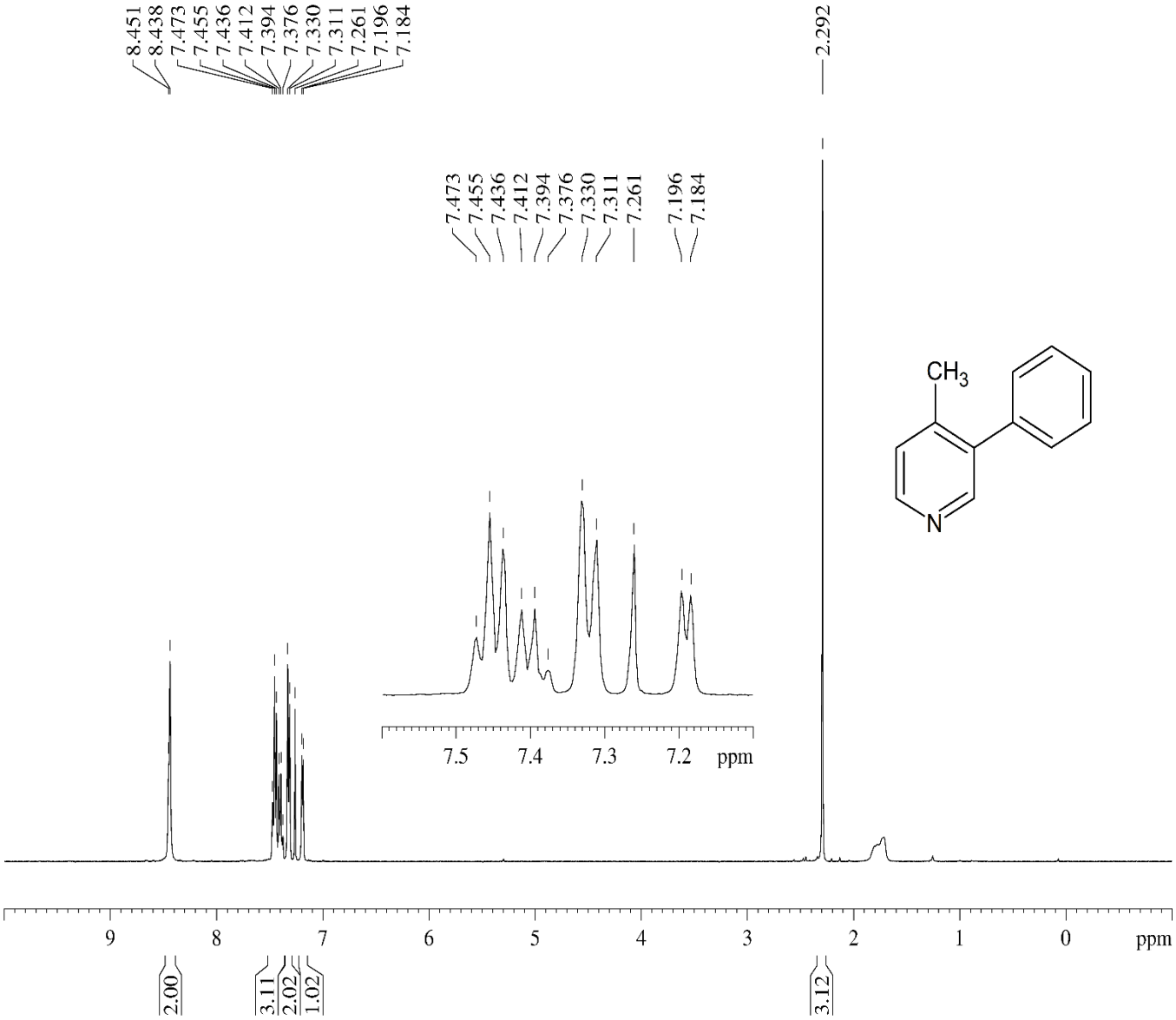

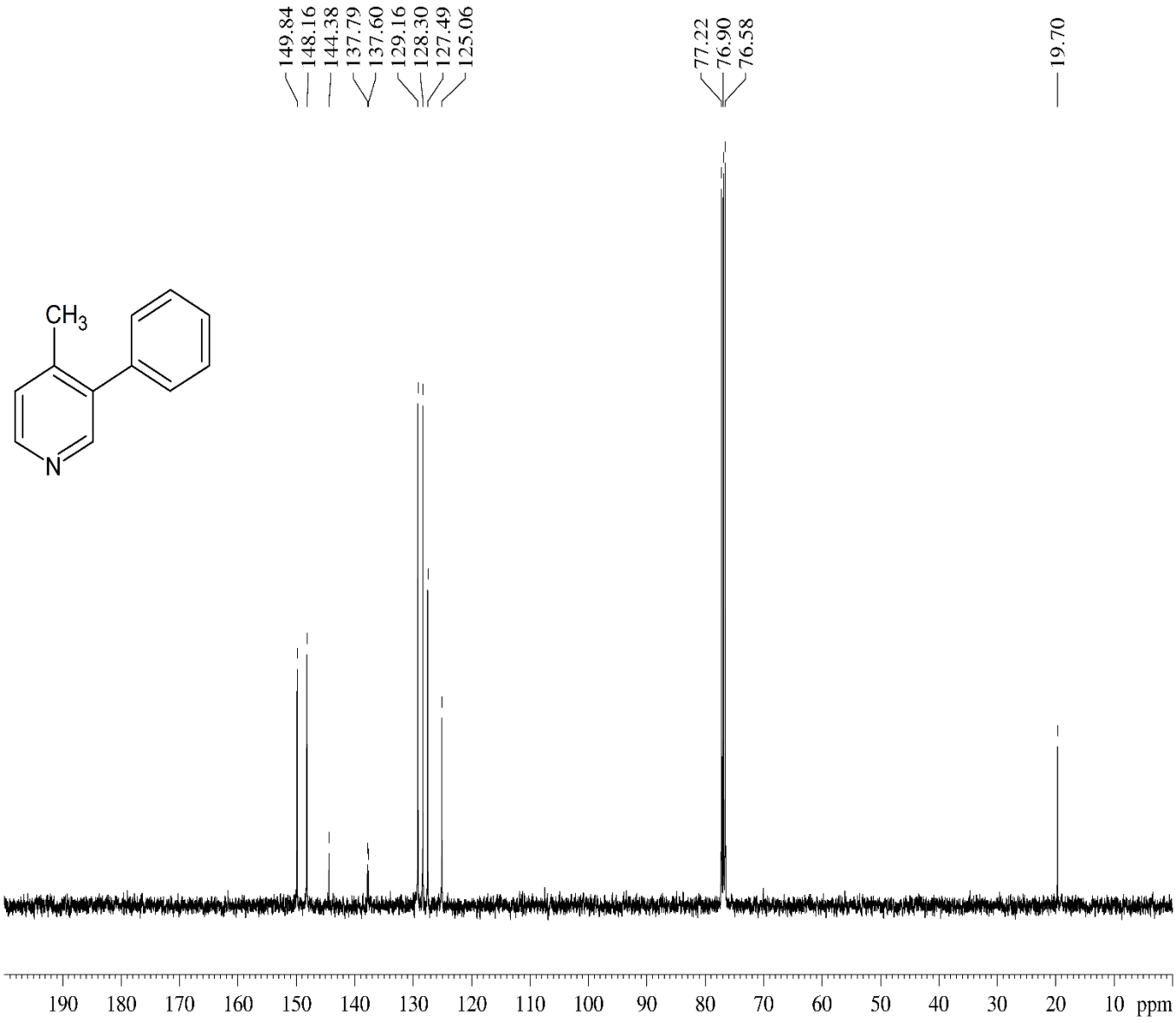
149.84
148.16
144.38
137.79
137.60
129.16
128.30
127.49
125.06
77.22
76.90
76.58
19.70
CH3
N
190 180 170 160 150 140 130 120 110 100 90 80 70 60 50 40 30 20 10 ppm

^{1}H (400 MHz, $CDCl_3$) and ^{13}C (100 MHz, $CDCl_3$) – NMR Spectra for **20**

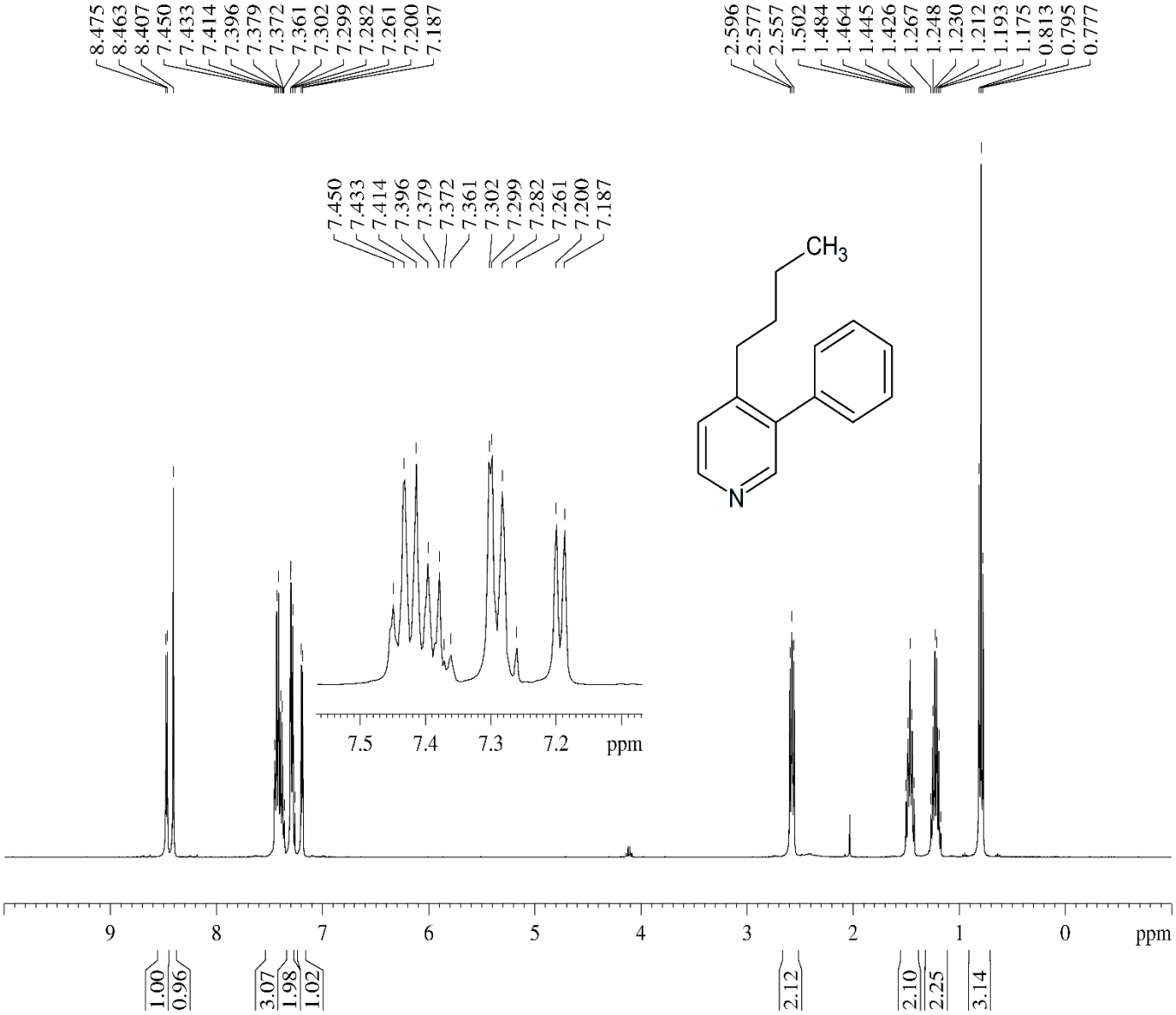

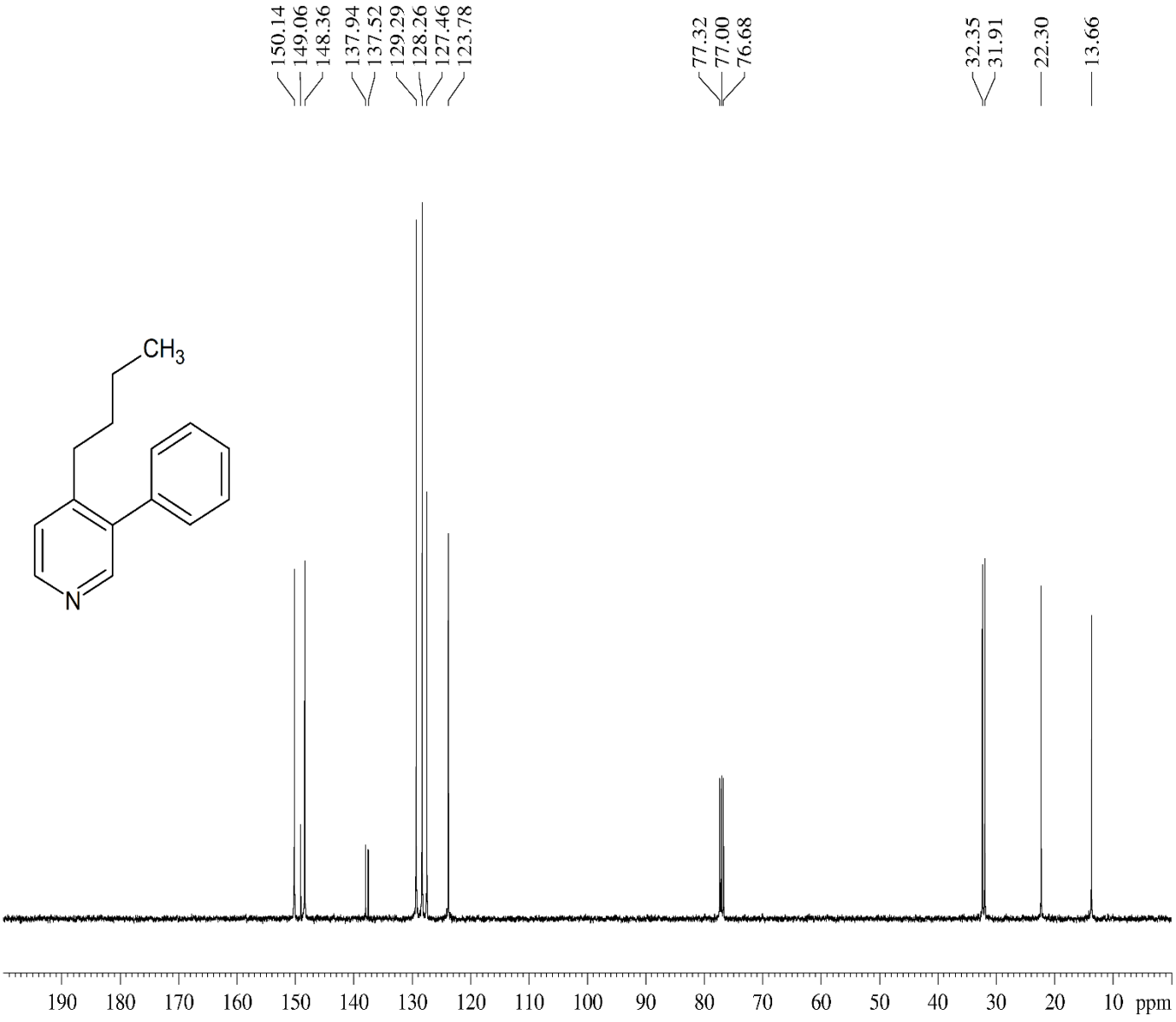
150.14
149.06
148.36
137.94
137.52
129.29
128.26
127.46
123.78
77.32
77.00
76.68
32.35
31.91
22.30
13.66
CH3
N
190 180 170 160 150 140 130 120 110 100 90 80 70 60 50 40 30 20 10 ppm

^{1}H (400 MHz, $CDCl_3$) and ^{13}C (100 MHz, $CDCl_3$) – NMR Spectra for **21.1**

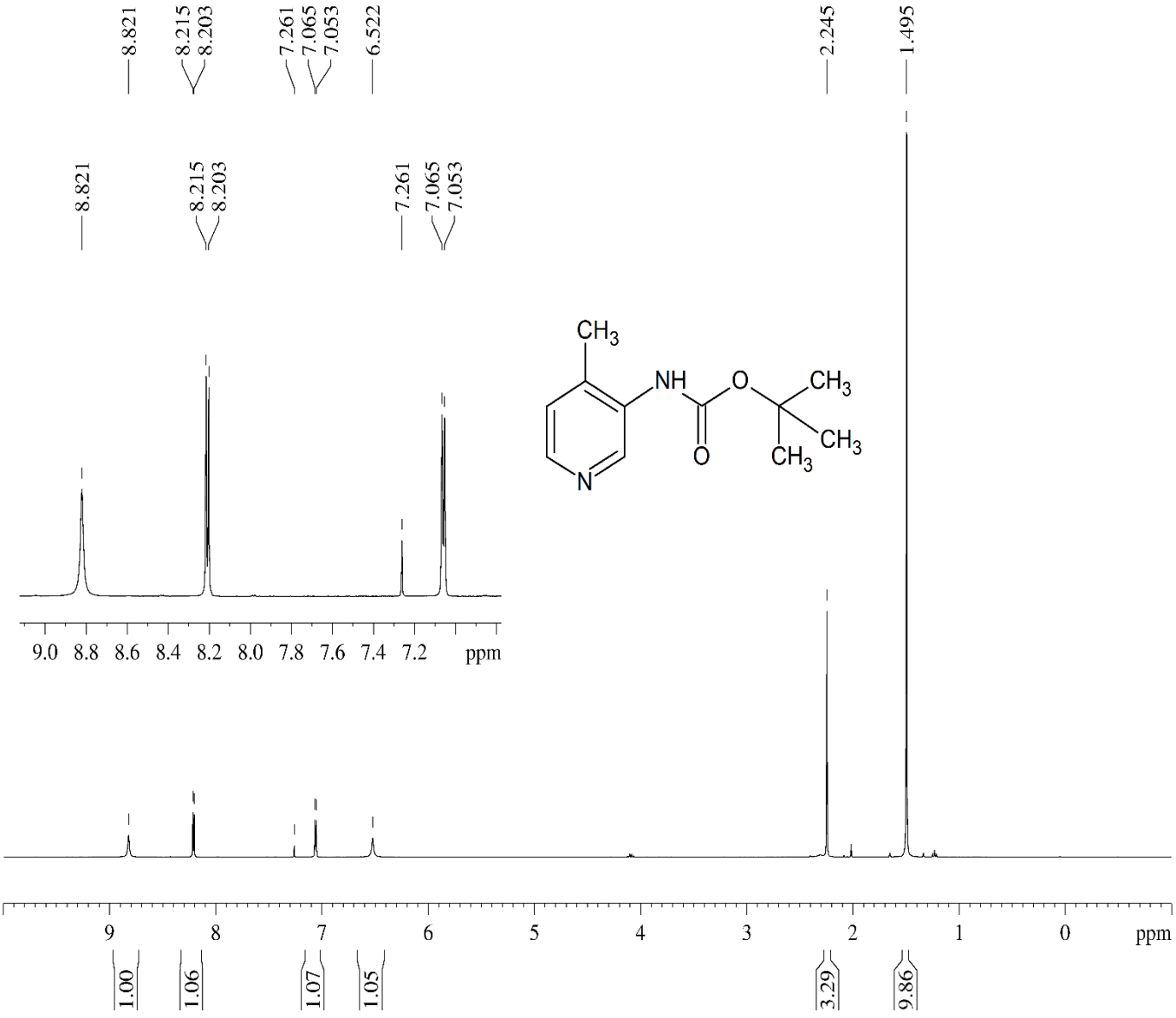

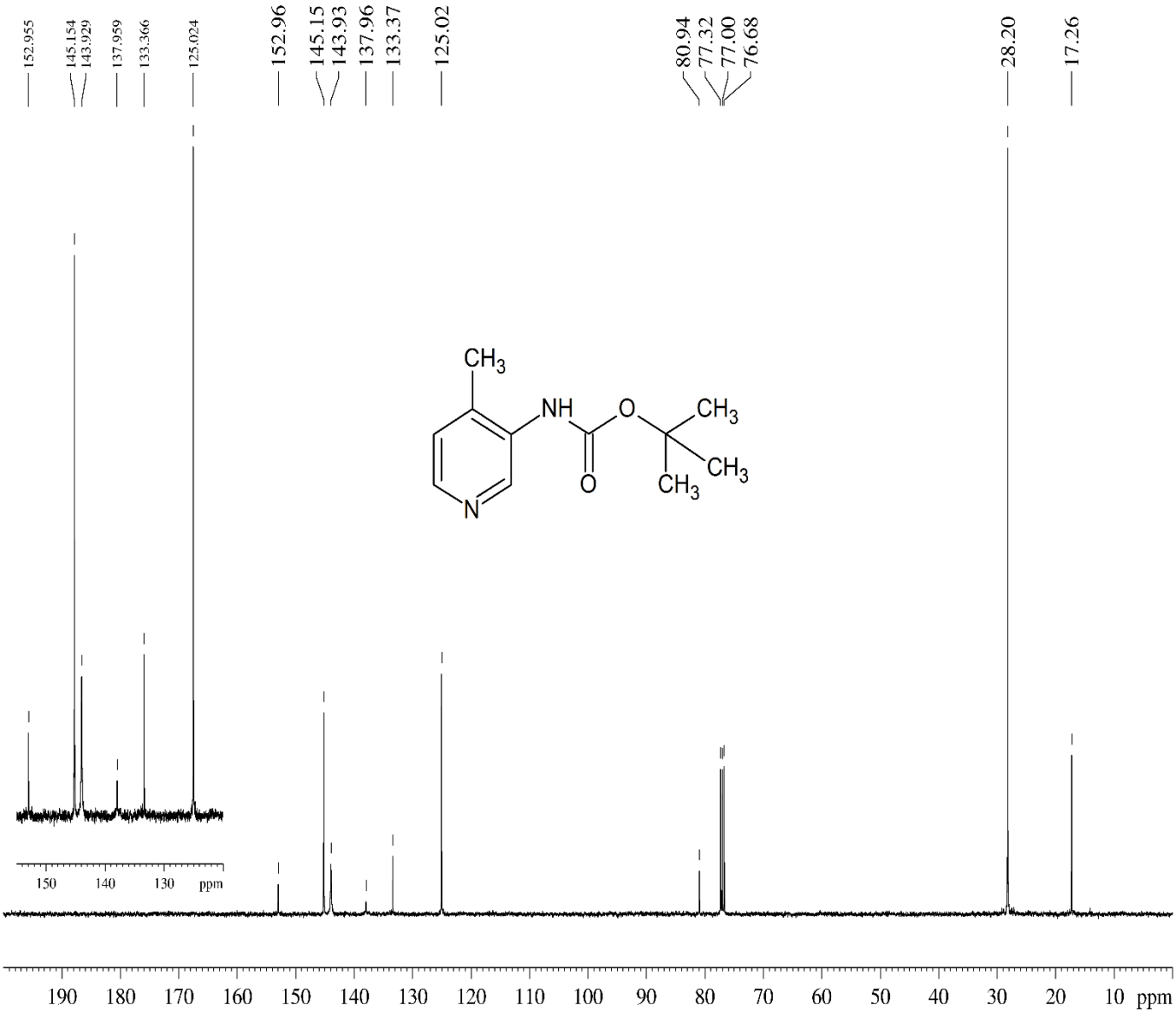
152.955
145.154
143.929
137.959
133.366
125.024
152.96
145.15
143.93
137.96
133.37
125.02
80.94
77.32
77.00
76.68
28.20
17.26
CH3
NH
O
CH3
CH3
CH3
O
N
150
140
130
ppm
190
180
170
160
150
140
130
120
110
100
90
80
70
60
50
40
30
20
10
ppm

^{1}H (400 MHz, $CDCl_3$) and ^{13}C (100 MHz, $CDCl_3$) – NMR Spectra for **21**

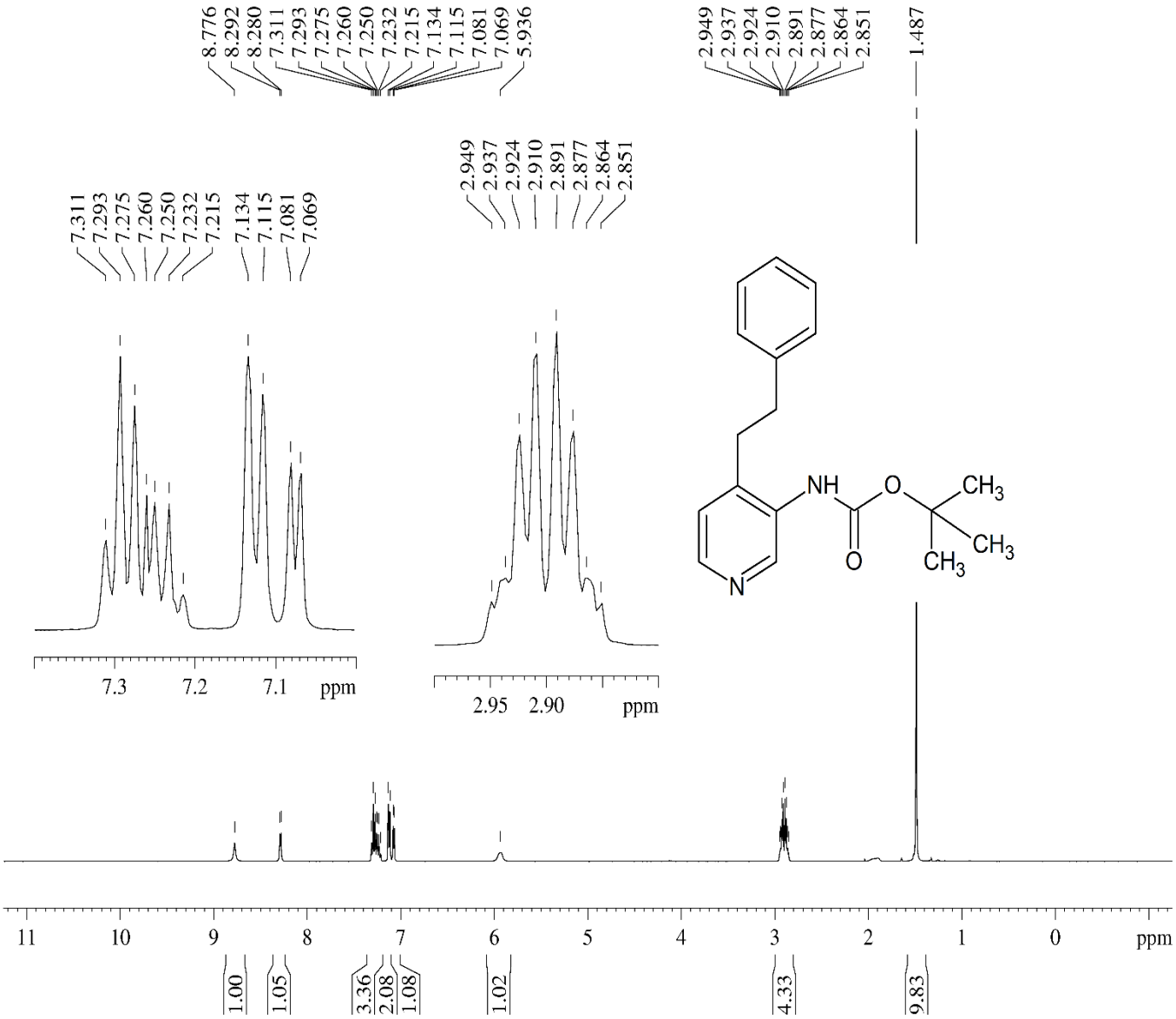

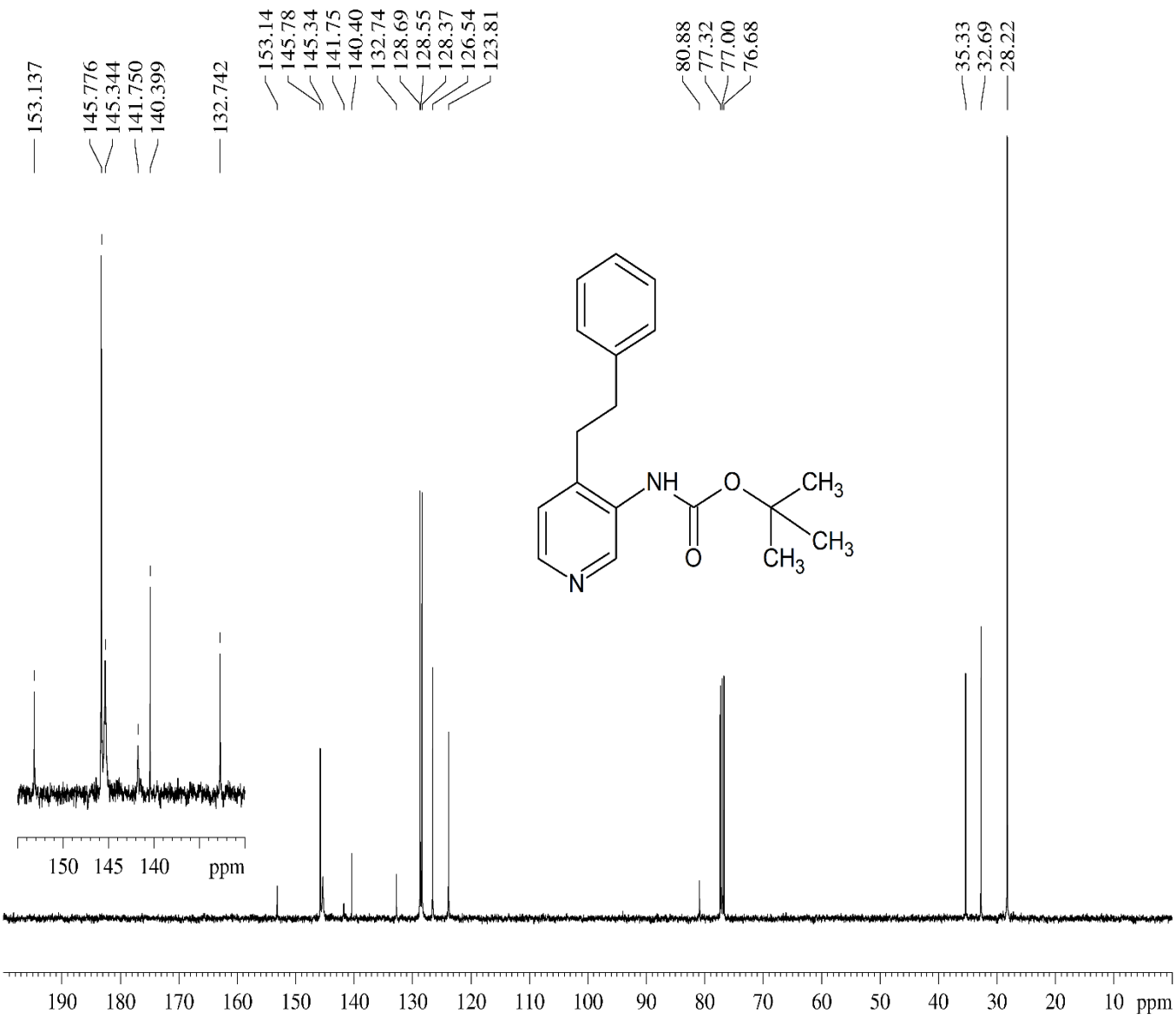
153.137
145.776
145.344
141.750
140.399
132.742
153.14
145.78
145.34
141.75
140.40
132.74
128.69
128.55
128.37
126.54
123.81
80.88
77.32
77.00
76.68
35.33
32.69
28.22
NH
O
O
N
CH3
CH3
CH3
150 145 140 ppm
190 180 170 160 150 140 130 120 110 100 90 80 70 60 50 40 30 20 10 ppm

^{1}H (400 MHz, $CDCl_3$) and ^{13}C (100 MHz, $CDCl_3$) – NMR Spectra for **22**

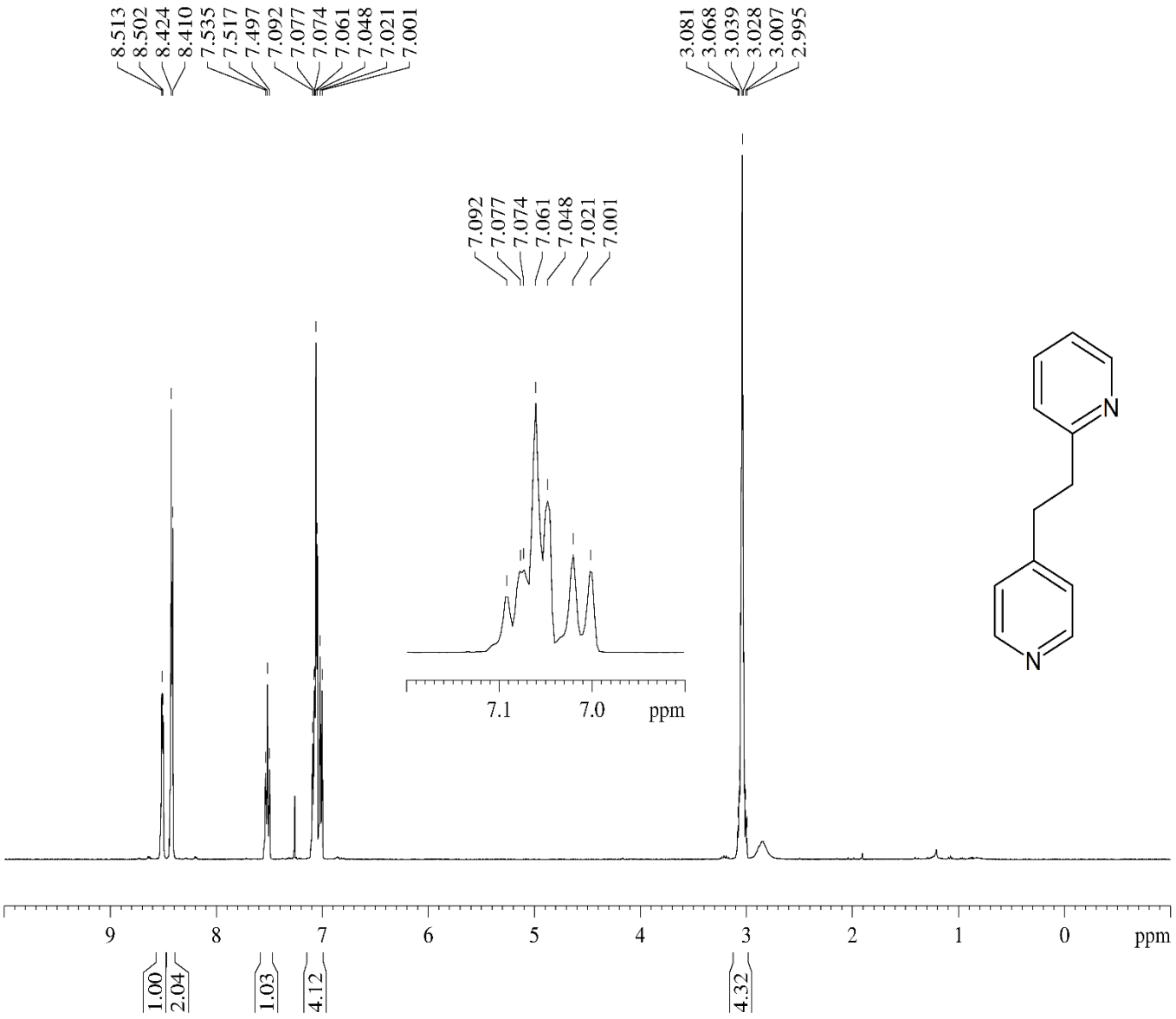

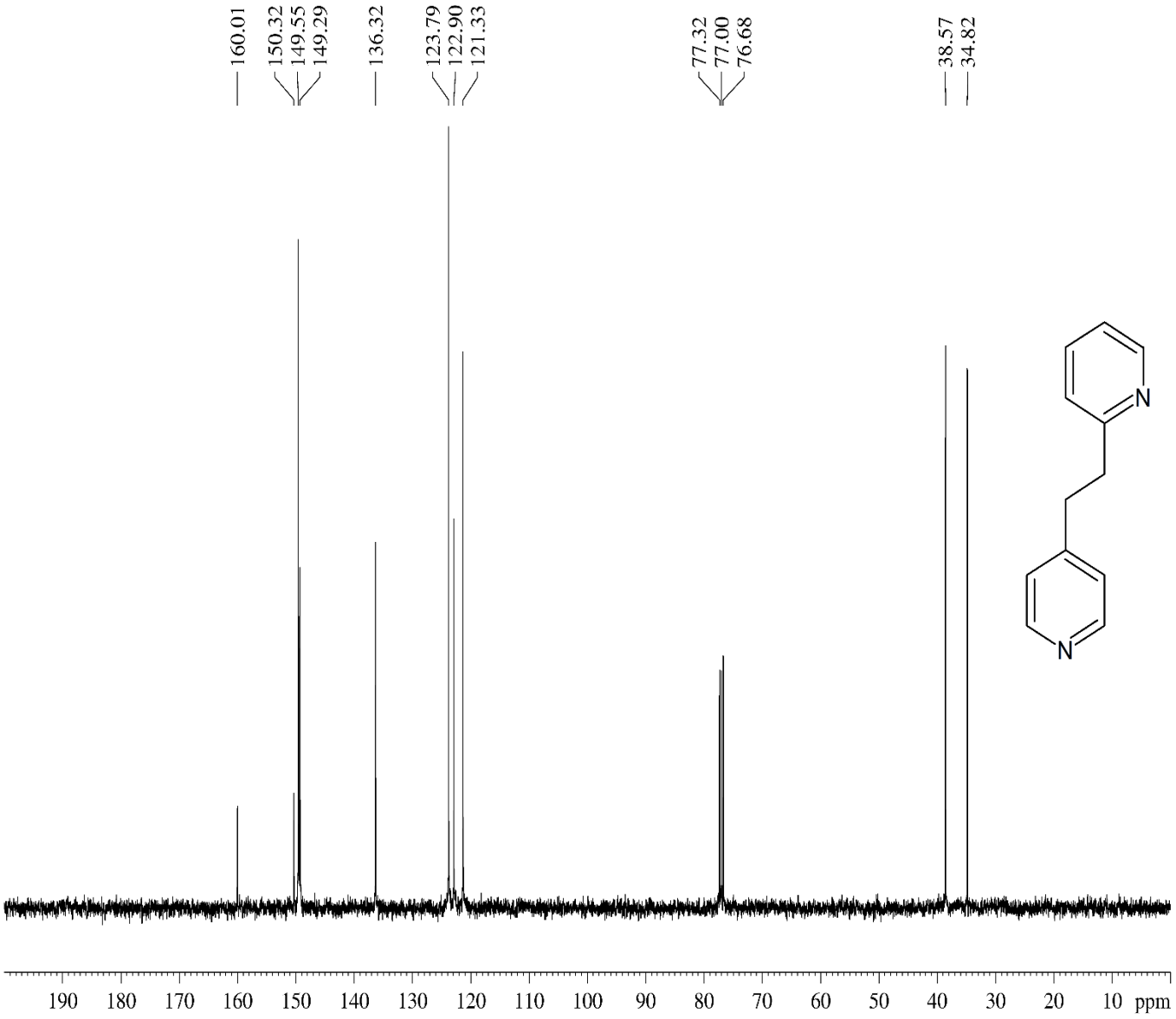
160.01
150.32
149.55
149.29
136.32
123.79
122.90
121.33
77.32
77.00
76.68
38.57
34.82
N
N
190 180 170 160 150 140 130 120 110 100 90 80 70 60 50 40 30 20 10 ppm

^{1}H (400 MHz, $CDCl_3$) and ^{13}C (100 MHz, $CDCl_3$) – NMR Spectra for **23.1**

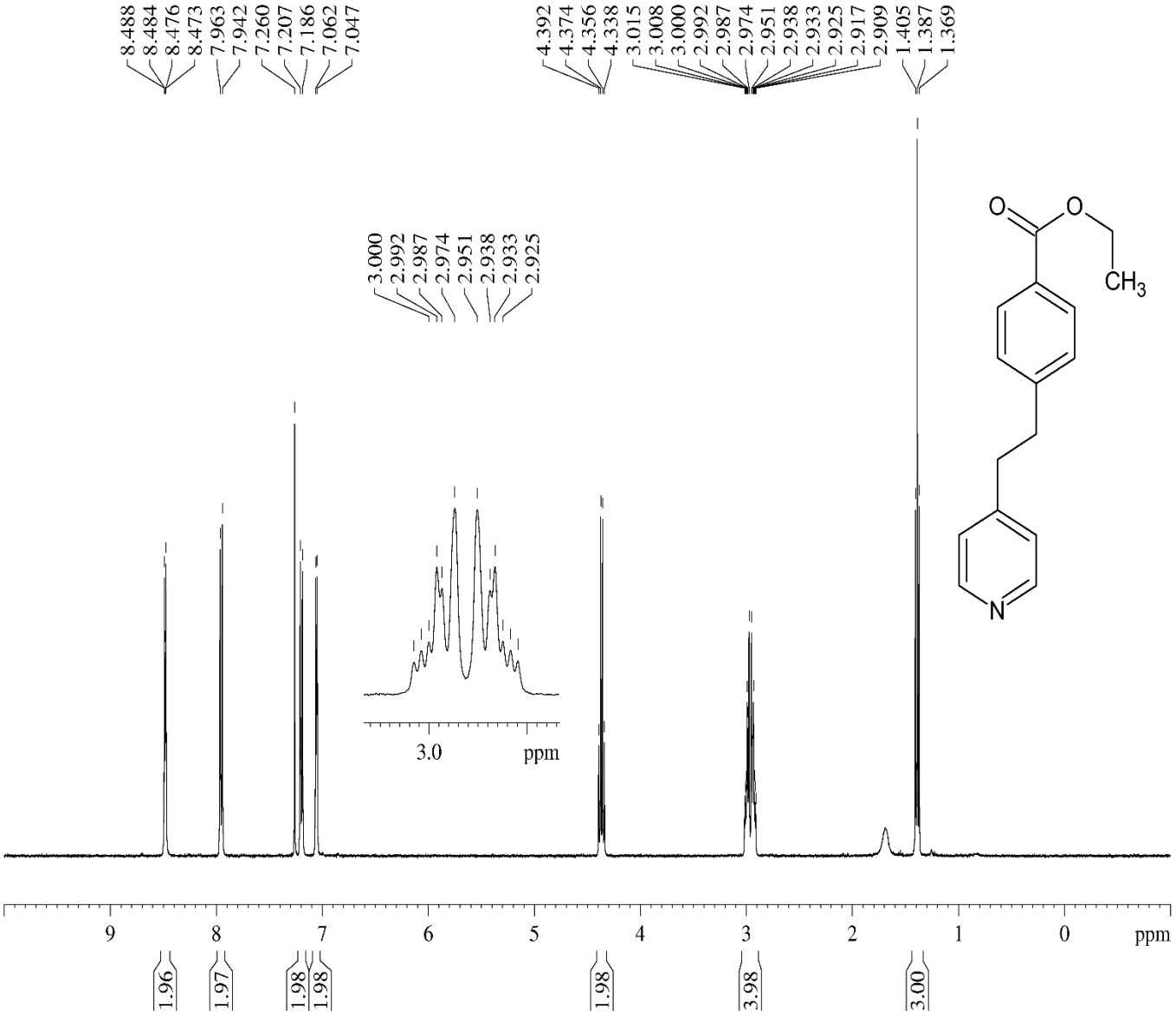

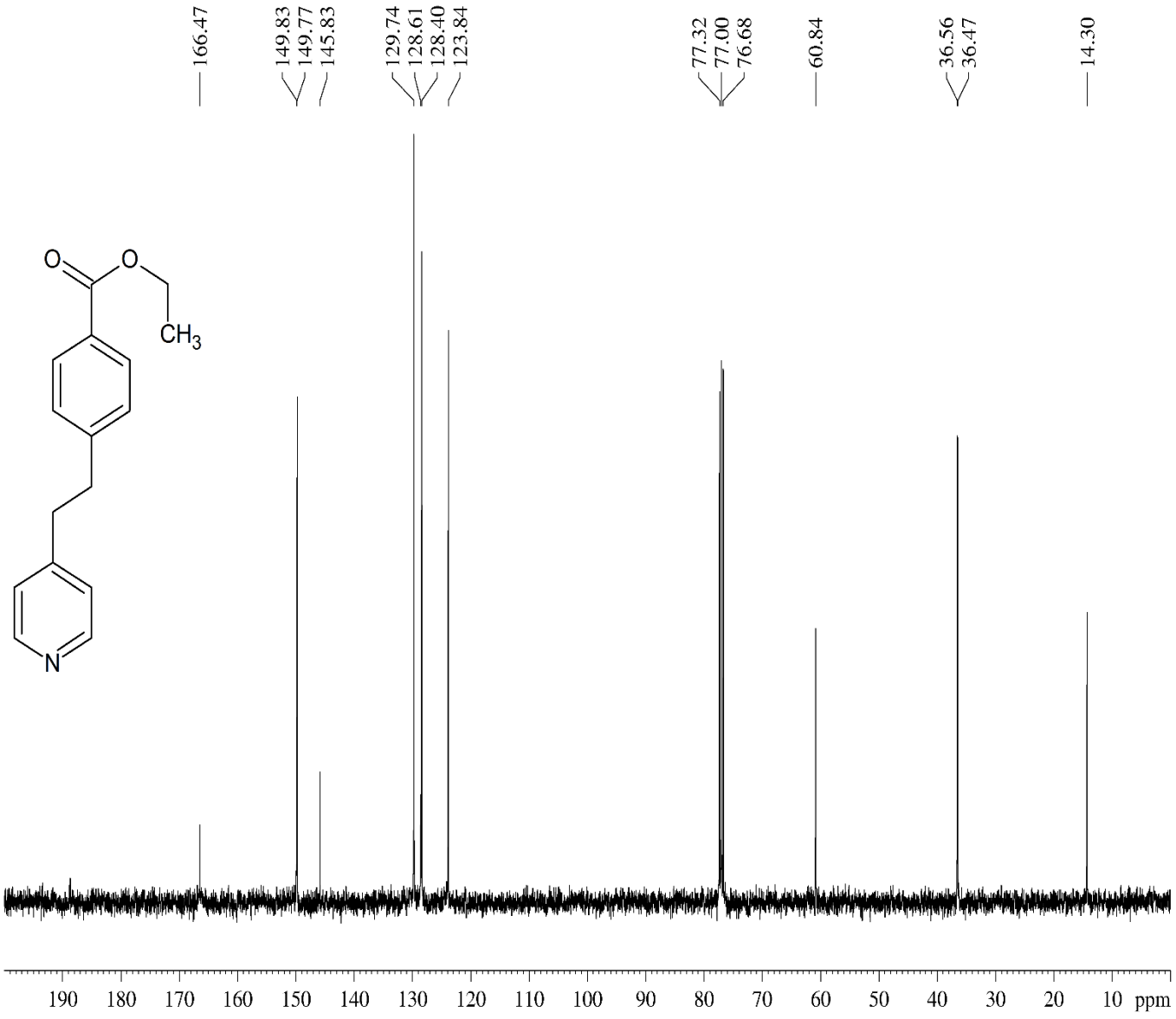
166.47
149.83
149.77
145.83
129.74
128.61
128.40
123.84
77.32
77.00
76.68
60.84
36.56
36.47
14.30
O
O
CH3
N
190 180 170 160 150 140 130 120 110 100 90 80 70 60 50 40 30 20 10 ppm

^{1}H (400 MHz, $CDCl_3$) and ^{13}C (100 MHz, $CDCl_3$) – NMR Spectra for **23.2**

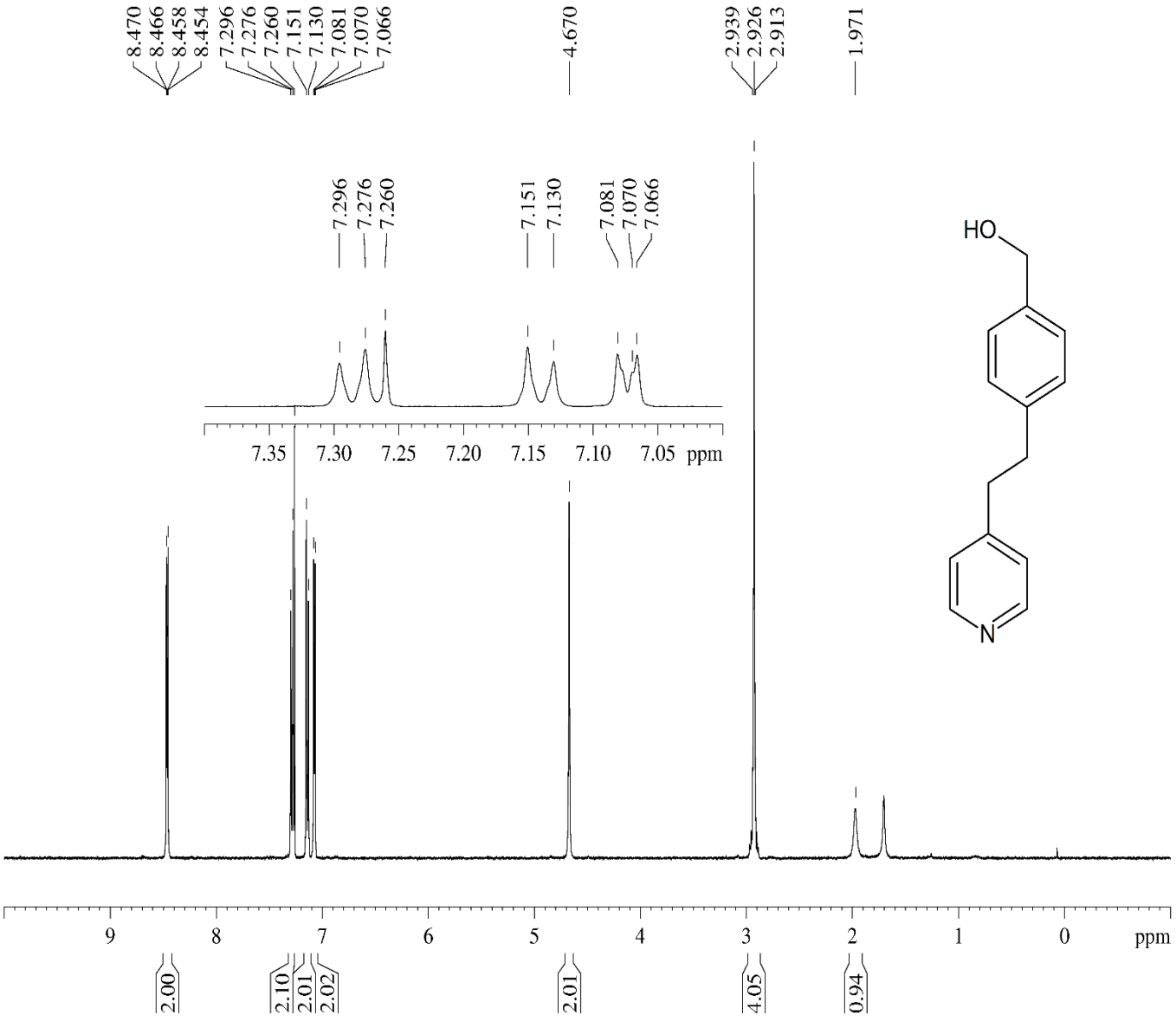

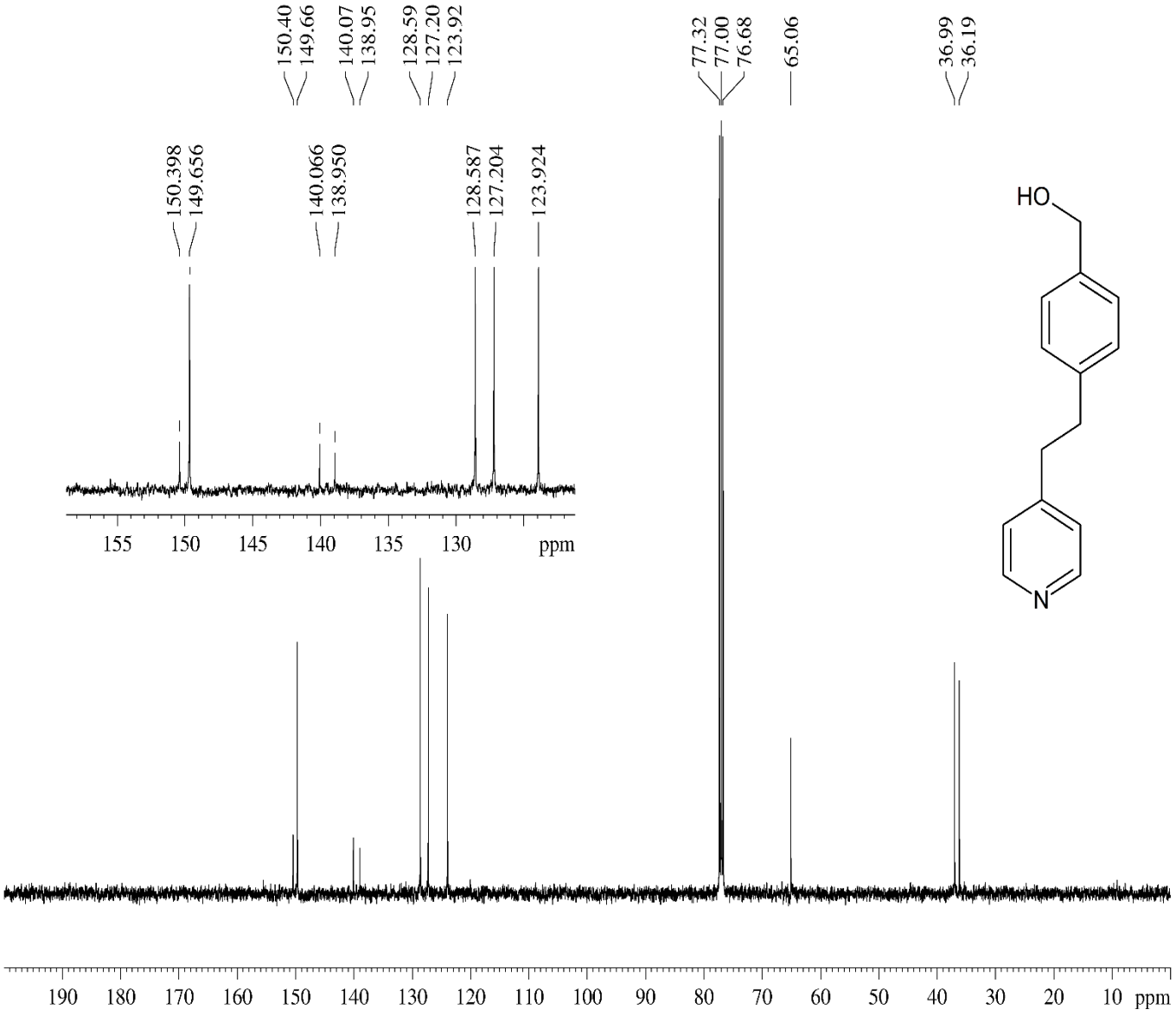
150.40
149.66
140.07
138.95
128.59
127.20
123.92
77.32
77.00
76.68
65.06
36.99
36.19
150.398
149.656
140.066
138.950
128.587
127.204
123.924
155
150
145
140
135
130
ppm
HO
N
190
180
170
160
150
140
130
120
110
100
90
80
70
60
50
40
30
20
10
ppm

^{1}H (400 MHz, $CDCl_3$) and ^{13}C (100 MHz, $CDCl_3$) – NMR Spectra for **23.3**

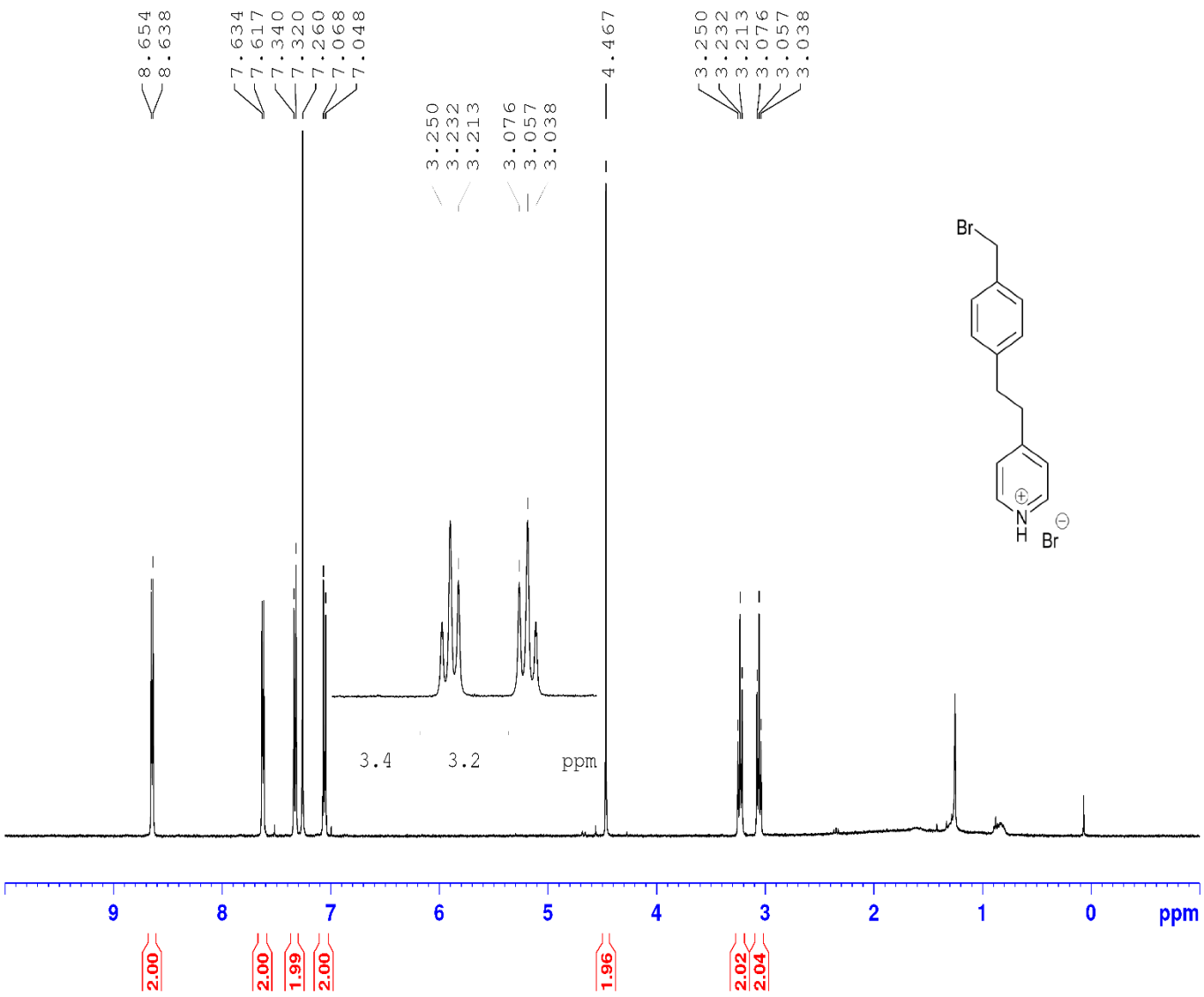

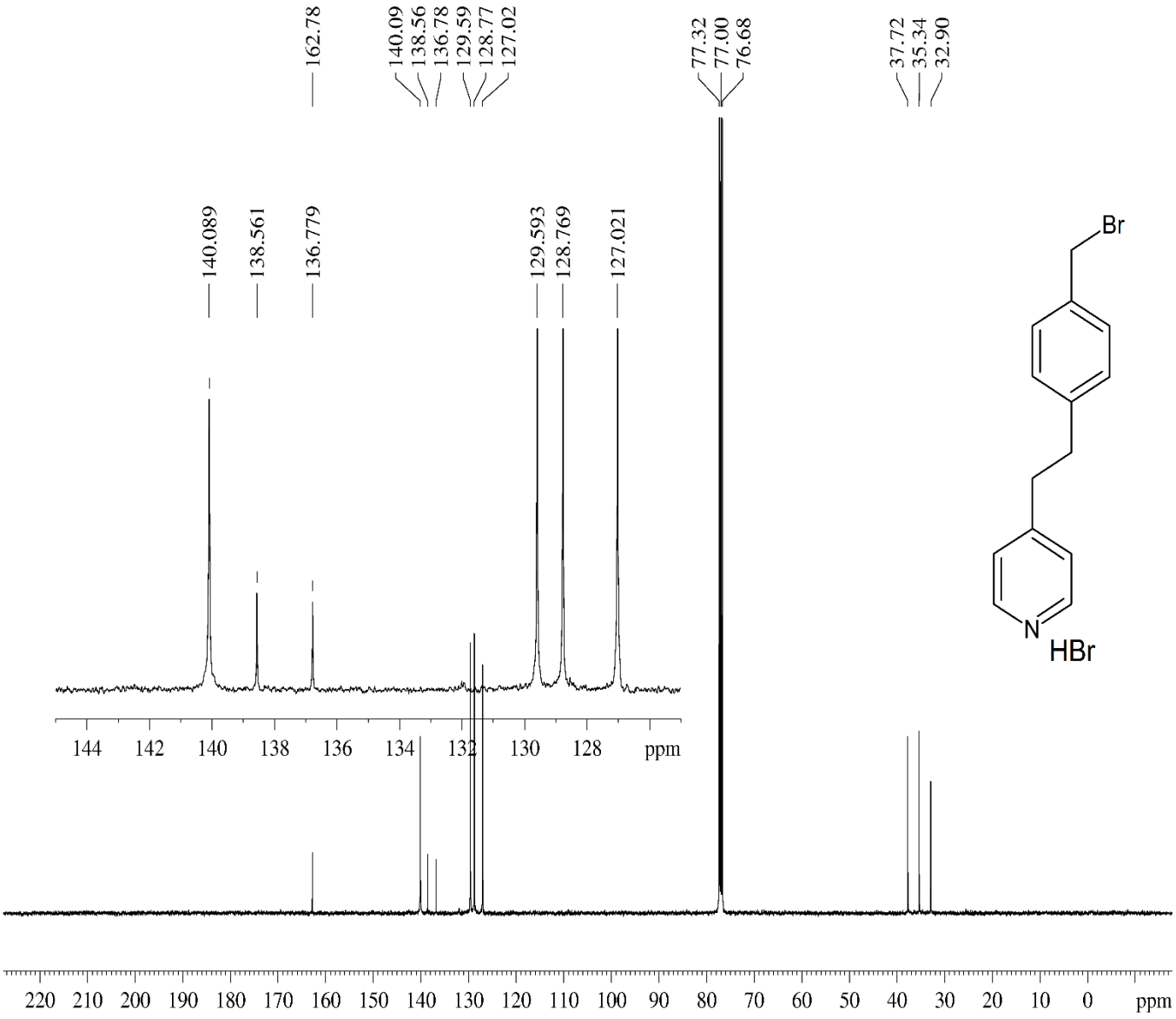
162.78
140.09
138.56
136.78
129.59
128.77
127.02
77.32
77.00
76.68
37.72
35.34
32.90
140.089
138.561
136.779
129.593
128.769
127.021
144
142
140
138
136
134
132
130
128
ppm
220
210
200
190
180
170
160
150
140
130
120
110
100
90
80
70
60
50
40
30
20
10
0
ppm
Br
N
HBr

^{1}H (400 MHz, $CDCl_3$) and ^{13}C (100 MHz, $CDCl_3$) – NMR Spectra for **23**

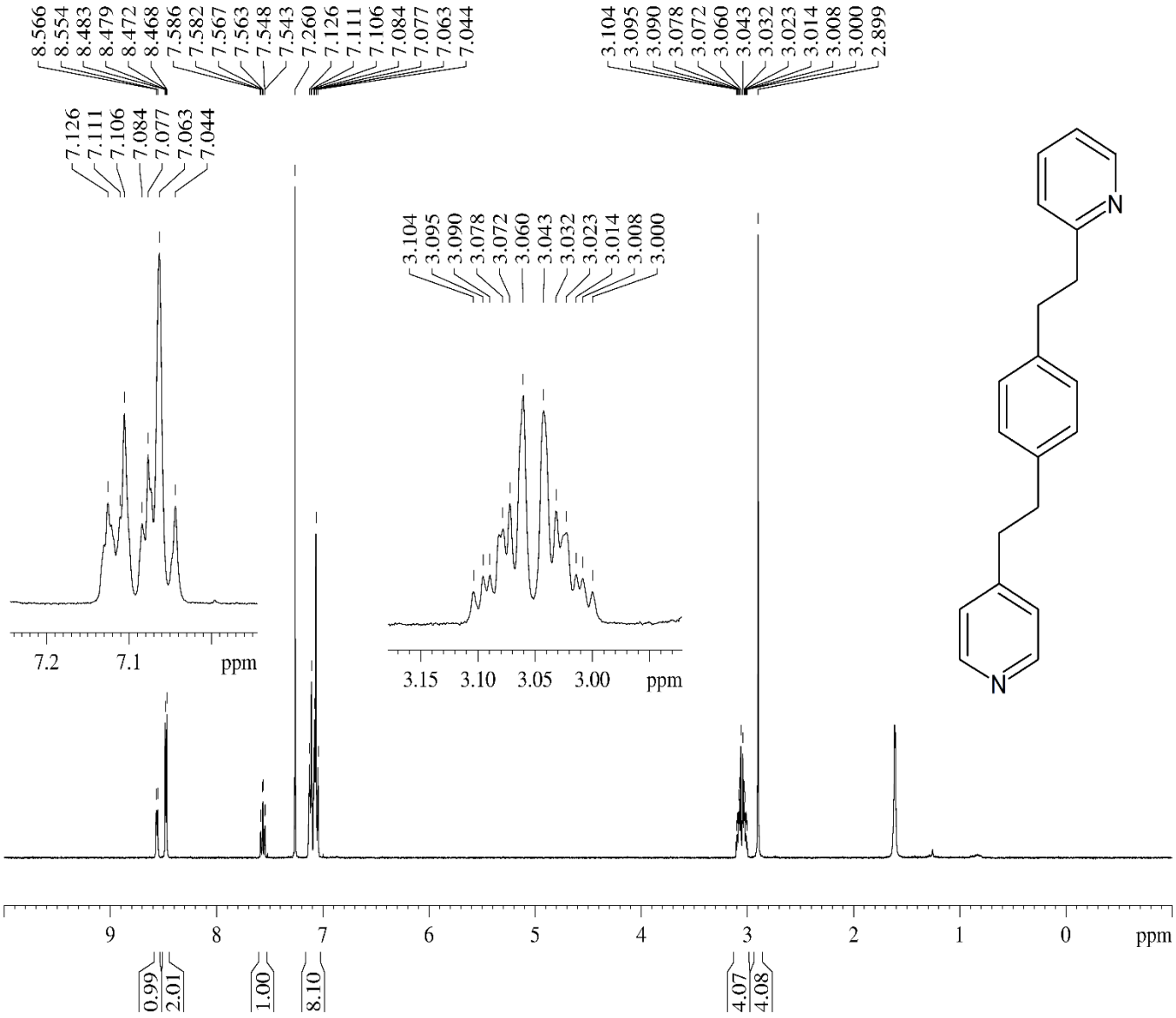

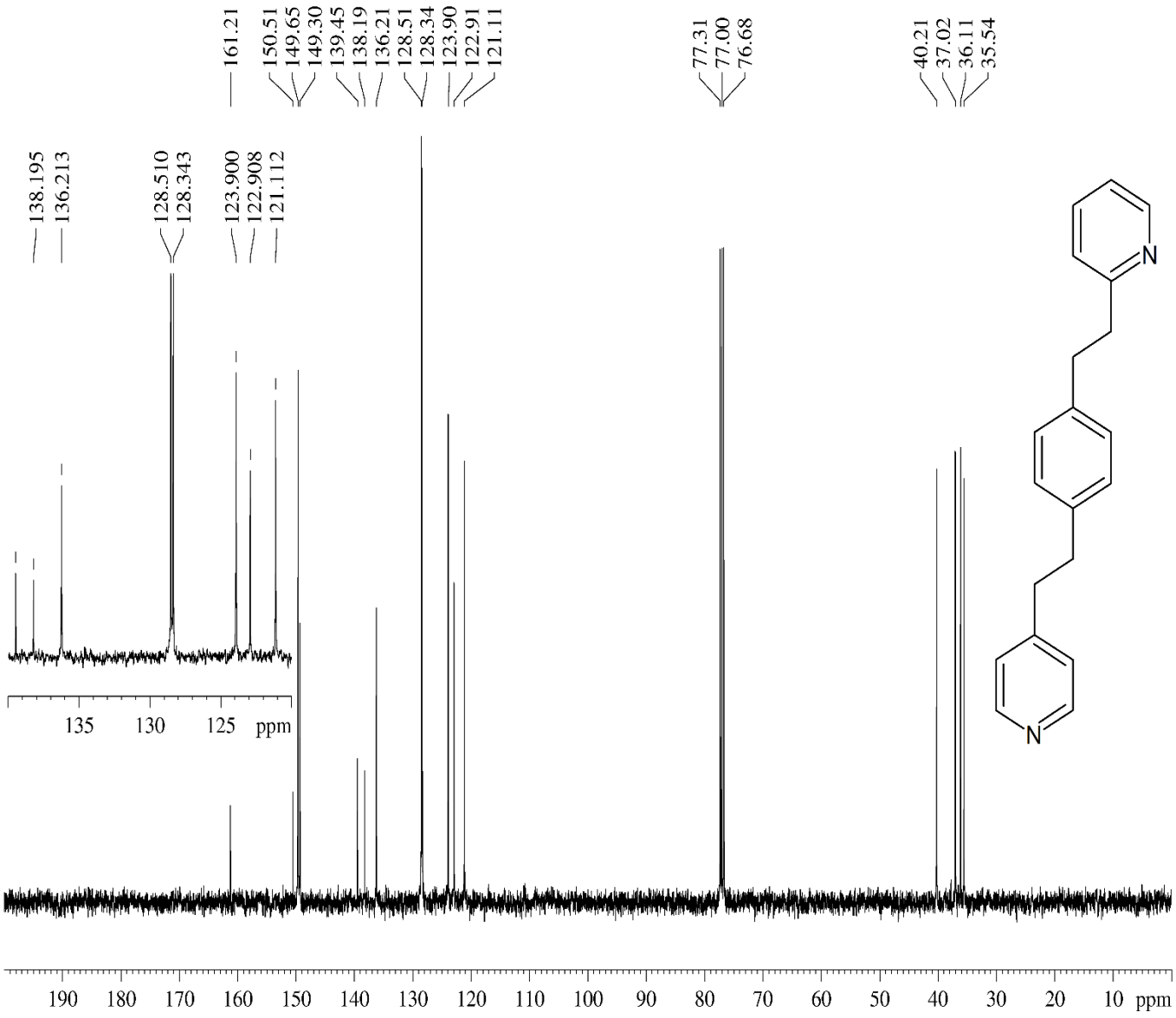
161.21
150.51
149.65
149.30
139.45
138.19
136.21
128.51
128.34
123.90
122.91
121.11
77.31
77.00
76.68
40.21
37.02
36.11
35.54
138.195
136.213
128.510
128.343
123.900
122.908
121.112
135
130
125
ppm
N
N
190
180
170
160
150
140
130
120
110
100
90
80
70
60
50
40
30
20
10
ppm

^{1}H (400 MHz, $CDCl_3$) and ^{13}C (100 MHz, $CDCl_3$) – NMR Spectra for **24.1**

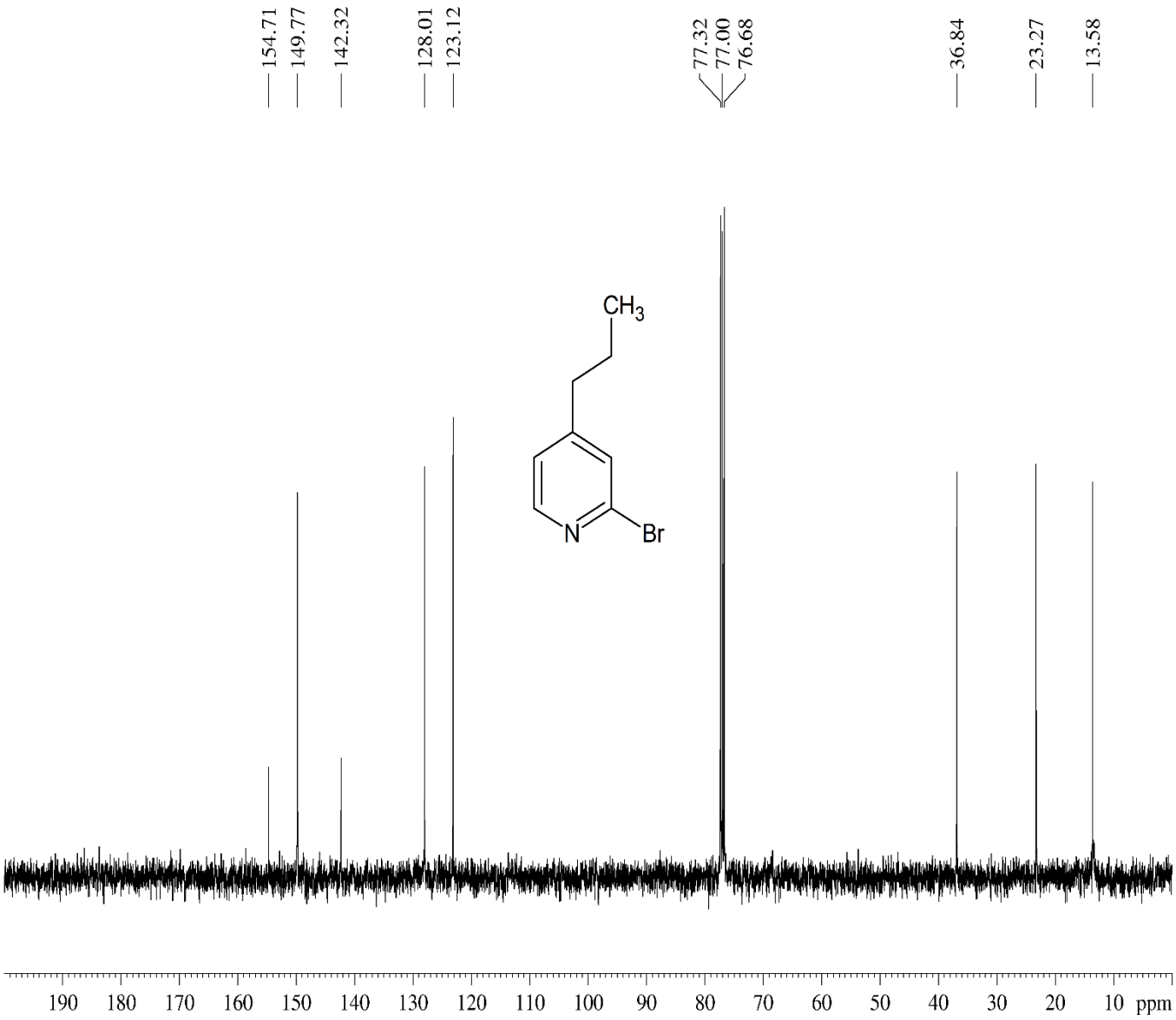

^{1}H (400 MHz, $CDCl_3$) and ^{13}C (100 MHz, $CDCl_3$) – NMR Spectra for **24**

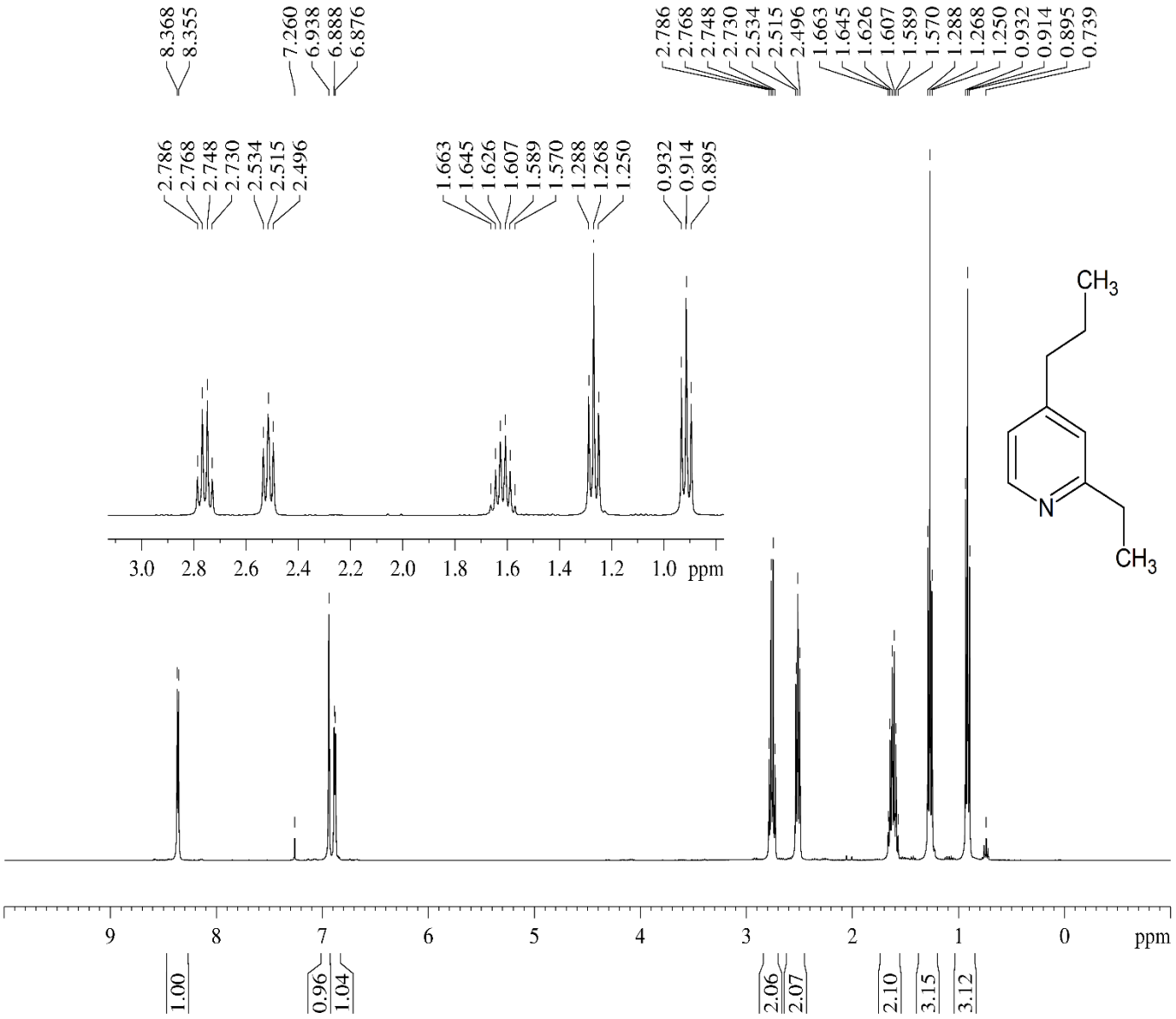

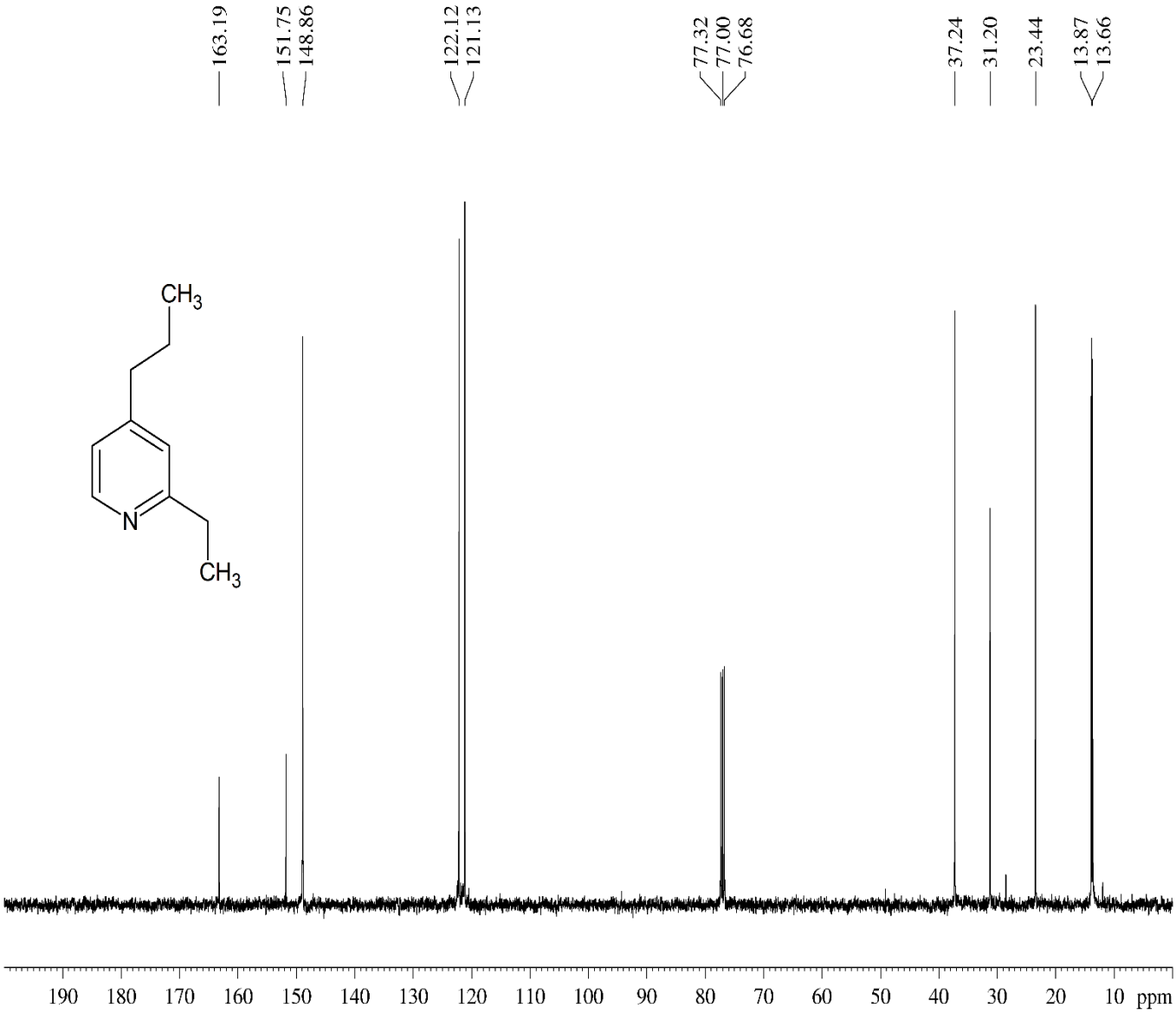
163.19
151.75
148.86
122.12
121.13
77.32
77.00
76.68
37.24
31.20
23.44
13.87
13.66
CH3
N
CH3
190 180 170 160 150 140 130 120 110 100 90 80 70 60 50 40 30 20 10 ppm

^{1}H (400 MHz, $CDCl_3$) and ^{13}C (100 MHz, $CDCl_3$) – NMR Spectra for **1a**

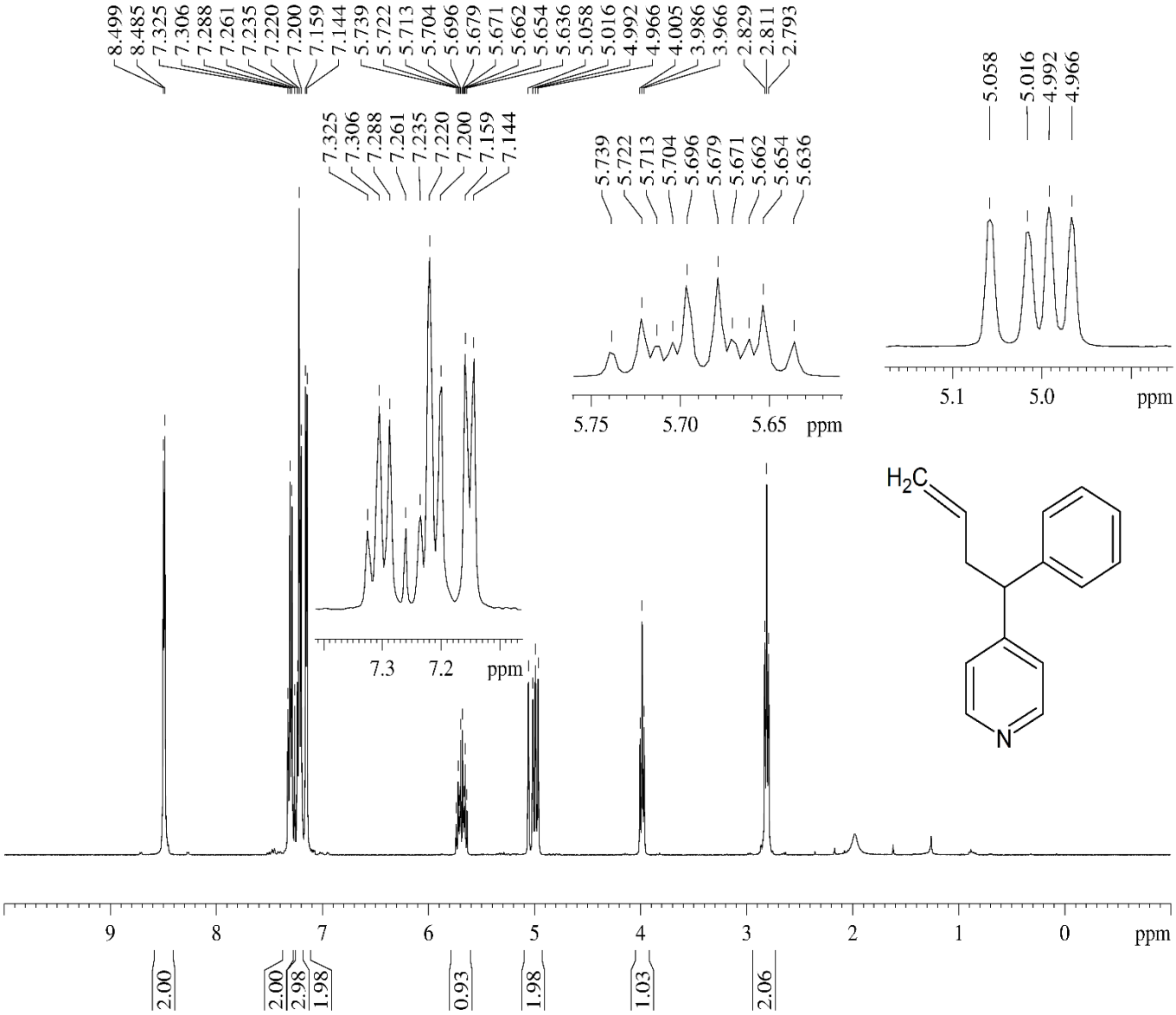

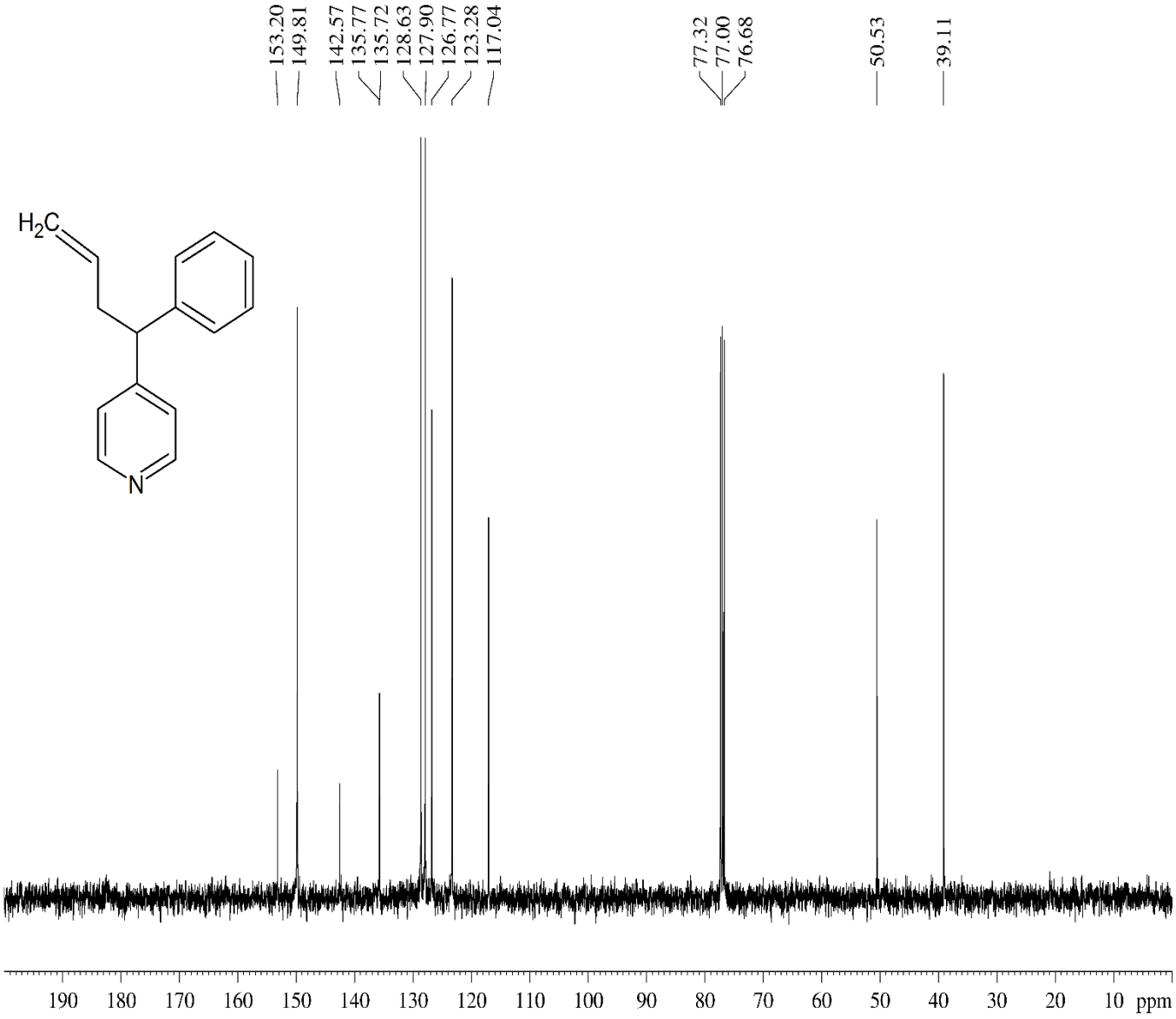
153.20
149.81
142.57
135.77
135.72
128.63
127.90
126.77
123.28
117.04
77.32
77.00
76.68
50.53
39.11
H2C
N
190 180 170 160 150 140 130 120 110 100 90 80 70 60 50 40 30 20 10 ppm

^{1}H (300 MHz, $CDCl_3$) and ^{13}C (75 MHz, $CDCl_3$) – NMR Spectra for **2a′**

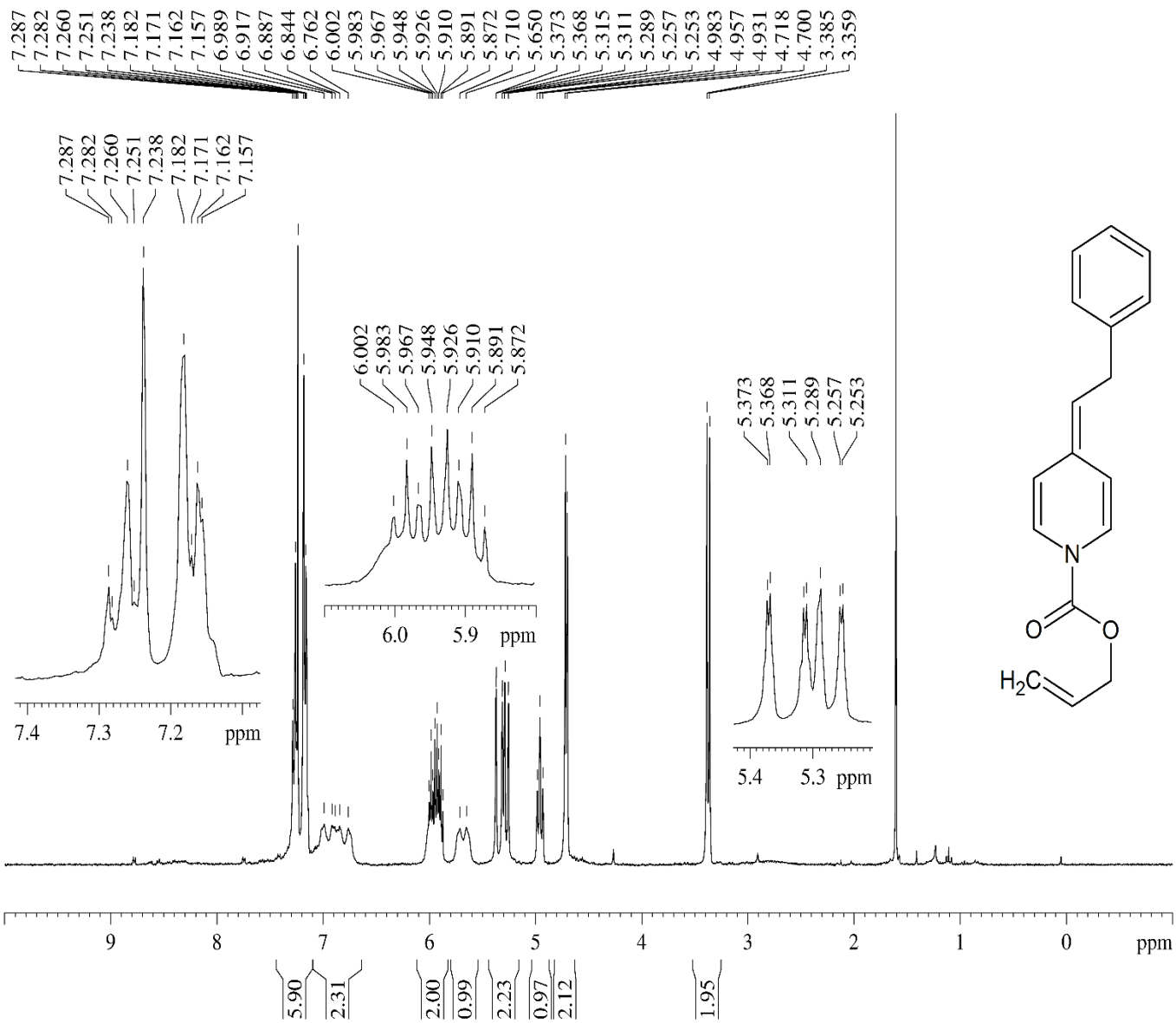

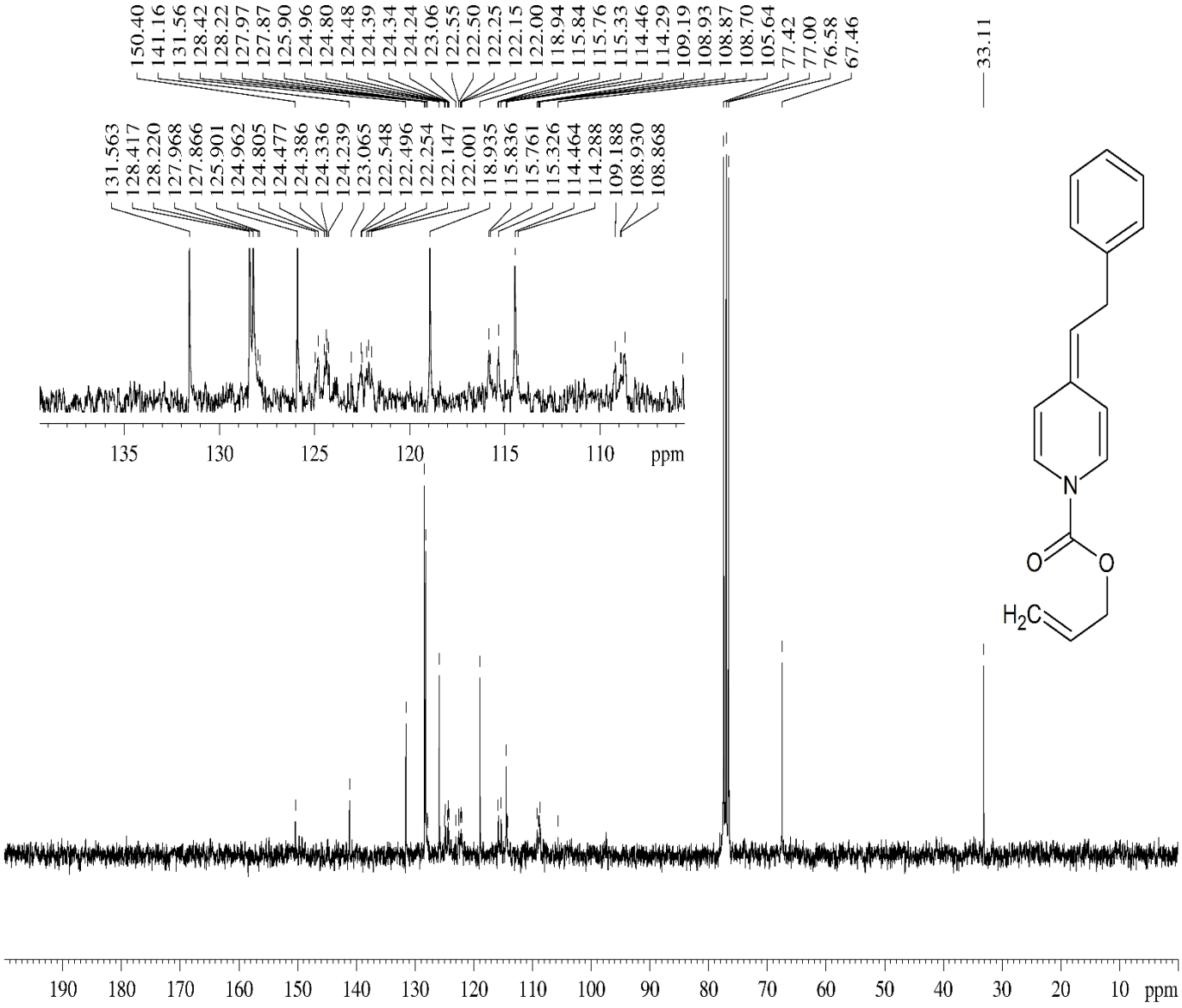
150.40
141.16
131.56
128.42
128.22
127.97
127.87
125.90
124.96
124.80
124.48
124.39
124.34
124.24
123.06
122.55
122.50
122.25
122.15
122.00
118.94
115.84
115.76
115.33
114.46
114.29
109.19
108.93
108.87
108.70
105.64
77.42
77.00
76.58
67.46
33.11
131.563
128.417
128.220
127.968
127.866
125.901
124.962
124.805
124.477
124.386
124.336
124.239
123.065
122.548
122.496
122.254
122.147
122.001
118.935
115.836
115.761
115.326
114.464
114.288
109.188
108.930
108.868
135
130
125
120
115
110
ppm
N
O
O
H2C
190
180
170
160
150
140
130
120
110
100
90
80
70
60
50
40
30
20
10
ppm

^{1}H (300 MHz, $CDCl_3$, at 42°C) and ^{13}C (75 MHz, $CDCl_3$, at 52°C) – NMR Spectra for **2a′**

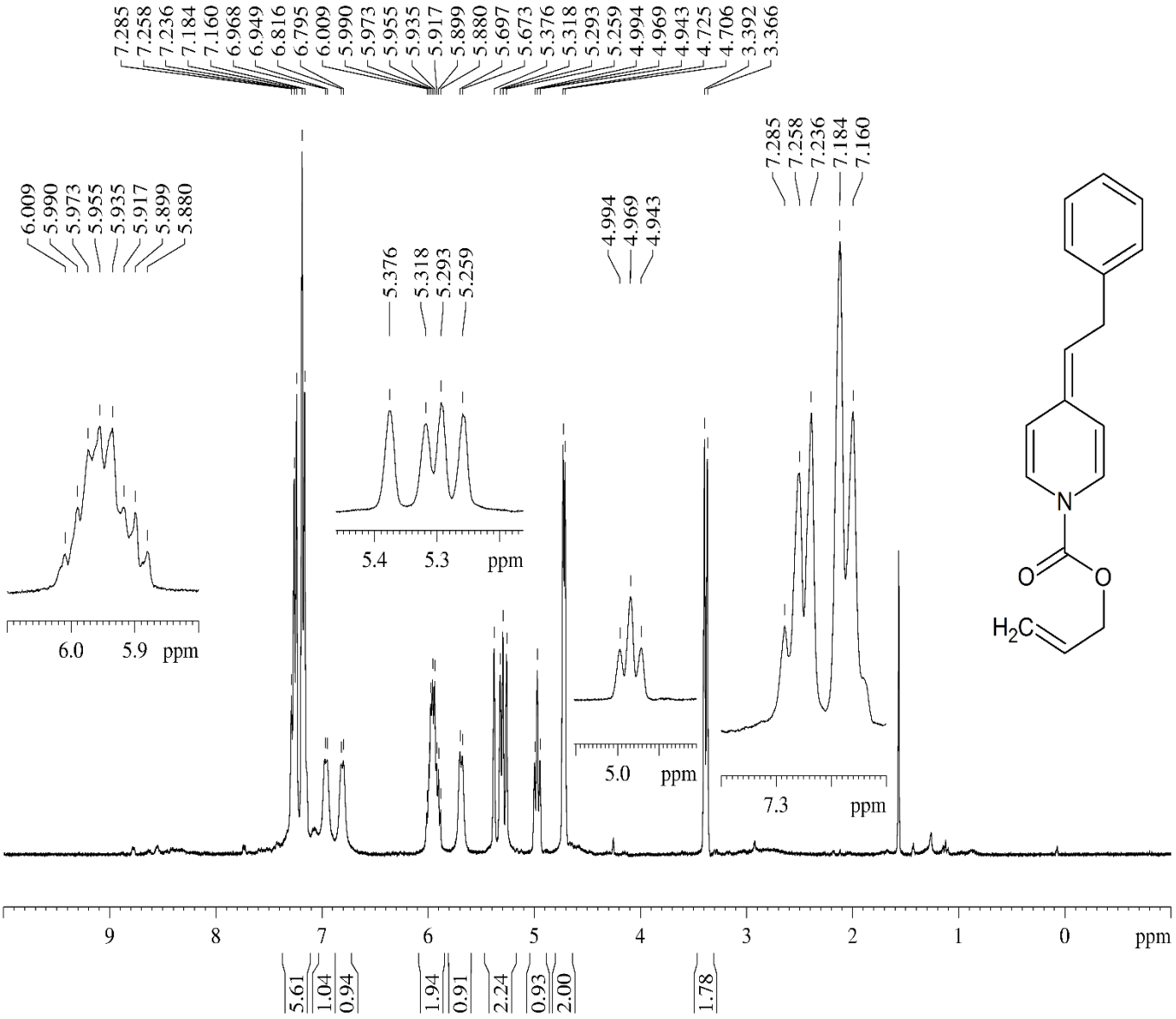

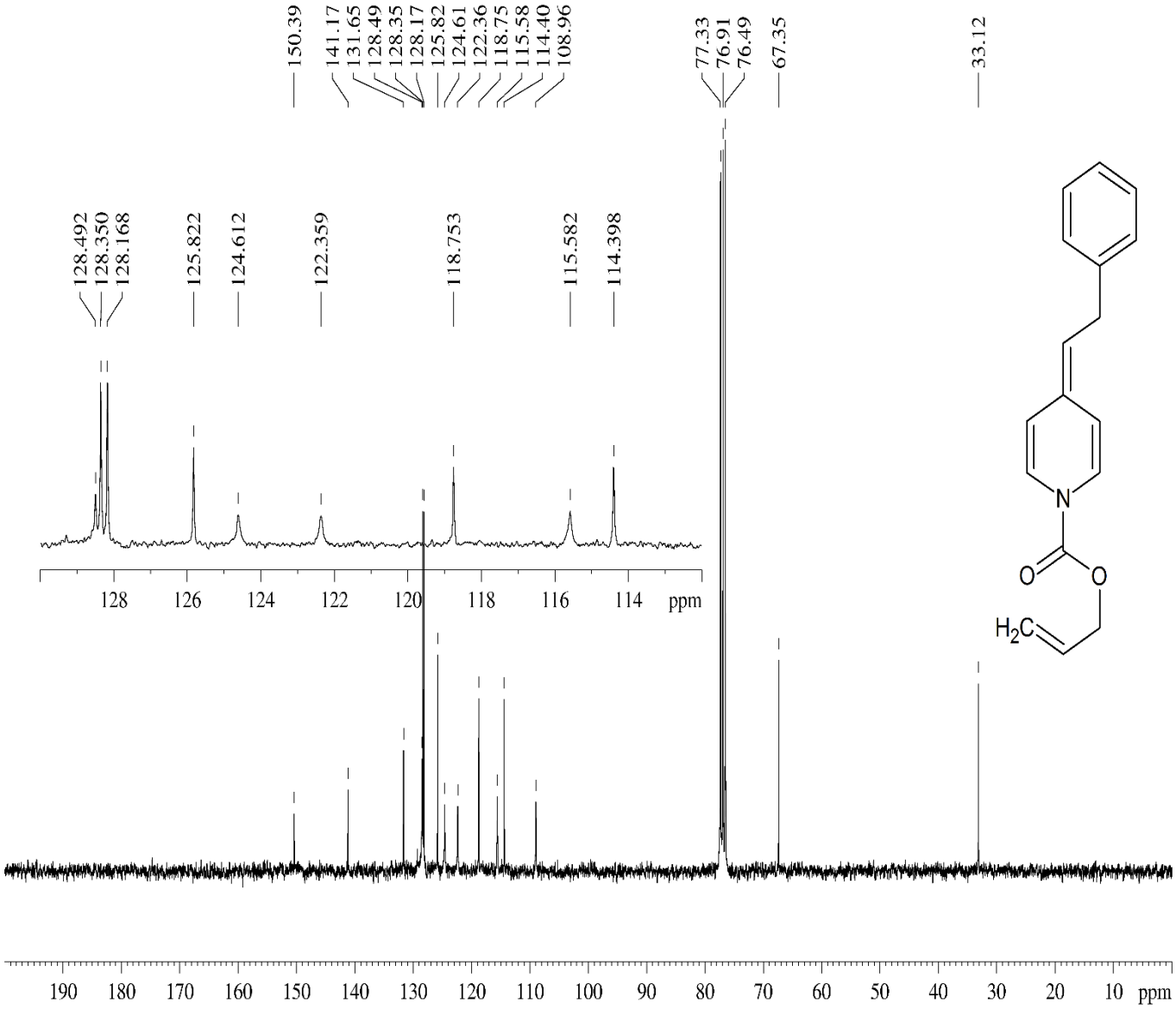
150.39
141.17
131.65
128.49
128.35
128.17
125.82
124.61
122.36
118.75
115.58
114.40
108.96
77.33
76.91
76.49
67.35
33.12
128.492
128.350
128.168
125.822
124.612
122.359
118.753
115.582
114.398
128
126
124
122
120
118
116
114
ppm
N
O
O
H2C
190
180
170
160
150
140
130
120
110
100
90
80
70
60
50
40
30
20
10
ppm

^{1}H (400 MHz, $CDCl_3$) and ^{13}C (100 MHz, $CDCl_3$) – NMR Spectra for **2a**

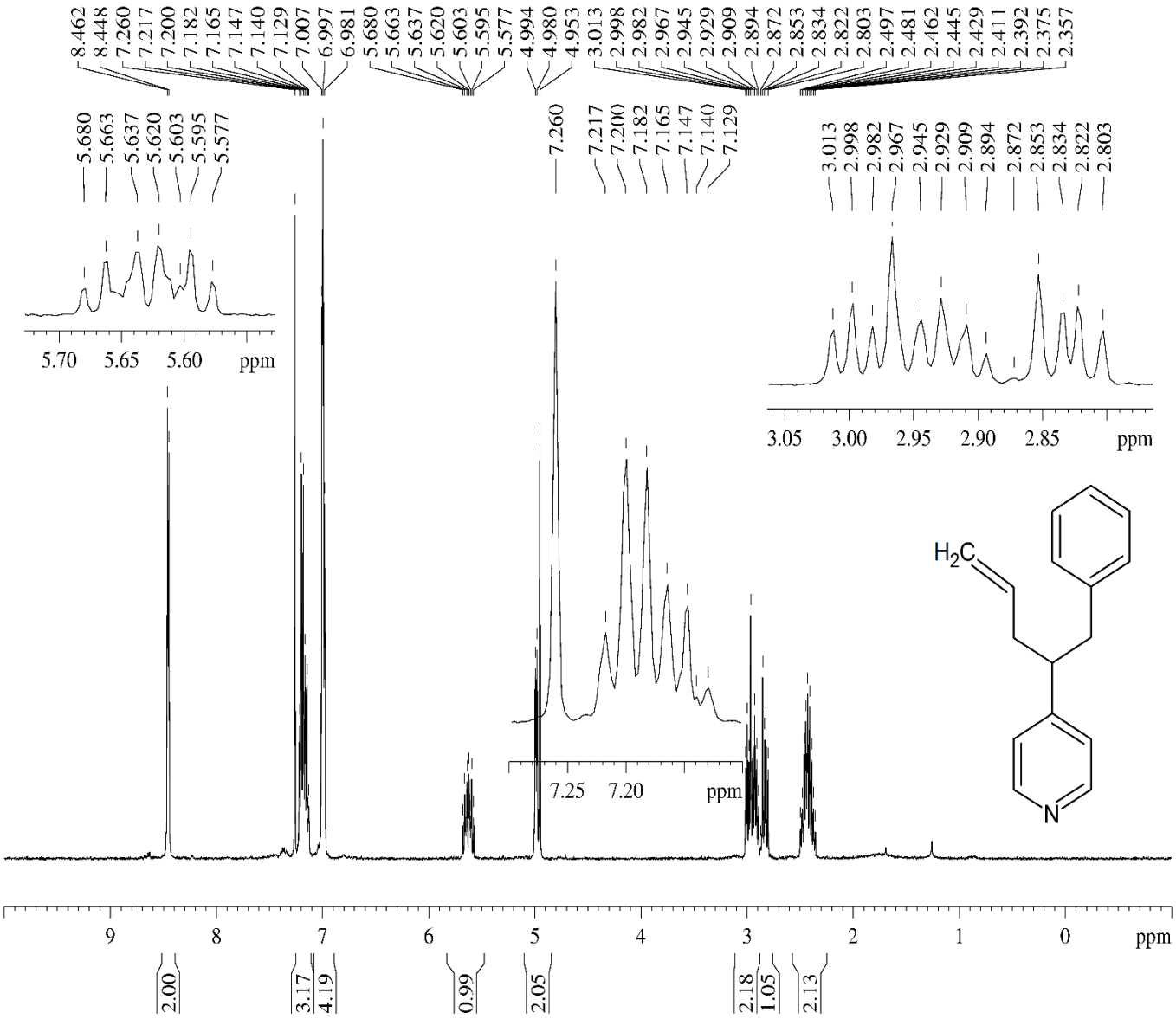

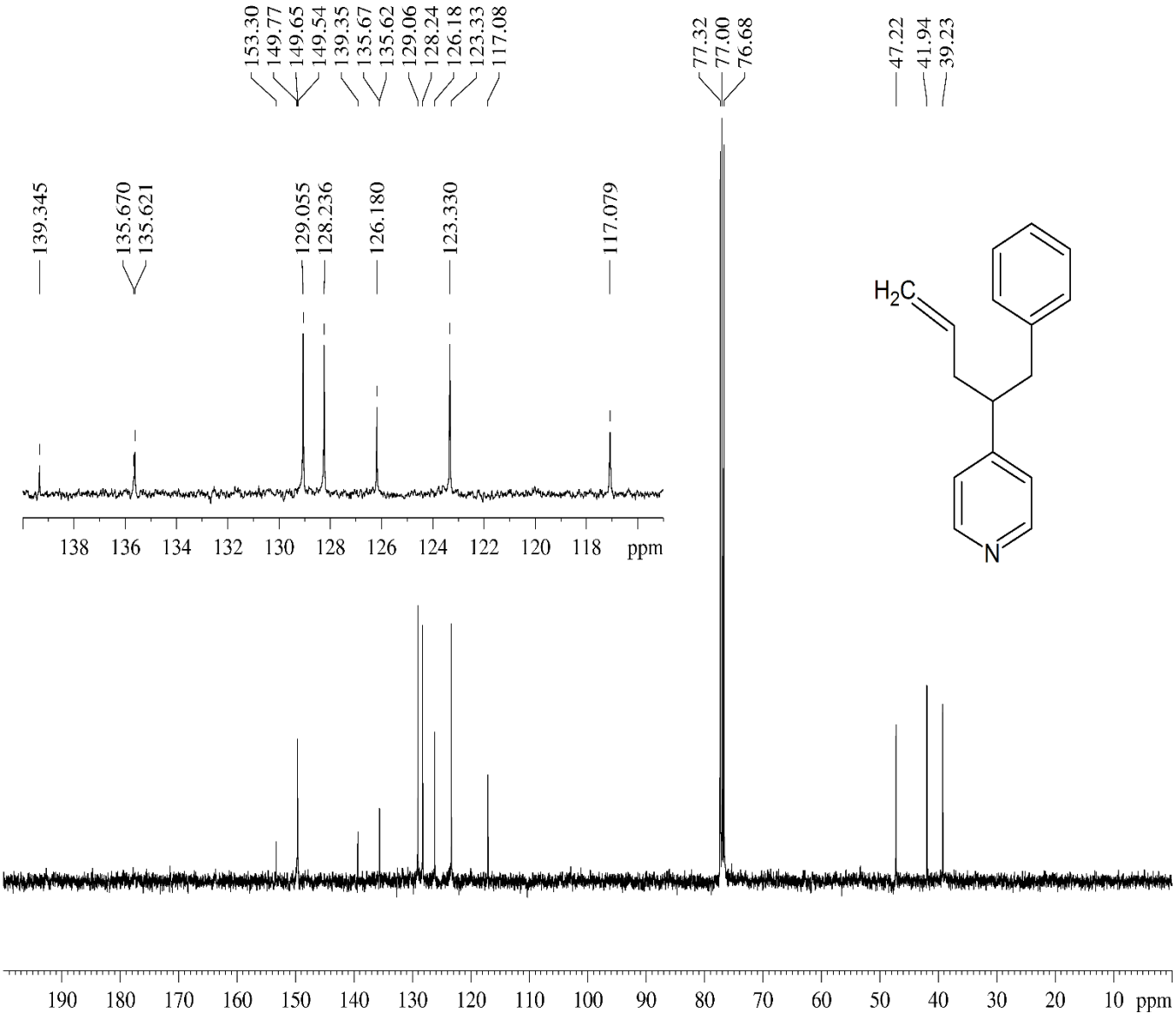
153.30
149.77
149.65
149.54
139.35
135.67
135.62
129.06
128.24
126.18
123.33
117.08
77.32
77.00
76.68
47.22
41.94
39.23
139.345
135.670
135.621
129.055
128.236
126.180
123.330
117.079
138 136 134 132 130 128 126 124 122 120 118 ppm
H2C
N
190 180 170 160 150 140 130 120 110 100 90 80 70 60 50 40 30 20 10 ppm

^{1}H (400 MHz, $CDCl_3$) and ^{13}C (100 MHz, $CDCl_3$) – NMR Spectra for **3a**

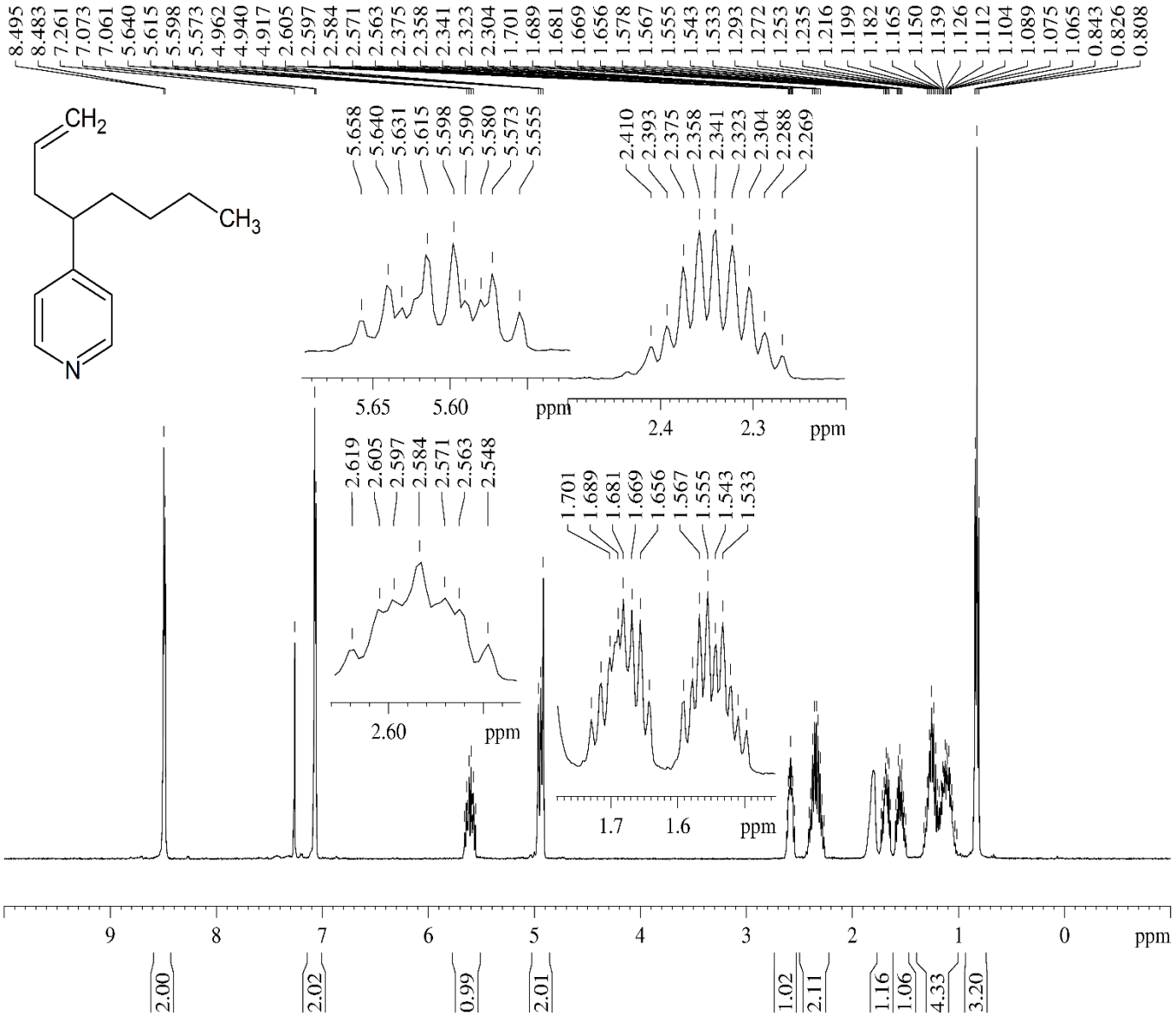

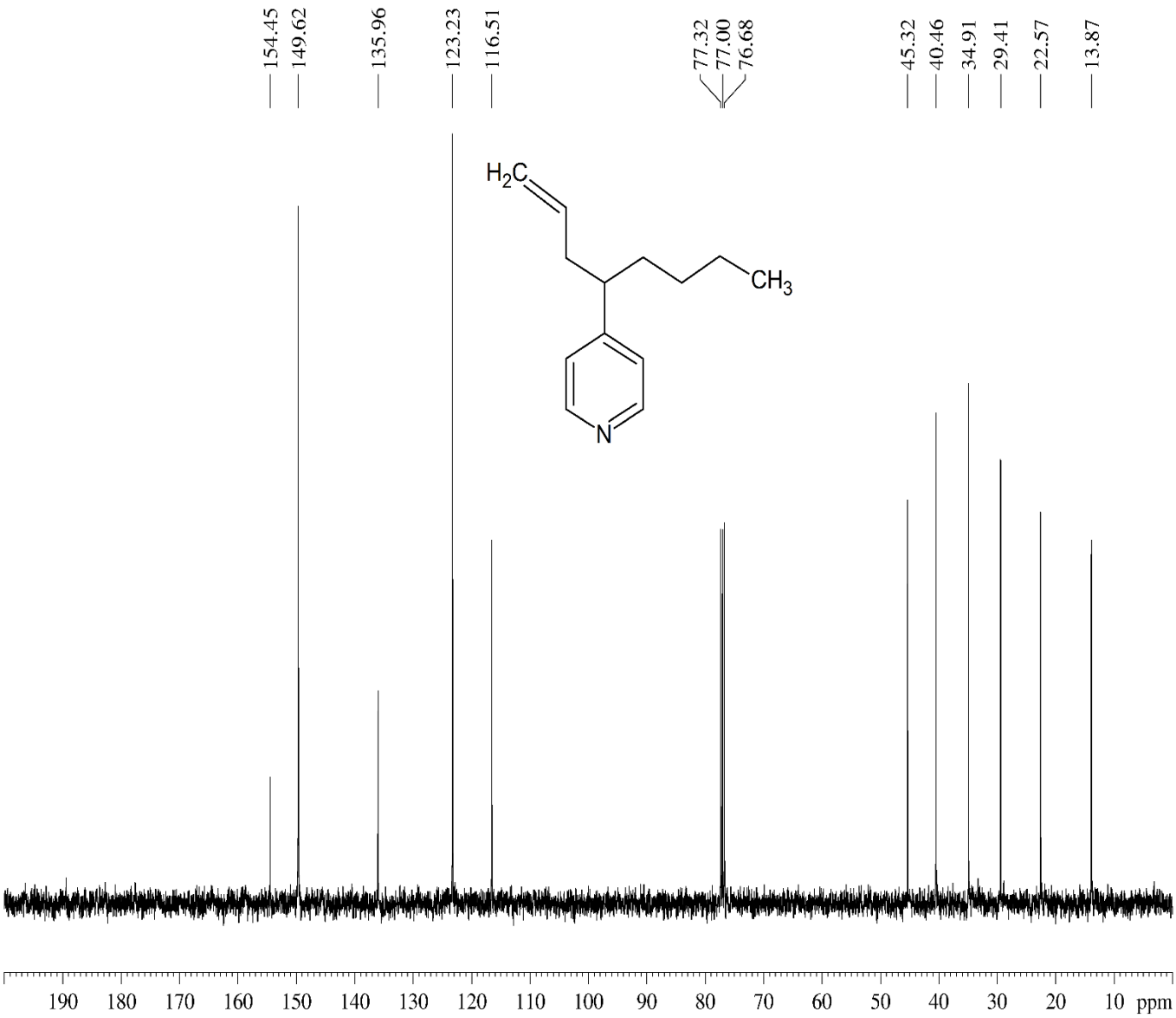
154.45
149.62
135.96
123.23
116.51
77.32
77.00
76.68
45.32
40.46
34.91
29.41
22.57
13.87
H2C
CH3
N
190 180 170 160 150 140 130 120 110 100 90 80 70 60 50 40 30 20 10 ppm

^{1}H (600 MHz, $CDCl_3$) and ^{13}C (100 MHz, $CDCl_3$) – NMR Spectra for **3aa**

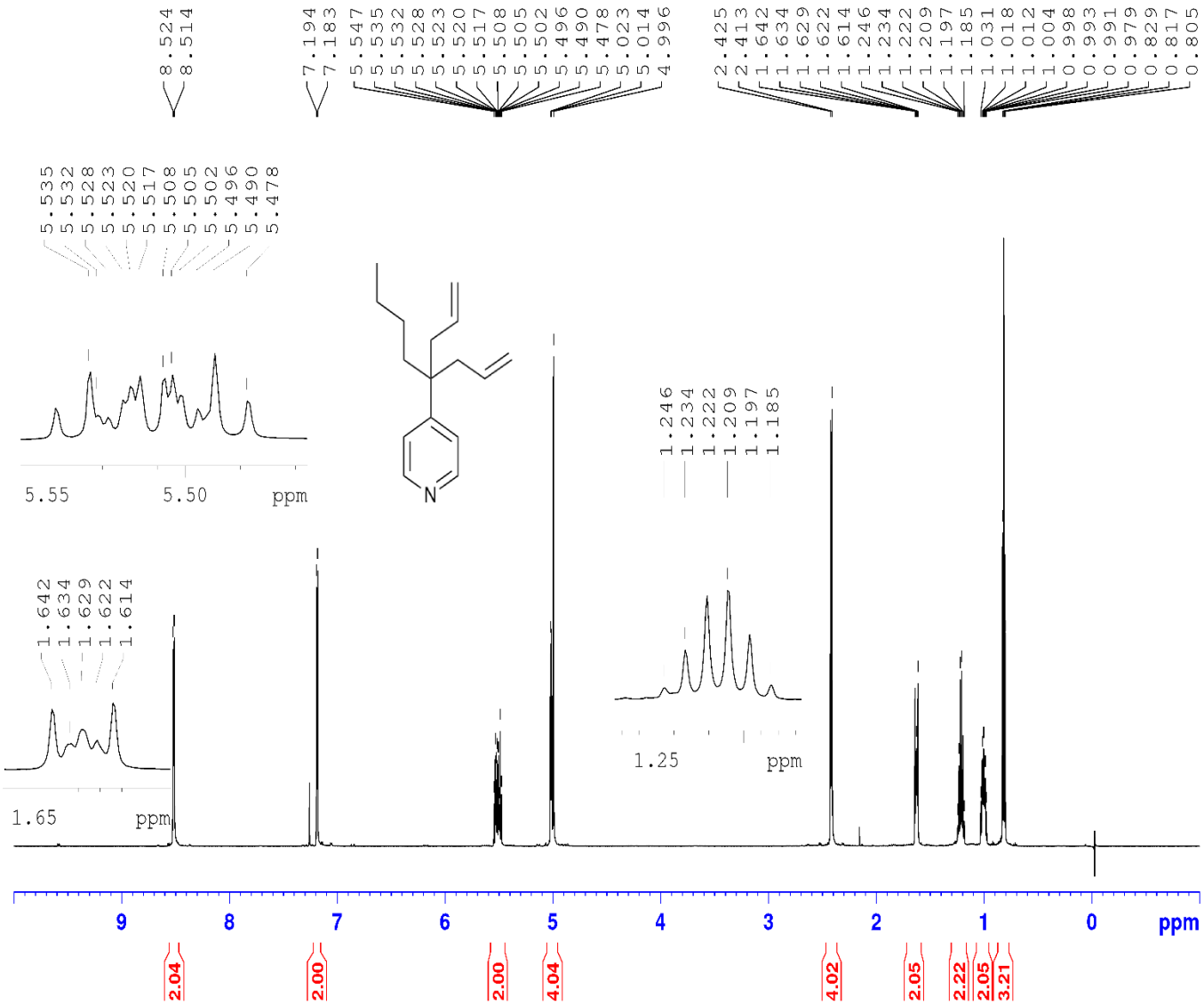

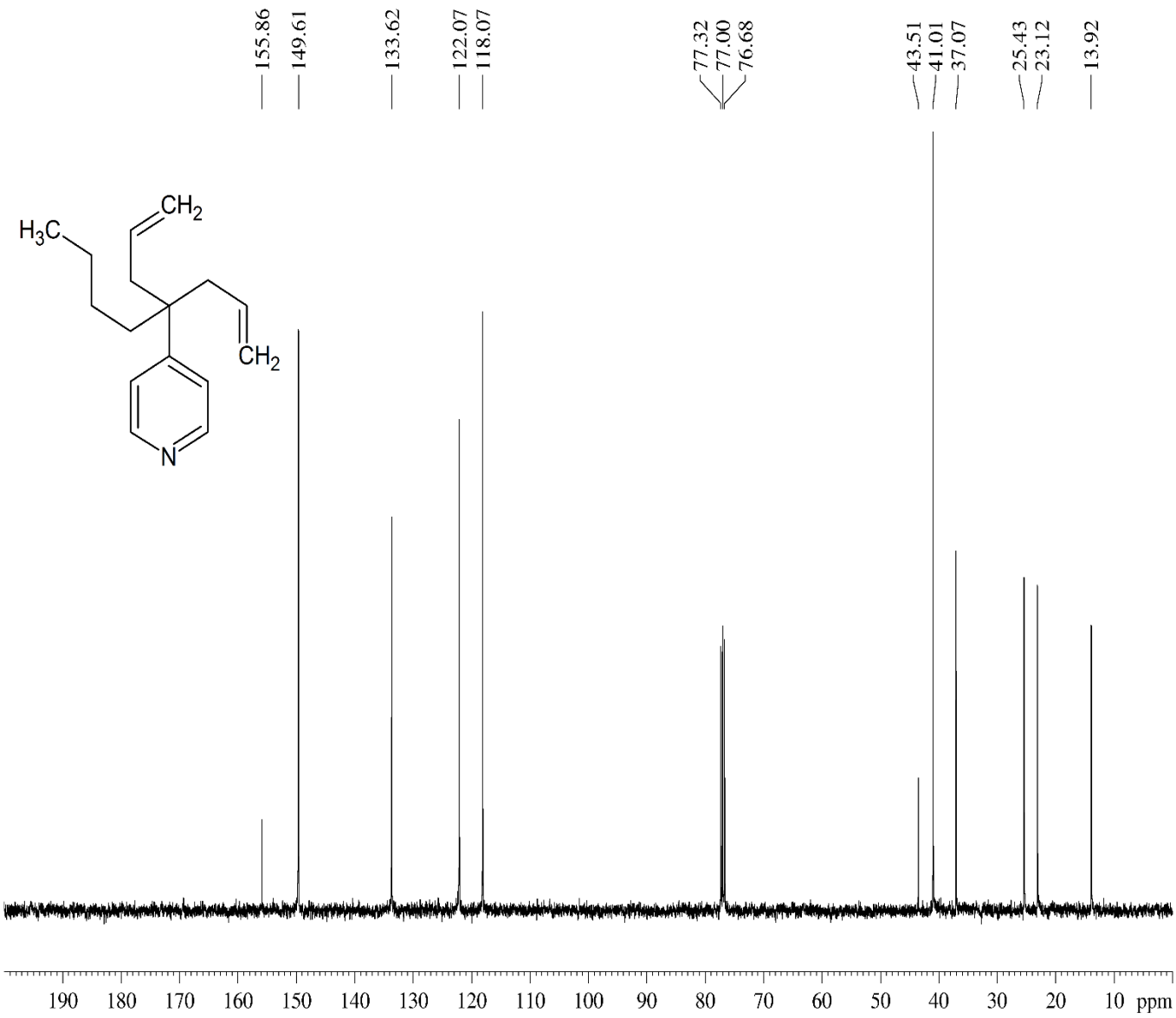
155.86
149.61
133.62
122.07
118.07
77.32
77.00
76.68
43.51
41.01
37.07
25.43
23.12
13.92
H3C
CH2
CH2
N
190 180 170 160 150 140 130 120 110 100 90 80 70 60 50 40 30 20 10 ppm

^{1}H (400 MHz, $CDCl_3$) and ^{13}C (100 MHz, $CDCl_3$) – NMR Spectra for **4a**

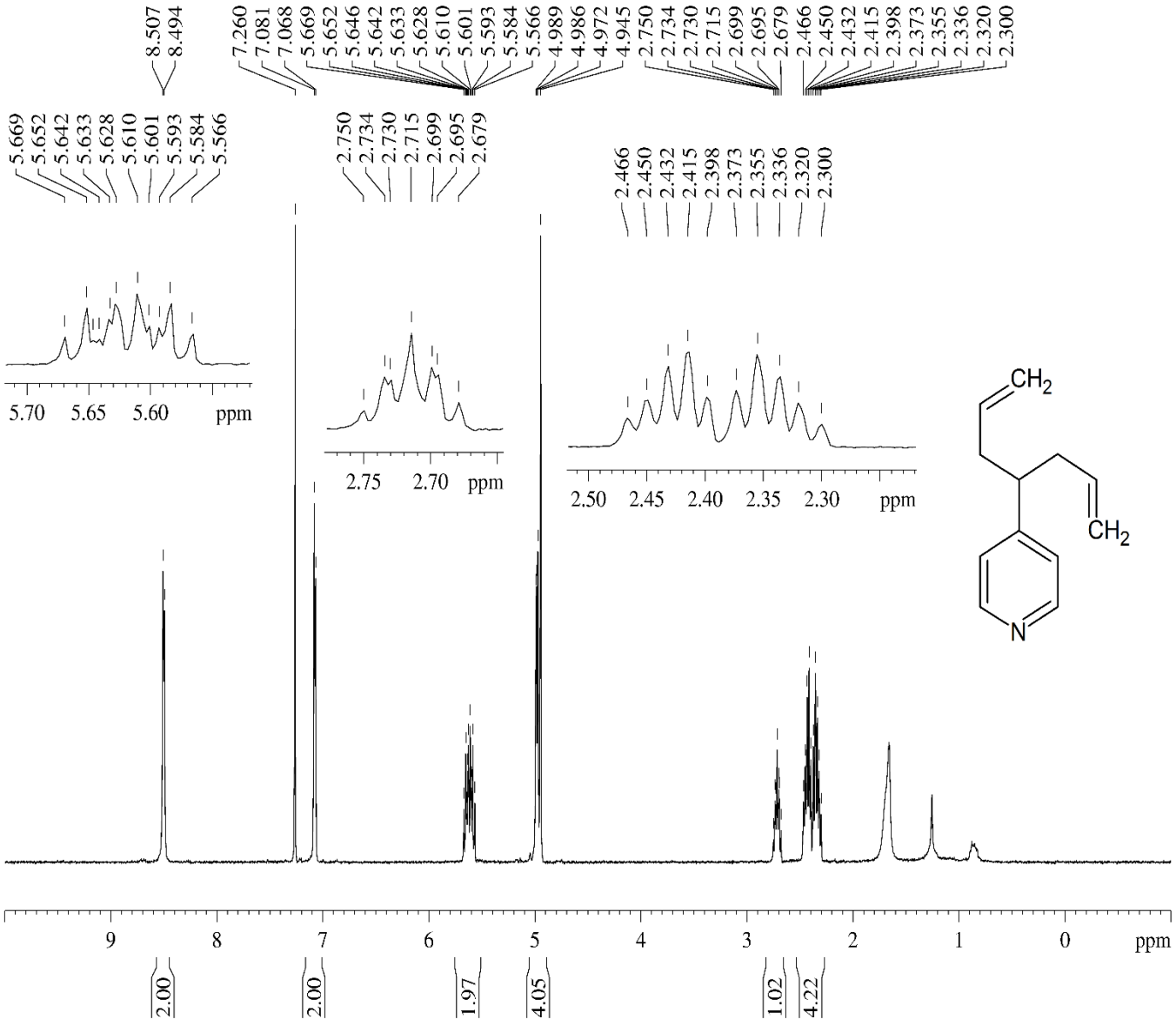

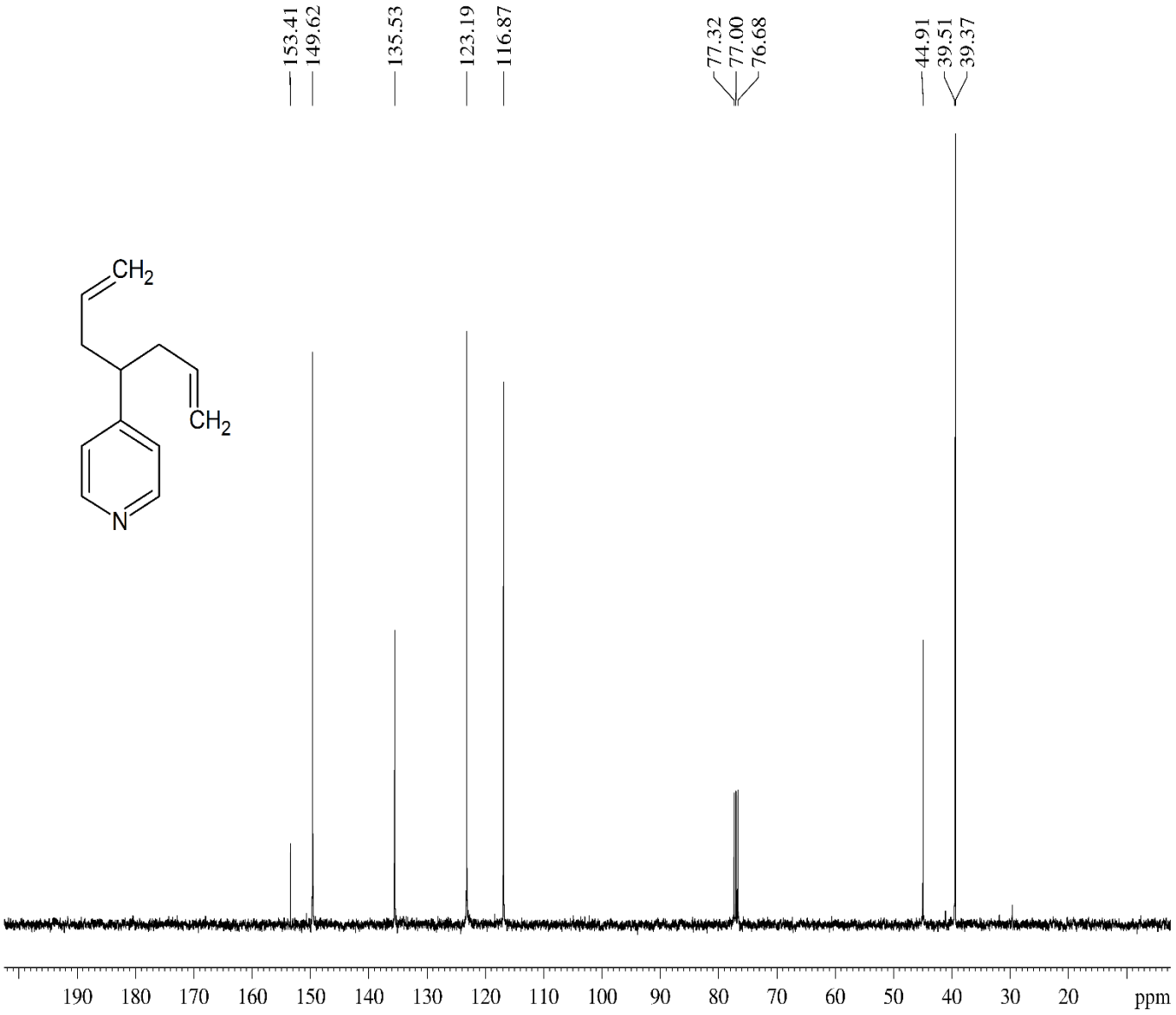
153.41
149.62
135.53
123.19
116.87
77.32
77.00
76.68
44.91
39.51
39.37
CH2
CH2
N
190
180
170
160
150
140
130
120
110
100
90
80
70
60
50
40
30
20
ppm

^{1}H (400 MHz, $CDCl_3$) and ^{13}C (100 MHz, $CDCl_3$) – NMR Spectra for **5a**

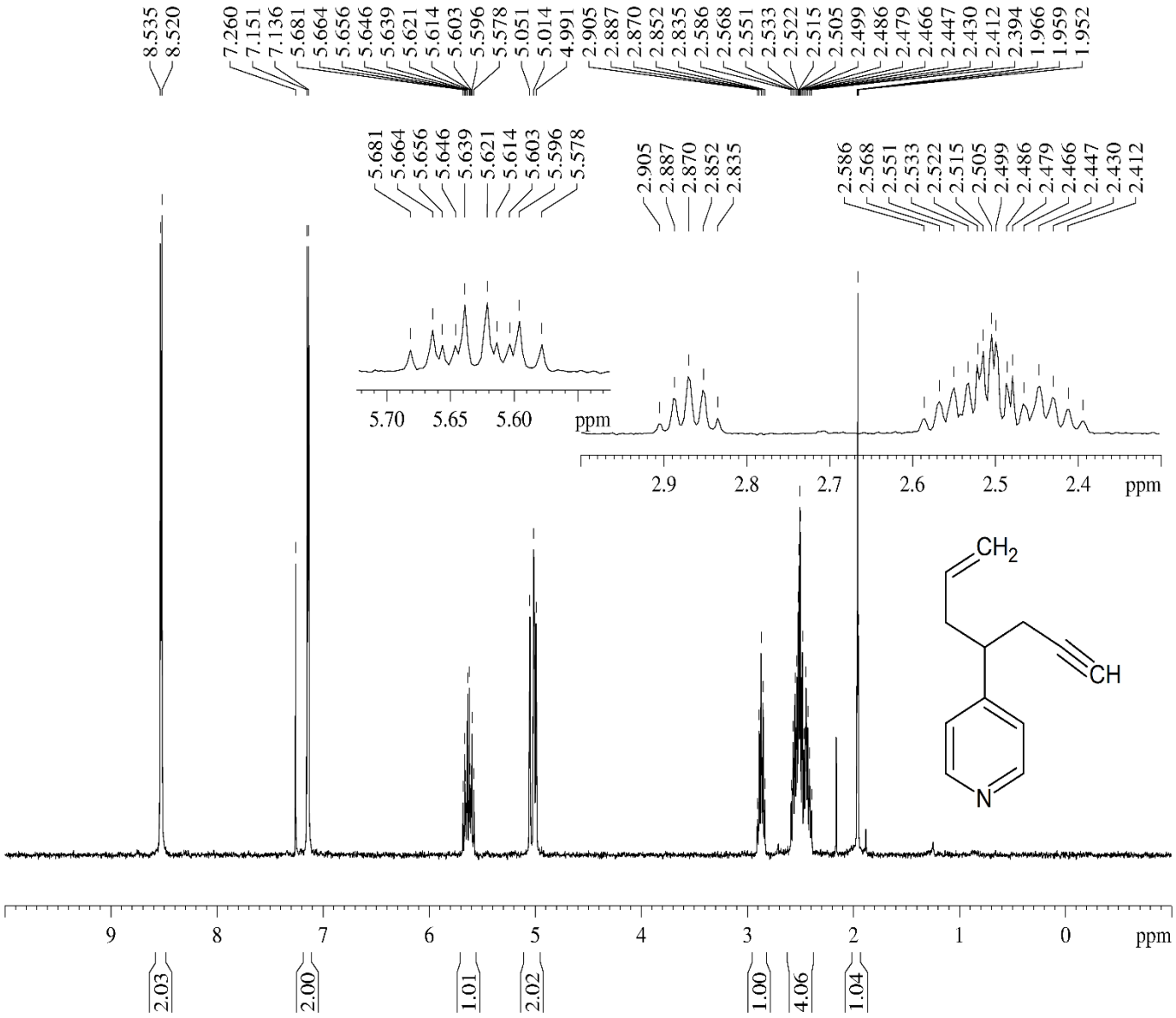

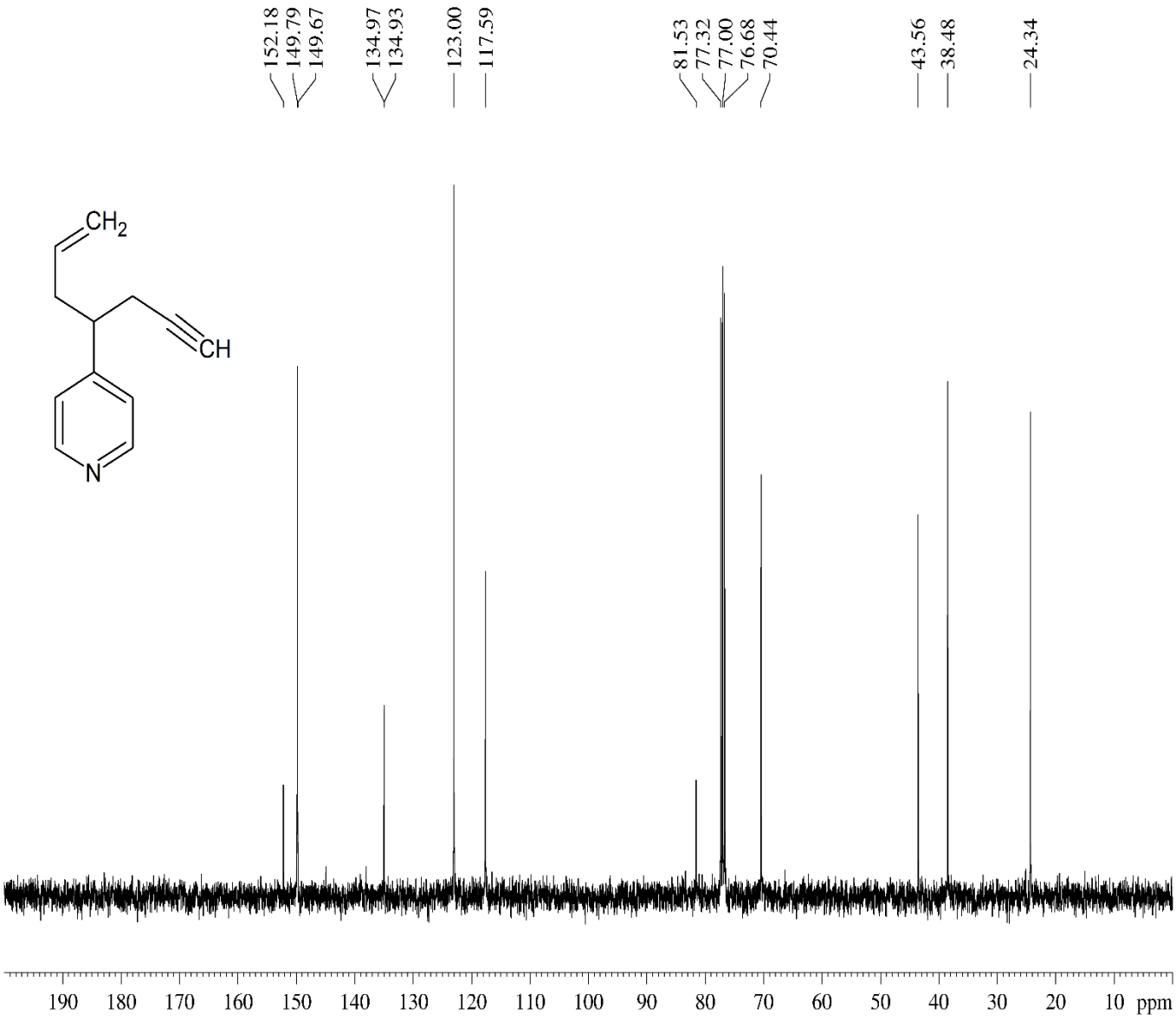
152.18
149.79
149.67
134.97
134.93
123.00
117.59
81.53
77.32
77.00
76.68
70.44
43.56
38.48
24.34
CH2
CH
N
190 180 170 160 150 140 130 120 110 100 90 80 70 60 50 40 30 20 10 ppm

^{1}H (400 MHz, $CDCl_3$) and ^{13}C (100 MHz, $CDCl_3$) – NMR Spectra for **6a**

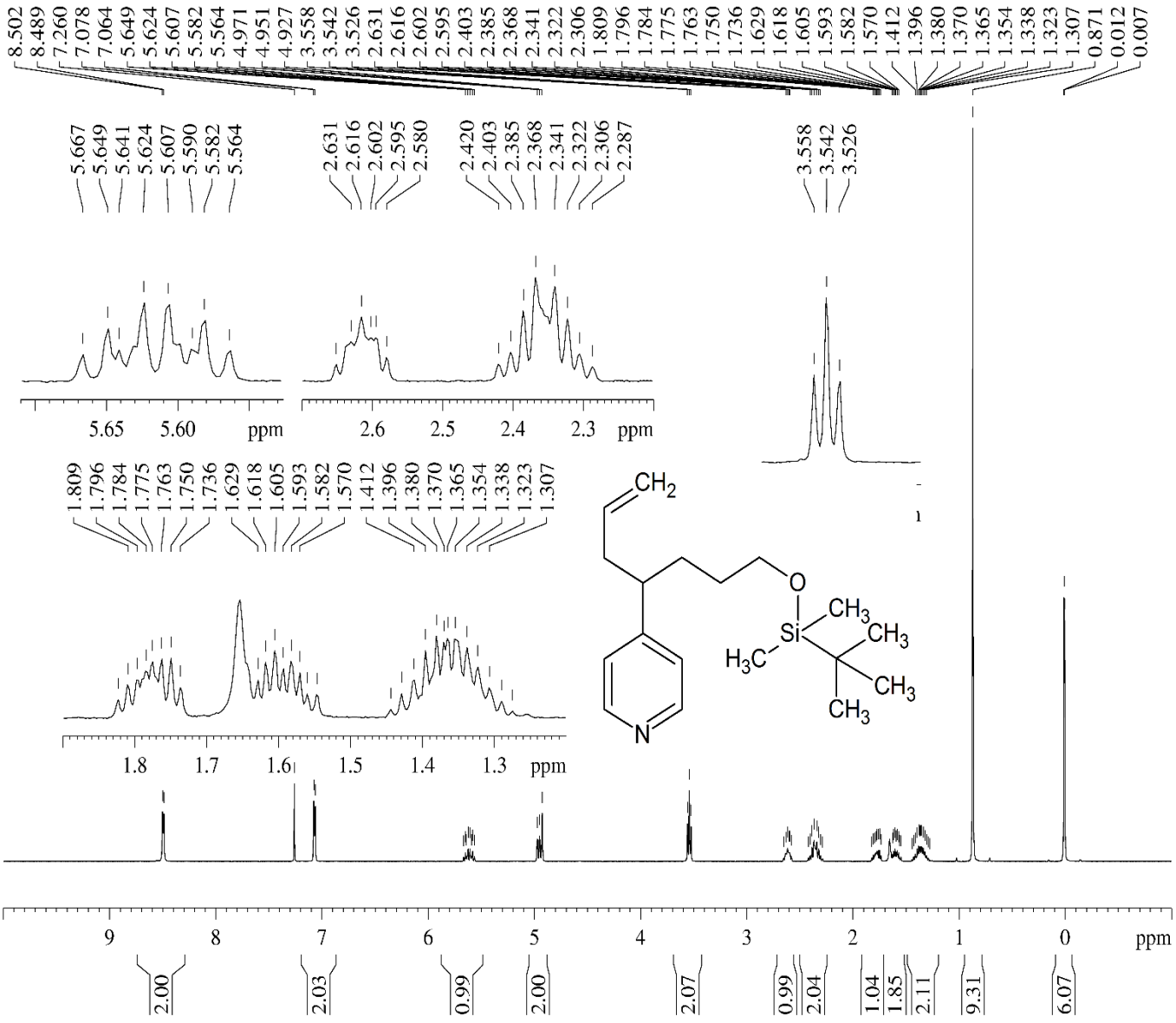

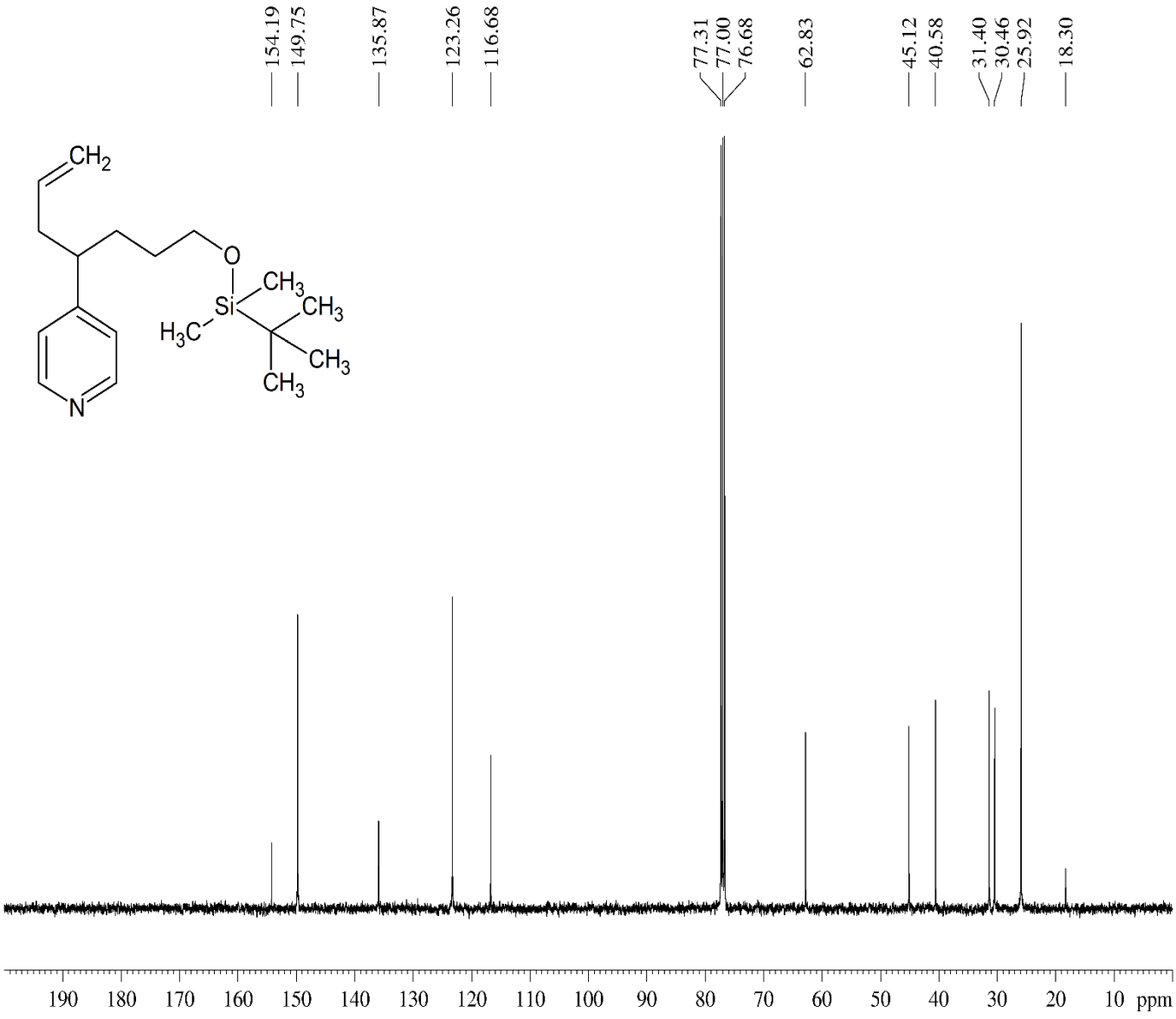
154.19
149.75
135.87
123.26
116.68
77.31
77.00
76.68
62.83
45.12
40.58
31.40
30.46
25.92
18.30
CH2
O
Si
CH3
CH3
H3C
CH3
CH3
N
190 180 170 160 150 140 130 120 110 100 90 80 70 60 50 40 30 20 10 ppm

^{29}Si NMR Spectra for **6a** (80 MHz, $CDCl_3$)

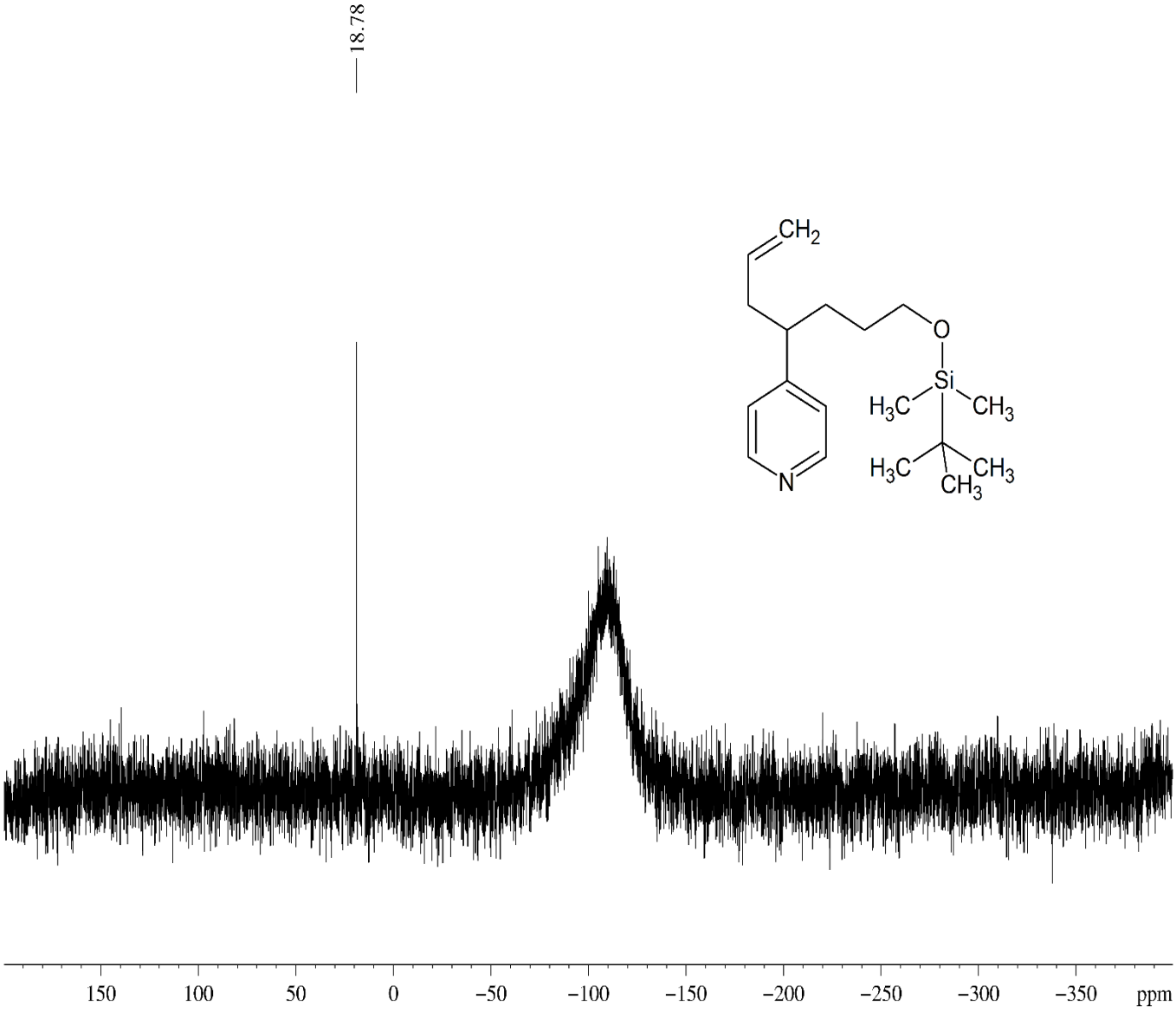

^{1}H (400 MHz, $CDCl_3$) and ^{13}C (100 MHz, $CDCl_3$) – NMR Spectra for **7a**

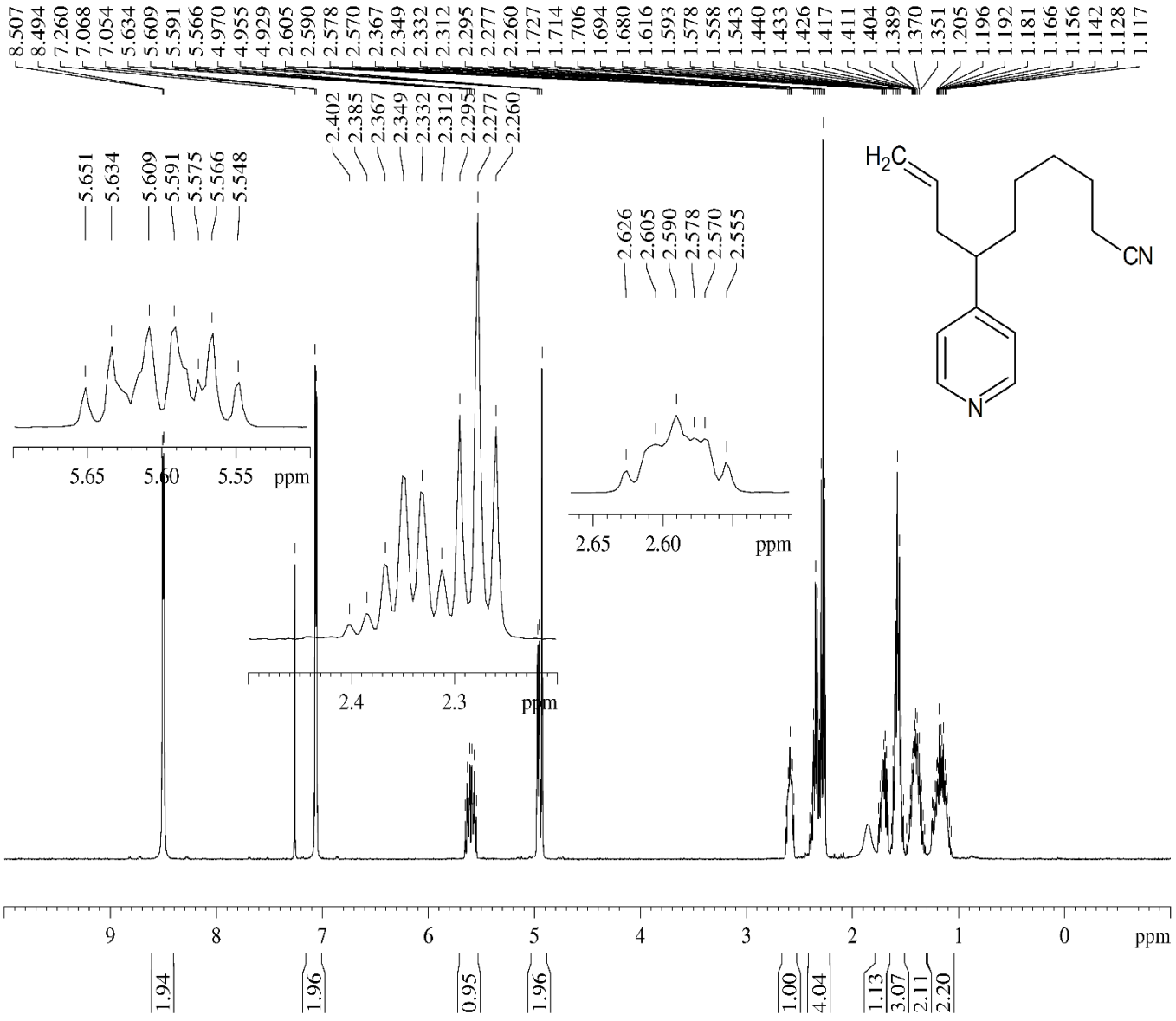

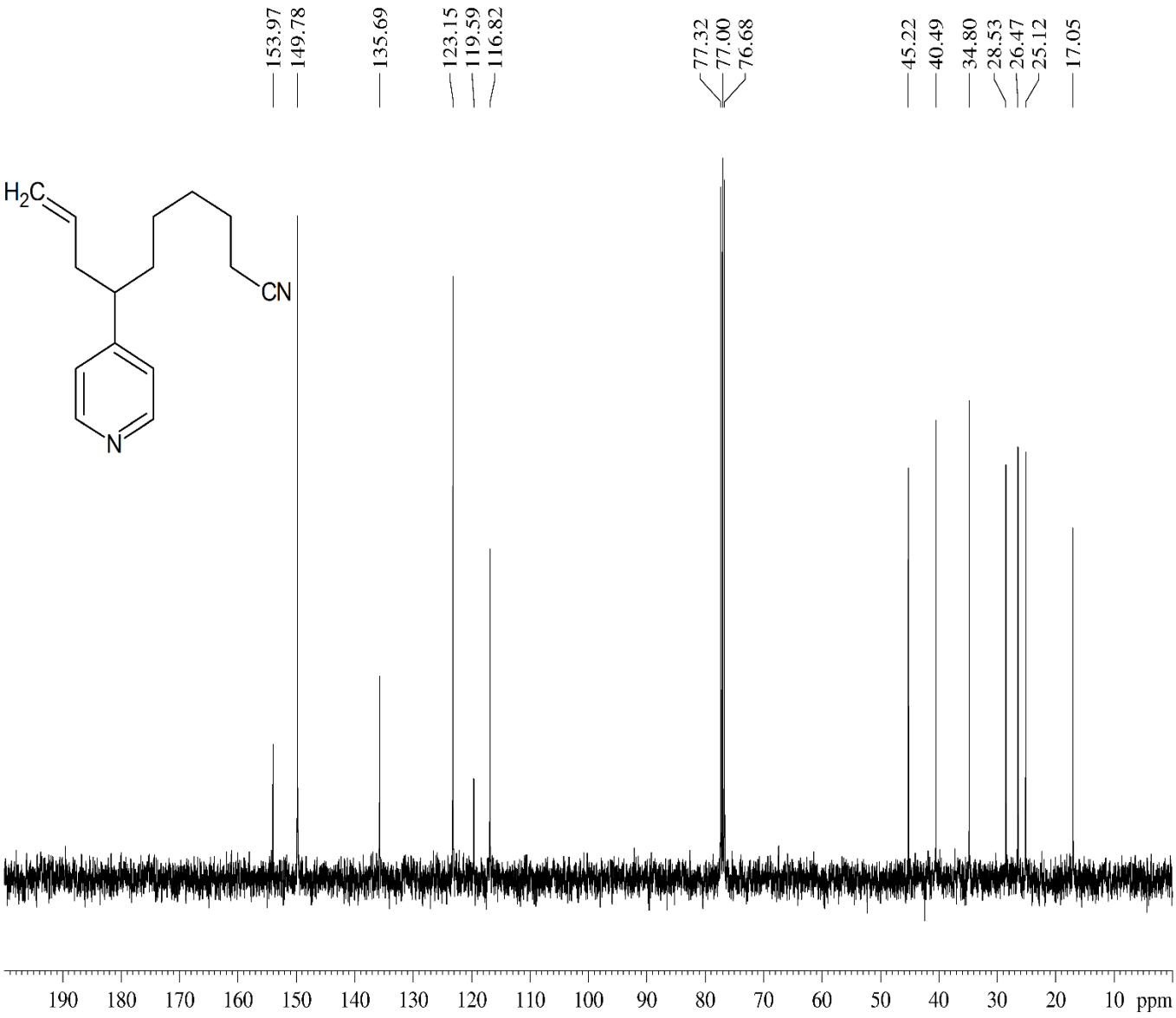
153.97
149.78
135.69
123.15
119.59
116.82
77.32
77.00
76.68
45.22
40.49
34.80
28.53
26.47
25.12
17.05
H2C
CN
N
190 180 170 160 150 140 130 120 110 100 90 80 70 60 50 40 30 20 10 ppm

^{1}H (400 MHz, $CDCl_3$) and ^{13}C (100 MHz, $CDCl_3$) – NMR Spectra for **8a**

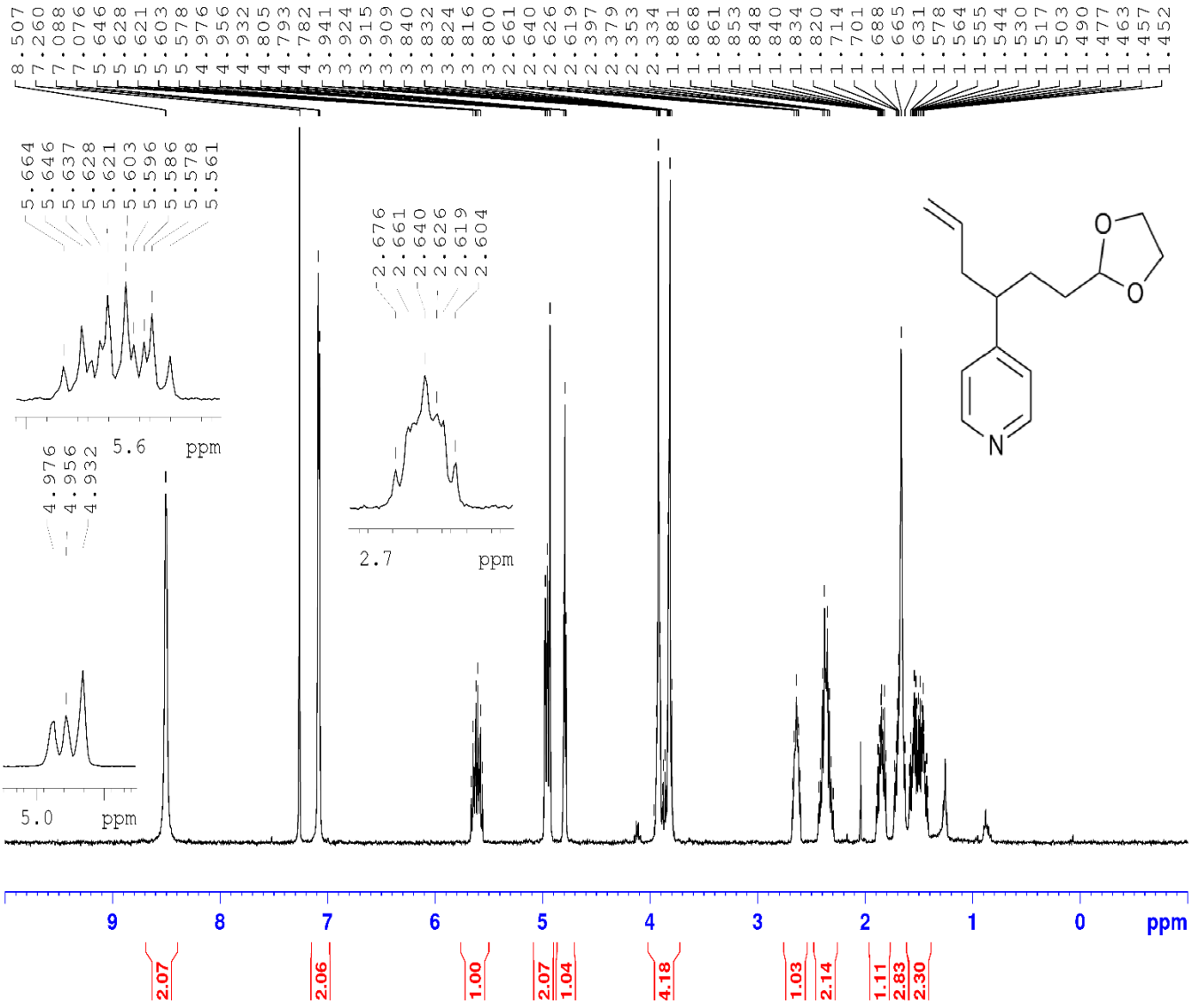

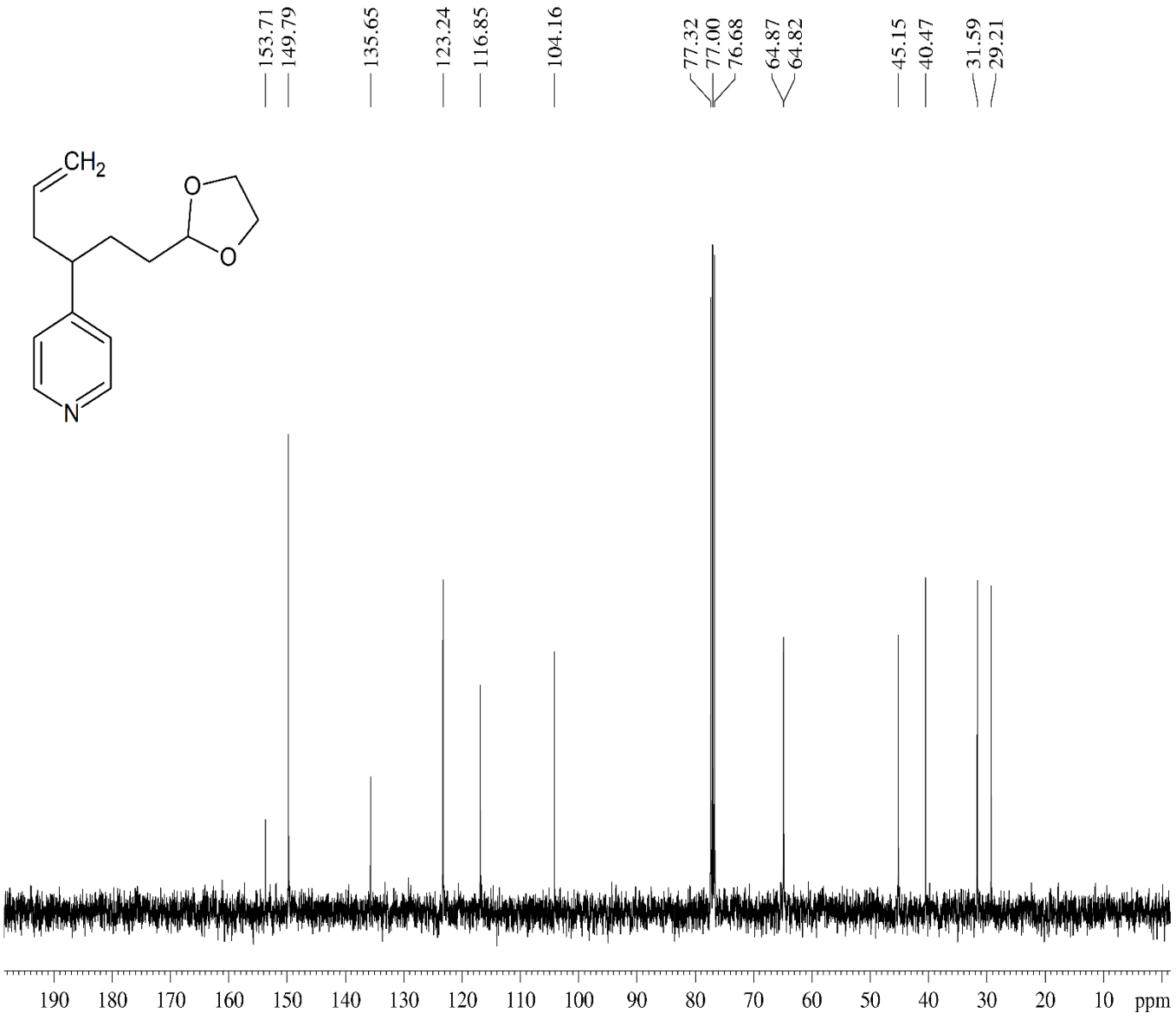
153.71
149.79
135.65
123.24
116.85
104.16
77.32
77.00
76.68
64.87
64.82
45.15
40.47
31.59
29.21
CH2
O
O
N
190 180 170 160 150 140 130 120 110 100 90 80 70 60 50 40 30 20 10 ppm

^{1}H (400 MHz, $CDCl_3$) and ^{13}C (100 MHz, $CDCl_3$) – NMR Spectra for **9a**

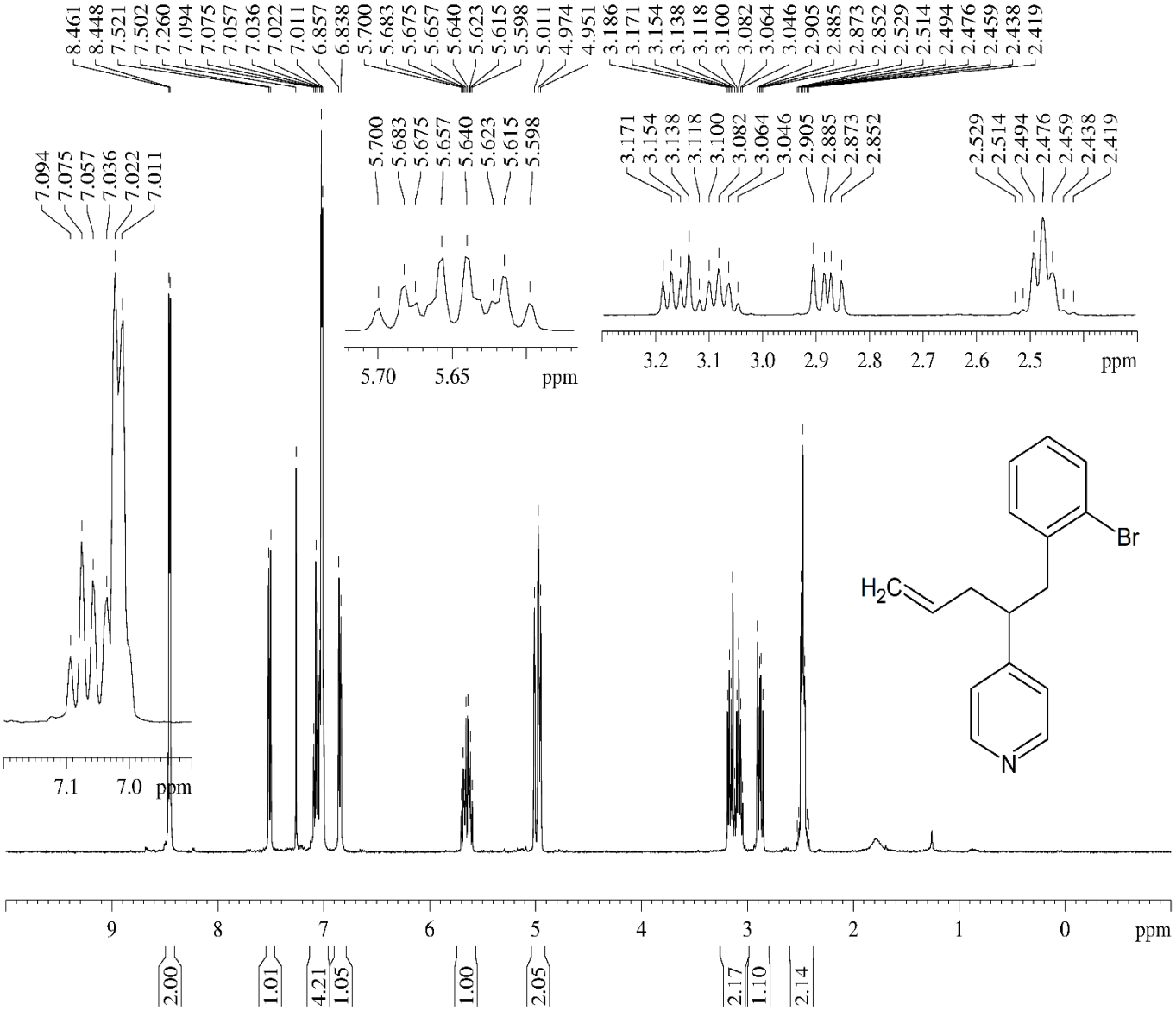

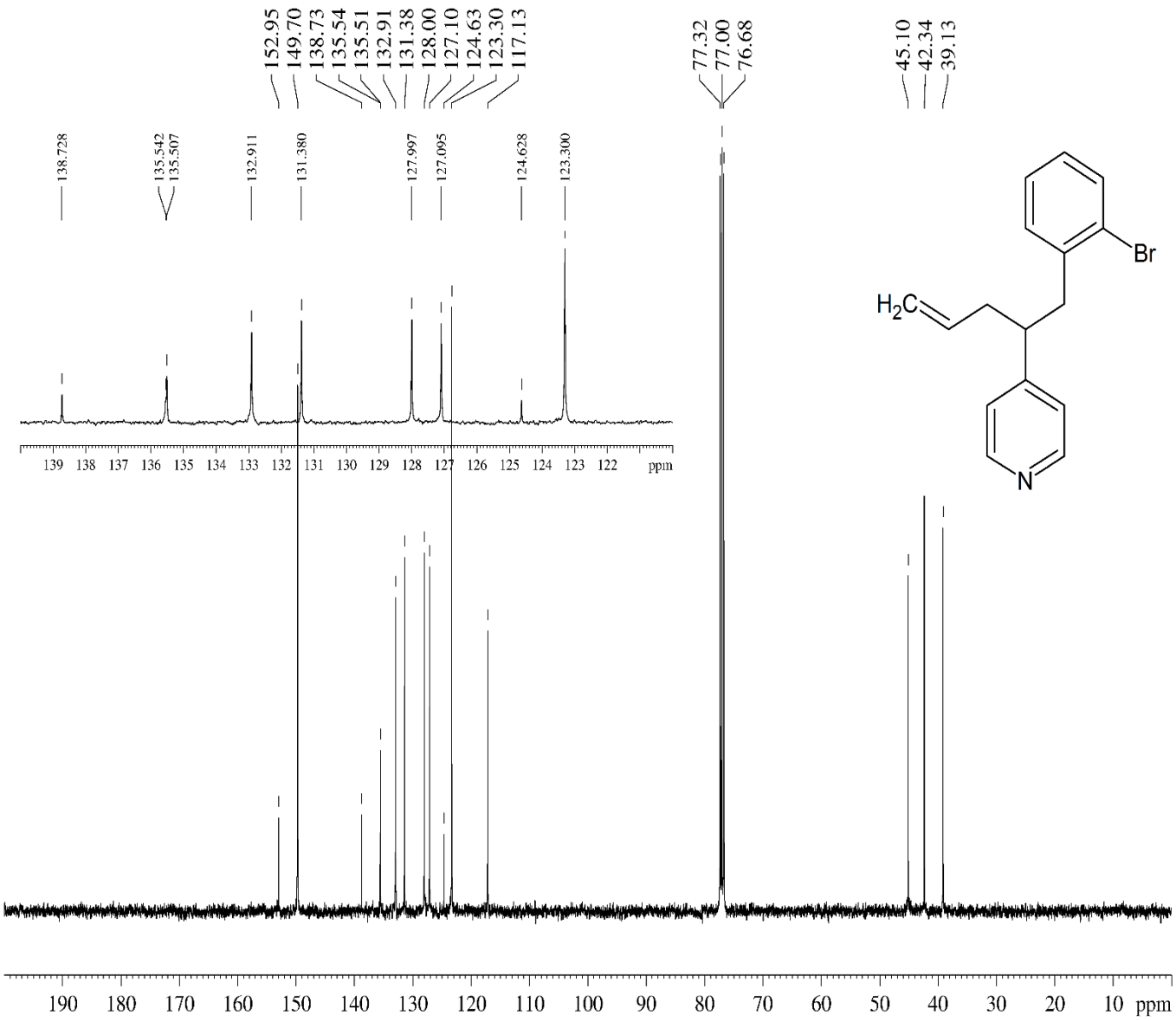
152.95
149.70
138.73
135.54
135.51
132.91
131.38
128.00
127.10
124.63
123.30
117.13
77.32
77.00
76.68
45.10
42.34
39.13
138.728
135.542
135.507
132.911
131.380
127.997
127.095
124.628
123.300
Br
H2C
N
139 138 137 136 135 134 133 132 131 130 129 128 127 126 125 124 123 122 ppm
190 180 170 160 150 140 130 120 110 100 90 80 70 60 50 40 30 20 10 ppm

^{1}H (400 MHz, $CDCl_3$) and ^{13}C (100 MHz, $CDCl_3$) – NMR Spectra for **10a**

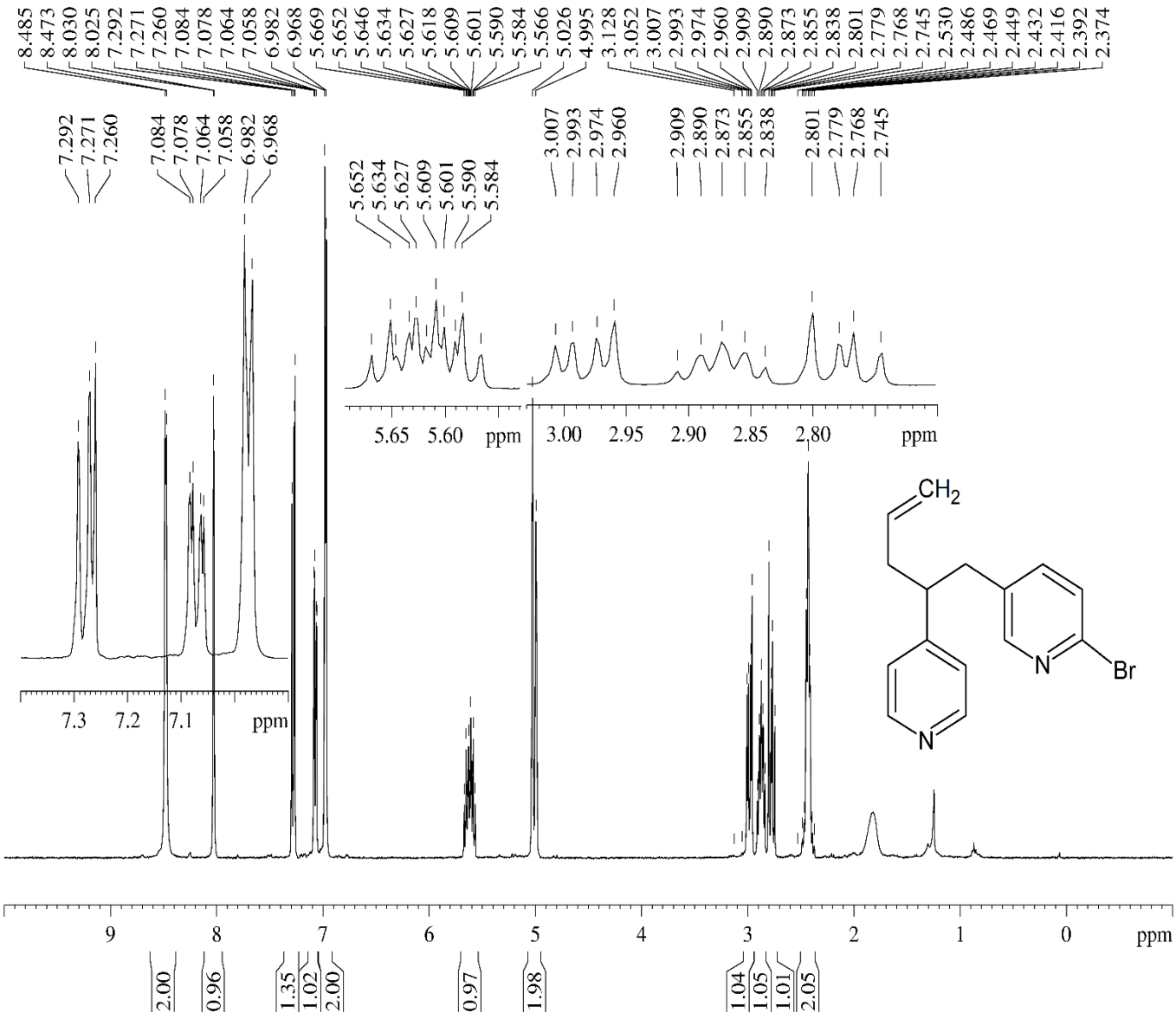

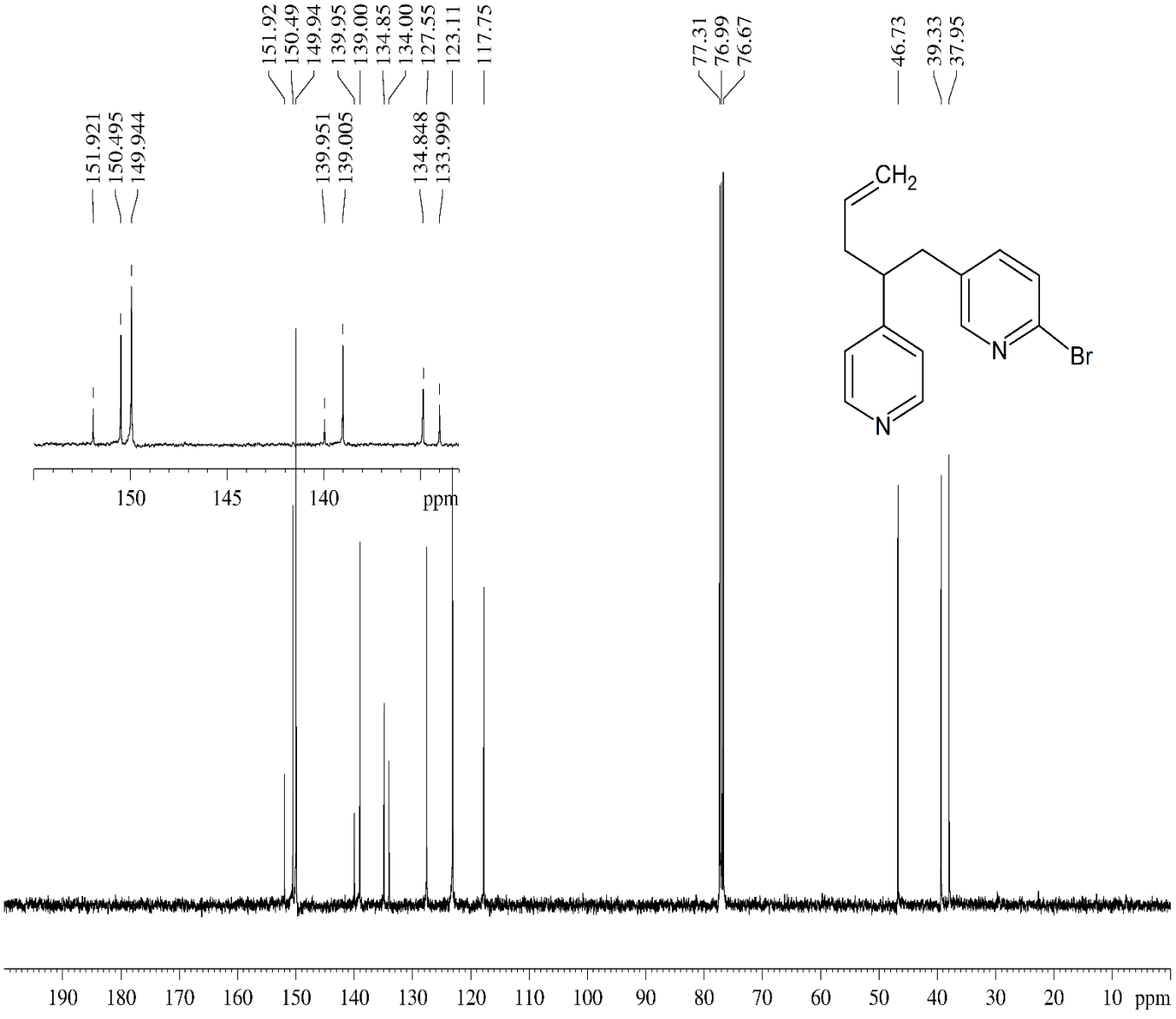
151.92
150.49
149.94
139.95
139.00
134.85
134.00
127.55
123.11
117.75
77.31
76.99
76.67
46.73
39.33
37.95
151.921
150.495
149.944
139.951
139.005
134.848
133.999
CH2
N
Br
N
150
145
140
ppm
190 180 170 160 150 140 130 120 110 100 90 80 70 60 50 40 30 20 10 ppm

^{1}H (400 MHz, $CDCl_3$) and ^{13}C (100 MHz, $CDCl_3$) – NMR Spectra for **12a**

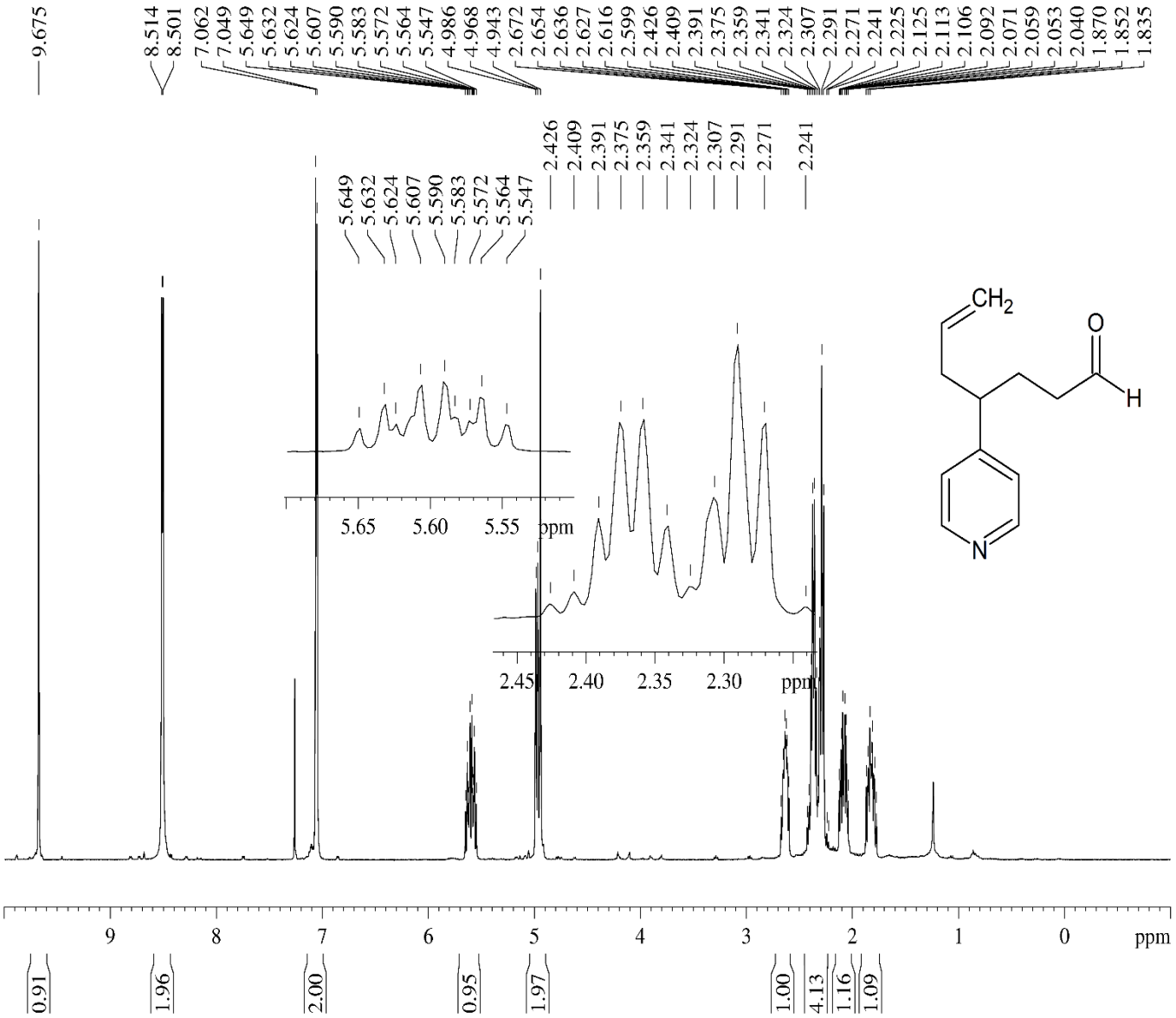

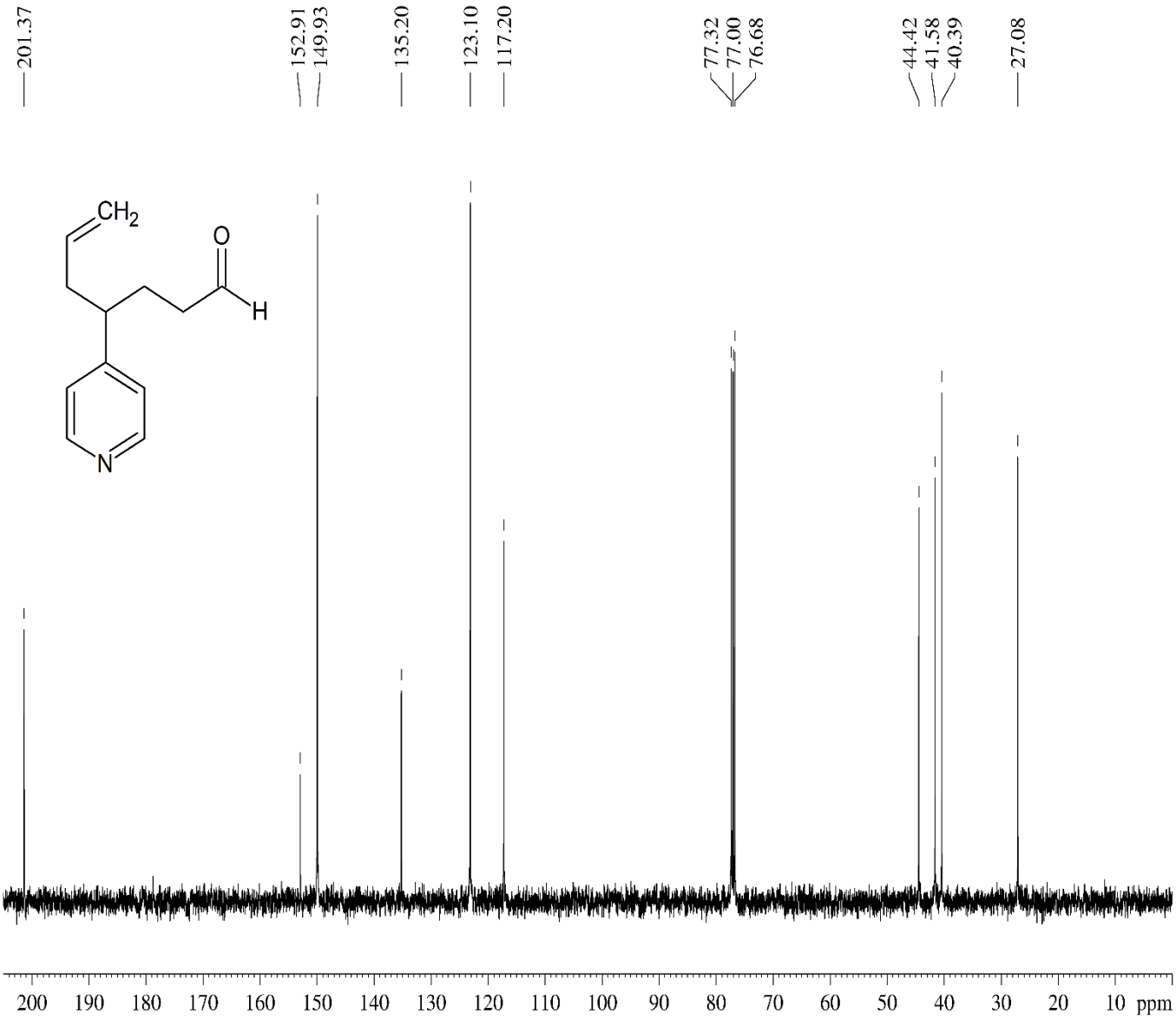
201.37
152.91
149.93
135.20
123.10
117.20
77.32
77.00
76.68
44.42
41.58
40.39
27.08
CH2
O
H
N
200 190 180 170 160 150 140 130 120 110 100 90 80 70 60 50 40 30 20 10 ppm

^{1}H (400 MHz, $CDCl_3$) and ^{13}C (100 MHz, $CDCl_3$) – NMR Spectra for **13a**

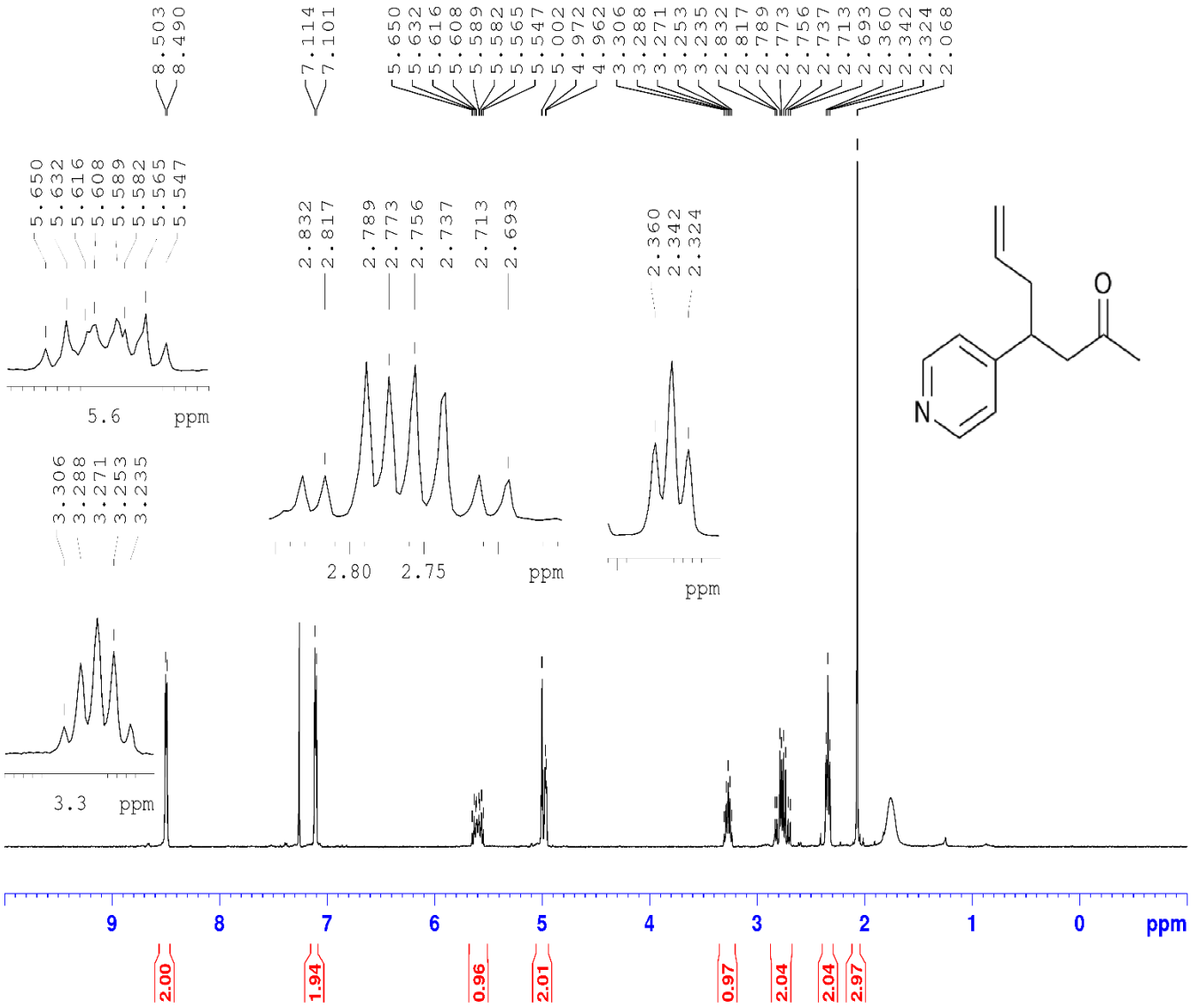

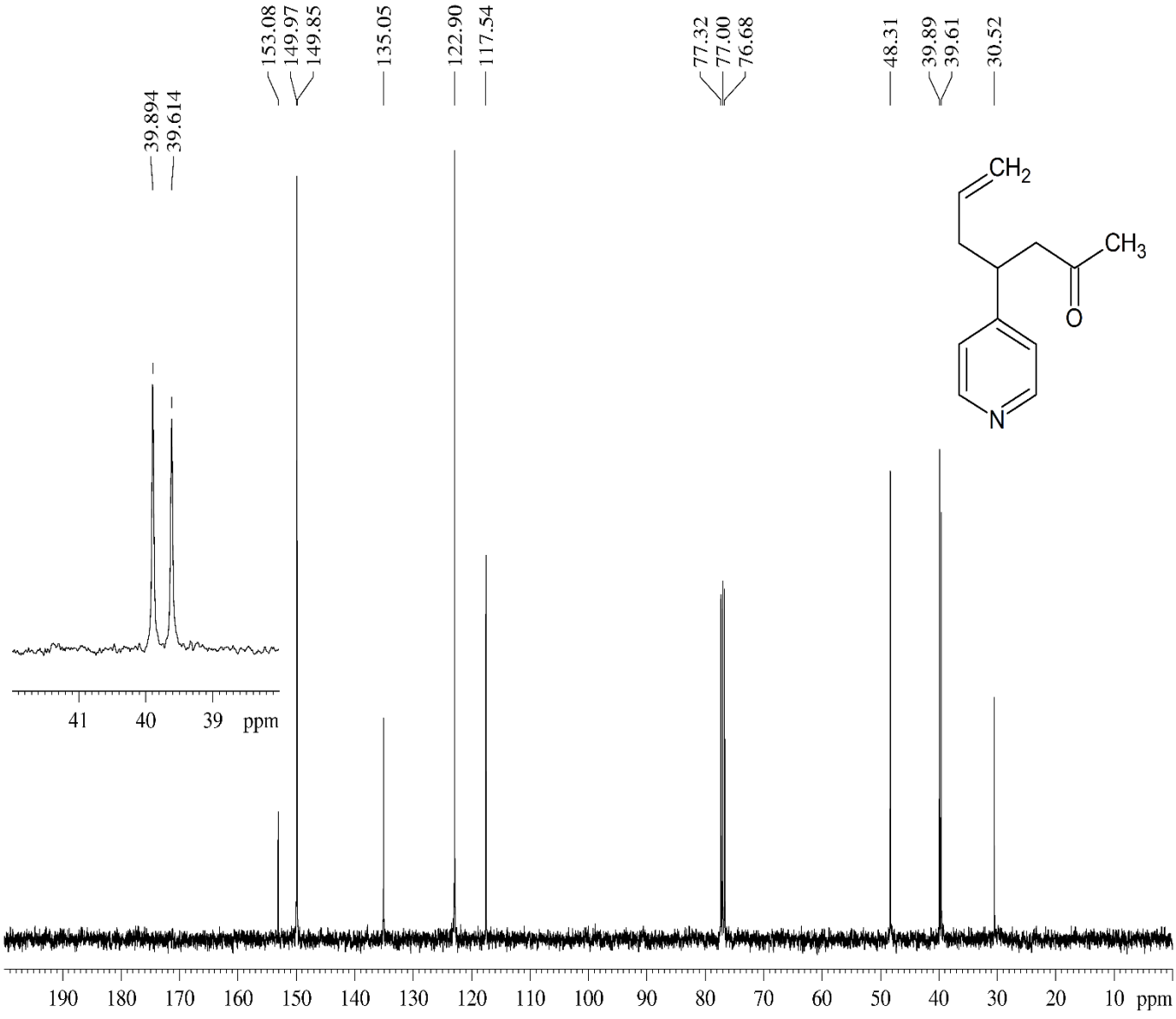
153.08
149.97
149.85
135.05
122.90
117.54
77.32
77.00
76.68
48.31
39.89
39.61
30.52
39.894
39.614
CH2
CH3
O
N
41
40
39
ppm
190
180
170
160
150
140
130
120
110
100
90
80
70
60
50
40
30
20
10
ppm

^{1}H (400 MHz, $CDCl_3$) and ^{13}C (100 MHz, $CDCl_3$) – NMR Spectra for **14a**

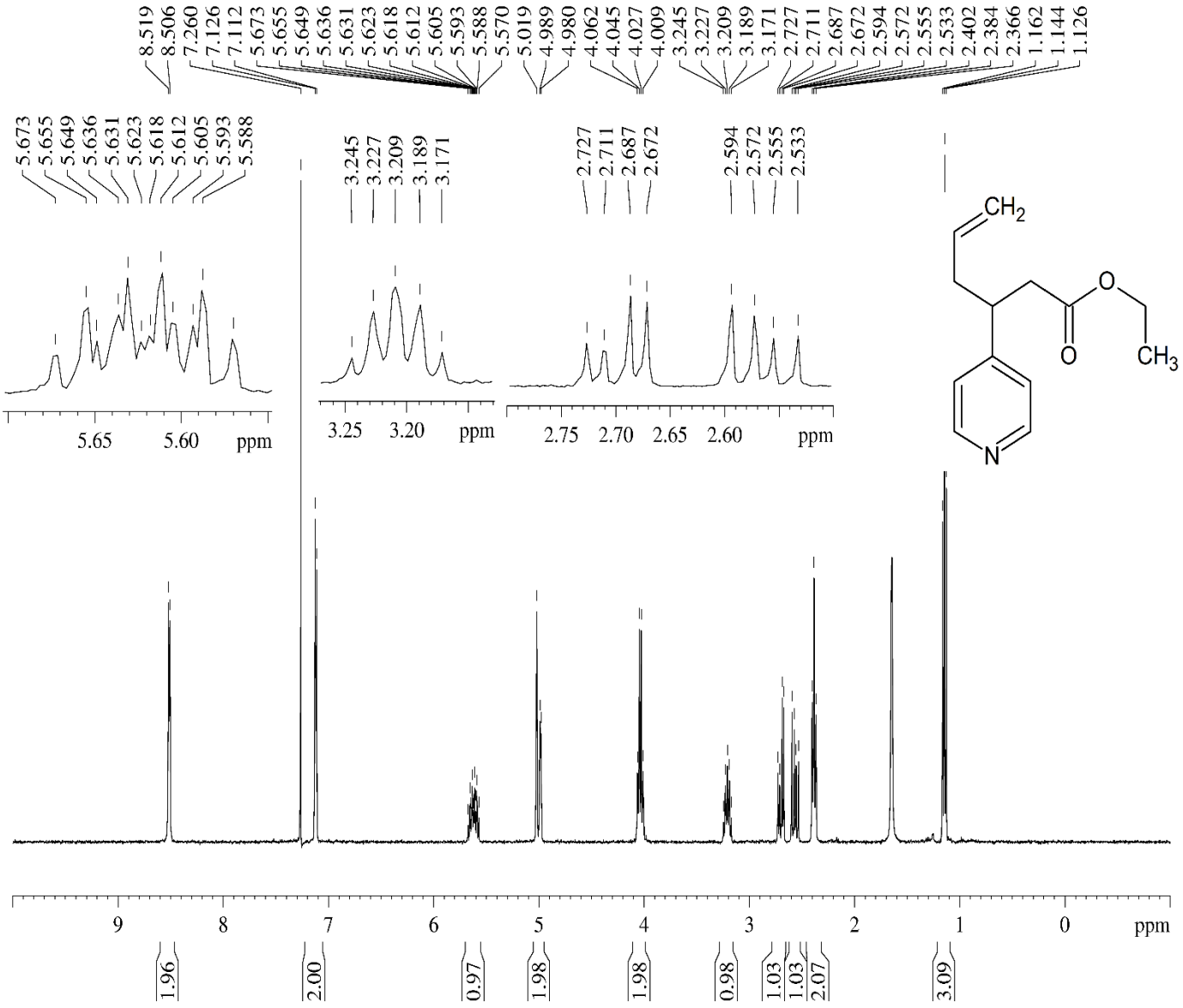

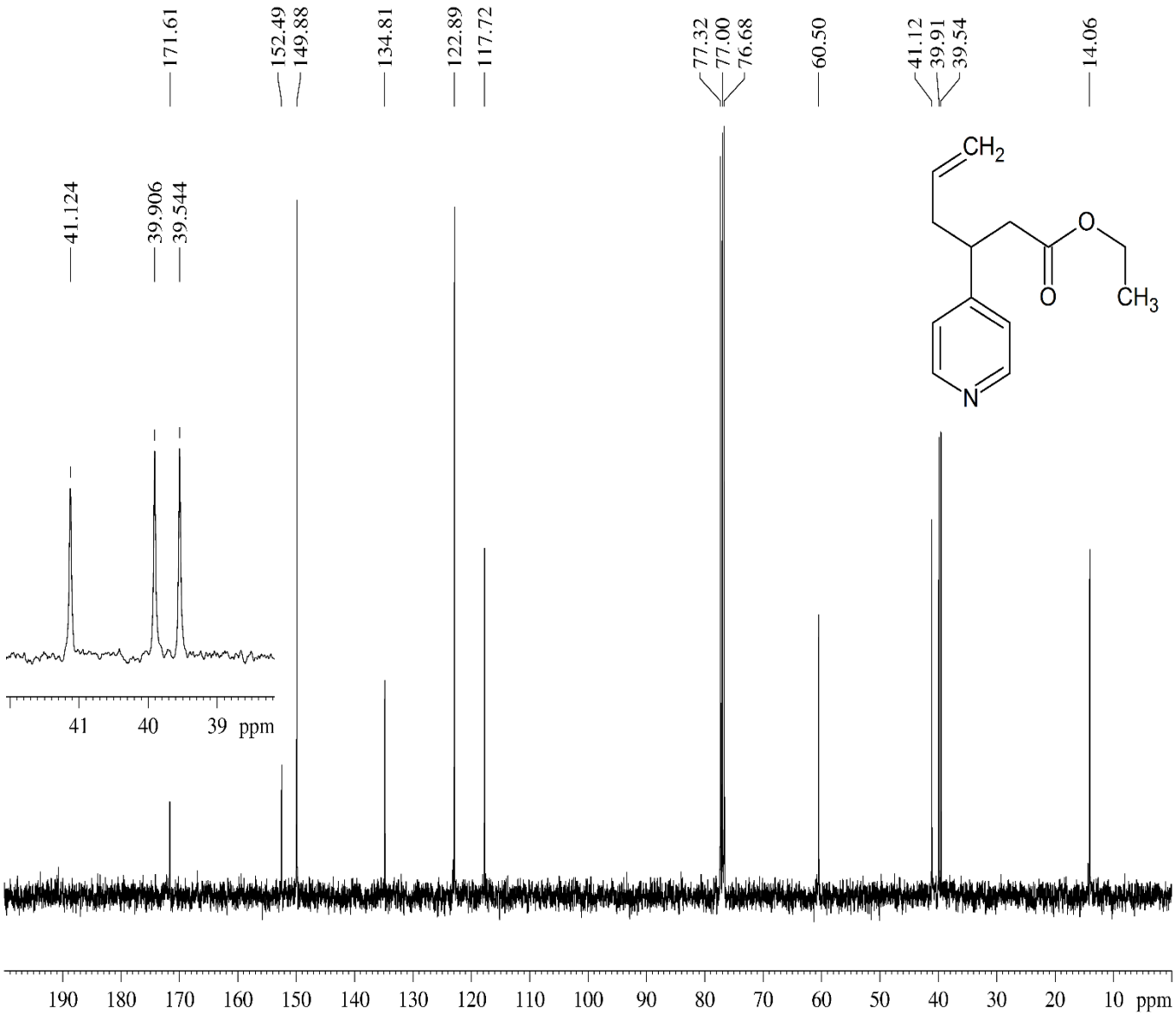
171.61
152.49
149.88
134.81
122.89
117.72
77.32
77.00
76.68
60.50
41.12
39.91
39.54
14.06
41.124
39.906
39.544
CH2
O
O
CH3
N
41
40
39 ppm
190
180
170
160
150
140
130
120
110
100
90
80
70
60
50
40
30
20
10 ppm

^{1}H (400 MHz, $CDCl_3$) and ^{13}C (100 MHz, $CDCl_3$) – NMR Spectra for **16a**

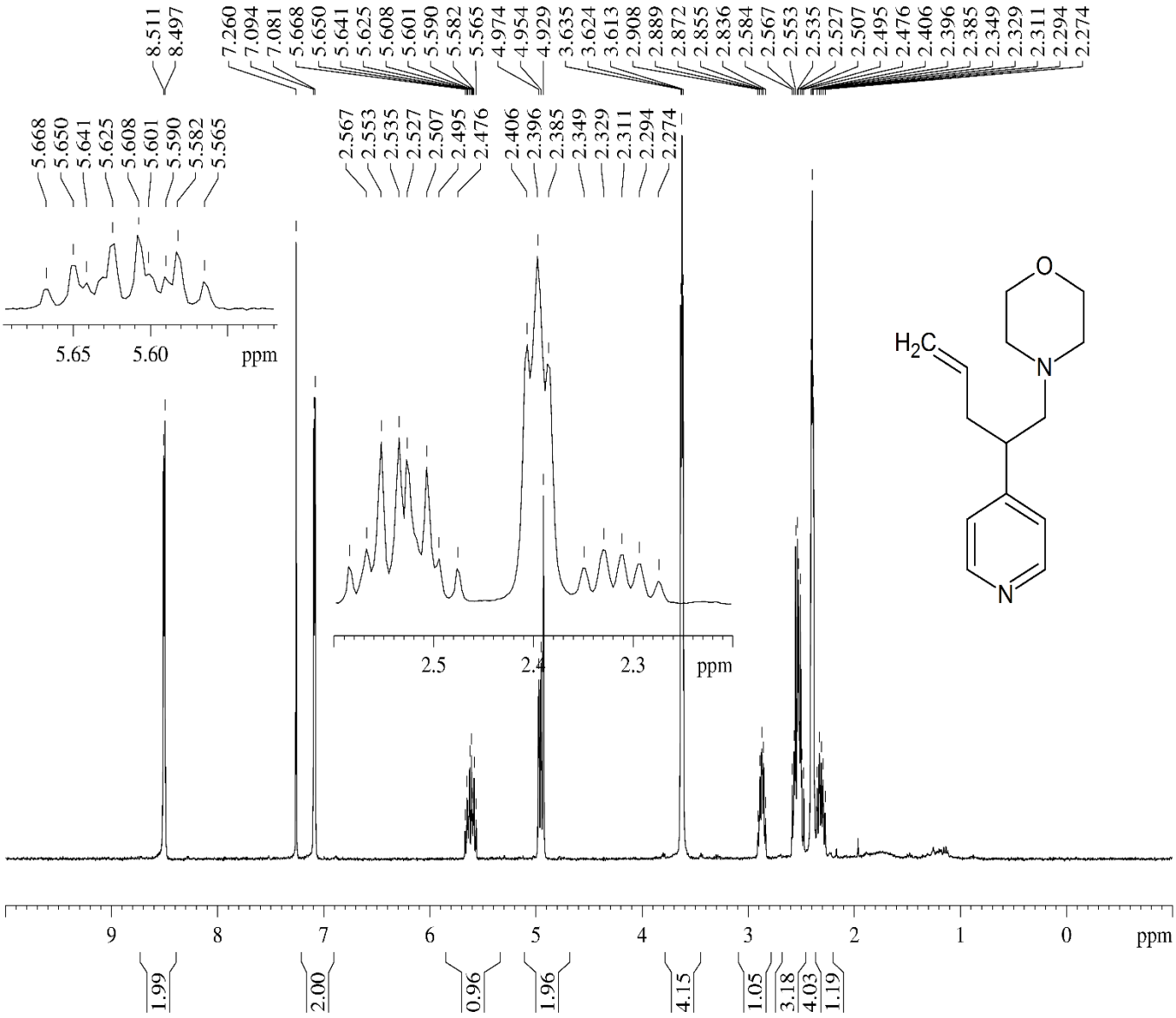

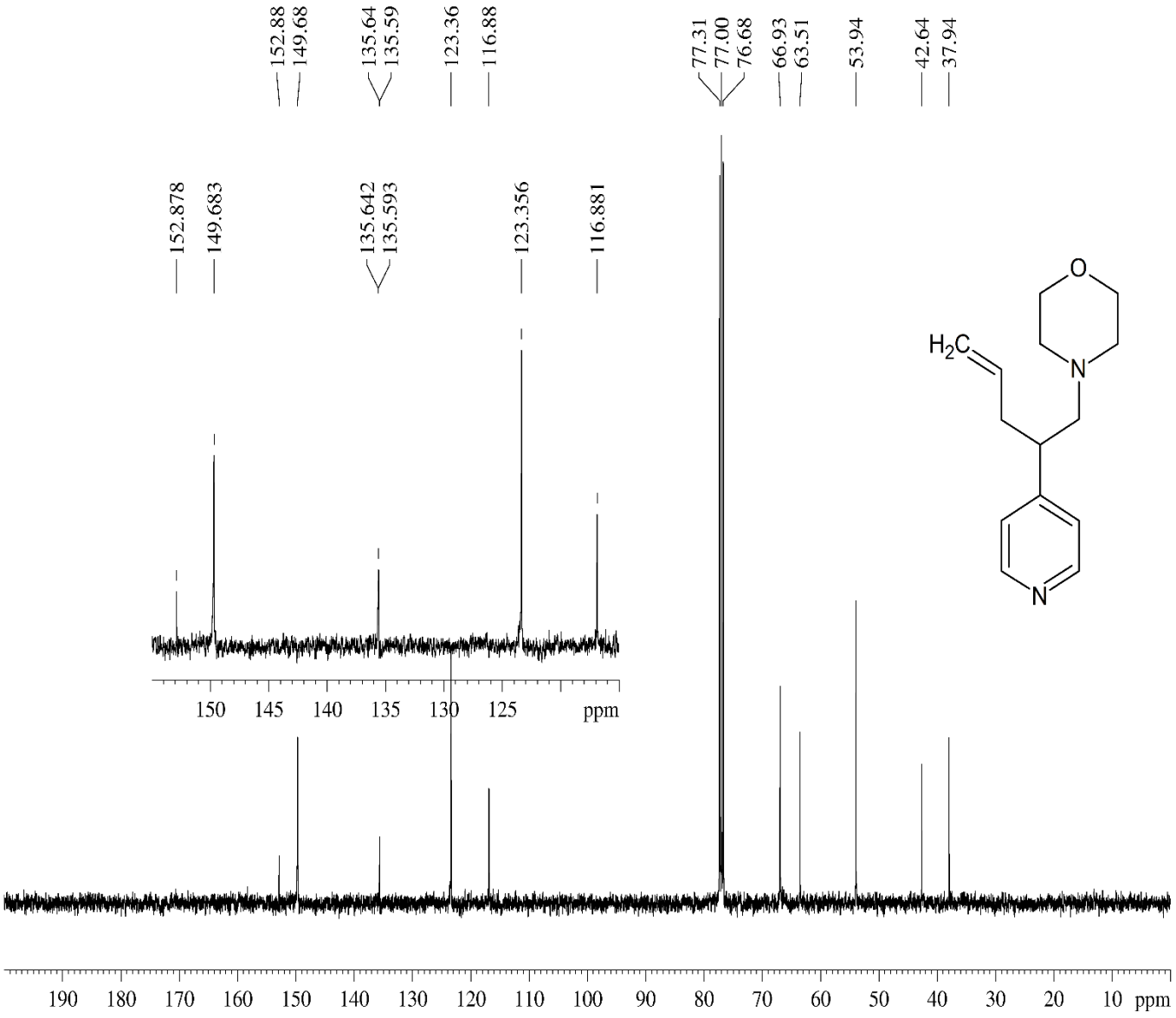
152.88
149.68
135.64
135.59
123.36
116.88
77.31
77.00
76.68
66.93
63.51
53.94
42.64
37.94
152.878
149.683
135.642
135.593
123.356
116.881
O
N
H2C
N
150 145 140 135 130 125 ppm
190 180 170 160 150 140 130 120 110 100 90 80 70 60 50 40 30 20 10 ppm

^{1}H (400 MHz, $CDCl_3$) and ^{13}C (100 MHz, $CDCl_3$) – NMR Spectra for **17a**

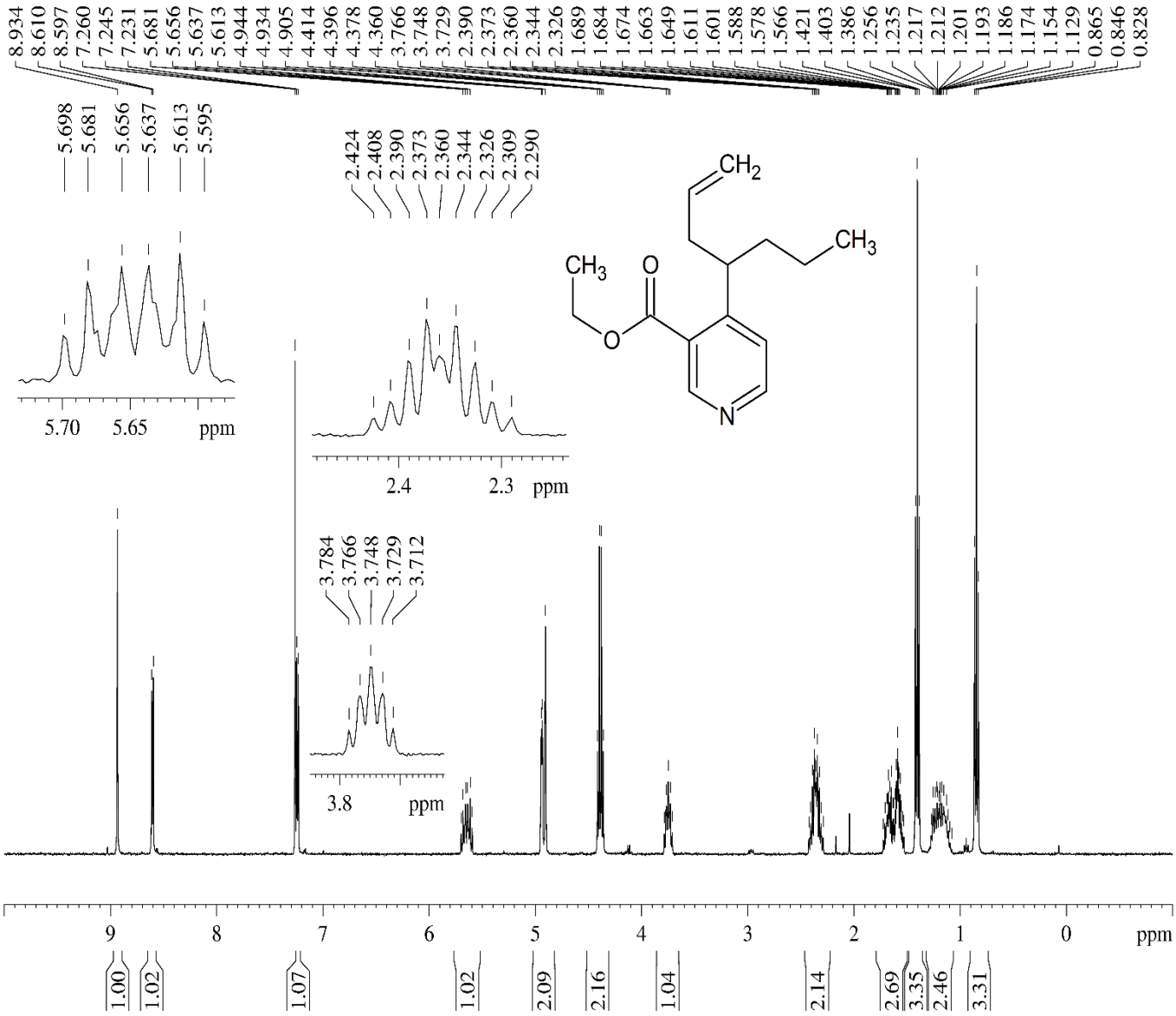

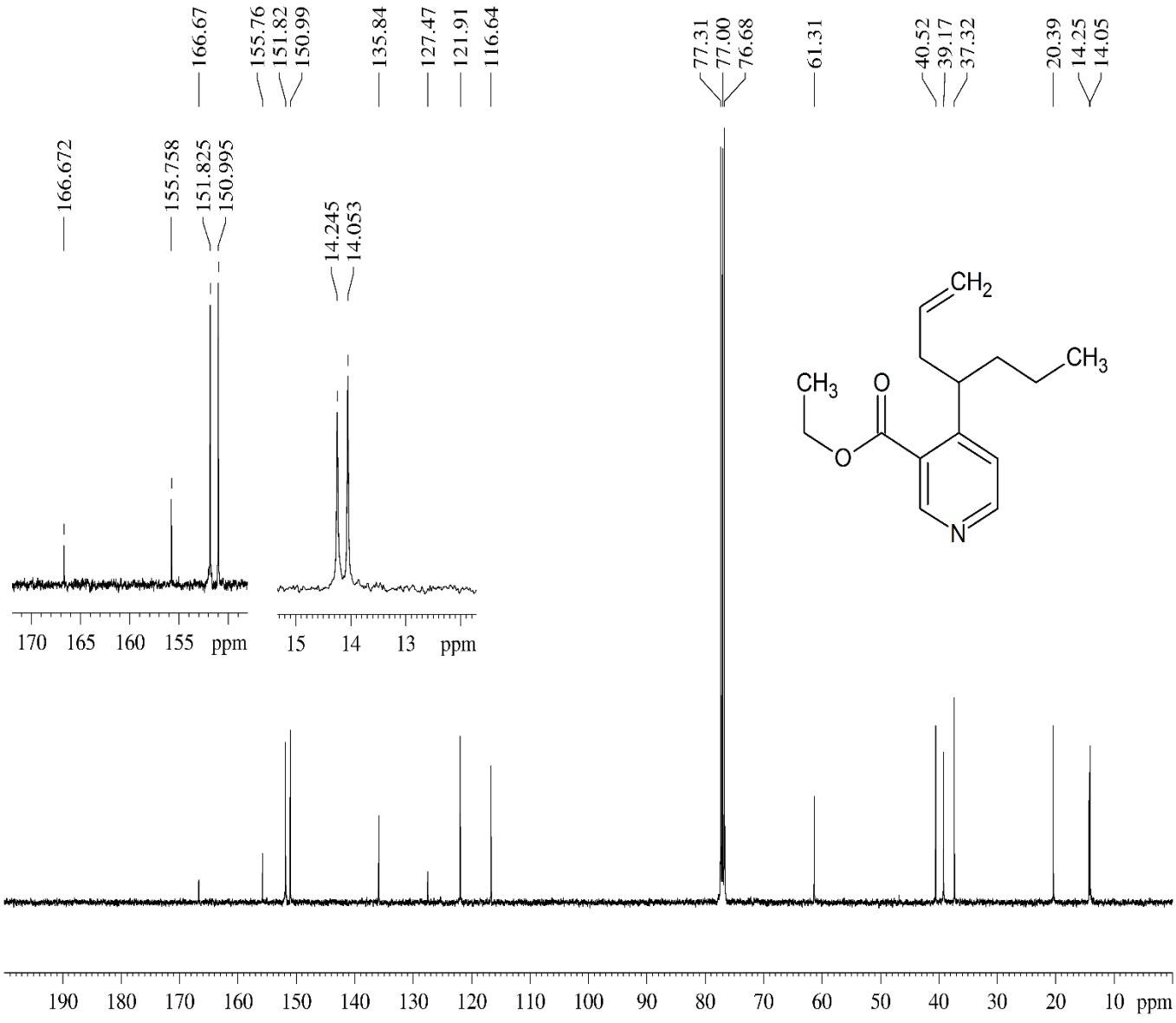
166.67
155.76
151.82
150.99
135.84
127.47
121.91
116.64
77.31
77.00
76.68
61.31
40.52
39.17
37.32
20.39
14.25
14.05
166.672
155.758
151.825
150.995
14.245
14.053
CH2
CH3
CH3
O
O
N
170 165 160 155 ppm
15 14 13 ppm
190 180 170 160 150 140 130 120 110 100 90 80 70 60 50 40 30 20 10 ppm

^{1}H (400 MHz, $CDCl_3$) and ^{13}C (100 MHz, $CDCl_3$) – NMR Spectra for **18a**

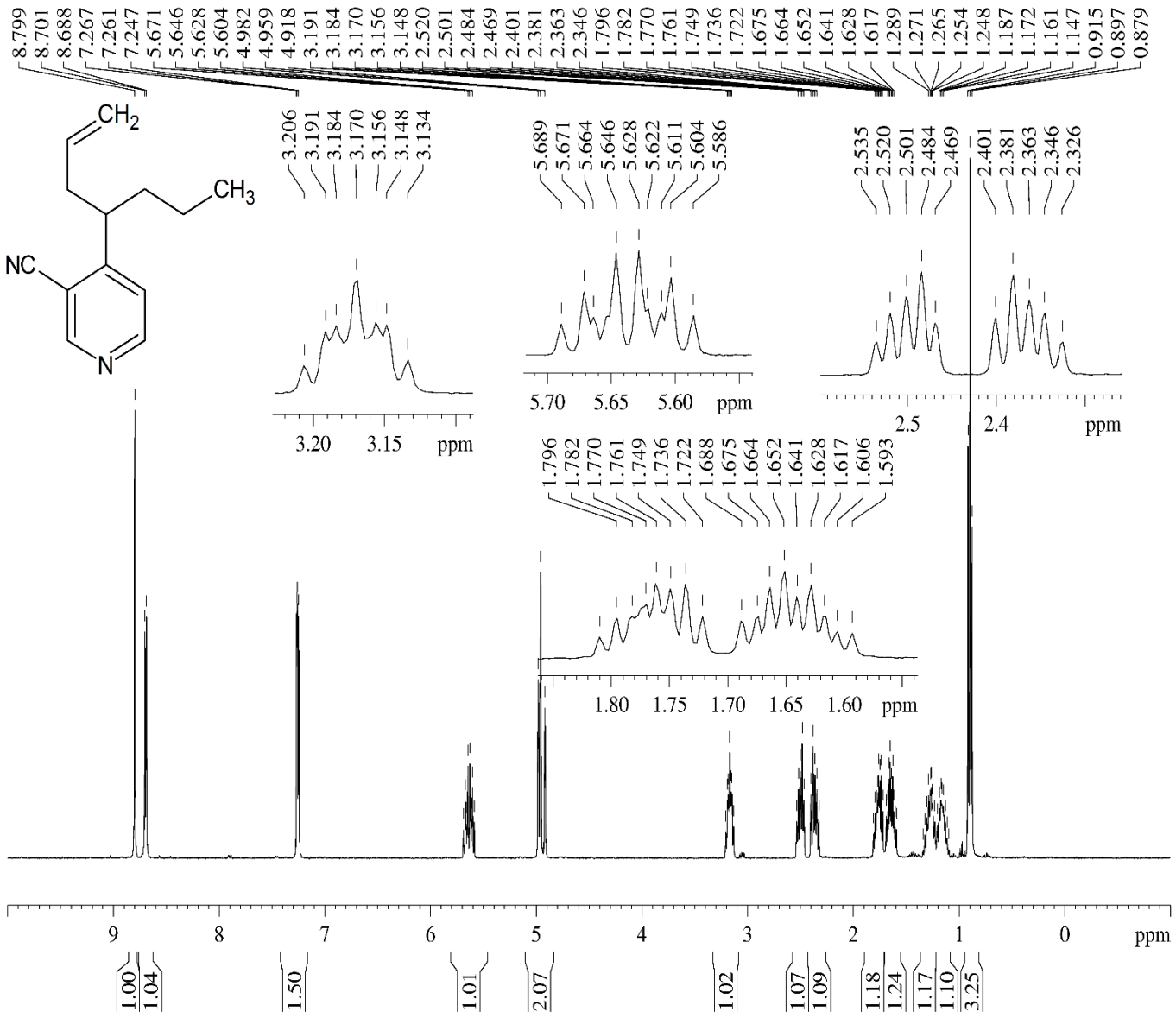

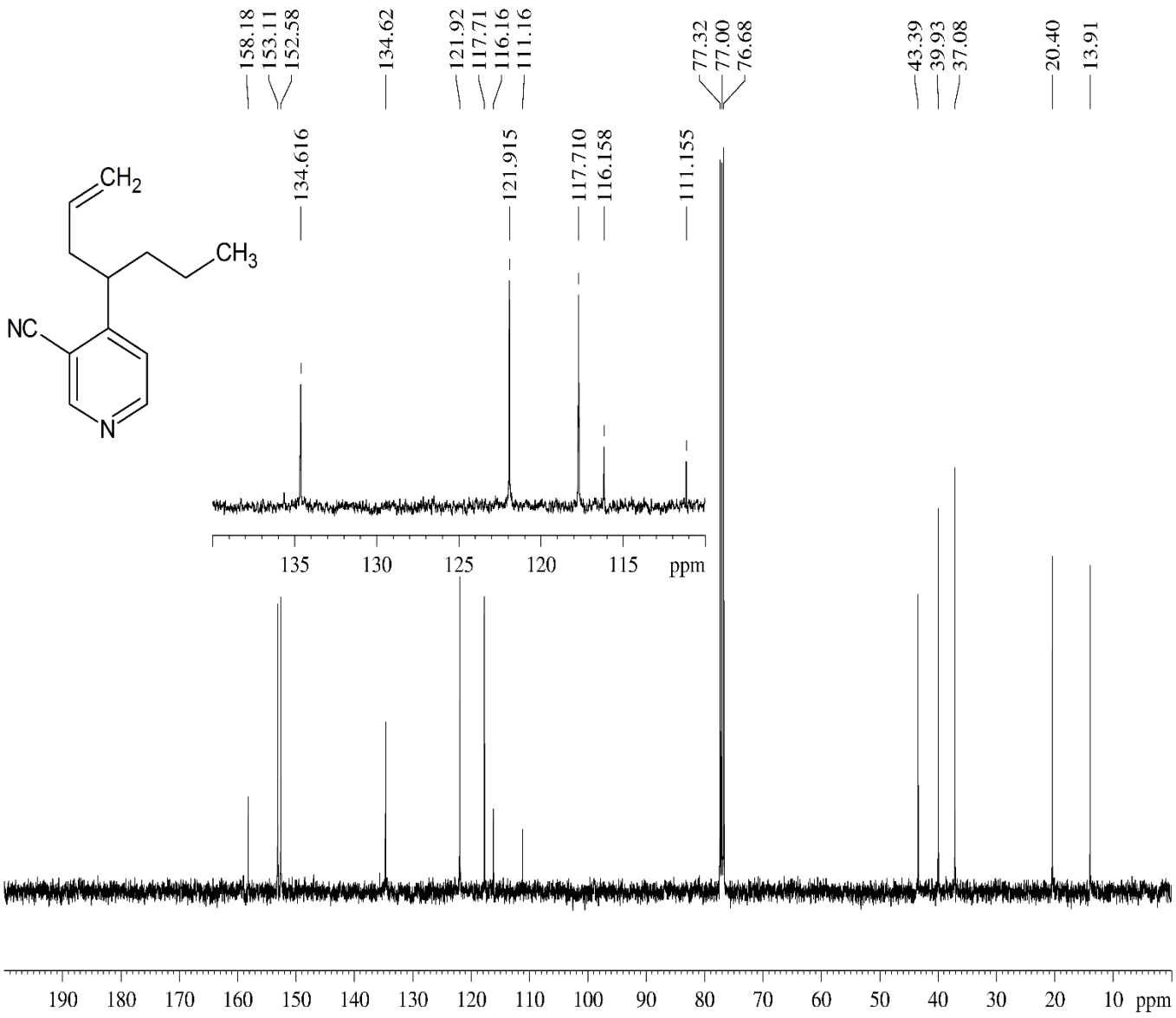
158.18
153.11
152.58
134.62
121.92
117.71
116.16
111.16
77.32
77.00
76.68
43.39
39.93
37.08
20.40
13.91
134.616
121.915
117.710
116.158
111.155
CH2
CH3
NC
N
135
130
125
120
115
ppm
190
180
170
160
150
140
130
120
110
100
90
80
70
60
50
40
30
20
10
ppm

^{1}H (400 MHz, $CDCl_3$) and ^{13}C (100 MHz, $CDCl_3$) – NMR Spectra for **19a**

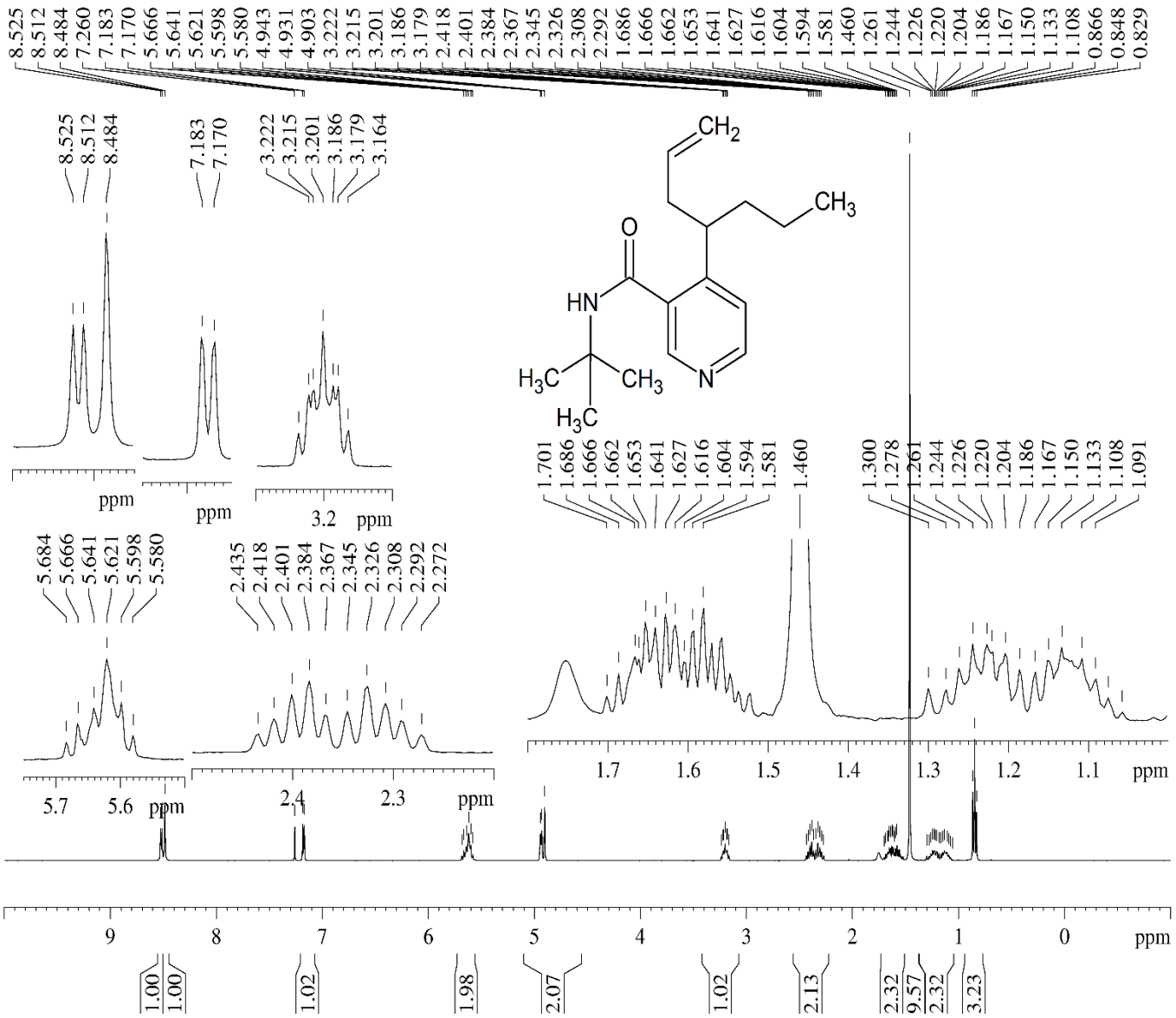

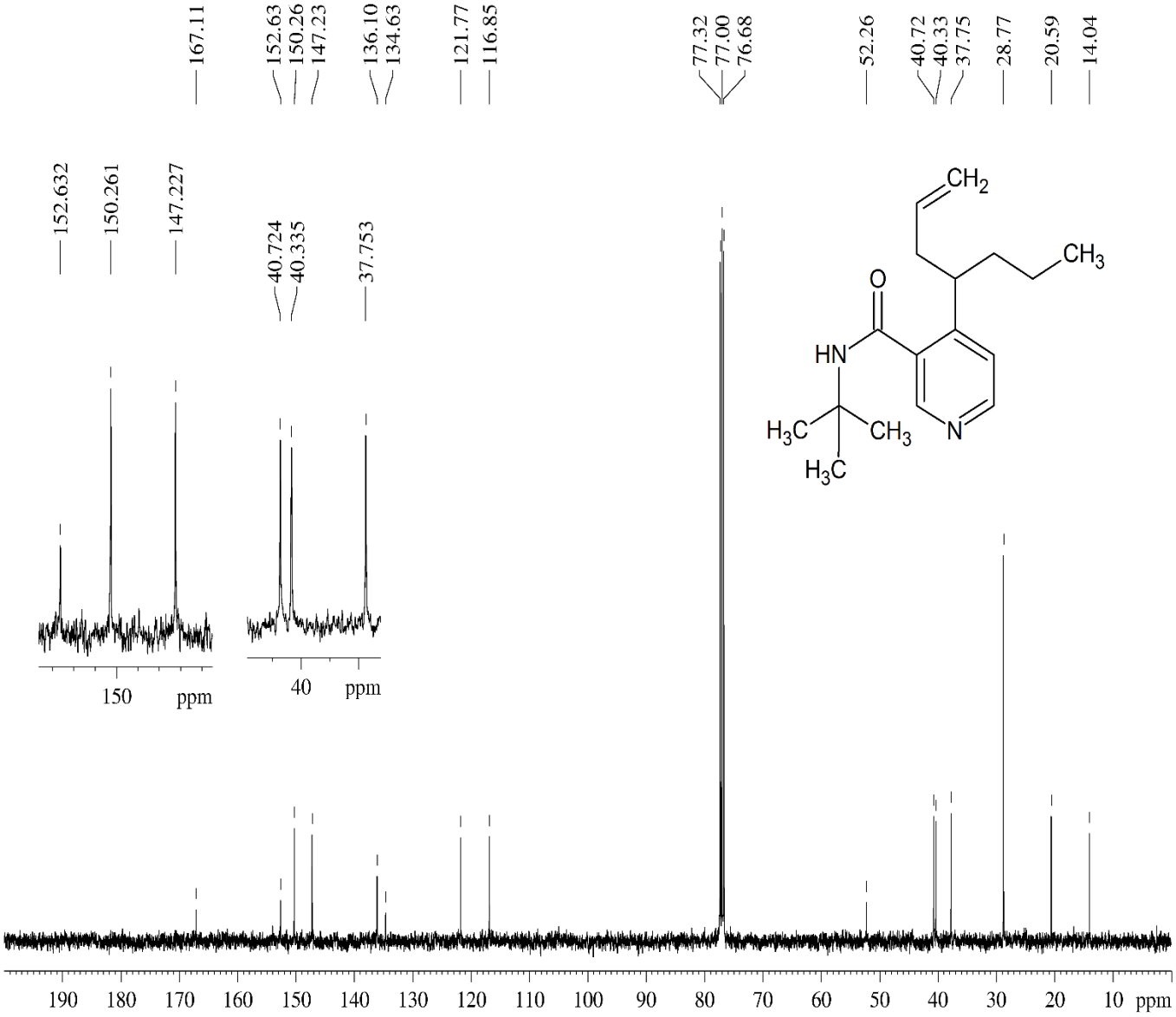
167.11
152.63
150.26
147.23
136.10
134.63
121.77
116.85
77.32
77.00
76.68
52.26
40.72
40.33
37.75
28.77
20.59
14.04
152.632
150.261
147.227
40.724
40.335
37.753
150 ppm
40 ppm
CH2
CH3
O
HN
H3C
CH3
H3C
N
190 180 170 160 150 140 130 120 110 100 90 80 70 60 50 40 30 20 10 ppm

^{1}H (400 MHz, $CDCl_3$) and ^{13}C (100 MHz, $CDCl_3$) – NMR Spectra for **20a**

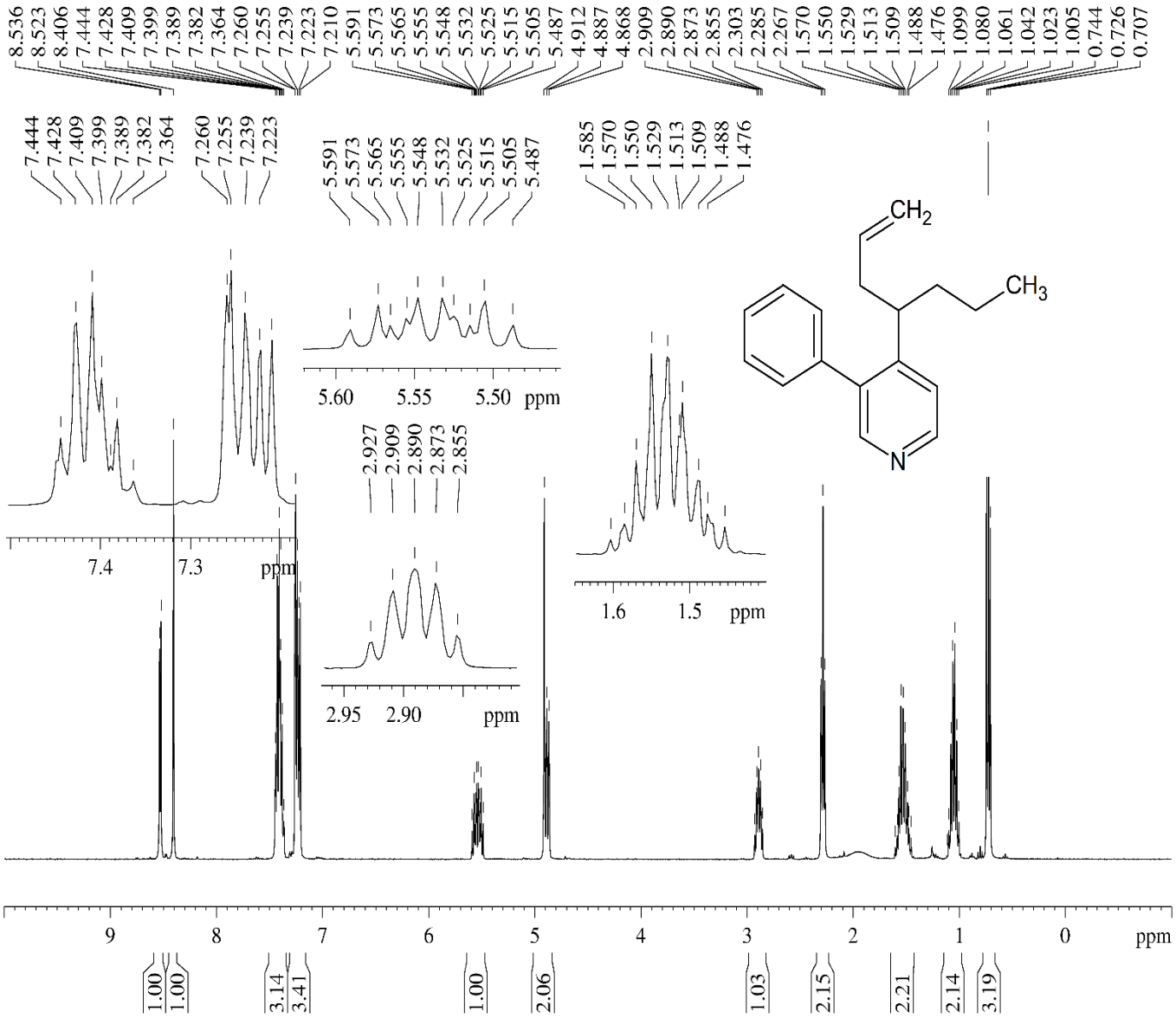

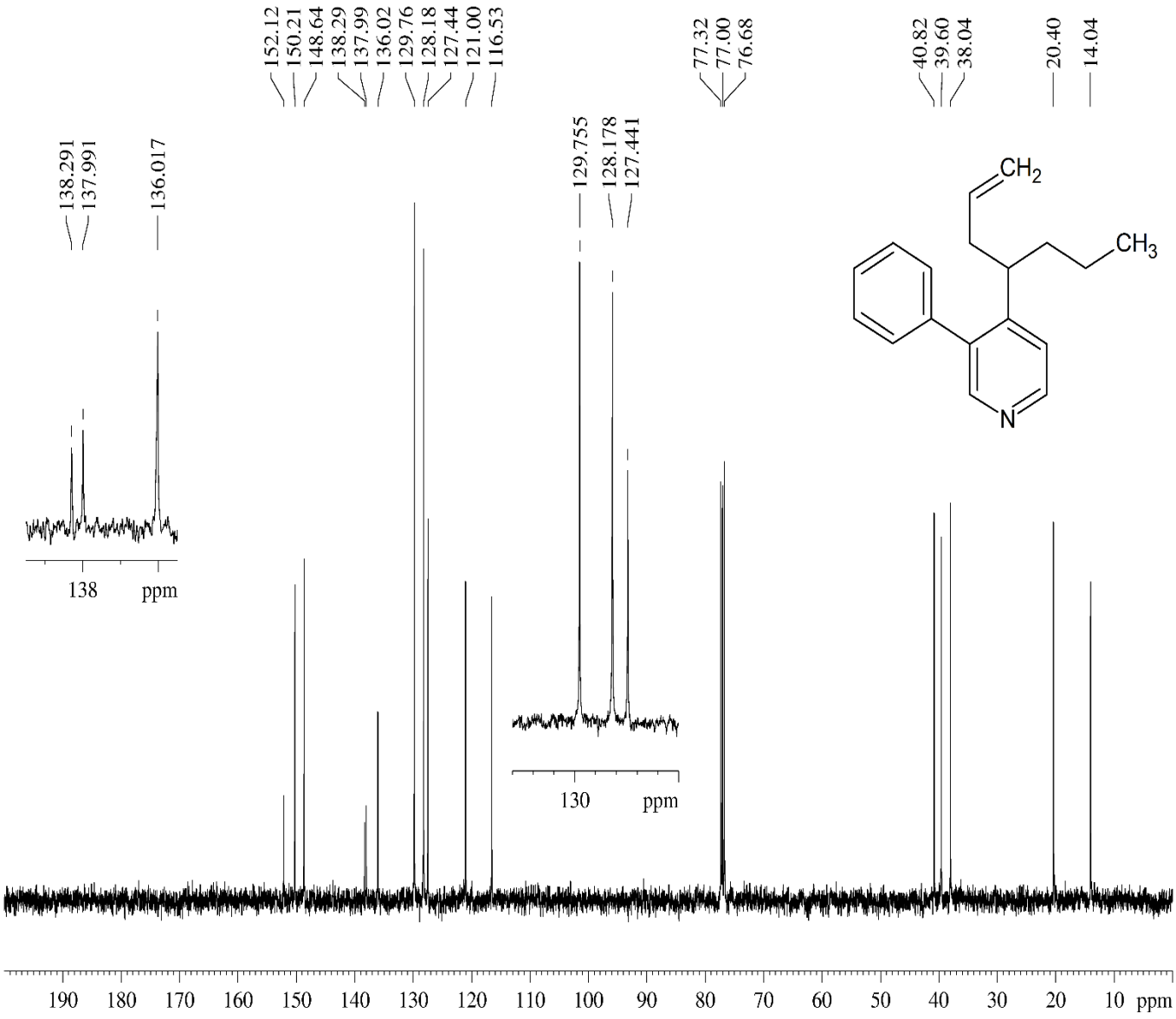
152.12
150.21
148.64
138.29
137.99
136.02
129.76
128.18
127.44
121.00
116.53
77.32
77.00
76.68
40.82
39.60
38.04
20.40
14.04
138.291
137.991
136.017
129.755
128.178
127.441
CH2
CH3
N
138 ppm
130 ppm
190 180 170 160 150 140 130 120 110 100 90 80 70 60 50 40 30 20 10 ppm

^{1}H (400 MHz, $CDCl_3$) and ^{13}C (100 MHz, $CDCl_3$) – NMR Spectra for **21a**

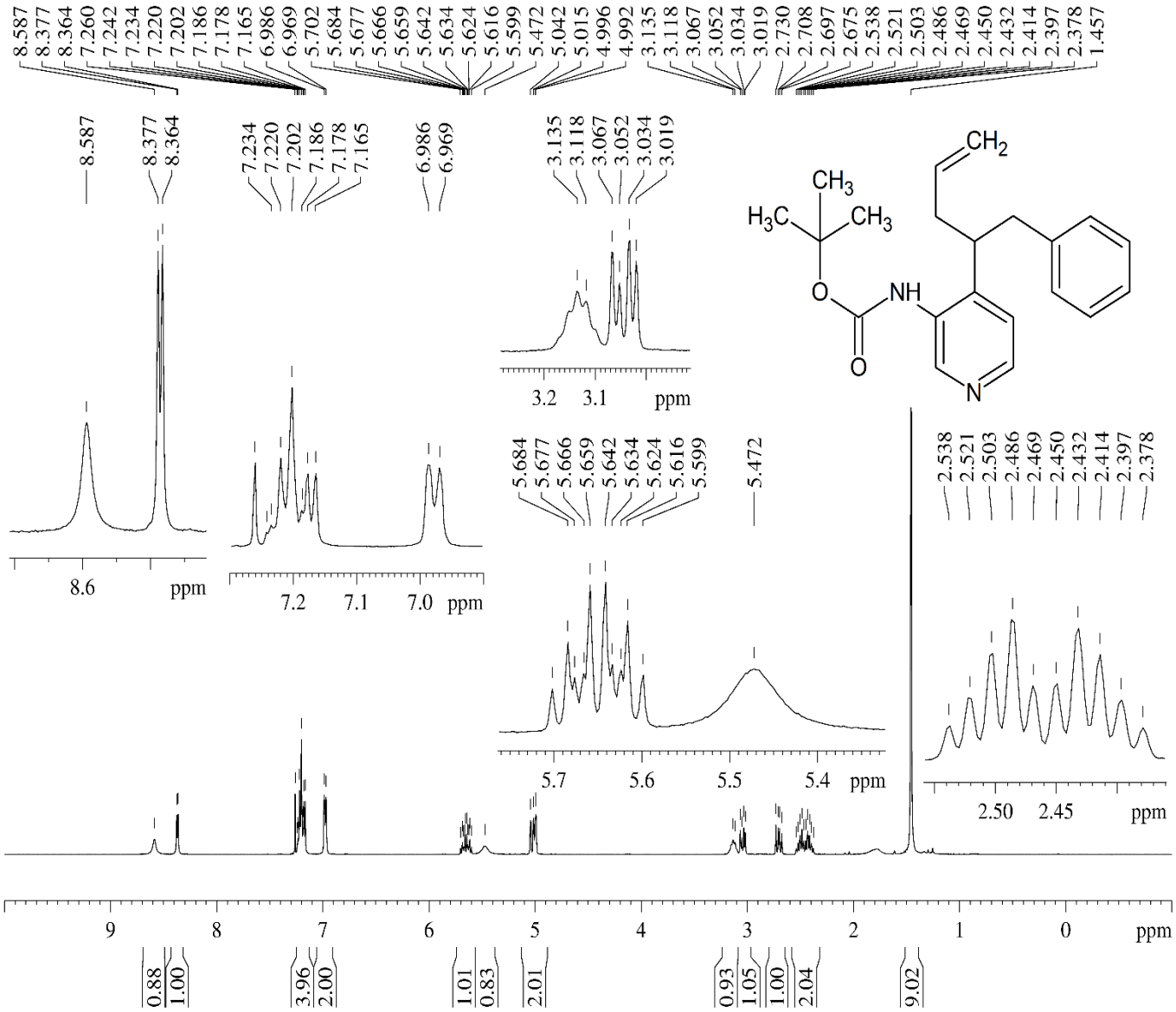

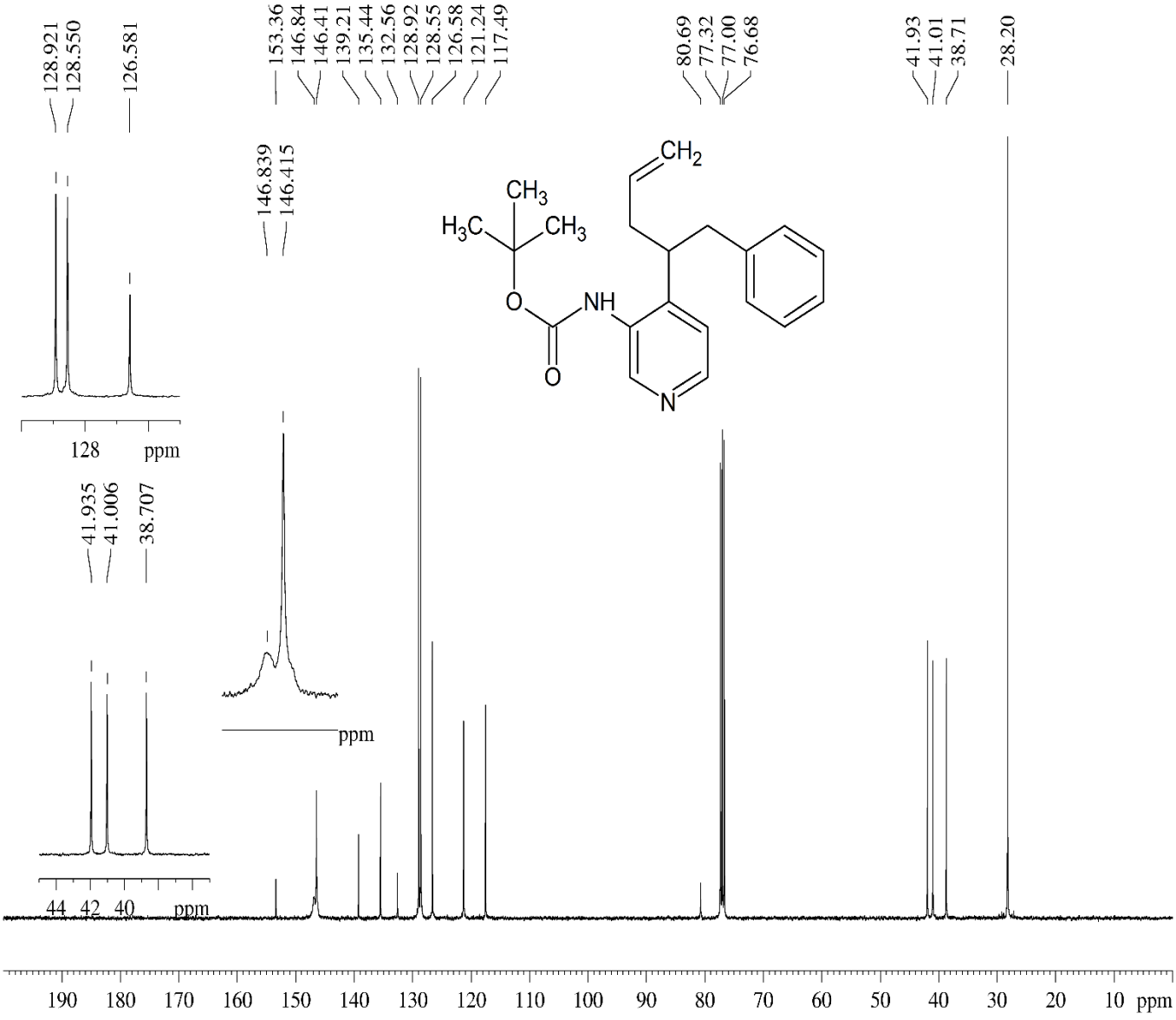
128.921
128.550
126.581
153.36
146.84
146.41
139.21
135.44
132.56
128.92
128.55
126.58
121.24
117.49
80.69
77.32
77.00
76.68
41.93
41.01
38.71
28.20
146.839
146.415
CH2
CH3
H3C
CH3
O
NH
O
N
128 ppm
41.935
41.006
38.707
ppm
44 42 40 ppm
190 180 170 160 150 140 130 120 110 100 90 80 70 60 50 40 30 20 10 ppm

^{1}H (300 MHz, $CDCl_3$, at r.t) and ^{13}C (100 MHz, $CDCl_3$, at r.t) – NMR Spectra for **22a′**

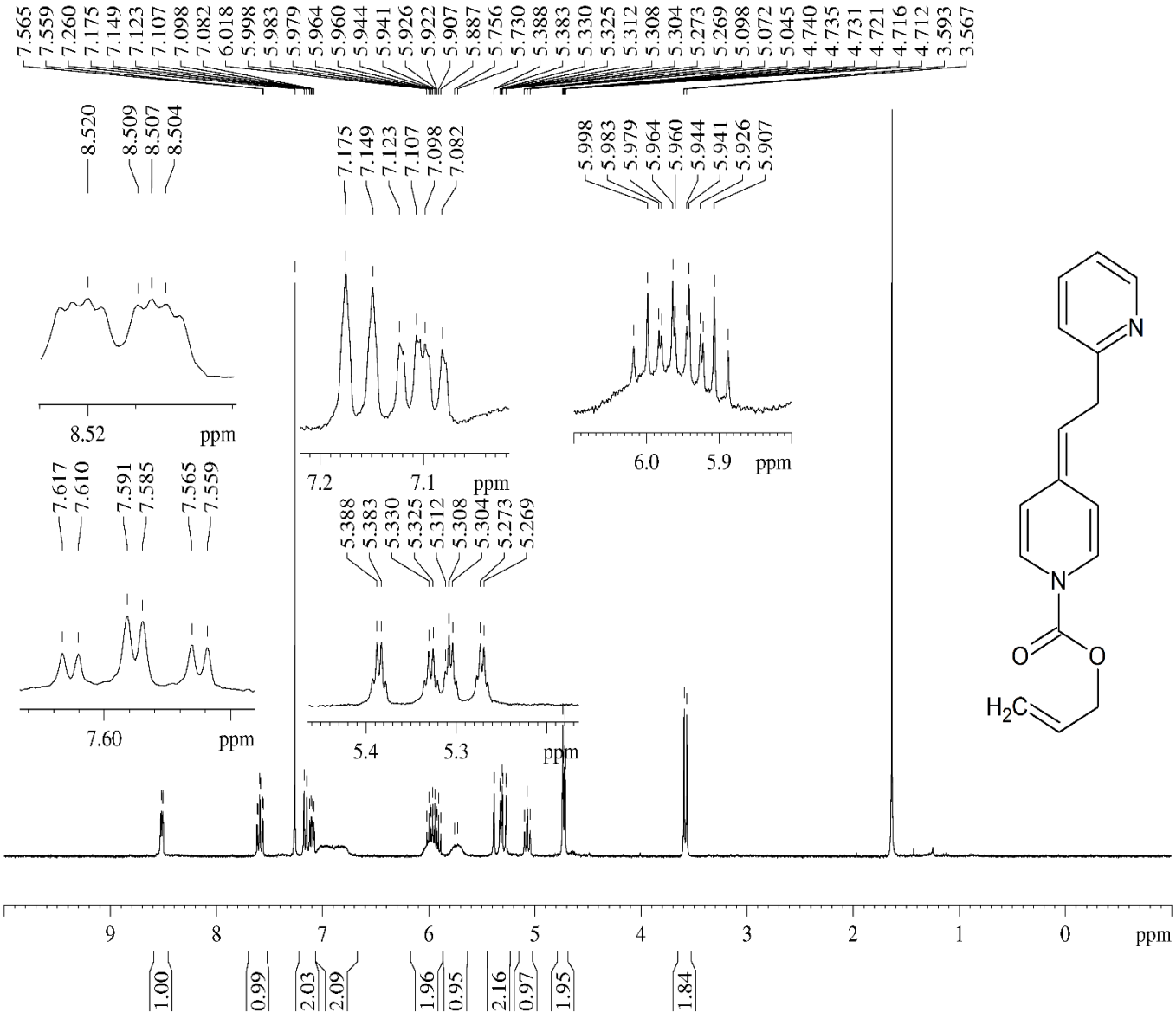

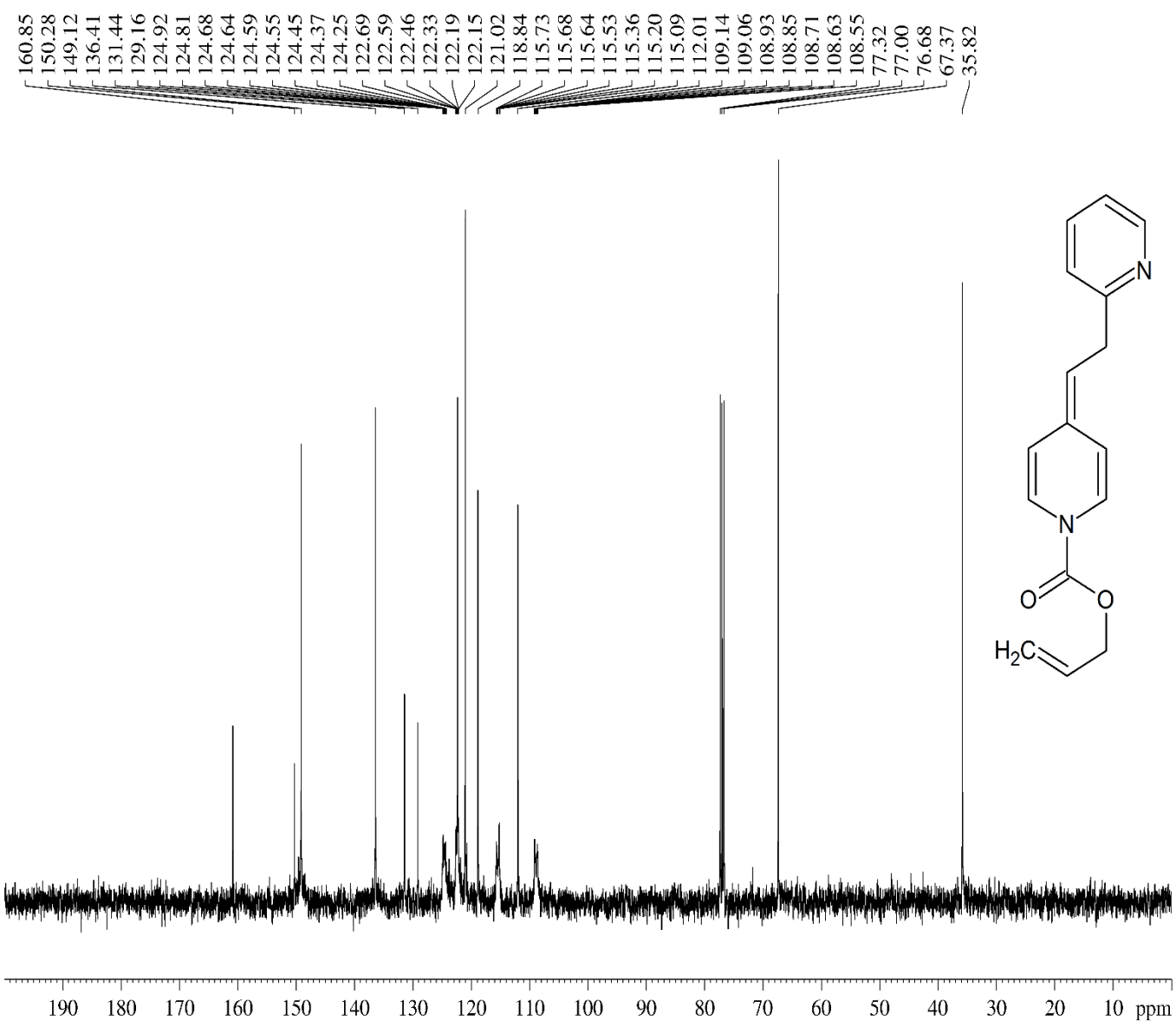
160.85
150.28
149.12
136.41
131.44
129.16
124.92
124.81
124.68
124.64
124.59
124.55
124.45
124.37
124.25
122.69
122.59
122.46
122.33
122.19
122.15
121.02
118.84
115.73
115.68
115.64
115.53
115.36
115.20
115.09
112.01
109.14
109.06
108.93
108.85
108.71
108.63
108.55
77.32
77.00
76.68
67.37
35.82
N
N
O
O
H2C
190
180
170
160
150
140
130
120
110
100
90
80
70
60
50
40
30
20
10
ppm

^{1}H (300 MHz, $CDCl_3$, at 40°C) and ^{13}C (100 MHz, $CDCl_3$, at 55°C) – NMR Spectra for **22a′**

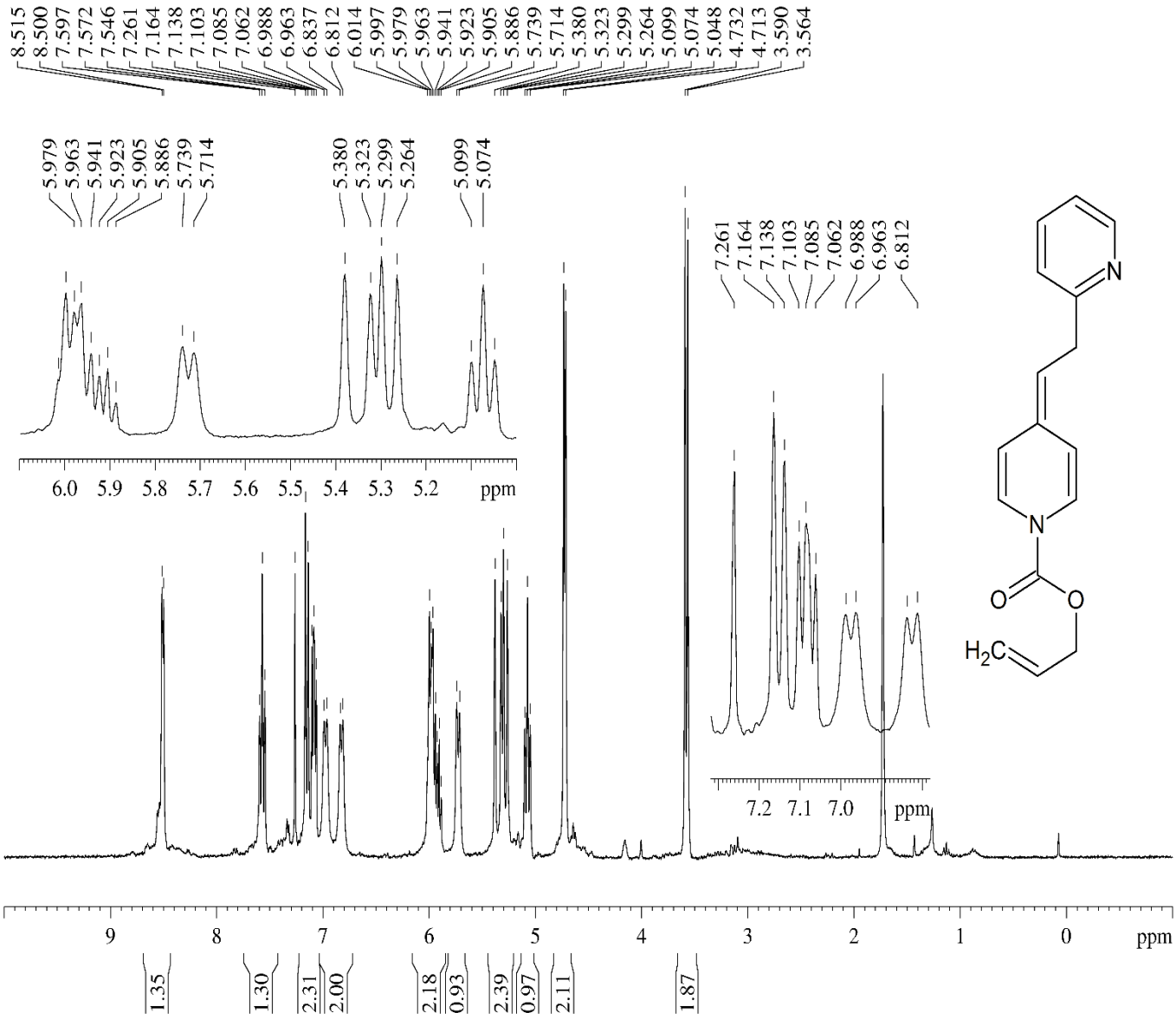

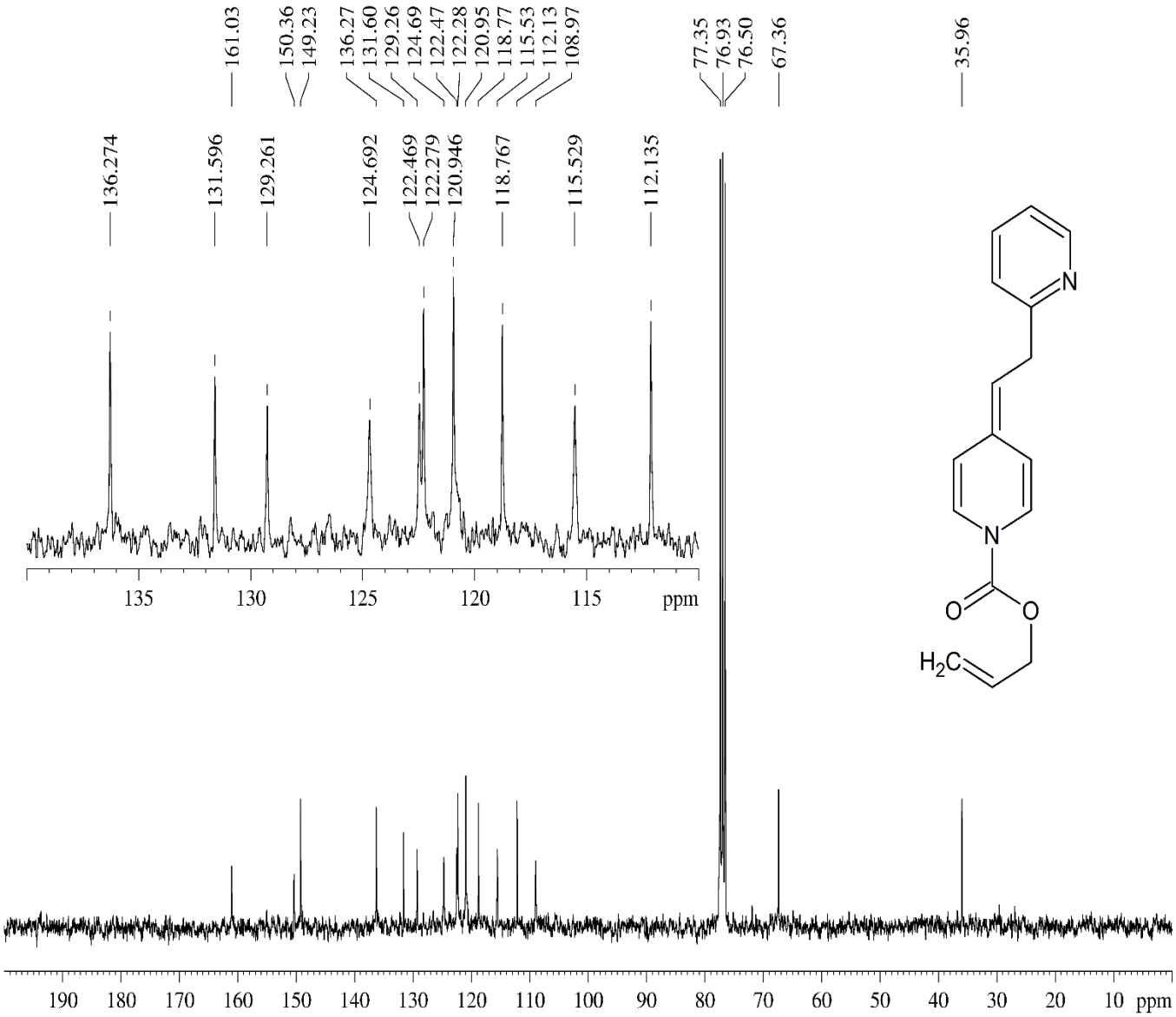
161.03
150.36
149.23
136.27
131.60
129.26
124.69
122.47
122.28
120.95
118.77
115.53
112.13
108.97
77.35
76.93
76.50
67.36
35.96
136.274
131.596
129.261
124.692
122.469
122.279
120.946
118.767
115.529
112.135
135
130
125
120
115
ppm
N
N
O
O
H2C
190
180
170
160
150
140
130
120
110
100
90
80
70
60
50
40
30
20
10
ppm

^{1}H (600 MHz, $CDCl_3$) and ^{13}C (150 MHz, $CDCl_3$) – NMR Spectra for **23a**

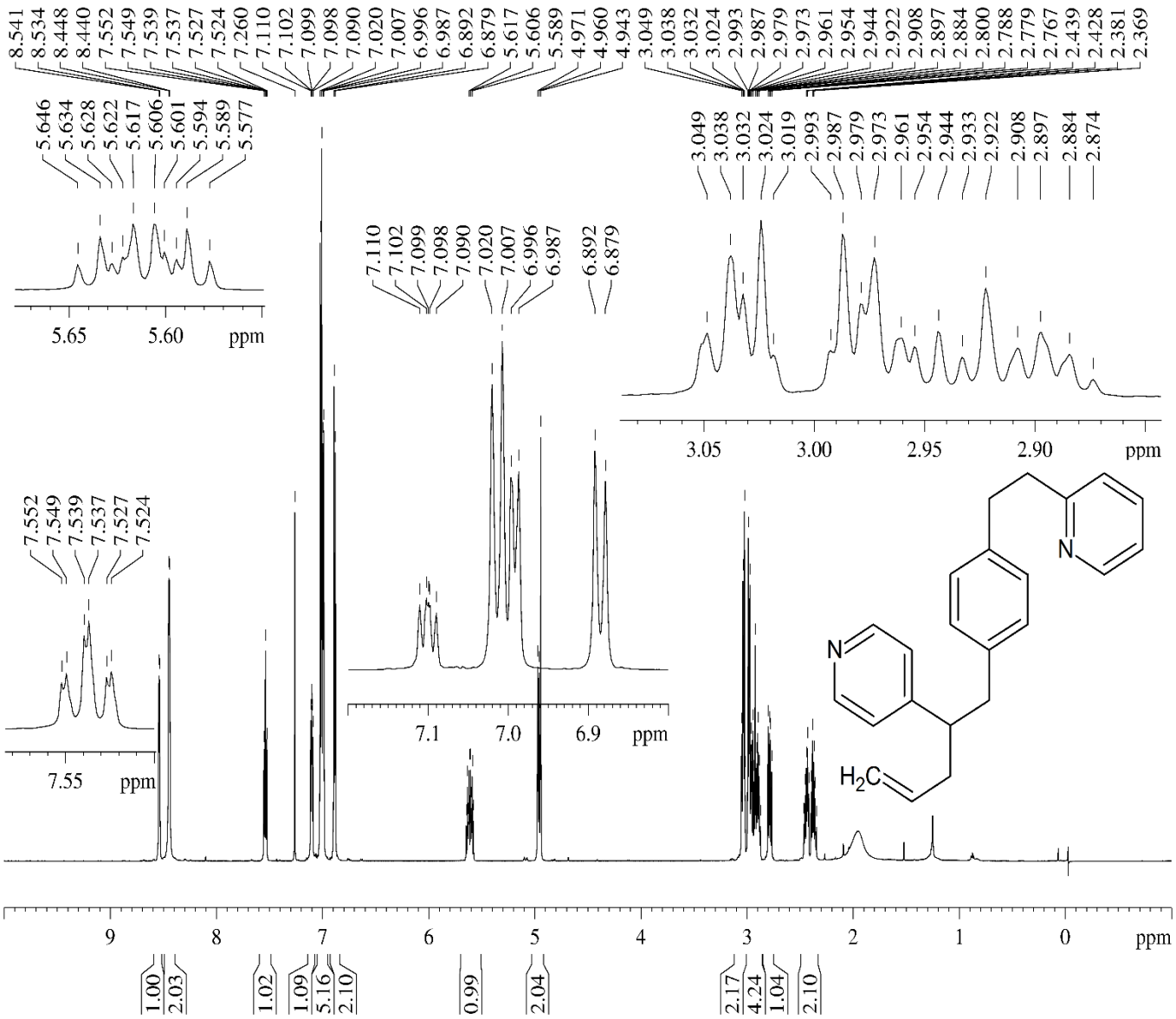

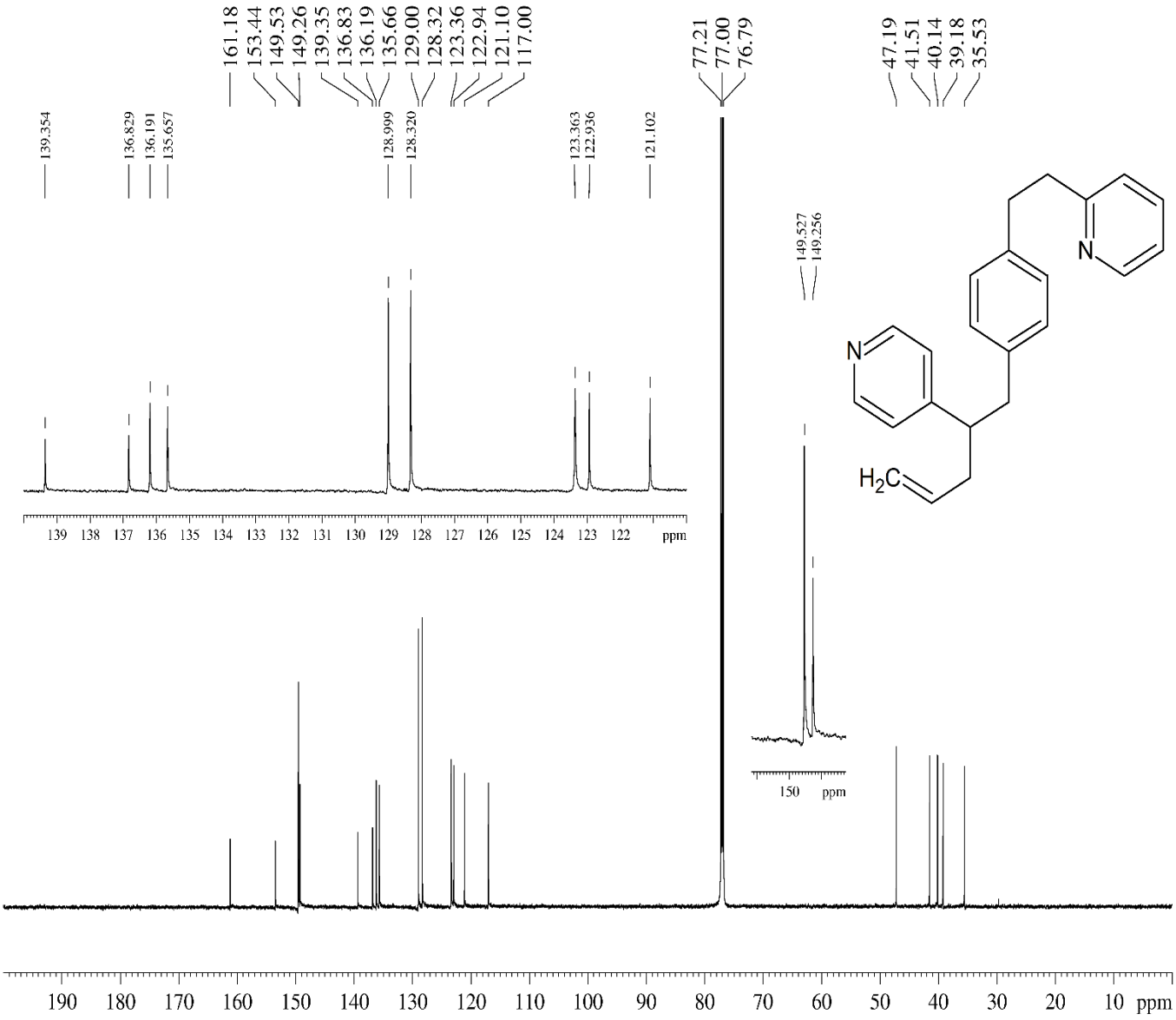
161.18
153.44
149.53
149.26
139.35
136.83
136.19
135.66
129.00
128.32
123.36
122.94
121.10
117.00
77.21
77.00
76.79
47.19
41.51
40.14
39.18
35.53
139.354
136.829
136.191
135.657
128.999
128.320
123.363
122.936
121.102
149.527
149.256
N
N
H2C
139 138 137 136 135 134 133 132 131 130 129 128 127 126 125 124 123 122 ppm
150 ppm
190 180 170 160 150 140 130 120 110 100 90 80 70 60 50 40 30 20 10 ppm

^{1}H (400 MHz, $CDCl_3$) and ^{13}C (100 MHz, $CDCl_3$) – NMR Spectra for **30a**

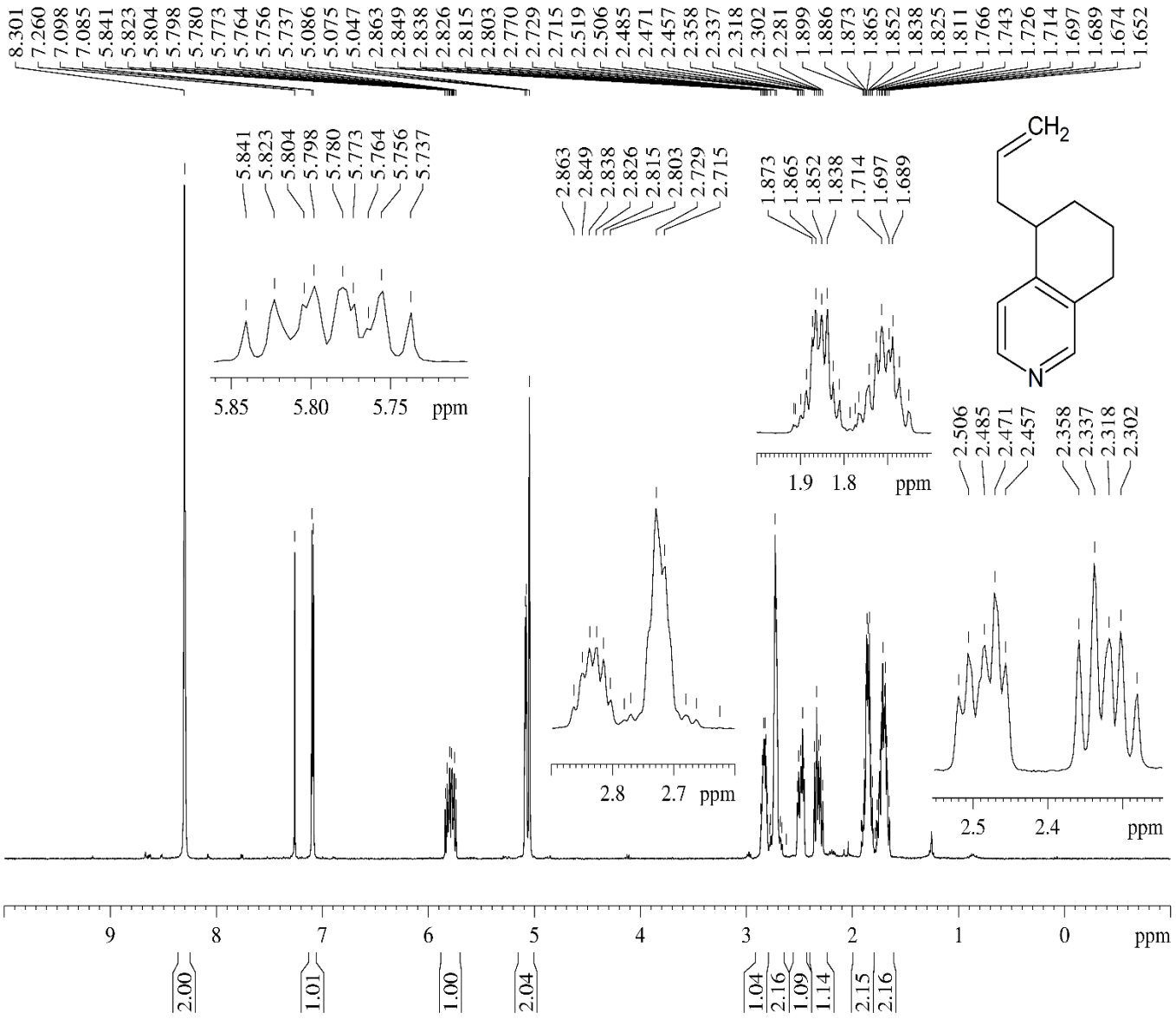

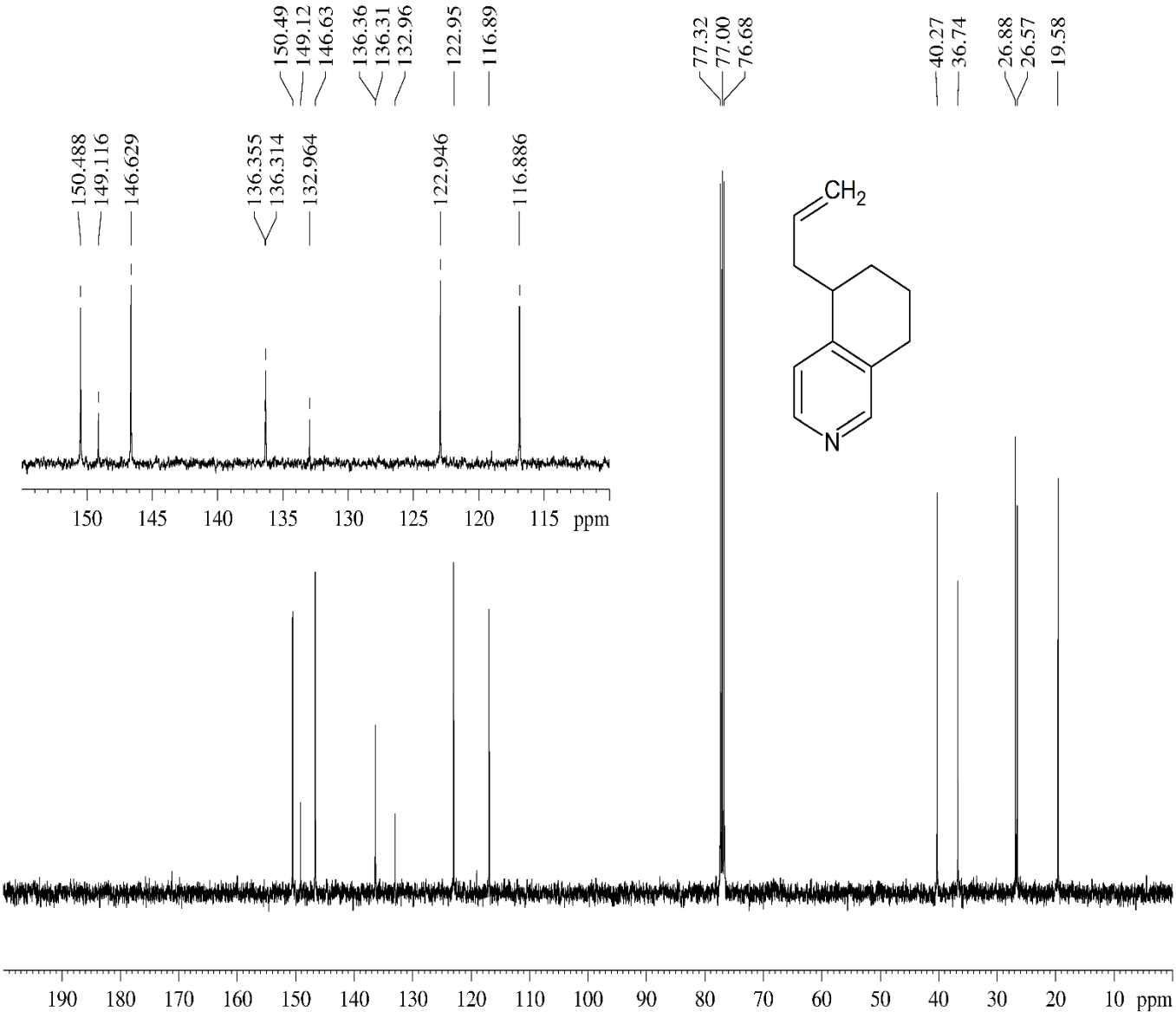
150.49
149.12
146.63
136.36
136.31
132.96
122.95
116.89
77.32
77.00
76.68
40.27
36.74
26.88
26.57
19.58
150.488
149.116
146.629
136.355
136.314
132.964
122.946
116.886
CH2
N
150 145 140 135 130 125 120 115 ppm
190 180 170 160 150 140 130 120 110 100 90 80 70 60 50 40 30 20 10 ppm

References:

(1) Hussain, I.; Capricho, J.; Yawer, M. A. *Adv. Synth. Catal.* **2016**, *358* (21), 3320–3349.

(2) Jonsson, R. *Scand. J. Immunol.* **2003**, *58* (6), 587.

(3) Casey, C. P. *J. Chem. Educ.* **2006**, *83* (2), 192.

(4) Colacot, T. J.; Matthey, J. *Platin. Met. Rev.* **2011**, *55* (2), 84–90.

(5) Choi, J.; Fu, G. C. *Science* **2017**, *356* (6334).

(6) Gensch, T.; Hopkinson, M. N.; Glorius, F.; Wencel-Delord, J. *Chem. Soc. Rev.* **2016**, *45* (10), 2900–2936.

(7) Roy, D.; Uozumi, Y. *Adv. Synth. Catal.* **2018**, *360* (4), 602–625.

(8) Chen, Q. A.; Ye, Z. S.; Duan, Y.; Zhou, Y. G. *Chem. Soc. Rev.* **2013**, *42* (2), 497–511.

(9) Nishimura, T.; Onoue, T.; Ohe, K.; Uemura, S. *J. Org. Chem.* **1999**, *64* (18), 6750–6755.

(10) Han, W.; Zhou, X.; Yang, S.; Xiang, G.; Cui, B.; Chen, Y. *J. Org. Chem.* **2015**, *80* (22), 11580–11587.

(11) Johansson Seechurn, C. C. C.; Kitching, M. O.; Colacot, T. J.; Snieckus, V. *Angew. Chem. Int. Ed.* **2012**, *51* (21), 5062–5085.

(12) Crabtree, R. H. *New J. Chem.* **2011**, *35* (1), 18–23.

(13) In *The Organometallic Chemistry of the Transition Metals*; John Wiley & Sons, Inc.: Hoboken, NJ, USA, 2005; pp 87–124.

(14) Tolman, C. A. *Chem. Rev.* **1977**, *77* (3), 313–348.

(15) Dierkes, P.; van Leeuwen, P. W. N. M. *J. Chem. Soc. Dalton Trans.* **1999**, 1519–1530.

(16) Ludwig, J. R.; Schindler, C. S. *Chem* **2017**, *2* (3), 313–316.

(17) Blakemore, D. C.; Castro, L.; Churcher, I.; Rees, D. C.; Thomas, A. W.; Wilson, D. M.; Wood, A. *Nat. Chem.* **2018**, *10* (4), 383–394.

(18) Netherton, M. R.; Fu, G. C. *Top. Organomet. Chem.* **2005**, 85–108.

(19) Miyaura, N.; Suzuki, A. *Chem. Rev.* **1995**, *95* (7), 2457–2483.

(20) Cordovilla, C.; Bartolomé, C.; Martínez-Ilarduya, J. M.; Espinet, P. *ACS Catal.* **2015**, *5* (5), 3040–3053.

(21) Zhou, J.; Fu, G. C. *J. Am. Chem. Soc.* **2003**, *125* (41), 12527–12530.

(22) Cabri, W.; Candiani, I. *Acc. Chem. Res.* **1995**, *28* (1), 2–7.

(23) Chinchilla, R.; Nájera, C. *Chem. Rev.* **2007**, *107* (3), 874–922.

(24) Tsuji, J.; Takahashi, H.; Morikawa, M. *Tetrahedron Lett.* **1965**, *6* (49), 4387–4388.

(25) Hata, G.; Takahashi, K.; Miyake, A. *Chem. Commun.* **1970**, *2* (1392), 1392–1393.

(26) Atkins, K. E.; Walker, W. E.; Manyik, R. M. *Tetrahedron Lett.* **1970**, *11*, 3821.

(27) Trost, B. M.; Strege, P. E. *J. Am. Chem. Soc.* **1977**, *99* (5), 1649–1651.

(28) Trost, B. M. *Tetrahedron* **2015**, *71* (35), 5708–5733.

(29) Amatore, C.; Jutand, A.; Meyer, G.; Mottier, L. *Chem. Eur. J.* **1999**, *5* (2), 466–473.

(30) Amatore, C.; Gamez, S.; Jutand, A. *J. Organomet. Chem.* **2001**, *624* (1–2), 217–222.

(31) Barry, M. T.; Keinan, E. *J. Org. Chem.* **1979**, *44* (20), 3451–3457.

(32) Trost, B. M.; Schmuff, N. R.; Miller, M. J. *J. Am. Chem. Soc.* **1980**, *102* (18), 5979–5981.

(33) Hutchins, R. O.; Learn, K. *J. Org. Chem.* **1982**, *47* (22), 4380–4382.

(34) Tanigawa, Y.; Nishimura, K.; Kawasaki, A.; Murahashi, S. I. *Tetrahedron Lett.* **1982**, *23* (52), 5549–5552.

(35) One, N.; Hamamoto, I.; Kaji, A. *J. Chem. Soc. Chem. Commun.* **1982**, No. 15, 821.

(36) Stevens, R. R.; Shier, G. D. *J. Organomet. Chem.* **1970**, *21* (2), 495–499.

(37) Ahmar, M.; Cazes, B.; Gore, J. *Tetrahedron Lett.* **1984**, *25* (40), 4505–4508.

(38) Chen, M. S.; White, M. C. *J. Am. Chem. Soc.* **2004**, *126* (5), 1346–1347.

(39) Trost, B. M.; Van Vranken, D. L. *Chem. Rev.* **1996**, *96* (1), 395–422.

(40) Trost, B. M.; Verhoeven, T. R. *J. Org. Chem.* **1976**, *41* (19), 3215–3216.

(41) Matsushita, H.; Negishi, E. *J. Chem. Soc. Chem. Commun.* **1982**, No. 3, 160.

(42) Ito, H.; Taguchi, T. *Chem. Soc. Rev.* **1999**, *28* (1), 43–50.

(43) Shimizu, I.; Yamada, T.; Tsuji, J. *Tetrahedron Lett.* **1980**, *21* (33), 3199–3202.

(44) Tsuda, T.; Chujo, Y.; Nishi, S. ichi; Tawara, K.; Saegusa, T. *J. Am. Chem. Soc.* **1980**, *102* (20), 6381–6384.

(45) Tsuji, J.; Shimizu, I.; Minami, I.; Ohashi, Y. *Tetrahedron Lett.* **1982**, *23* (46), 4809–4812.

(46) Rodríguez, N.; Goossen, L. J. *Chem. Soc. Rev.* **2011**, *40* (10), 5030–5048.

(47) Vitaku, E.; Smith, D. T.; Njardarson, J. T. *J. Med. Chem.* **2014**, *57* (24), 10257–10274.

(48) Gomtsyan, A. *Chem. Heterocycl. Compd.* **2012**, *48* (1), 7–10.

(49) Foley, D. J.; Nelson, A.; Marsden, S. P. *Angew. Chem. Int. Ed.* **2016**, *55* (44), 13650–13657.

(50) Tollefson, E. J.; Hanna, L. E.; Jarvo, E. R. *Acc. Chem. Res.* **2015**, *48* (8), 2344–2353.

(51) Fisher, T. J.; Dussault, P. H. *Tetrahedron* **2017**, *73* (30), 4233–4258.

(52) Grigoropoulou, G.; Clark, J. H.; Elings, J. A. *Green Chem.* **2003**, *5* (1), 1–7.

(53) Crudden, C. M.; Edwards, D. *Eur. J. Org. Chem.* **2003**, No. 24, 4695–4712.

(54) Bataille, C. J. R.; Donohoe, T. J. *Chem. Soc. Rev.* **2011**, *40* (1), 114–128.

(55) Ogba, O. M.; Warner, N. C.; O'Leary, D. J.; Grubbs, R. H. *Chem. Soc. Rev.* **2018**, *47* (12), 4510–4544.

(56) Waetzig, S. R.; Tunge, J. A. *J. Am. Chem. Soc.* **2007**, *129* (14), 4138–4139.

(57) Trost, B.; Thaisrivongs, D. *Synfacts* **2009**, *2009*, 1254–1254.

(58) Trost, B. M.; Thaisrivongs, D. A.; Hartwig, J. *J. Am. Chem. Soc.* **2011**, *133* (32), 12439–12441.

(59) Sha, S. C.; Zhang, J.; Carroll, P. J.; Walsh, P. J. *J. Am. Chem. Soc.* **2013**, *135* (46), 17602–17609.

(60) Murakami, R.; Sano, K.; Iwai, T.; Taniguchi, T.; Monde, K.; Sawamura, M. *Angew. Chem. Int. Ed.* **2018**, *57* (30), 9465–9469.

(61) Liu, X.-J.; You, S.-L. *Angew. Chem. Int. Ed.* **2017**, *56* (14), 4002–4005.

(62) Moon, P. J.; Wei, Z.; Lundgren, R. J. *J. Am. Chem. Soc.* **2018**, jacs.8b11390.

(63) Bull, J. A.; Mousseau, J. J.; Pelletier, G.; Charette, A. B. *Chem. Rev.* **2012**, *112* (5), 2642–2713.

(64) Parameswarappa, S. G.; Pigge, F. C. *J. Org. Chem.* **2012**, *77* (18), 8038–8048.

(65) Niwa, T.; Yorimitsu, H.; Oshima, K. *Angew. Chem. Int. Ed.* **2007**, *46* (15), 2643–2645.

(66) Kagawa, N.; Malerich, J. P.; Rawal, V. H. *Org. Lett.* **2008**, *10* (12), 2381–2384.

(67) Lansakara, A. I.; Mariappan, S. V. S.; Pigge, F. C. *J. Org. Chem.* **2016**, *81* (21), 10266–10278.

(68) Joshi, M. S.; Pigge, F. C. *ACS Catal.* **2016**, *6* (7), 4465–4469.

(69) Lansakara, A. I.; Farrell, D. P.; Pigge, F. C. *Org Biomol Chem* **2014**, *12* (7), 1090–1099.

(70) Pawar, L.; Pigge, F. C. *Tetrahedron Lett.* **2013**, *54* (45), 6067–6070.

(71) Hu, D. X.; Grice, P.; Ley, S. V. *J. Org. Chem.* **2012**, *77* (11), 5198–5202.

(72) Montgomery, T. D.; Zhu, Y.; Kagawa, N.; Rawal, V. H. *Org. Lett.* **2013**, *15* (5), 1140–1143.

(73) Amatore, C.; Jutand, A.; M'Barki, M. A. *Organometallics* **1992**, *11* (9), 3009–3013.

(74) Van Leeuwen, P. W. N. M.; Kamer, P. C. J.; Reek, J. N. H.; Dierkes, P. *Chem. Rev.* **2000**, *100* (8), 2741–2769.

(75) Van Leeuwen, P. W. N. M.; Kamer, P. C. J. *Catal. Sci. Technol.* **2018**, *8* (1), 26–113.

(76) Trost, B. M.; Thaisrivongs, D. A. *J. Am. Chem. Soc.* **2008**, *130* (43), 14092–14093.

(77) Wadsworth, W. S.; Emmons, W. D. *J. Am. Chem. Soc.* **1961**, *83* (7), 1733–1738.

(78) Robiette, R.; Richardson, J.; Aggarwal, V. K.; Harvey, J. N. *J. Am. Chem. Soc.* **2006**, *128* (7), 2394–2409.

(79) Abou-Shehada, S.; Teasdale, M. C.; Bull, S. D.; Wade, C. E.; Williams, J. M. J. *ChemSusChem* **2015**, *8* (6), 1083–1087.

(80) Chen, Q.; du Jourdin, X. M.; Knochel, P. *J. Am. Chem. Soc.* **2013**, *135* (13), 4958–4961.

(81) Li-Yuan Bao, R.; Zhao, R.; Shi, L. *Chem. Commun.* **2015**, *51* (32), 6884–6900.

(82) Sha, S.; Zhang, J.; Carroll, P. J.; Walsh, P. J. *J. Am. Chem. Soc.* **2013**, *135* (46), 17602–17609.

(83) Jaramillo, P.; Pérez, P.; Fuentealba, P. *J. Phys. Org. Chem.* **2007**, *20* (12), 1050–1057.

(84) Oh, H. K.; Lee, J. M.; Lee, H. W.; Lee, I. *Int. J. Chem. Kinet.* **2004**, *36* (8), 434–440.

(85) Güven, A. *Int. J. Mol. Sci.* **2005**, *6* (11), 257–275.

(86) Still, W. C.; Kahn, M.; Mitra, A. *J. Org. Chem.* **1978**, *43* (14), 2923–2925.

(87) Hoye, T. R.; Zhao, H. *J. Org. Chem.* **2002**, *67* (12), 4014–4016.

(88) Chen, Q.; Mollat, X.; Knochel, P. **2013**, 2–5.

(89) Lautens, M.; Roy, A.; Fukuoka, K.; Fagnou, K.; Martín-Matute, B. *J. Am. Chem. Soc.* **2001**, *123* (22), 5358–5359.

(90) Howell, J. M.; Feng, K.; Clark, J. R.; Trzepkowski, L. J.; White, M. C. *J. Am. Chem. Soc.* **2015**, *137* (46), 14590–14593.

(91) Lebel, H.; Davi, M.; Díez-González, S.; Nolan, S. P. *J. Org. Chem.* **2007**, *72* (1), 144–149.

(92) Brundish, D.; Bull, A.; Donovan, V.; Fullerton, J. D.; Garman, S. M.; Hayler, J. F.; Janus, D.; Kane, P. D.; McDonnell, M.; Smith, G. P.; Wakeford, R.; Walker, C. V.; Howarth, G.; Hoyle, W.; Allen, M. C.; Ambler, J.; Butler, K.; Talbot, M. D. *J. Med. Chem.* **1999**, *42* (22), 4584–4603.

(93) Kitbunnadaj, R.; Zuiderveld, O. P.; Christophe, B.; Hulscher, S.; Menge, W. M. P. B.; Gelens, E.; Snip, E.; Bakker, R. A.; Celanire, S.; Gillard, M.; Talaga, P.; Timmerman, H.; Leurs, R. *J. Med. Chem.* **2004**, *47* (10), 2414–2417.

(94) Massaro, A.; Mordini, A.; Mingardi, A.; Klein, J.; Andreotti, D. *Eur. J. Org. Chem.* **2011**, *2011* (2), 271–279.

(95) Benington, F.; Morin, R. D.; Khaled, M. A. *Synthesis* **1984**, *1984* (07), 619–620.

(96) Evans, O. R.; Lin, W. *Chem. Mater.* **2001**, *13* (8), 2705–2712.

(97) Hunter, C. A.; Misuraca, M. C.; Turega, S. M. *J. Am. Chem. Soc.* **2011**, *133* (3), 582–594.

(98) O'Neil, G. W.; Drake, N. D.; Storvick, J. M. *Tetrahedron Lett.* **2013**, *54* (7), 715–717.

(99) Bonnet, V.; Mongin, F.; Trécourt, F.; Quéguiner, G. *J. Chem. Soc. Perkin Trans.* **2000**, 4245–4249.

(100) Konishi, H.; Tanaka, H.; Manabe, K. *Org. Lett.* **2017**, *19* (7), 1578–1581.

(101) Kuriyama, M.; Matsuo, S.; Shinozawa, M.; Onomura, O. *Org. Lett.* **2013**, *15* (11), 2716–2719.

(102) Huestis, M. P.; Fagnou, K. *Org. Lett.* **2009**, *11* (6), 1357–1360.

(103) Maekawa, H.; Nishiyama, Y. *Tetrahedron* **2015**, *71* (38), 6694–6700.